Chair of Materials Science and Testing of Polymers

Doctoral Thesis

WEATHERING STABILITY OF POLYMERIC MATERIALS DEVELOPED FOR PV MODULES OPERATING IN HARSH CLIMATIC CONDITIONS

Antonia Omazic

April 2019

Dissertation

WEATHERING STABILITY OF POLYMERIC MATERIALS DEVELOPED FOR PV MODULES OPERATING IN HARSH CLIMATIC CONDITIONS

Authored by

Mag Ing Cheming Antonia Omazić

Submitted to

**Chair of Materials Science and Testing
of Polymers**

Department Polymer Engineering and Science

University of Leoben

Leoben, Austria

Conducted at

Polymer Competence Center Leoben GmbH

Leoben, Austria

Reviewer

Univ.-Prof. DI Dr. mont. Gerald Pinter

Chair of Materials Science and Testing of Polymers

University of Leoben

Supervisor

DI Dr. mont. Gernot Oreški

Polymer Competence Center Leoben GmbH

Affidavit

I declare in lieu of oath, that I wrote this thesis and performed the associated research myself, using only the support indicated in the literature cited in this thesis.

Mag Ing Cheming Antonia Omazić   Leoben, February 2019

Acknowledgment

Funding

Abstract

Harsh environmental conditions lead to the deterioration of optical, thermal and mechanical properties of polymeric components in photovoltaic (PV) modules. Therefore, an increased reliability represents one of the main challenges for current and future PV modules. However, an increased reliability has to be achieved within cost-reduction and sustainability frameworks, which makes it even more challenging. In order to meet an increased demand for reliability, cost-reduction and sustainability, some of the options are: (i) change of materials for PV components, (ii) change in PV design and/or production process and (iii) development of new or adjusting the current qualification and reliability tests. However, the influence of each of those steps on reliability of PV modules has to be well understood.

Hence the main aims of this thesis are to understand the influence of the replacement of state-of-the-art materials with alternatives, PV design and customized climate-specific accelerated tests on reliability of PV modules. In order to assess weathering stability of polymeric materials for PV components, suitable characterization methods and evaluation procedures are proposed. The results obtained in this work enhance knowledge about polymer degradation and give valuable input to state-of-the-art knowledge on PV modules' reliability and could help in the optimization of current and the development of new qualification and reliability tests.

After an introduction and an in-depth literature review on the relation between degradation of polymeric PV components and climatic conditions in Chapter 1, results of the feasibility study for replacement of state-of-the-art PET/fluoropolymer backsheets via alternative co-extruded polyolefin backsheets are presented in Chapter 2. In order to determine the weathering stability of alternative polyolefin backsheets, a systematic investigation in terms of UV/Vis/NIR spectroscopy, FTIR-ATR spectroscopy, differential scanning calorimetry (DSC), tensile test and thermo-mechanical analysis (TMA) was conducted. The results pointed to excellent weathering stability of the polyolefin backsheet even after extended aging. Inherent hydrolysis resistance, retained flexibility and selective permeation properties are great features that could lead to reduced cracking and embrittlement in the field, especially under harsh operating conditions.

Major drawbacks of EVA are peroxide-crosslinking and production of acetic acid upon degradation, which are linked to many PV failure modes. Therefore, Chapter 3 deals with weathering stability of alternative polyolefin encapsulants (thermoplastic polyolefin, TPO, and polyolefin elastomer, POE) on the PV module level. The special focus was on the

influence of the microclimate within the module and permeation properties of the backsheet on their degradation. Therefore PV modules were prepared with a polymeric (PET-laminate) and impermeable glass backsheet. Changes of optical, chemical and thermal properties were determined after accelerated aging. FTIR-ATR spectroscopy revealed strong influence of the type of the backsheet and microclimate within the test module on degradation of front encapsulants. As opposed to a polymeric backsheet, an impermeable glass backsheet prevents moisture and oxygen ingress towards cell and front encapsulant, which results in different degradation mechanisms. TPO showed very good weathering stability in both types of modules. The results of these investigations have confirmed that PV design, i.e. type of the backsheet plays an important role in the degradation of front encapsulants in PV modules.

Chapter 4 deals with thermo-mechanical stability of state-of-the-art and alternative polyolefin encapsulants. In order to understand the influence of aging on thermo-mechanical behaviour of encapsulants, thermo-mechanical analysis (TMA) was conducted on laminated encapsulants before and after 1000h of damp heat aging. The results have shown strong influence of morphology, i.e. crystallinity on the thermo-mechanical behaviour of encapsulants. Due to the highest crystalline content, TPO showed the most stable thermo-mechanical behaviour among the investigated encapsulants before and after aging. On the other hand, EVA with the lowest crystalline content showed the highest thermal expansion, which could lead to the formation of stresses within the PV module during production and service time and give rise to different failure modes. The findings from this work proved that thermo-mechanical analysis combined with differential scanning calorimetry is a suitable method for the systematic investigation of thermo-mechanical stability of polyolefin encapsulants.

In order to predict long term performance under different operating conditions as accurately as possible, the development of climate-specific tests is necessary. According to the state-of-the-art IEC 61215 qualification test, damp heat testing of modules performed at 85°C and 85% RH for 1000h provides the most information on aging and degradation of encapsulation materials, but this test is recognized as not predictive of long term performance. Therefore, Chapter 5 deals with the influence of climate-specific accelerated tests on degradation of EVA at the PV module level. The main focus in this part was on the application of non-destructive methods, whereas Raman confocal spectroscopy proved to be a great tool for fast and non-destructive qualitative and quantitative assessment of EVA degradation. The results showed significant difference in EVA degradation behaviour under different aging conditions compared to standard tests. These findings provided valuable input for

understanding EVA degradation under different aging conditions, which could be of great importance for the development of optimized accelerated tests.

Kurzfassung

Die Einwirkung unterschiedlichster Umwelteinflüsse kann zu Veränderungen der optischen, thermischen und mechanischen Eigenschaften der in Photovoltaik (PV)-Modulen verbauten Kunststoffkomponenten führen und dadurch in weiterer Folge die Leistung des PV-Moduls über die Zeit verringern. Die Zuverlässigkeit von PV-Modulen ist jedoch ein wesentlicher Qualitätsfaktor und stellt die Hersteller somit vor eine große Herausforderung. Auch andere Faktoren, wie die Nachhaltigkeit des Produktes und die Herstellungskosten müssen mitberücksichtigt werden, um wettbewerbsfähig zu bleiben. Um eine ausreichende Zuverlässigkeit und ein nachhaltiges Produkt mit möglichst niedrigen Kosten zu erreichen, können mehrere Ansätze verfolgt werden: (i) Änderung der Materialien der Modulkomponenten, (ii) Änderungen im Design und Herstellungsprozess des Moduls und (iii) Optimierung beziehungsweise Weiterentwicklung der derzeitigen Qualitäts- und Zuverlässigkeitstests. Inwieweit diese Ansätze die Zuverlässigkeit eines PV-Moduls erhöhen muss allerdings noch genauer untersucht und verstanden werden.

Das Hauptziel dieser Arbeit ist daher zu verstehen, inwiefern sich der Ersatz von gegenwärtig verwendeten Materialien durch alternative Materialien, Änderungen im Moduldesign und klimaspezifisch beschleunigte Alterungstests auf die Beständigkeit von PV-Modulen auswirken. Um die Beständigkeit von Kunststoffkomponenten im PV-Modul zu untersuchen, werden geeignete Charakterisierungsmethoden und Evaluierungsverfahren vorgestellt. Die Ergebnisse, die im Rahmen dieser Dissertation erarbeitet wurden, erweitern das Verständnis über Alterung von Kunststoffen und liefern einen wertvollen Beitrag zu den bisherigen Kenntnissen über die Zuverlässigkeit von PV-Modulen. Sie ermöglichen darüber hinaus eine Optimierung und Weiterentwicklung der aktuell angewandten Qualitäts- und Zuverlässigkeitsprüfungen.

Nach einer Einführung und einer Übersicht über den Zusammenhang zwischen vorherrschenden Klimabedingungen und der daraus folgenden Alterung von Kunststoffkomponenten im PV-Modul im Kapitel 1, beschäftigt sich Kapitel 2 mit den Ergebnissen einer Machbarkeitsstudie zum Einsatz von Rückseitenfolien aus co-extrudiertem Polyolefin anstatt der Verwendung der herkömmlichen Rückseitenfolien aus einer Kombination von Polyethylenterephtalat (PET) und Fluorpolymeren. Um die Bewitterungsstabilität der neuen Rückseitenfolien zu charakterisieren, wurde eine systematische Untersuchung des Materials mittels UV/Vis/NIR-Spektroskopie, Fourier-Transform-Infrared (FTIR)-Spektroskopie im Attenuated-Total-Reflection (ATR)-Modus, Differential-Thermoanalyse (DSC), uniaxialen Zugversuchen und Thermomechanischer

Analyse (TMA) durchgeführt. Die Ergebnisse dieser Untersuchungen zeigen eine hervorragende Stabilität der neuen Polyolefin-Rückseitenfolien auch nach ausgedehnter Bewitterung des Materials. Polyolefine sind unempfindlich gegenüber Hydrolyse, bleiben flexibel und zeigen selektive Permeationseigenschaften. Diese Eigenschaften können zu einer Verringerung der Versprödung und Rissbildung von Rückseitenfolien führen, auch unter den strengen Witterungsbedingungen, die im freien Feld herrschen.

Ein großer Nachteil von Ethylen-Vinylacetat (EVA), das üblicherweise als Einbettungsmaterial in PV-Modulen verwendet wird, ist die peroxidische Vernetzung im Herstellungsprozess und die Bildung von Essigsäure beim Abbau des Materials, was zu diversen Versagensmechanismen im Modul führen kann. Kapitel 3 beschäftigt sich daher mit der Bewitterungsstabilität von alternativen Einbettungsmaterialien aus Polyolefinen (Thermoplastisches Polyolefin (TPO) und Polyolefin-Elastomer (POE)) auf Modulebene. Das Hauptaugenmerk wurde dabei auf den Einfluss des Mikroklimas im Modul und die Permeationseigenschaften der Rückseitenfolien gelegt. Dafür wurden PV-Module mit unterschiedlichen Einbettungsmaterialien (EVA, TPO und POE) und einer herkömmlichen PET-Rückseitenfolie beziehungsweise alternativ einer undurchlässigen Glasrückseite hergestellt. Nach einer beschleunigten, künstlichen Bewitterung wurden die Änderungen der optischen, chemischen und thermischen Eigenschaften der Einbettungsmaterialien bestimmt. Mittels FTIR-Spektroskopie im ATR-Modus konnte ein starker Einfluss des Rückseitenmaterials und des Mikroklimas im Modul auf die Alterung der vorderen Einbettungsfolie nachgewiesen werden. Module mit Glasrückseite verhindern das Eindringen von Feuchtigkeit und Sauerstoff und verändern so die Alterungsmechanismen. TPO zeigte eine sehr gute Stabilität sowohl im Modul mit PET-Rückseite, als auch im Modul mit Glasrückseite. Die Ergebnisse dieser Untersuchungen bestätigen, dass das PV-Design (Rückseitenmaterial) eine wichtige Rolle bei der Beständigkeit der vorderen Einbettungsfolie spielt.

In Kapitel 4 wird der Unterschied der thermomechanischen Stabilität von herkömmlichen und alternativen Einbettungsfolien beschrieben. Um den Einfluss von Alterungsmechanismen auf das thermomechanische Verhalten von Einbettungsfolien zu untersuchen, wurden mittels Thermomechanischer Analyse (TMA) Messungen an laminierten Einbettungsfolien vor und nach 1000 Stunden Damp-Heat-Bewitterung durchgeführt. Die Ergebnisse zeigten einen starken Einfluss der Morphologie (z.B. Kristallinität) auf das thermomechanische Verhalten. Aufgrund der hohen Kristallinität zeigte TPO die geringsten thermomechanischen Veränderungen unter den untersuchten Materialien sowohl vor, als auch nach Bewitterung. Hingegen zeigte EVA, das Material mit

der geringsten Kristallinität die höchste thermische Ausdehnung, welche im Herstellungsprozess und während der Betriebszeit eines PV-Moduls zur Bildung von Eigenspannungen im Modul führen und verschiedene Versagensmechanismen begünstigen kann. Die Ergebnisse dieses Teils der Arbeit zeigen, dass die Kombination von TMA und DSC eine geeignete Methode zur systematischen Untersuchung der thermomechanischen Stabilität von Polyolefin-Einbettungsfolien darstellt.

Um die Langzeitstabilität unter verschiedenen Betriebsbedingungen so genau wie möglich vorherzusagen, ist die Entwicklung klimaspezifischer Tests notwendig. Gemäß der letztgültigen Norm IEC 61215, liefert die Damp-Heat-Bewitterung von Modulen bei 85°C und 85% relativer Luftfeuchtigkeit für 1000 Stunden die meisten Informationen über die Alterung von Einbettungsmaterialien. Allerdings ist dieser Test nicht für eine Vorhersage der Langzeitperformance geeignet. In Kapitel 5 werden daher Einflüsse klimaspezifischer beschleunigter Bewitterungstests auf die Alterung von EVA-Einbettungsfolien auf Modulebene untersucht. Das Hauptaugenmerk in diesem Teil der Arbeit liegt in der Anwendung nicht zerstörender Prüfungsmethoden. Mit der Raman-Konfokal-Spektroskopie konnte eine geeignete Methode für eine schnelle, zerstörungsfreie, qualitative und quantitative Beurteilung der Alterung von EVA in den PV-Modulen gefunden werden. Im Vergleich zu standardisierten Untersuchungen zeigten Messungen mittels Raman-Konfokal-Spektroskopie signifikante Unterschiede in der Degradation von EVA, das im Modul verschiedenen Bewitterungsbedienungen ausgesetzt war. Diese Erkenntnisse liefern einen wertvollen Beitrag zum Verständnis von Alterungsmechanismen von EVA in PV-Modulen in verschiedenen Klimas, was in Folge hilfreich bei der Weiterentwicklung und Optimierung beschleunigter Bewitterungsverfahren sein kann.

Table of contents

Introduction

Solar energy demand

The interest for renewable energy is constantly increasing due to a number of factors such as falling costs, increased investments, advances in technologies, different government initiatives, etc. In 2017, solar PV capacity installations showed a remarkable increase compared to other renewables with an increase of 31 % (see Figure 1.) [1–3].
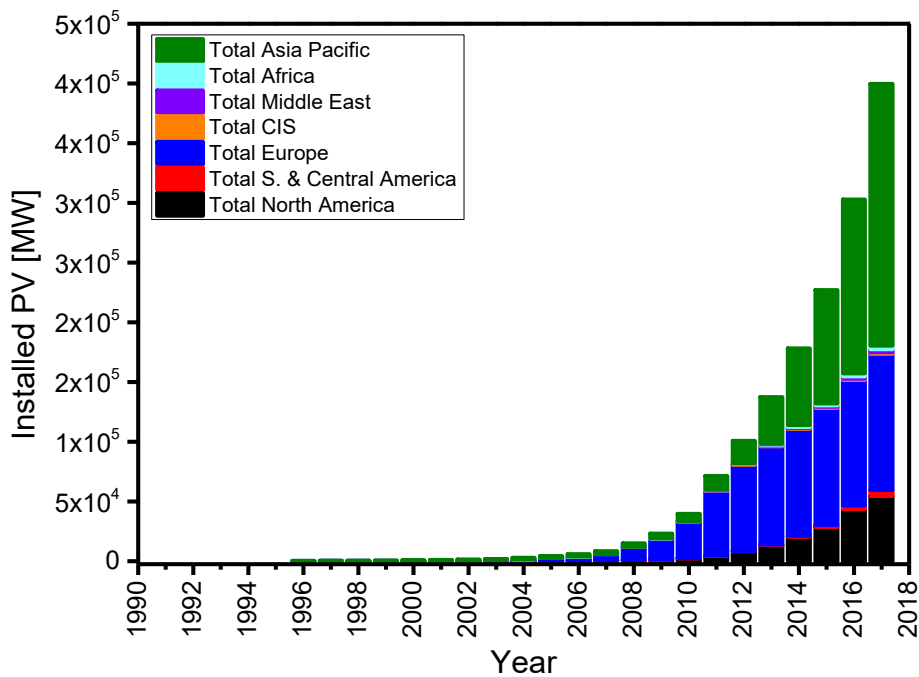
Figure 1. Overview of PV installations in the last decade (data from [3])

According to the [4], solar PV is already a low-cost renewable energy source and soon it will be the cheapest form of electricity production in many regions of the world including the remote ones.

Currently, there are many types of photovoltaic (PV) technology on the market ranging from Si-based (mono- and multi-crystalline) to thin-film based (*Cadmium Indium Gallium Selenide*-CIGS, *Cadmium-Telluride*-CdTe). However, as the cheaper and more available alternative over thin-film, the c-Si-based solar cell technology became the prevailing technology with 85–90% global market share [5]. Improvements in slicing technology and reduced kerf loss led to reduction of the c-Si cell thickness from previous 400 µm to 180 µm thick cell [5,6]. This reduces the usage of Si in g/Wp significantly, which affects

the final price and return of investments i.e. the energy payback time (EPBT) [6]. It is assumed that the thickness of the multi crystalline Si-cell will decrease even more approaching 150 µm until 2025. [7].

Challenges of increasing demand for solar PV energy

The rapid growth of the PV market and decrease of PV module prices entail an intense pressure on production costs and the costs of PV module components. This is inducing a considerable expansion of the encapsulation material market towards new materials and suppliers [7,8]. Another always-present challenge is the reliability of all the current and future PV modules, which is of major importance for users and producers. PV modules are degrading before meeting the manufacturer's warranty life time of ≥25 years due to different failures of PV components [9–12]. In fact, the failure of PV modules was found to be dependent on operating conditions (climate) [13]. Many of the failure modes are triggered/promoted by degradation of polymeric components (encapsulant and backsheet) such as discoloration, corrosion, backsheet cracking, etc... The reason is the different set of external stresses (temperature, humidity, irradiance, mechanical loads…) that drive the degradation of polymeric components to a different extent. However, PV modules have the same composition regardless on different operating conditions and external stress factors (see Figure 2.).
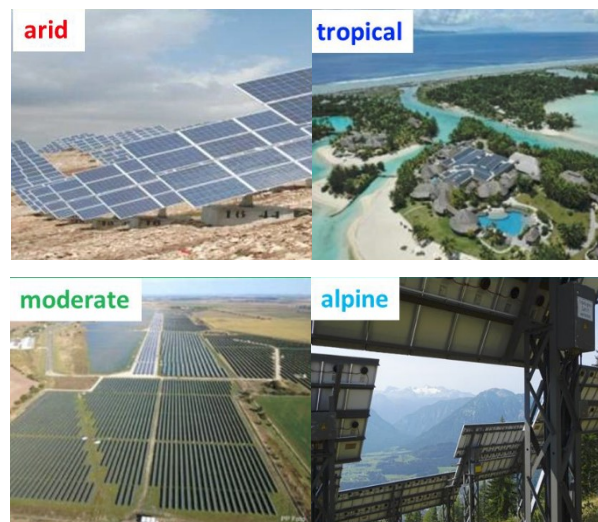
Figure 2. PV modules operating under different climatic conditions (© Infinity)

In order to overcome the common reliability issues related to the standard used encapsulant ethylene vinyl-acetate (EVA) (e.g. yellowing, delamination and corrosion of metallization) and to reduce the lamination time needed for the peroxide-induced crosslinking, new alternative encapsulation materials (polyolefin-based) are penetrating the market. In fact, it is expected that the EVA encapsulant will show decrease in its

market share in the following years due to penetration of the new encapsulating materials (see Figure 3.) [7]. Furthermore, due to reliability issues related to the common PET-based material, new backsheet materials based on polyolefins and polyamides are emerging at the market as well.
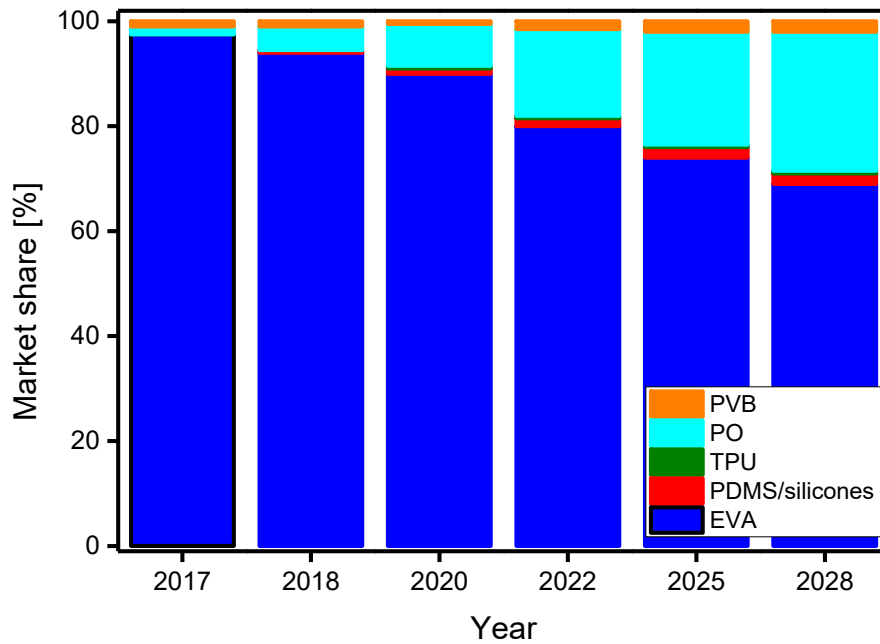
Figure 3. Expected world market share [%] for different encapsulation materials (adjusted from [7])

Aside of costs and reliability, PV industry is faced with up-coming sustainability issues as well. An increase in PV installations leads to an increased amount of PV waste, where 1GW of installed PV modules brings upon around 2.500 tons of backsheet waste only [14]. Not only the amount of waste itself represents a problem, but also that materials for certain components are toxic and/or not applicable for conventional recycling procedures such as pyrolysis. For example, the commonly used fluoropolymers in the PET-based backsheet could be replaced by other alternatives such as polyolefin- or polyamide-based backsheets because they are not applicable for conventional recycling methods such as pyrolysis due to evolution of toxic by-products [7,14,15]. Not only the composition of the standard backsheets, but also their design is changing from multilayer laminates towards co-extruded and monolayer backsheets, which eliminates application of different environmentally non-friendly adhesives and solvents. Toxic lead (Pb), which is usually used for soldering, could soon be replaced by more eco-friendly lead-free alternatives such as tin (Sn), silver (Ag), bismuth (Bi), copper (Cu) or electrically

conductive adhesives (ECA), which are also more compliant with the up-coming reduced wafer thickness. Therefore, it is evident that the issues related to the life cycle and sustainability of PV modules need to represent another important requirement when considering PV module design and materials.

Hence, in order to support sustainable PV growth, reduce costs and increase the reliability of PV modules, PV manufacturers need to come up with certain solutions, which is possible via [7,12]:

1. Changes in design (e.g. reduction of the materials' thickness)
2. Application of cheaper and/or environmental friendly materials for PV components and/or
3. Change in processes (e.g. reduction of lamination time, peroxide-free encapsulants…).

However, any of those changes could induce the adjustment of the standard PV module assembly i.e. design. For example, the changes in the reduction of the wafer thickness could lead to higher brittleness of the c-Si cell, which would require replacement of the standard interconnections. In those terms, the application of electrically conductive adhesives (ECA) seems as a great solution since they provide lower thermal stresses, which is of major importance for ever thinner cells [7]. Moreover, it is always questionable whether the changes in design, process and/or materials would affect PV module reliability or not. Therefore, thorough testing of new PV components and their interactions with other PV components is required [12]. Hence, challenged by *reduction of the PV components' costs*, always-present *reliability issues* related to commonly used polymeric materials and *rising sustainability challenges*, the *selection of materials and production technologies present a very important and critical step for PV manufacturers*.

Structure of the thesis

The thesis is divided into the following parts:

0. Introduction
1. State of the art
2. Weathering stability of alternative polyolefin-based backsheets
3. Weathering stability of polyolefin encapsulants in standard and double glass modules
4. Influence of damp heat aging on thermo-mechanical stability of polyolefin encapsulants at single film level
5. Non-destructive investigation of influence of climate-specific accelerated tests on degradation of EVA at module level
6. Summary

Firstly, a short overview on the main challenges that are rising with increasing demand for solar energy and thesis structure with the objectives will be presented.

Chapter 1 represents state of the art in PV industry in terms of (i) reliability issues of the PV modules concerning polymeric components, (ii) relation between the climatic conditions and degradation of polymeric components and (iii) possibility of replacement of the commonly used materials in PV modules - optimization of the PV module design. Parts of this chapter are published in the Journal of Solar Energy Materials & Solar Cells under the name "Relation between degradation of polymeric components in crystalline silicon PV module and climatic conditions: A literature review" and doi number: 10.1016/j.solmat.2018.12.027.

In **Chapter 2** the weathering stability of the newly developed alternative co-extruded polyolefin-based backsheet is investigated and compared to standard polyester-based backsheet. Co-extruded polyolefin-based backsheet provides numerous advantages such as selective permeation properties, hydrolysis resistance, high flexibility and fluoropolymer-free and adhesive-free composition. Such set of properties goes along with higher reliability requirements of the modules operating under harsh climatic conditions, cost-reduction and sustainability. The main aim of the chapter is to investigate whether the weathering stability of the alternative backsheet stand-alone films is sufficient in terms of PV reliability. Different set of characterization methods is proposed and conducted in order to understand the degradation processes occurring with aging time. Parts of this chapter were accepted for publication in the Journal of Applied Polymer Science under the title "Increased reliability of modified polyolefin backsheets over

commonly used polyester backsheets for crystalline PV modules" with doi number: 10.1002/app.20183117.

Chapter 3 deals with weathering stability of the standard (EVA) and alternative (TPO, POE) encapsulants on PV module level. In order to investigate the influence of permeation properties of the backsheet material on degradation of encapsulant, single-cell test modules were prepared with different types of backsheet materials: polymeric PET-laminate and impermeable glass backsheet. In order to understand the influence of microclimate within PV module on degradation of PV encapsulants, the encapsulants were manually delaminated above the cell and above the backsheet. Their optical, thermal and structural properties were investigated and findings were correlated with microclimate effects and permeation properties of the backsheet.

Thermo-mechanical properties of PV components are very important during the production and service of PV modules. Mismatches in coefficient of thermal expansion (CTE) and changes in the thermo-mechanical properties upon aging can induce additional internal stresses within the PV module. Consequently, failure modes such as delamination and/or cracking of solders and cells may rise. Therefore, **Chapter 4** deals with thermo-mechanical properties of stand-alone laminated polyolefin encapsulants before and after aging under damp heat conditions. Their thermomechanical properties are correlated with morphology before and after aging.

Chapter 5 deals with the optimization of accelerated aging tests and non-destructive analysis of PV module degradation. In order to predict reliability of PV modules during their outdoor exposure, it is necessary to conduct accelerated tests that replicate outdoor conditions as close as possible. Furthermore, it is of great importance to investigate the degradation of the encapsulants within a PV module, since the degradation of the encapsulants was shown to be influenced by microclimate. Therefore, the PV modules were aged under climate-specific aging tests (for tropical, moderate, alpine and arid climate). The applicability of Raman confocal spectroscopy as a non-destructive tool for qualitative and quantitative assessment of EVA degradation in PV modules was investigated. Results of Raman confocal spectroscopy were compared with another non-destructive method (UV-fluorescence imaging) in order to discuss their advantages in terms of outcomes, relevance and complexity.

In the end, summary and the final remarks are given.

References

[1]   REN21, Renewables 2018: Global Status Report: A comprehensive annual overview of the state of renewable energy, 2018.

[2]   IEA - International Energy Agency, World energy balances: Overview, 2018.

[3]   BP Global, BP Statistical Review of World Energy June 2018, 2018. https://www.bp.com/en/global/corporate/energy-economics/statistical-review-of-world-energy.html (accessed 17 September 2018).

[4]   Fraunhofer ISE, Current and Future Cost of Photovoltaics: Long-term Scenarios for Market Development, System Prices and LCOE of Utility-Scale PV Systems. Study on behalf of Agora Energiewende, 2015. www.agora-energiewende.de.

[5]   H.S. C.S. Solanki, Anti-reflection and Light Trapping in c-Si Solar cells. Chapter 2: c-Si Solar Cells: Physics and Technology, 1st ed., Springer Singapore, 2017.

[6]   S. Philipps and W. Warmuth, Photovoltaics Report, 2018.

[7]   International Technology Roadmap for Photovoltaic, Results 2017 inculding maturity report 2018: Ninth Edition, September 2018, 2017. http://www.itrpv.net.

[8]   C. Peike, I. Häldrich, K.-A. Weiß, I. Dürr, Overview of PV module encapsulation materials, Photovoltaics International (19) (2013) 85–92.

[9]   M. Vázquez, I. Rey-Stolle, Photovoltaic module reliability model based on field degradation studies, Prog. Photovolt: Res. Appl. 16 (5) (2008) 419–433. https://doi.org/10.1002/pip.825.

[10] E.Parnham, A.Whitehead, S.Pain, W.Brennan, Comparison of Accelerated UV Test Methods With Florida Exposure for Photovoltaic Backsheet Materials EU PVSEC 2017, in: 33rd European Photovoltaic Solar Energy Conference and Exhibition, Amsterdam, 2017.

[11] Report IEA-PVPS T1-25:2014, Trends 2014 in Photovoltaic Applications: Survey report of Selected IEA Countries between 1992 and 2013.

[12] J. Wohlgemuth and S. Kurtz, Reliability testing beyond qualification as a key component in photovoltaic's progress toward grid parity, in: IEEE Internationl Reliability Physics Symposium, Monterey, CA, USA, 2011.

[13] A. Omazic, G. Oreski, M. Halwachs, G.C. Eder, C. Hirschl, L. Neumaier, G. Pinter, M. Erceg, Relation between degradation of polymeric components in crystalline silicon PV module and climatic conditions: A literature review, Solar Energy Materials and Solar Cells 192 (2019) 123–133. https://doi.org/10.1016/j.solmat.2018.12.027.

[14] L. Maras, Environmental challenges disposing of backsheets at PV module EOL, in: EU PVSEC, Munich, Germany 2016.

[15] S.Huber, M.K. Moe, N. Schmidbauer, G. Hansen and D. Herzke, Emissions from incineration of fluoropolymer materials: A literature survey, 2009.

1 State-of-the-art

Parts of this chapter are published in the Journal of Solar Energy Materials & Solar Cells under the name "Relation between degradation of polymeric components in crystalline silicon PV module and climatic conditions: A literature review" and doi number: 10.1016/j.solmat.2018.12.027.

1.1 Reliability of c-Si photovoltaic modules

Even though photovoltaic (PV) modules are designed to operate outdoors ≥25 years [1–4], exposure to mechanical stresses, moisture, elevated temperature and ultraviolet radiation eventually degrades protective materials in PV modules, giving rise to occurrence of different failure modes. As a consequence, the solar cell performance is reduced before meeting the manufacturer's warranty of 25 years lifetime [1,5,6]. A PV failure mode is an effect that either degrades the module power, which is not reversed by normal operation, or creates a safety issue. On the other hand, a purely cosmetic issue, which does not affect the module´s performance or safety, is not considered as a PV module failure [6]. Nevertheless, purely cosmetic issues may trigger/enhance other failure modes or indicate presence of other visually not observable failures that do affect power output. For instance, a rather newly addressed failure mode "snail trails" are discolorations on the cell and there is no yet an indication that they cause a significant decrease of module efficiency. However, the presence of "snail trails" is an indication of cell cracks [7–9]. Furthermore, during transport and installation, which are the first critical stages in a PV module's life, glass breakage is one of the most occurring defects. Although this observation is not a failure mode that affects cell performance directly, it is still promoting or even causing other failure modes to occur like failed electrical insulation, corrosion, delamination, etc. [6].

Failure modes are typically divided into the following categories: infant failures, midlife failures and wear-out failures (see Figure 1.1.) [6]. Most failures occur in the beginning of the working life of PV module (infant failures). In fact, around of 5% of all failure cases occur due to transportation damages [6]. In Figure 1.1. it can be seen that in the midlife phase of PV working-life (before the warranty end) failure modes related to polymeric components start to occur.
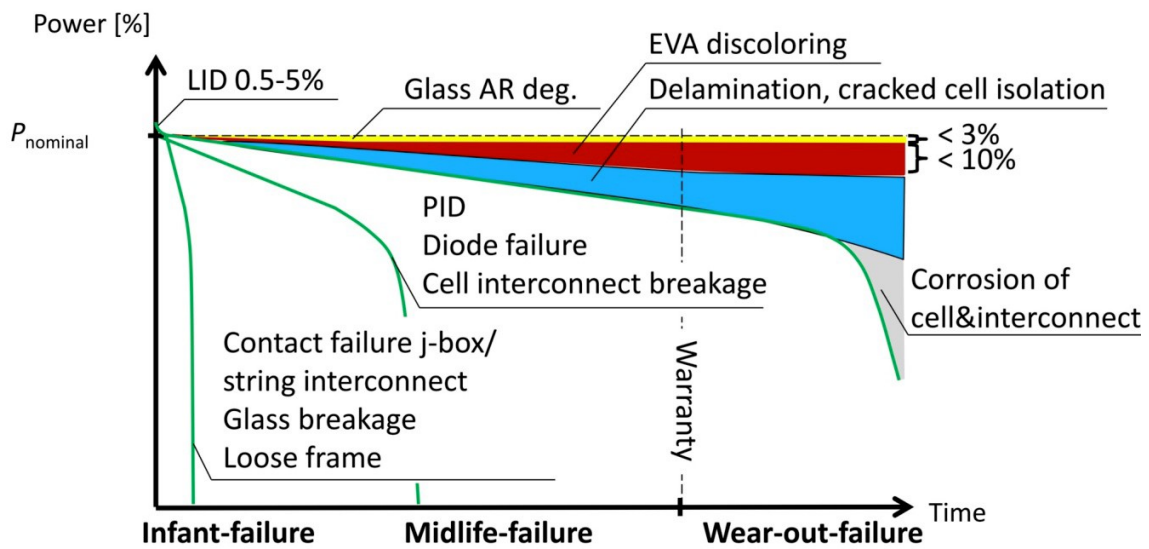
Figure 1.1. Three typical failure scenarios for wafer based crystalline photovoltaic modules (LID – Light Induced Degradation, PID – Potential Induced Degradation, EVA – Ethylene Vinyl Acetate, j-box – junction box) [6]

1.2   Role of polymeric materials in degradation of c-Si PV modules

In order to provide the best possible efficiency, sensitive PV components, i.e. brittle solar cells and metallization need to be protected from direct environmental factors such as mechanical stresses, humidity and UV irradiation. Due to their low weight, low price and ease of production, polymeric materials were chosen already from the beginning as the best option to serve that purpose [10]. They embed solar cells as an encapsulant, and protect the module from the backside as backsheet (see Figure 1.2.). However, up to now field experiences have shown that the performance losses of PV modules might be caused, or at least enhanced, by polymeric materials related failures, such as discoloration of EVA, delamination of encapsulant at the front glass and/or backsheet interface and backsheet delamination, cracking and chalking [6,11].
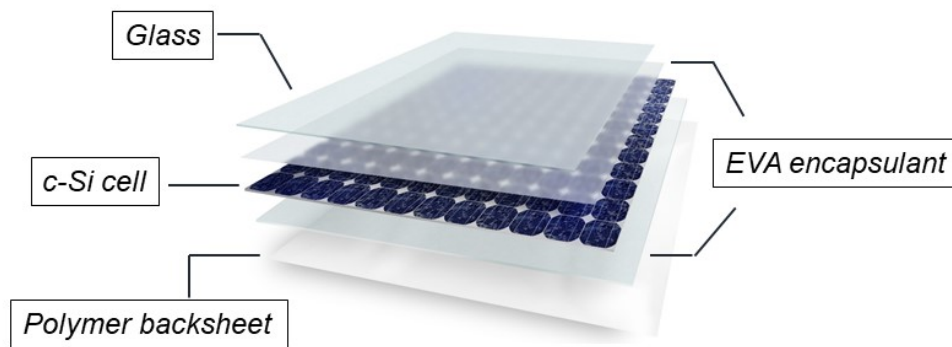
Figure 1.2. Schematic picture of standard c-Si PV module

As can be seen in Figure 1.2. PV modules are multilayer systems of different components bonded adhesively to each other resulting in numerous interfaces of different types of materials: glass-polymeric encapsulant, polymeric encapsulant-cell, metallic interconnections-polymeric encapsulant, polymeric encapsulant-polymeric backsheet. These interfaces are potential paths for contamination ingress and/or different interfacial reactions, which can lead to degradation and leakage currents [12]. Although certain polymers may meet the requirements concerning solar applications, their interaction with other materials in a PV-module can trigger degradation. As shown in Figure 1.3., interactions between components at their interfaces can drive certain failure modes. Migration of additives between encapsulant, cell and backsheet can drive the occurrence of discoloration, delamination and snail trails. Furthermore, acetic acid, which is by-product of EVA-degradation, drives Na^+ diffusion from the glass and gives rise to occurrence of potential induced degradation (PID). Water ingress from the edges of the PV modules and through the backsheet drives corrosion of metallization and degradation of EVA, which again results in acetic acid. If the permeability of the backsheets (in terms of acetic acid transmission rate, AATR) is too low, than the retained acetic acid at interfaces accelerates corrosion, delamination, discoloration and maybe other following degradation mechanisms [13]. Therefore, the combination of specific external factors (climatic conditions-solar irradiation, temperature and humidity cycles, wind or snow loads …) and existing internal factors (additives, morphology, internal residual stresses, CTE mismatches) can result in limitations for the usage of given materials or combinations thereof as they can cause failures of PV modules before meeting the expected 25 years lifetime [14]. However, during outdoor exposure, many factors are acting simultaneously and it is often hard or almost impossible to distinguish one specific primary driving factor of degradation.
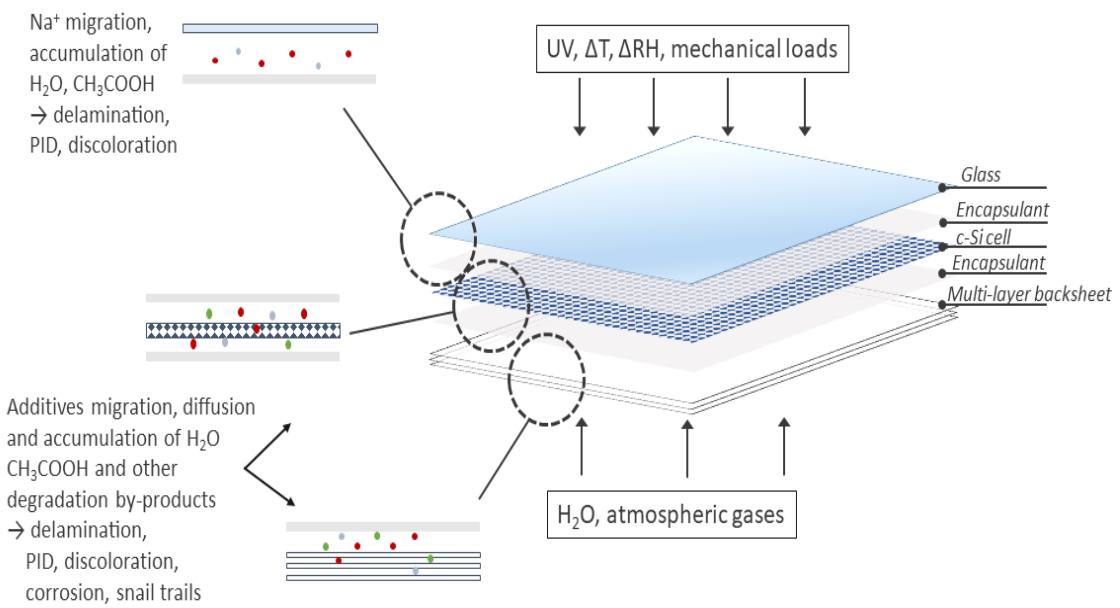
Figure 1.3. Schematic of interactions between PV components

Depending on the molecular structure and conditions of use, properties of polymeric PV components can change drastically during outdoor exposure [15,16]. Therefore, they have to be stabilized with a different set of additives, such as UV-absorbers, light and thermal stabilizers [15,17–19]. Even though the main purpose of additives is to prevent material degradation, very often they are either consumed over time, consumed in unwanted side reactions or even extracted (water soluble additives), which reduces their performance and allows degradation of the base polymer [17,18]. They might react with other compounds within the material, such as processing additives or cross-linker (peroxides in EVA) or impurities, leading to formation of different by-products [7,20,20– 22]. Furthermore, due to elevated temperature they can migrate into more vulnerable amorphous zones of semi-crystalline polymers (like EVA), which can accelerate degradation of the material in the depleted polymer zones [15,17,23,24].

1.2.1 Encapsulant

The main purposes of the encapsulating material are to provide structural support, optical coupling, electrical isolation, physical isolation/protection for the brittle silicon cell and circuit components from exposure to hazardous or degrading environmental factors [14,20,25–27]. The nature of the encapsulant also has an influence on the heat dissipation amongst different layers of the module, which can be of high importance for PV modules operating under high temperatures [28,29]. Only few polymers such as ethylene-vinyl acetate copolymer (EVA), poly(vinyl butyral) (PVB),

poly(dimethylsiloxane) (PDMS-silicones), ionomers, thermoplastic polyolefins (TPO) and thermoplastic silicone elastomers (TPSE) were found to be suitable for application in PV modules (see Table 1.1.) [25,27].

Table 1.1. Typical physical properties of encapsulating materials (adjusted from [26,27])

Polymer	Group	Parameter				
		T_g [°C]	E [MPa]	Refractive index [-]	Volume resistivity @ 23°C [Ωcm]	Moisture ingress [g d^{-1}]
EVA	Elastomer	-40 to -34	≤68	1.48-1.49	10^{14}	115
Silicone		-50	≤10	1.38-1.58	10^{14}-10^{15}	310
PVB	Thermoplastic	+12 to +20	≤11	1.48	10^{10}-10^{12}	310
Ionomer		+40 to +50	≤300	1.49	10^{16}	55
TPSE	Thermoplastic elastomer	-100	≤280	1.42	10^{16}	-
TPO		-60 to -40	≤32	1.48	10^{14}-10^{18}	-

Ethylene vinyl-acetate (EVA) encapsulant

Due to their exceptional UV- and thermal stability, the earliest modules built in 1960s and 1970s used silicone encapsulants. In order to reduce the price, silicone was gradually replaced first by PVB and then by EVA [26,30]. The most commonly used encapsulant today is still EVA, not because of its best combination of properties, but because it is an economical option with an established history of acceptable durability [31]. However, being and organic polymer, EVA is susceptible to degradation when it is exposed outdoor. In fact, in the first decades (up to 2000.), the prevailing degradation mode of field-aged PV modules was discoloration (yellowing or browning) of EVA [14,26,32]. Discoloration is not only an aesthetic problem; even slight discoloration can lead to an increase in surface temperature by radiation absorption, which results in lower efficiencies [17]. Since the degradation processes are temperature dependent, an increase in surface temperature due to the discoloration can have a significant impact on the rate of degradation. Even though power output may seem not be affected by the discoloration in the moment of the power analysis, it should be kept in mind that discoloration is usually accompanied by changes in the mechanical properties as well [38] which can induce further degradation modes (e.g. delamination).

Degradation mechanism of EVA is proposed to be via Norrish I and II reactions, which result in a deacetylation of the EVA chains forming ketones, aldehyde, acetic acid and radicals, as depicted in Figure 1.4. [14,25,33,34].
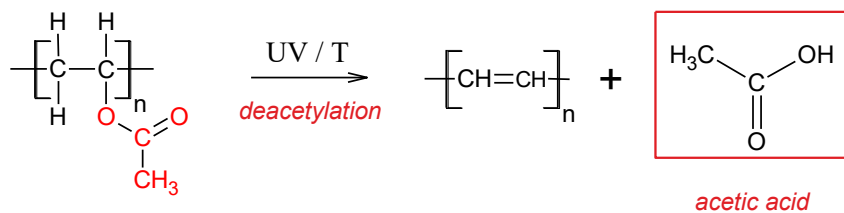
Figure 1.4. Deacetylation of EVA via Norrish II reaction

Radicals further lead to chain scission as well as crosslinking [33]. The α,β-unsaturated carbonyl groups, that are initially present in the polymer, give rise to deacetylation [25,35]. In general, the species with conjugated double bonds are acting as chromophores and under UV-light irradiation at wavelengths above 300 nm, the degradation of non-chromophore polymers is likely to be initiated by chromophore impurities [36]. However, in newer studies it was shown that the interactions between some stabilizing additives and the curing agent might generate chromophores as well [20,21,25,33]. For instance, Klemchuk et al. [21] found that conjugated double bonds are not the reason for the discoloration of EVA. Instead, authors [21] have shown that peroxide-additive interactions, mainly peroxide-UV absorber and peroxide-phosphite interactions, are leading to the discoloration of EVA. Jentsch et al. [20] investigated the influence of typical stabilizers (benzophenone-type UV absorbers, HALS and arylphosphite) on yellowing and delamination of EVA encapsulants. They found that decomposition of UV absorber and phosphite upon photo-degradation leads to the formation of benzoic acid and a phenol product [20]. Benzoic acid catalyses adhesion loss at the EVA/glass interface while the phenol leads to discoloration. [20,37] If the oxygen is diffusing through the edges of the module and/or permeable backsheet, oxidation of chromophore species can occur, known as photo-bleaching effect (see Figure 1.5.) [14,33]. It is usually leaving the circular area of yellow-to-brown encapsulant above the cell. If cell cracks are present, the oxygen can diffuse through them as well, leaving behind an uneven discoloration [38]. The existence of snail trails is correlated to the discoloration of the encapsulant as well, i.e. additives in formulation. Therefore, the type of the encapsulant, backsheet and cell metallization play a significant role in occurrence of this phenomenon [8,9,82,83].
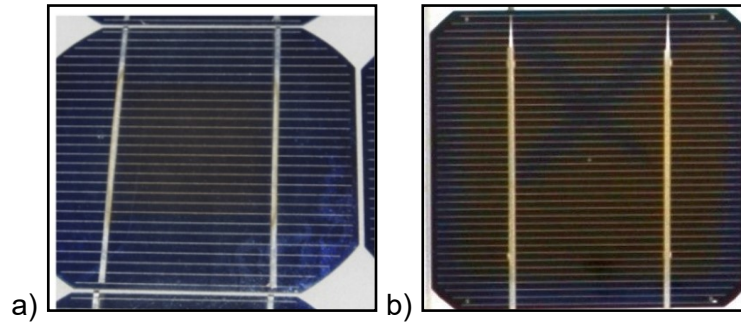
Figure 1.5. a) Photobleaching effect due to the oxygen permeation through the edges; b) photobleaching effect due to the oxygen permeation through cracks [6]

It is observed that discoloration is usually followed by certain degree of delamination (see Figure 1.6.), which can occur at glass/encapsulant, encapsulant/cell, encapsulant/backsheet, encapsulant/ribbon interface or even within the backsheet layers [39]. It promotes cell corrosion and affects the transmission of the light onto the cell, which reduces power output [12,30,40–43]. Aside from benzoic acid [20], delamination can also be initiated due to changes in thermal and thermo-mechanical properties of EVA upon field exposure [43,44]. Wang et al. [44] assume that UV exposure is favouring crystallization in EVA resulting in a higher Young's modulus of the encapsulants (increased stiffness), which can initiate delamination. Delamination of the encapsulant at the interface with glass and/or cell is among common degradation modes observed in the field [4,6,39,41,45–48].

In order to promote better adhesion at glass/EVA interface, EVA is formulated with adhesion promoters, normally in the form of coupling agents that enhance adhesion via silicon-oxygen (Si-O-Si) covalent bonds [12,49]. Even small amounts of moisture that can penetrate from the edges of the PV module can cause decomposition of the adhesive bonds. Promoted by its high water uptake potential of 115 g d^{-1} [26] EVA can hydrolyse, which results in formation of acetic acid. Acetic acid in turn is able to catalyse the decomposition of Si-O-Si bonds at the glass/encapsulant interface [11,12]. Acetic acid is not only representing a problem for adhesion with the glass but it is also accelerating corrosion of cells and interconnectors [50–52]. According to Dhere et al. [43,53] delamination of the front encapsulant can be promoted by contaminations (mainly Na, P and Sn) at the surface of the cell as well. However, Sánchez-Friera et al. [41] noticed in their study that delamination at the encapsulant/cell interface is always located between metallization fingers in the proximity of the cell busbars and at the cell perimeter where no additional P or Na concentrations are expected. Therefore, authors [41] believe that this delamination is likely to be related to geometrical factors, as the highest device thickness discontinuities are found at these areas.
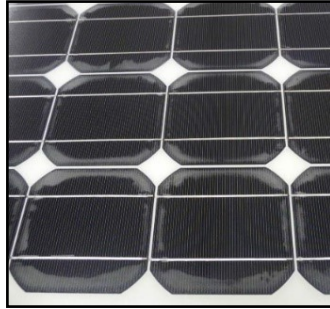
Figure 1.6. Delamination of the front encapsulant [6]

Another failure mode that seems to be influenced by the encapsulant properties is potential induced degradation (PID). When it comes to this failure mode, the volume resistivity of the material is of high importance since it influences the ionic current flow through the encapsulant. Therefore, a higher volume resistivity will reduce ion mass transfer. EVA has a high volume resistivity, but it is decreasing as temperature increases [36]. Another factor promoting PID is acetic acid since it accelerates diffusion of Na^+ from the glass. Therefore, materials like PVB, TPO, silicones or ionomers are good alternative to EVA (see Table 1.). However, regarding the water vapour transmission rate (WVTR) values and production conditions, polyolefins and ionomers represent the best candidates for PID reduction. PID occurrence is highly influenced by environmental conditions and it seems that higher temperatures and humidity values are accelerating degradation [36,54].

1.2.2 Backsheet

PV backsheets typically have a multilayer (mostly three layers) structure, where each layer fulfils a specific function (see Figure 1.7.). The layer in contact with the encapsulant needs to provide durable adhesion and chemical compatibility with the encapsulant and to be stable to the direct solar exposure filtered through the glass and encapsulant layers. Usually materials like polyamide (PA), polyethylene (PE) or EVA are used. The central or core layer is typically thicker and provides the required mechanical stability and electrical insulation of the whole composite. This layer is usually made of poly(ethylene terephthalate) (PET), while few backsheet types have polyamide or polyolefin as core layers. The outer layer needs to be highly reliable and stable since it provides environmental protection for the other layers and is directly exposed to the environment including indirect short UV. Therefore, it is usually made of PET, poly(vinylidene fluorid) (PVDF) or poly(vinyl fluorid) (PVF) [2,55]. These layers are usually laminated together with addition of adhesives. Only few material combinations can be co-extruded to multi-layer backsheets.
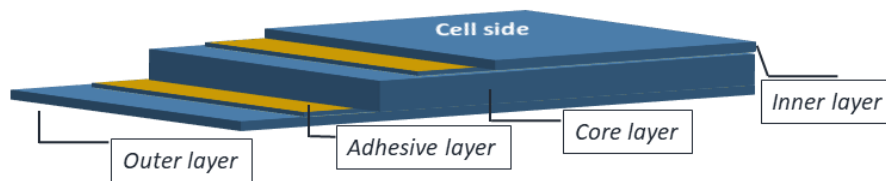
Figure 1.7. Schematic figure of the multi-layer laminated PV backsheet

Since each of the backsheet layers is exposed to a different set of stresses in outdoor exposure, their individual performance affects the performance of the whole backsheet and at the end, of the entire PV module [55]. The main degradation modes of backsheets include delamination, formation of cracks, chalking, burns, formation of bubbles and discoloration (see Figure 1.8.).
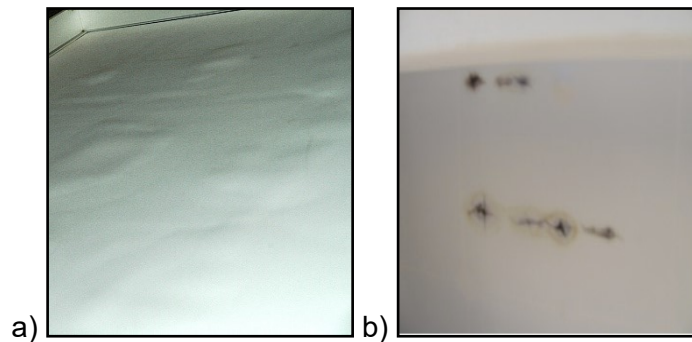
Figure 1.8. a) Delamination and bubbles, b) Burn-marks [6]

In order to prevent delamination between encapsulant and backsheet, some backsheets contain EVA layers as inner layer of the backsheet (e.g. PET/PET/EVA or PPE). This EVA layer (or commonly named "E-layer") is prone to degradation, i.e. discoloration [56]. As shown by Kempe et al. [57], the EVA layer can also experience shrinkage, causing changes in dimensional stability and cracking.

Delamination can also occur between the individual backsheet layers mostly due to degradation and adhesion loss of the adhesives (for example aromatic polyester-based polyurethane [56,58]) that are bonding backsheet layers. Namely, due to high affinity of adhesives towards water, hydrolytic degradation (and thermal degradation at elevated temperature) of adhesive layer can occur, which causes its depletion [41,56,59]. Depletion of the adhesive layer is not only leading to delamination, but it also affects the dimensional stability of the backsheet due to higher internal residual stresses. Therefore, cracking of the outer layer can occur [56] leading to reduction of the insulating ability of the backsheet, which exposes modules to a higher risk for failure. According to [10,60,61], cracking is mainly observed for the non-fluoropolymer backsheets with PET-

or PA- outer layers. Namely, unmodified polyesters and polyamides belong to the group of polycondensates that are in general sensitive to water, which can cause chain scission processes due to hydrolysis that is main dominating aging factor for these materials [62–66]. Chain scission results in chemo-crystallization due to presence of a high number of nucleation end-points formed by chain scission of the PET molecules by hydrolytic degradation. It can induce volume shrinkage, which promotes loss of mechanical properties, i.e. cracking [16,17,62,63,65]. Hydrolysis of polyesters is shown to be autocatalytic and dependent upon the concentration of initial carboxyl end-groups [65]. The lower the value of carboxyl end groups in the original material is, the higher the hydrolysis resistance [66,67]. However, the hydrolysis resistance of PET films for PV application can be increased via incorporation of anti-hydrolysis additives, which chemically react with free moisture during processing and service (act as acid and water scavengers), which converts them into nonreactive urea structures [62,66]. Such additives are usually based on carbodiimides [62,66,68]. In that way, initial viscosity is maintained, which affects mechanical properties [66]. This is very important step since as little as 0.01 wt.% of active water can lead to noticeable loss of viscosity and molecular weight [17]. Sorption and diffusion of the water play important role in the progress of hydrolysis [17]. A factor that is directly influencing sorption and diffusion of the penetrant in general is the morphological structure of the polymer, in particular free fractional volume (FFV) that is available to assist in penetrant transport through the polymer [17,69]. At elevated temperature, in particular above the glass transition, segmental mobility increases and affects diffusion of the penetrant [69]. Since the hydrolysis occurs in amorphous regions [17,65] it is important to reduce amorphous content as well, i.e. to increase crystalline content in the polymer. This can be achieved via biaxial stretching during production, which increases crystallinity and therefore directly reduces water absorption and hydrolysis [65,66,70]. Recently Shi et al. [70] showed that the hydrolytic stability of PET films for PV purposes can be enhanced by introducing three processes: polycondensation process that leads to considerably high molecular weights, a sophisticated extrusion technique that suppresses damages of resins caused by frictional heat and improved mechanical stretching process using temperature control programs.

Due to their high UV- and thermal-stability, fluoropolymers are usually used as protective outer layer for the hydrolysis-sensitive PET layers. It was shown [62,71] that PVF in particular remains relatively stable over the longer time range. However, it was observed by Hu et al. [72] that PVDF backsheets are showing a high percentage of cracking and delamination, especially in arid climates and explained this effect by reduction in

thickness and dimensional stability. Oreski et al. [71] found that PVDF is susceptible to post- and re-crystallization processes which leads to embrittlement of the material and cracking.

Discoloration is not that often observed for backsheets as for encapsulants, but it can also appear on either the inner or the outer layer of the backsheet (depending on the ground surface type and its albedo) [60,61]. PVDF/PET/PVDF backsheets usually show yellowing from the inner side (already within 5 years of operation), while solely PET-based backsheets are yellowing from the outer side [72]. PET strongly absorbs radiation in the wavelength range from 300-350 nm, which can lead to chemical changes causing yellowing and loss in mechanical performance. As observed by Felder et al. [60], it seems that there is a correlation between yellowing and loss in elongation at break, which can lead to cracking of PET-based backsheets.

Chalking of the backsheet is also one of the frequently observed failure modes. It is a result of strong surface degradation of the polymer binder of the outer layer, which leads to an uncovering of the pigments and fillers at the surface resulting in their easy abrasion. According to [73], it is observed mostly for PA-outer layers of backsheets. In order to reduce this abrasion at the outer surfaces and the resulting loss in mechanical stability upon outdoor exposure, the backsheet materials are usually stabilized, with either UV absorbers or titanium dioxide (TiO_2) or combination of both. Such stabilization is known for PET and PVF [2]. Namely, TiO_2 is protecting the polymer binder from direct photochemical degradation [23]. However, since the TiO_2 is photo-catalytically active at wavelengths below 380 nm, exposure to such energy can lead to over acceleration of photo-catalytic degradation of the polymer binder [2,23]. Since the rate of photo-catalysis is dependent on the temperature and UV irradiation, one can assume that the degradation of the mechanical properties is more likely to occur in warmer climates.

1.3 Climate as an influencing factor in degradation of polymeric components in c-Si PV modules

The degradation of field-aged PV modules has been investigated for a long time starting already in the mid-1980s [37,40,46,47,74–85]. Back then, the most reported degradation mechanisms were severe discoloration, delamination and corrosion [85]. However, the results obtained in these early field inspections are not representative for today's PV modules since the type of lamination materials being responsible for the observed delamination and discolouration were replaced with new formulations. It is also important to note that some of the mechanisms observed recently (like cell cracks or hot spots), could not be detected in former times due to lack of required technology. Nevertheless, the knowledge of the most important long-term degradation mechanisms for sure helped in quantifying long-term behaviour and lifetime of PV modules, tailoring the properties of materials for PV components and qualification tests of today's PV modules [6,76].

The operating conditions (climate) were already recognized as an important driving factors of PV degradation and their influence on failure rates of PV modules was reported in many publications [46,74,75][14,30,46,76,86–88].

According to a comprehensive study [60] from 2016 conducted on 1,919,000 modules installed in different climates, cell and metallization degradation showed less or small dependency on climate conditions, while degradation of polymer components showed a stronger trend. In that study, the dependency of polymeric material degradation on climate conditions was found to be in order: hot arid> tropical> moderate (see Figure 1.9.).
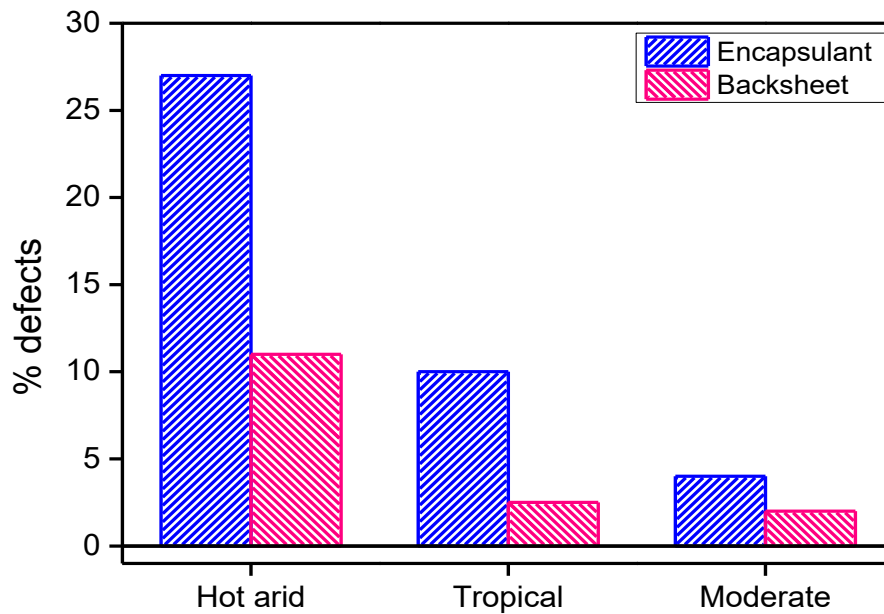
Figure 1.9. Degradation of polymeric components in dependence on climate (data taken from [60])

However, for certain climate types it is hard to draw conclusion since not so many data on degradation of PV modules is available. In fact, the distribution of the data presented in the Figure 1.10. clearly shows that most of the data are coming from moderate climate zones. Another problem in understanding the degradation of the PV modules is the fact that the information of PV module's composition is usually either very poor or even missing.
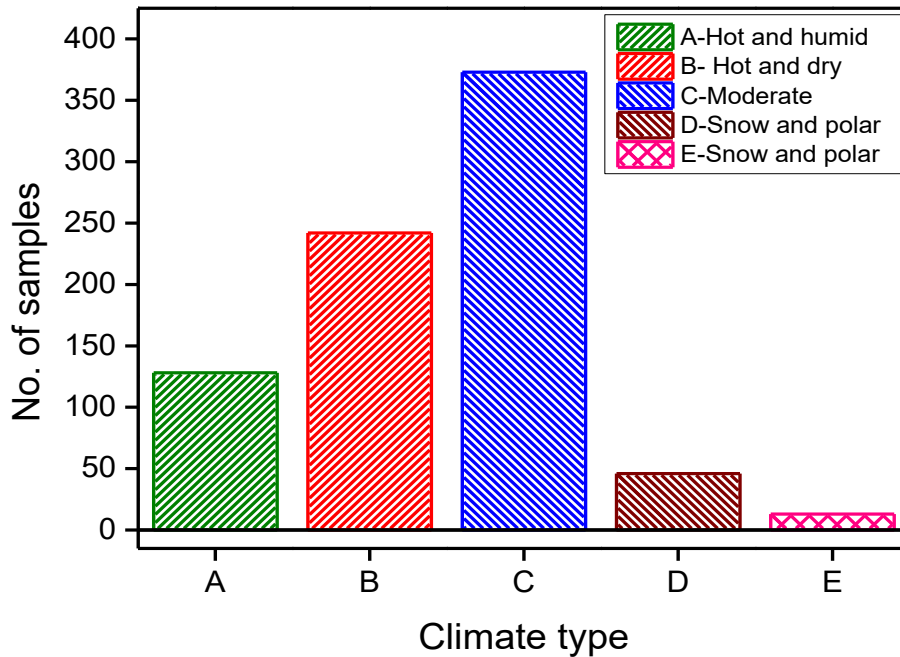
Figure 1.10. Distribution of the collected data on degradation of PV modules according to Köppen-Geiger classification system (data from [74,89])

Since the temperature and humidity are shown to be the most influencing degradation factors, in this subchapter the analysis of degradation will start by analysis of the most harsh conditions of hot and dry climate (high temperature; low humidity) and will follow in the order hot and dry > hot and humid > moderate> snow and polar. Reason for such approach is to depict the difference in degradation behaviour with introduction of humidity or change in the intensity of temperature and /or humidity.

<u>Arid climate</u>

The hot and dry climatic zones (B), in literature known as arid or desert, present the most difficult environment for PV modules. In desert climate, PV modules are submitted to harsh climatic stress factors like high solar and UV irradiation, temperature cycles and sand. Therefore, the most common failure modes observed in desert environment are discoloration of the EVA encapsulant, accompanied with delamination above the cell and certain degree of corrosion [14,29,32,38,87,90–93]. This observation is in accordance with an assumption of Jentsch et al. [20] that discoloration of EVA results in formation of benzoic acid and phenol products, which enhance delamination and discoloration. Few authors even managed to establish the correlation between degree of discoloration and reduction in power output [30,32,87,94]. UV exposure and/or high temperature is causing changes in thermal and thermo-mechanical properties of EVA as well, and affect thermo-

mechanical fatigue of interconnections. Therefore, another observed failure mode is deterioration of the solder bonds, which leads to increased series resistance (Rs) [87]. Regarding backsheet degradation, the most commonly observed failure mode is chalking, discoloration and/or cracking (depending on the backsheet type) [30,38]. On the other hand, Quintana [95] investigated modules with PVB encapsulant and Mylar® backsheet in the hot and dry climate of southeaster Utah (hot and dry, but cold winter). The modules actually showed very good performance and the authors believe that it is due to the contribution of PVB encapsulant, expanded metal interconnects, silicon oxide anti-reflective coating, and excellent solder/substrate solderability. Hu et al. [72] examined the backsheets in different climates of China and found that in arid climate (either hot or cold) the main degradation mechanism of PVDF-based backsheets are yellowing from the inner side and cracking and delamination of the outer layer due to the serious thickness reduction. On the other hand, PET-based backsheets were found to mainly discolour from the outer side and suffer from hot-spots, bubbles and cracking due to the increased brittleness. The PA-based backsheets resulted in micro-cracking already within one year of exposure.

Tropical climate

Hot and humid conditions in the tropical climates (A) drive the degradation of PV modules much more rapidly and severely in comparison to other environmental conditions [46,96,97]. The delamination is more frequent and severe [41,43,97]. Novoa et al. [98] showed that de-bond energy of EVA/glass decreases from 2.15 kJ/m^2 to 1.75 kJ/m^2 when temperature rises up from 25°C to 50°C. Moreover, the de-bond growth rate of EVA is enhanced by 1000 times with merely 10°C increase of temperature or 15% moisture ingress. In addition, corrosion is driven by humidity ingress through the backsheet and/or edges of module and is further accelerated through high temperature. Since most of the polymer backsheets are laminates of different polymeric materials with different properties (PA, PP, EVA, PET, fluoropolymers), moisture or atmospheric gases can be trapped in the backsheet due to the different permeation properties, which leads to the formation of bubbles. Bubbles can also be a result of hydrogen gas evolution in corrosion process of interconnections [99,99]. The degradation product of EVA degradation, i.e. acetic acid speeds up corrosion of inner components of the module as well, which raises question of its operation under humid climates [26,100–102]. It seems then reasonable that corrosion of metallization together with degradation of backsheet have been found to occur more in modules placed in the hot and humid zones [30,38]. Dechthummarong et al. [103] investigated the physical deterioration of EVA encapsulant in 15 years old field-aged PV modules in hot and humid Thailand. The key defects they

found were discoloration, delamination and corrosion of the bus-bars on the cell. The corrosion they noticed was higher (87% of the modules) in comparison to hot and dry environment where corrosion mainly occurred around the junction box or around the fingers. The humidity ingress further influenced detachment of the backsheet and brittle fracture of edge sealant, which in turn led to the formation of bubbles near the busbars, at the centre of the cell and at the edges of the cell [103]. Higher corrosion, accompanied by delamination and bubbles in the backsheet, was also observed by Chattopadhyay et al. [30] in hot and humid climate of India. Hu et al. [72] reported about formation of the bubbles in PVDF-based outer layer of backsheets at shoreline of subtropical climate in China. These degradation modes are not observed in the same extent in cold climates [30,104]. According to the [75], the another degradation mode that appears 15 times more often in hot-dry and hot-humid climates than in other climates is PID, which is mainly affected by the volume resistivity of the encapsulant.

Moderate climate

In warm and temperate climate (C) beside EVA discoloration, one of the observed problems are also encapsulant delamination and corrosion due to the moisture ingress [42,105–107]. Based on results reported in [36], another prominent failure type for the moderate climate is the snail tracks phenomenon. Atmaram et al. [107] measured long-term performance and reliability of ~12 years old PV modules in the warm, humid and ocean-salts environments of coastal Florida (Cfa). Investigated modules contained EVA and PVB encapsulants. The modules with EVA showed cell delamination in about half of the investigated modules. Modules with PVB did not show significant delamination, which is very surprising since the water uptake of PVB (310 g d^{-1}) is much higher than the one of EVA (115 g d^{-1}) [26]. Furthermore, the adhesion of PVB to glass is lower (≤ 50 N/10 mm) than the adhesion of EVA to glass (≤60 N/10 mm) [108]. The backsheet type is reported only for the modules with PVB and it is Tedlar®. Since PVB is sensitive to hydrolysis, it can be assumed that the reason for reduced delamination in PVB modules is Tedlar® backsheet, which is known for its low permeability (did not allow for moisture ingress). Similar behaviour was confirmed also by [109].

Continental and polar climate

In continental (D) and polar climates (E) lower temperatures are expected to retard any thermal degradation modes. Therefore, the most observed degradation modes in these climates are related to the mechanical stresses (high snowfall and/or wind stresses) and those are cell cracks, frame breakage or bending and glass breakage. Frame distortions change assembly of the modules (strain for which ordinary module frames are not

designed) [6,74,75,88]. Another issue in snow or polar climates is the compliancy of EVA since the glass transition temperature (Tg) of EVA (-15°C) is lying in the operating range. Lower modulus of elasticity affects stress transfer to the bonds [26]. Therefore, brittleness of EVA at lower temperatures can lead to interconnect breakage [46,88]. Low temperatures can also cause embrittlement of the edge-sealant adhesives and reduce further stability. It was shown that modules with silicone-based adhesives could resist loads of up to nearly 500 kg without any frame bending or permanent damage while the tape-based adhesives can sustain only 230-360 kg [6]. Bradley at al. [104] investigated the degradation of the PV modules in snow climate of Quebec, Canada. The investigated modules consisted of EVA encapsulant and PVF/PET/Tie layer backsheet. Even-though cell cracks are the most observed degradation mode for this climate, authors did not observe any of the cell cracks after 20 years of the exposure. However, they noticed that 21% of the modules resulted in delaminated backsheet and 10% suffered from the cell corrosion and encapsulant delamination (without discoloration). The reason for delamination is probably the increased stiffness at lower temperature of both, EVA and tie layer (usually polyethylene copolymers) in the backsheet. Chattopadhyay et al. [38] investigated PV modules of two different manufacturers exposed in snow climate of India (Ladakh) and noticed that the encapsulant of one type of modules showed severe discoloration, while the another had no signs of discoloration. The UV radiation content in Ladakh (at an altitude of 4500 m) is very high and probably the formulation of discoloured encapsulant was not adjusted to sustain these conditions.

1.4   Concept of optimized materials combination

In recent studies [8,13,21,82,93,109–114], reaction mechanisms at module interfaces have been addressed as an important influencing factor of PV degradation as well, which led to an assumption that some failure modes could be reduced or even avoided with the right combination of materials (depending on operational conditions). While certain polymers have desirable properties concerning solar application requirements, their interfaces with the other materials in modules must be carefully examined [36]. Hülsmann et al. [109] investigated the concept of the "breathable backsheets" and showed how the permeation properties of the backsheet can influence the degradation of the encapsulant. It was shown that reactions requiring oxygen proceed much more effectively in a module with a polyamide (PA) backsheet due to higher values of oxygen transmission rate (OTR). Hence, the encapsulants prone to discoloration due to UV irradiation should be combined with a PA backsheet. On the other hand, encapsulants sensitive to hydrolysis, like PVB, should be combined with a backsheet of a low WVTR. In another study [13], the interface encapsulant/backsheet was studied and it was shown how the permeation properties of backsheet (in terms of acetic acid transmission rate - AATR) can affect the degradation of encapsulant due to the retention of the acetic acid at the interface. Since the acetic acid has an autocatalytic effect, its retention promotes degradation of EVA, i.e. even higher production of acetic acid. Therefore, when combined with the backsheet of a higher AATR such as PA-based backsheet, the degradation of EVA is lower than when combined with the backsheet of a lower AATR (e.g. PET) [13,115]. Suleske [93] found that the composition, i.e. permeation properties of the polymer backsheets, could play role in delamination of field-aged PV modules. Namely, it was observed that the particular backsheets could maintain the lower temperature of the module and provide permeation of oxygen necessary for the photo-bleaching effect, which finally resulted in the reduced occurrence of the encapsulant delamination. Cabrera et al. [116] found that, regarding preliminary results on a module prototype in Atacama desert, thinner glass-glass modules with thermoplastic encapsulant are a better solution than standard modules (EVA/polymeric backsheet). Skoczek et al. [82] reported about different degradation rates of PV modules with glass and polymeric backsheet (Tedlar®) in moderate subtropical climate of Italy. According to authors, glass-glass modules degraded more than glass-polymer backsheet modules due to the temperature differences between cells, which could cause additional thermomechanical fatigue to interconnections i.e. changes in solder-joint geometry ("coarsening" as a result of segregation of the metals, SnPb, in the soldering alloy)

[40,82]. Furthermore, in-permeability of glass backsheets influences accumulation of degradation products of EVA, which could affect cell interconnections containing aluminium (Al). Klemchuk et al. [21] suggested using backsheets with higher OTR values in order to reduce EVA discoloration via photo-bleaching reactions. Govaerts et al. [110] investigated the possibility of corrosion reduction via application of POE encapsulant instead of standard EVA and densely plated metallization instead of screen-printed Ag. It was shown that, either by application of POE or plated metallization, corrosion could be reduced. Kapur et el. [117] found that ionomer combined with EVA could be good solution for PID reduction. Meyer et al. [8] found that not only the encapsulation or backsheet alone, but rather their combination has a crucial factor for snail-trail formation. The vast numbers of the field-studies presented above and the results of accelerated aging tests have shown that the certain degradation modes may not be influenced by solely climate but also by materials combination, which indicated that attention should be given to the proper choice of suited materials for particular climatic conditions [13,30,82,86,93,109,118]. However, the PV module composition is still quite the same no matter on the operation conditions (climate). In order to avoid certain failure modes and increase reliability of PV-module, PV components could be optimized based on their operating conditions. With new materials, it may be possible to realize the concept of optimized, climate-specific PV module design and to avoid premature PV failure modes. However, substitution of currently used materials with alternative ones is neither a fast nor an easy process; the properties of the materials have to be carefully adjusted to meet all the requirements for solar application, be easy and cheap to produce, and among all have to combine well with the other components in a PV module. This requires thorough research on the current failure modes of the standard PV modules and possible failure modes of the new PV module assembly. This information is necessary for improving accelerated aging tests, constituting materials and their combinations, characterization and evaluation methods.

1.5   Summary and conclusions

Due to harsh environmental conditions and different internal stresses, PV modules are degrading before meeting the manufacturers' warranty of 25 years lifetime. Based on the findings presented in this paper, it is obvious that the degradation of the PV modules is highly dependent on the climatic (operating) conditions and materials used.

Higher reliability could be accomplished by changes in materials properties of PV components, design and/or processes, which could require development of new or adjusting the current qualification and reliability tests. If the new alternative materials are to be employed, their behaviour under different climatic conditions should be well analysed and their usage should be reconsidered together with power degradation and economical aspects. However, prior to these actions it is necessary to understand degradation mechanisms of the PV components and interactions at their interfaces under different climatic conditions.

Lessons learned from the field-aged PV modules combined with the results of accelerated tests could be very helpful for improvements of accelerated aging tests, tailoring properties of new materials and provide information about the preferable material combinations for different climatic conditions.

1.6 References

[1] M. Vázquez, I. Rey-Stolle, Photovoltaic module reliability model based on field degradation studies, Prog. Photovolt: Res. Appl. 16 (5) (2008) 419–433. https://doi.org/10.1002/pip.825.

[2] E.Parnham, A.Whitehead, S.Pain, W.Brennan, Comparison of Accelerated UV Test Methods With Florida Exposure for Photovoltaic Backsheet Materials EU PVSEC 2017, in: 33rd European Photovoltaic Solar Energy Conference and Exhibition, Amsterdam, 2017.

[3] Report IEA-PVPS T1-25:2014, Trends 2014 in Photovoltaic Applications: Survey report of Selected IEA Countries between 1992 and 2013.

[4] J. Wohlgemuth and S. Kurtz, Reliability testing beyond qualification as a key component in photovoltaic's progress toward grid parity, in: IEEE Internationl Reliability Physics Symposium, Monterey, CA, USA, 2011.

[5] J. Tracy, N. Bosco, F. Novoa, R. Dauskardt, Encapsulation and backsheet adhesion metrology for photovoltaic modules, Prog. Photovolt: Res. Appl. 25 (1) (2017) 87–96. https://doi.org/10.1002/pip.2817.

[6] Report IEA-PVPS T13-01:2013, Performance and Reliability of Photovoltaic Systems: Subtask 3.2: Review on failures of PV modules. IEA PVPS Task 13, External final draft report IEA-PVPS, November/2013. http://iea-pvps.org/index.php?id=95&eID=dam_frontend_push&docID=2064.

[7] S. Meyer, S. Timmel, M. Gläser, U. Braun, V. Wachtendorf, C. Hagendorf, Polymer foil additives trigger the formation of snail trails in photovoltaic modules, Solar Energy Materials and Solar Cells 130 (0) (2014) 64–70. https://doi.org/10.1016/j.solmat.2014.06.028.

[8] S. Meyer, S. Timmel, U. Braun, C. Hagendorf, Polymer Foil Additives Trigger the Formation of Snail Trails in Photovoltaic Modules, Energy Procedia 55 (2014) 494–497. https://doi.org/10.1016/j.egypro.2014.08.014.

[9] P. Peng, A. Hu, W. Zheng, P. Su, D. He, K.D. Oakes, A. Fu, R. Han, S.L. Lee, J. Tang, Y.N. Zhou, Microscopy study of snail trail phenomenon on photovoltaic modules, RSC Adv. 2 (30) (2012) 11359. https://doi.org/10.1039/c2ra22280a.

[10] G. Griffini, S. Turri, Polymeric materials for long-term durability of photovoltaic systems, Journal of Applied Polymer Science 133 (11) (2016). https://doi.org/10.1002/app.43080.

[11] D. Wu, J. Zhu, D. Montiel-Chicharro, T.R. Betts, R. Gottschalg, Influence of different lamination conditions on the reliability of encapsulation of PV modules, in: 29th European Photovoltaic Solar Energy Conference and Exhibition, Amsterdam, Netherlands, 2014.

[12] D. Wu, J. Zhu, T.R. Betts, R. Gottschalg, Degradation of interfacial adhesion strength within photovoltaic mini-modules during damp-heat exposure, Prog. Photovolt: Res. Appl. 22 (7) (2014) 796–809. https://doi.org/10.1002/pip.2460.

[13] A.Mihaljevic, G.Oreski, G.Pinter, Influence of Backsheet Type on Formation of Acetic Acid in PV Modules, in: 32nd European Photovoltaic Specialists Conference and Exhibition, Munich, 2016.

[14] A.W. Czanderna, F. J. Pern, Encapsulation of PV modules using ethylene vinyl acetate copolymer as a pottant: A critical review, Solar Energy Materials and Solar Cells (43) (1996) 101–181.

[15] H. Zweifel, Macromolecular Systems - Materials Approach: Stabilization of Polymeric Materials, Springer, 1998.

[16] Z. Xia, J.H. Wohlgemuth and D.W. Cunningham, A Lifetime Prediction of PV Encapsulant and Backsheet via Time Temperature Superposition Principle, in: 34th IEEE Photovoltaic Specialists Conference (PVSC), Philadelphia, Pennsylvania, USA, 7-12 June, 2009.

[17] G.W. Ehrenstein, S. Pongratz, Resistance and stability of polymers, Hanser Publishers, Munich, 2013.

[18] J. Fink, Additives. Version 1.1 at 28th April 2009, Preliminary Version, 2009.

[19] F. Gugumus, The performance of light stabilizers in accelerated and natural weathering, Polymer Degradation and Stability (58) (1995).

[20] A. Jentsch, K.-J. Eichhorn, B. Voit, Influence of typical stabilizers on the aging behavior of EVA foils for photovoltaic applications during artificial UV-weathering, Polymer Testing 44 (2015) 242–247. https://doi.org/10.1016/j.polymertesting.2015.03.022.

[21] P. Klemchuk, E. Ezrin, G. Lavigne, W. Holley, J. Galica, S. Agro, Investigation of the degradation and stabilization of EVA-based encapsulant in field-aged solar energy modules, Polymer Degradation and Stability (55) (1997) 347–365.

[22] F.J. Pern, A.W. Czanderna, Characterization of ethylene vinyl acetate (EVA) encapsulant: Effects of thermal processing and weathering degradation on its discoloration, Solar Energy Materials and Solar Cells (25) (1992) 3–23.

[23] L.K. Massey, The effects of UV light and weather on plastics and elastomers, 2nd ed., William Andrew Pub, Norwich NY, 2007.

[24] G.W. Ehrenstein, G. Riedel, P. Trawiel, Thermal analysis of plastics: Theory and practice, Carl Hanser Verlag, Munich, 2004.

[25] S. Isarankura Na Ayutthaya, J. Wootthikanokkhan, Investigation of the photodegradation behaviors of an ethylene/vinyl acetate copolymer solar cell encapsulant and effects of antioxidants on the photostability of the material, J. Appl. Polym. Sci. 107 (6) (2008) 3853–3863. https://doi.org/10.1002/app.27428.

[26] O. Hasan, Arif, A. F. M., Performance and life prediction model for photovoltaic modules: Effect of encapsulant constitutive behavior, Solar Energy Materials and Solar Cells 122 (0) (2014) 75–87. https://doi.org/10.1016/j.solmat.2013.11.016.

[27] C. Peike, I. Häldrich, K.-A. Weiß, I. Dürr, Overview of PV module encapsulation materials, Photovoltaics International (19) (2013) 85–92.

[28] A.R. Gxasheka, E.E. van Dyk, E.L. Meyer, Evaluation of performance parameters of PV modules deployed outdoors, Renewable Energy 30 (4) (2005) 611–620. https://doi.org/10.1016/j.renene.2004.06.005.

[29] E. Kaplani, Detection of Degradation Effects in Field-Aged c-Si Solar Cells through IR Thermography and Digital Image Processing, International Journal of Photoenergy 2012 (1) (2012) 1–11. https://doi.org/10.1155/2012/396792.

[30] S. Chattopadhyay, R. Dubey, V. Kuthanazhi, J.J. John, C.S. Solanki, A. Kottantharayil, B.M. Arora, K.L. Narasimhan, J. Vasi, B. Bora, Y.K. Singh, O.S. Sastry, All India Survey of Photovoltaic Module Degradation 2014: Survey methodology and statistics, pp. 1–6.

[31] A. Reinders, P. Verlinden, W. van Sark and A. Freundlich, Photovoltaic Solar Energy: From Fundamentals to Applications. Ch. 10.2. Encapsulant Materials for PV Modules, John Wiley & Sons, Ltd, 2017.

[32] F. Bandou, A. Hadj Arab, M.S. Belkaid, P.-O. Logerais, O. Riou, A. Charki, Evaluation performance of photovoltaic modules after a long time operation in Saharan environment, International Journal of Hydrogen Energy 40 (39) (2015) 13839–13848. https://doi.org/10.1016/j.ijhydene.2015.04.091.

[33] A. Beinert, C. Peike, I. Dürr, M. Kempe, K.-A. Weiß, The Influence of the Additive Composition on the Photochemical Degradation of EVA, in: 29th European Photovoltaic Solar Energy Conference and Exhibition, Amsterdam, Netherlands, 2014.

[34] M. Rodríguez-Vázquez, C.M. Liauw, N.S. Allen, M. Edge, E. Fontan, Degradation and stabilisation of poly(ethylene-stat-vinyl acetate): 1 – Spectroscopic and rheological examination of thermal and thermo-oxidative degradation mechanisms, Polymer Degradation and Stability 91 (1) (2006) 154–164. https://doi.org/10.1016/j.polymdegradstab.2005.04.034.

[35] N.S. Allen, M. Edge, M. Rodriguez, C.M. Liauw, E. Fontan, Aspects of the thermal oxidation, yellowing and stabilisation of ethylene vinyl acetate copolymer, Polymer Degradation and Stability (71) (2001) 1–14.

[36] Report IEA-PVPS T13-09:2017, Assessment of Photovoltaic Module Failures in the Field: IEA PVPS Task 13, Subtask 3, Final draft May 2017, May/2017.

[37] M.C.C de Oliveira, A.S.A.C. Diniz, M. M. Viana, L.V.F. Cunha, The causes and effects of degradation of encapsulant ethylene vinyl acetate copolymer (EVA) in crystalline silicon photovoltaic modules: A review, Renewable and Sustainable Energy Reviews 81 (2018) 2299–2317. https://doi.org/10.1016/j.rser.2017.06.039.

[38] S. Chattopadhyay, R. Dubey, V. Kuthanazhi, J.J. John, C.S. Solanki, A. Kottantharayil, B.M. Arora, K.L. Narasimhan, V. Kuber, J. Vasi, A. Kumar, O.S. Sastry, Visual Degradation in Field-Aged Crystalline Silicon PV Modules in India and Correlation With Electrical Degradation, IEEE J. Photovoltaics 4 (6) (2014) 1470–1476. https://doi.org/10.1109/JPHOTOV.2014.2356717.

[39] J.H. Wohlgemuth, P. Hacke, N. Bosco, D.C. Miller, M.D. Kempe and S.R. Kurtz, Assessing the Causes of Encapsulant Delamination in PV Modules, in: Proceedings of the 2016 IEEE 43rd Photovoltaic Specialists Conference (PVSC), 5-10 June 2016, Portland, Oregon.

[40] M.A.Quintana and D.L.King, Commonly observed degradation in field-aged photovoltaic modules, in: 29th IEEE Photovoltaic Specialists Conference, New Orleans, 2002.

[41] P. Sánchez-Friera, M. Piliougine, J. Peláez, J. Carretero, M. Sidrach de Cardona, Analysis of degradation mechanisms of crystalline silicon PV modules after 12 years of operation in Southern Europe, Prog. Photovolt: Res. Appl. 19 (6) (2011) 658–666. https://doi.org/10.1002/pip.1083.

[42] N.C. Park, J.S. Jeong, B.J. Kang, D.H. Kim, The effect of encapsulant discoloration and delamination on the electrical characteristics of photovoltaic module, Microelectronics Reliability 53 (9-11) (2013) 1818–1822. https://doi.org/10.1016/j.microrel.2013.07.062.

[43] Neelkanth G. Dhere, Reliability of PV Modules and Balance-of-System Components, in: Proceedings of the 31st IEEE Photovoltaic Specialist Conference, 2005., pp. 1570–1576.

[44] E. Wang, H.E. Yang, J. Yen, S. Chi, C. Wang, Failure Modes Evaluation of PV Module via Materials Degradation Approach, Energy Procedia 33 (2013) 256–264. https://doi.org/10.1016/j.egypro.2013.05.066.

[45] J. Wohlgemuth, D.W. Cunningham, A. Nguyen, G. Kelly and D. Amin, Failure Modes of Crystalline Silicon Modules, in: PV Module Reliability Workshop 2010.

[46] D. C. Jordan, J. H. Wohlgemuth, and S. R. Kurtz, Technology and Climate Trends in PV Module Degradation, in: 27th European Photovoltaic Solar Energy Conference and Exhibition, Frankfurt, 2012.

[47] S. Djordjevic, D. Parlevliet, P. Jennings, Detectable faults on recently installed solar modules in Western Australia, Renewable Energy 67 (2014) 215–221. https://doi.org/10.1016/j.renene.2013.11.036.

[48] G. TamizhMani, Reliability Evaluation of PV Power Plants: Input Data for Warranty, Bankability and Energy Estimation Models, in: PV Module Reliability Workshop, Golden, CO, 2014.

[49] Edwin P. Plueddemann, Silane Coupling Agents, 2nd ed., Springer Science+Business Media, LLC, New York, 1991.

[50] U. Weber, R. Eiden, C. Strubel, T. Soegding, M. Heiss, P. Zachmann, K. Nattermann, H. Engelmann, A. Dethlefsen, N. Lenck, Acetic Acid Production, Migration and Corrosion Effects in Ethylene-Vinyl-Acetate- (EVA-) Based PV Modules, in: 27th European Photovoltaic Solar Energy Conference and Exhibition, Frankfurt, 2012.

[51] T. Geipel, M. Moeller, A. Kraft, U. Eitner, A Comprehensive Study of Intermetallic Compounds in Solar Cell Interconnections and their Growth Kinetics, Energy Procedia 98 (2016) 86–97. https://doi.org/10.1016/j.egypro.2016.10.084.

[52] C. Peike, S. Hoffmann, P. Hülsmann, B. Thaidigsmann, K.-A. Weiß, M. Koehl, P. Bentz, Origin of damp-heat induced cell degradation, Solar Energy Materials and Solar Cells 116 (2013) 49–54. https://doi.org/10.1016/j.solmat.2013.03.022.

[53] N.G. Dhere, N.R. Raravikar, Adhesional shear strength and surface analysis of a PV module deployed in harsh coastal climate, Solar Energy Materials and Solar Cells 67 (1-4) (2001) 363–367. https://doi.org/10.1016/S0927-0248(00)00304-4.

[54] M. López-Escalante, L.J. Caballero, F. Martín, M. Gabás, A. Cuevas, J. Ramos-Barrado, Polyolefin as PID-resistant encapsulant material in 5PV6 modules, Solar Energy Materials and Solar Cells 144 (2016) 691–699. https://doi.org/10.1016/j.solmat.2015.10.009.

[55] W.J. Gambogi, Comparative Performance of Backsheets for Photovoltaic Modules, in: 25th European Photovoltaic Solar Energy Conference and Exhibition, Valencia, Spain, 2010, pp. 4079–4083.

[56] Chiao-Chi Lin, Peter J. Krommenhoek, Stephanie S. Watson, Xiaohong Gu, Depth profiling of degradation of multilayer photovoltaic backsheets after accelerated laboratory weathering: Cross-sectional Raman imaging, Solar Energy Materials and Solar Cells 144 (2016) 289–299. https://doi.org/10.1016/j.solmat.2015.09.021.

[57] M.D. Kempe, D.C. Miller, A. Zielnik, D. Montiel-Chicharro, J. Zhu, R. Gottschalg, Survey of Mechanical Durability of PV Backsheets, in: 4th Atlas/NIST Workshop on Photovoltaic Materials Durability, 2017.

[58] Y. Voronko, B.S. Chernev, G.C. Eder, Spectroscopic investigations on thin adhesive layers in multi-material laminates, Applied Spectroscopy 68 (5) (2014) 584–592. https://doi.org/10.1366/13-07291.

[59] Fernando D. Novoa, David C. Miller, Reinhold H. Dauskardt, Environmental mechanisms of debonding in photovoltaic backsheets, Solar Energy Materials and Solar Cells 120, Part A (0) (2014) 87–93. https://doi.org/10.1016/j.solmat.2013.08.020.

[60] T. Felder, H. Hu, W. Gambogi, K.R. Choudhury, S. MacMaster, L. Garreau-Iles and J. Trout, Field Study and Analysis of Backsheet Degradation in 450MW+ PV Installations, in: 4th Atlas/NIST Workshop on Photovoltaic Materials Durability, 2017.

[61] A. Fairbrother, PV Array Differential Backside Exposure Conditions: Backsheet Degradation and Site Design, in: 4th Atlas/NIST Workshop on Photovoltaic Materials Durability, 2017.

[62] B. Ottersböck, G. Oreski, G. Pinter, Correlation study of damp heat and pressure cooker testing on backsheets, J. Appl. Polym. Sci. (2016). https://doi.org/10.1002/APP.44230.

[63] M. Knausz, G. Oreski, G.C. Eder, Y. Voronko, B. Duscher, T. Koch, G. Pinter, K.A. Berger, Degradation of photovoltaic backsheets: Comparison of the aging induced changes on module and component level, J. Appl. Polym. Sci. 132 (42093) (2015) 1–8. https://doi.org/10.1002/app.42093.

[64] G. Oreski, G. Pinter, Aging Characterization of Multi-Layer Films Used As Photovoltaic Module Backsheets: 4AV.4.13, in: 28th European Photovoltaic Solar Energy Conference and Exhibition, Paris, France, 2013, pp. 3050–3054.

[65] N.S. Allen, M. Edge, M. Mohammadian, K. Jones, Physicochemical aspects of the environmental degradation of poly(ethylene terephthalate), Polymer Degradation and Stability 43 (2) (1994) 229–237. https://doi.org/10.1016/0141-3910(94)90074-4.

[66] J. Scheirs, T.E. Long, Modern polyesters: Chemistry and technology of polyesters and copolyesters, John Wiley & Sons, Hoboken, N.J., 2003.

[67] K. Looney, B. Brennan, Modelling the correlation between DHT and true field lifetimes for PET based backsheets, in: 29th European Photovoltaic Solar Energy Conference and Exhibition, Amsterdam, Netherlands, 2014, pp. 2467–2470.

[68] H. Kliesch, B. Kuhmann, T. Kiehne, I. Fischer, G. Hilkert, V. Schaefer US 7.241,507 B2, Sep. 8.

[69] John Wiley and Sons, Encyclopedia of Polymer Science and Technology - Barrier polymers, 1999-2012.

[70] Z. Shi, A. Fujita, Extremely enhanced hydrolytic stability of poly(ethylene terephthalate) films, Polym Eng Sci 58 (3) (2018) 261–271. https://doi.org/10.1002/pen.24562.

[71] G. Oreski, G.M. Wallner, Aging mechanisms of polymeric films for PV encapsulation, Solar Energy 79 (6) (2005) 612–617. https://doi.org/10.1016/j.solener.2005.02.008.

[72] H. Hu, W.M. Wang, O. Fu, A. Bradley, T. Felder, W. Gambogi and T.J. Trout, Typical Photovoltaic Backsheet Failure Mode Analysis Under Different Climates in China, in: SNEC 2016, Shanghai.

[73] A. Lefebvre, G. O'Brien, D. Althouse, B. Douglas, G. Moeller, D. Garcia, T. Fine, A. Bonnet, Weathering Performance of PV Backsheets, in: 2013 PV Module Reliability Workshop.

[74] M.Halwachs, K.A.Berger, L.Maul, L.Neumaier, Y.Voronko, A.Mihaljevic, N.Vollert, W.Mühleisen, M.Schwark, R.Ebner, C.Hirschl, Descriptive Statistics on the Climate Related Performance and Reliability Issues from Global PV Installations, in: 33rd European Photovoltaic Solar Energy Conference and Exhibition, Amsterdam, 2017., pp. 1–3.

[75] M.Köntges, S.Altmann, T.Heimberg, U.Jahn, K.- A. Berger, Mean Degradation Rates in PV Systems for Various Kinds of PV Module Failures, in: 32nd European Photovoltaic Solar Energy Conference and Exhibition, Munich, 2016.

[76] D.C. Jordan, S.R. Kurtz, Photovoltaic Degradation Rates-an Analytical Review, Prog. Photovolt: Res. Appl. 21 (1) (2013) 12–29. https://doi.org/10.1002/pip.1182.

[77] E.D. Dunlop, D. Halton, The performance of crystalline silicon photovoltaic solar modules after 22 years of continuous outdoor exposure, Progress in Photovoltaics: Research and Application 14 (1) (2006) 53–64. https://doi.org/10.1002/pip.627.

[78] R.Dubey, S. Chattopadhyay, V. Kuthanazhi, J.J. John, B.M. Arora, A. Kottantharayil, K.L. Narasimhan, C. S. Solanki, V. Kuber, J. Vasi, A. Kumar, O. S. Sastry, All India Survey of Photovoltaic Module Degradation: 2013, 2013.

[79] A. Jacobson, R. Duke, D.M. Kammen, M. Hankins, Field Performance Measurements of Amorphous Silicon Photovoltaic Modules in Kenya, in: Conference proceedings of The American Solar Energy Society, Madison, Wisconsin, USA, June 16-21, 2000.

[80] A.B. Maish, C. Alcitty, S. Hester, D. Greenberg, D. Osborn, D. Collier, Photovoltaic system reliability, in: 26th IEEE PVSC Conference, Sept.30-Oct.3, 1997., Anaheim, CA.

[81] K. Kato, PVRessQ!: a research activity on reliability of PV systems from an user's viewpoint in Japan, Proc. of SPIE 8112. https://doi.org/10.1117/12.896135.

[82] A. Skoczek, T. Sample, E.D. Dunlop, The results of performance measurements of field-aged crystalline silicon photovoltaic modules, Progress in Photovoltaics: Research and Application (2009) 227–240. https://doi.org/10.1002/pip.874.

[83] Robert J van der Plas and Mark Hankins, Solar electricity in Africa: a reality, Energy Policy 26 (4) (1997) 295–305.

[84] J. Wohlgemuth, T. Silverman, D.C. Miller, P. McNutt, M. Kempe and M. Deceglie, Evaluation of PV Module Field Performance, in: IEEE 42nd Photovoltaic Specialist, New Orleans, LA, 14-19 June, 2015.

[85] J. Schaefer, L. Schlueter, A. Rosenthal, H.Wenger, Electrical Degradation of the Carrisa Plains Power Plant, in: 10th European Photovoltaic Solar Energy, Lisbon, 1991.

[86] E. Urrejola, J. Antonanzas, P. Ayala, M. Salgado, G. Ramírez-Sagner, C. Cortés, A. Pino, R. Escobar, Effect of soiling and sunlight exposure on the performance ratio of photovoltaic technologies in Santiago, Chile, Energy Conversion and Management 114 (2016) 338–347. https://doi.org/10.1016/j.enconman.2016.02.016.

[87] K.Yedidi, S.Tatapudi, J.Mallineni, B.Knisely, K.Kutiche, G.TamizhMani, Failure and Degradation Modes and Rates of PV Modules in a Hot-Dry Climate: Results after 16 years of field exposure, in: Photovoltaic Specialist Conference (PVSC), 2014 IEEE 40th, pp. 3245–3247.

[88] N.Bogdanski, W.Herrmann, F.Reil, M.Köhl, K.-A.Weiss, M.Heck, PV reliability (cluster II): Results of a German four-year joint project: Part II, results of three years module weathering in four different climates, in: 25th European Photovoltaic Solar Energy Conference and Exhibition/ 5th World Conference on Photovoltaic Energy Conversion, 6-10 September 2010, Valencia, Spain.

[89] M. Halwachs, L. Neumaier, N. Vollert, L. Maul, S. Dimitriadis, Y. Voronko, G. C. Eder, A. Omazic, W. Mühleisen, C. Hirschl, M. Schwark, K. A. Berger, Statistical evaluation of PV system performance and failure data among different climate zones, Submitted in Renewable Energy Manuscript Number RENE-S-18-04734 (2018.).

[90] Y.Tang, B.Raghuraman, J.Kuitche, G.TamizhMani, C.E.Backus, C.Osterwald, An evaluation of 27+ years old photovoltaic modules operated in a hot-dessert climatic conditions, in: 2006 IEEE 4th World Conference on Photovoltaic Energy Conversion, Waikoloa, Hawai, 2006.

[91] M. Chicca, G. TamizhMani, Nondestructive techniques to determine degradation modes: Experimentation with 18 years old photovoltaic modules, in: IEEE 42nd Photovoltaic Specialists Conference (PVSC), New Orleans, 2015., pp. 1–5.

[92] A. Bouraiou, M. Hamouda, A. Chaker, M. Mostefaoui, S. Lachtar, M. Sadok, N. Boutasseta, M. Othmani, A. Issam, Analysis and evaluation of the impact of climatic conditions on the photovoltaic modules performance in the desert environment, Energy Conversion and Management 106 (2015) 1345–1355. https://doi.org/10.1016/j.enconman.2015.10.073.

[93] A.A.Suleske, Performance Degradation of Grid-Tied Photovoltaic Modules in a Desert Climatic Condition. Master Thesis, 2010.

[94] D. Chianese, A. Realini, N. Cereghetti, G. Friesen, Analysis of weathered c-Si PV modules, in: Proceedings of 3rd World Conference on Photovoltaic Energy Conversion, Osaka, Japan, 11-18 May, 2003.

[95] M.A.Quintana, D.L.King, F.M.Hosking, J.A.Kratochvil, R.W.Johnson, B.R.Hansen, Diagnostic Analysis of Silicon Photovoltaic Modules After 20-year Field Exposure, in: IEEE 28th Photovoltaic Specialists Conference, Piscataway, NJ, 2000.

[96] A. Limmanee, S. Songtrai, N. Udomdachanut, S. Kaewniyompanit, Y. Sato, M. Nakaishi, S. Kittisontirak, K. Sriprapha, Y. Sakamoto, Degradation analysis of photovoltaic modules under tropical climatic conditions and its impacts on LCOE, Renewable Energy 102 (2017) 199–204. https://doi.org/10.1016/j.renene.2016.10.052.

[97] M.Makenzi, N.Timonah, M.Benedict, I.Abisai, Degradation Prevalence Study of Field-Aged Photovoltaic Modules Operating Under Kenyan Climatic Conditions, SJEE 3 (1) (2015) 1. https://doi.org/10.11648/j.sjee.20150301.11.

[98] F.D. Novoa, D.C. Miller, R.H. Dauskardt, Adhesion and debonding kinetics of photovoltaic encapsulation in moist environments, Prog. Photovolt: Res. Appl. 24 (2) (2016) 183–194. https://doi.org/10.1002/pip.2657.

[99] W. Oh, S. Kim, S. Bae, N. Park, S.-I. Chan, Y. Kang, H.-S. Lee, D. Kim, Migration of Sn and Pb from Solder Ribbon onto Ag Fingers in Field-Aged Silicon Photovoltaic Modules, International Journal of Photoenergy 2015 (2015) 1–7. https://doi.org/10.1155/2015/257343.

[100] Th. Swonke and U. Hoyer, Diffusion of Moisture and Impact of UV Irradiance in Photovoltaic Encapsulants, in: 24th European Photovoltaic Solar Energy Conference, Hamburg, 2009.

[101] B. Ketola, A. Norris, The Role of Encapsulant Moisture Permeability in the Durability of Solar Photovoltaic Modules, in: 25th European Photovoltaic Solar Energy Conference and Exhibition/ 5th World Conference on Photovoltaic Energy Conversion, Valencia, 2010.

[102] M.D. Kempe, G.J. Jorgensen, K.M. Terwilliger, T.J. McMahon, C.E. Kennedy, T.T. Borek, Acetic acid production and glass transition concerns with ethylene-vinyl acetate used in photovoltaic devices, Solar Energy Materials and Solar Cells 91 (4) (2007) 315–329. https://doi.org/10.1016/j.solmat.2006.10.009.

[103] C. Dechthummarong, B. Wiengmoon, D. Chenvidhya, C. Jivacate, K. Kirtikara, Physical deterioration of encapsulation and electrical insulation properties of PV modules after long-term operation in Thailand, Solar Energy Materials and Solar Cells 94 (9) (2010) 1437–1440. https://doi.org/10.1016/j.solmat.2010.03.038.

[104] A. Bradley, T. Dhir, Y. Poissant, Initial analysis of 22-year old PV system in Quebec, Canada, in: PV Module Reliability Workshop (PVMRW), February 24-27, Golden, Colorado, 2015.

[105] J.Vanek, J.Hylsky, D.Strachala, L.Simonova and Z.Chobola, Assessment of the longest operating photovoltaic power station in the Chech Republic, in: 31st European Photovoltaic Solar Energy Conference and Exhibition, Hamburg, 2015.

[106] E.D.Dunlop, D. Halton, H.A. Ossenbrink, 20 years of life and more: where is the end of life of a PV module? in: 31st IEEE Photovoltaics Specialists Conference, Piscataway, NJ, 2005.

[107] G.H.Atmaram, G.G.Ventre, C.W.Maytrott, J.P.Dunlop and R.Swamy, Long-Term Performance and Reliability of Crystalline Silicon Photovoltaic Modules, in: 25th PVSC, Washington, D.C., 1996.

[108] L.-M.Huang, H.-Y.Hsu, R.-C.Lai, F.-M.Lin, C.-Y.Peng and F.-Y.Yeh, Physical Properties of EVA and PVB Encapsulant Materials for Thin Film Photovoltaic Module Applications, in: 24th European Photovoltaic Solar Energy Conference, Hamburg, 2009.

[109] P. Hülsmann, C. Peike, M. Blüml, P. Schmid, K.-A. Weiß, M. Köhl, Impact of permeation properties and back sheet/encapsulation interactions on the reliability of PV modules, ASME 2011 International Mechanical Engineering Congress and Exposition, IMECE 2011 4 (PARTS A AND B) (2011).

[110] J. Govaerts, B.Geyer, A.van der Heide, T.Borgers, S.Hellstrom, B.Broeders, E.Voroshazi, J.Szlufcik and J.Poortmans, Extended Qualification Testing of 1-cell Crystalline Si PV Laminates: Impacts of Advanced Cell Metallization and Encapsulation Schemes, in: 33rd European Photovoltaic Solar Energy Conference and Exhibition, Amsterdam, 2017.

[111] G. Stollwerck, W. Schoeppel, A. Graichen, C. Jaeger, Polyolefin Backsheet and New Encapsulant Supress Cell Degradation in the Module, in: 28th European Photovoltaic Solar Energy Conference and Exhibition, Paris, France, 2013.

[112] A. Carr, T. Pryor, A comparison of the performance of different PV module types in temperate climates, Solar Energy 76 (1-3) (2004) 285–294. https://doi.org/10.1016/j.solener.2003.07.026.

[113] K. Akhmad, A. Kitamura, F. Yamamoto, H. Okamoto, H. Takakura, Y. Hamakawa, Outdoor performance of amorphous silicon and polycrystalline silicon PV modules, Solar Energy Materials and Solar Cells 46 (3) (1997) 209–218. https://doi.org/10.1016/S0927-0248(97)00003-2.

[114] W. Meike, Hot Climate Performance Comparison Between Poly-Crystalline and Amorphous Silicon Cells Connected to an Utility Mini-Grid, in: Proceedings of Solar 98, 36th Annual Conference of the Australian and New Zealand Solar Energy Society, Christchurch, New Zealand, November, 1998., pp. 464–470.

[115] G. Oreski, A. Mihaljevic, Y. Voronko, G.C. Eder, Acetic acid permeation through photovoltaic backsheets: Influence of the composition on the permeation rate, Polymer Testing 60 (2017) 374–380. https://doi.org/10.1016/j.polymertesting.2017.04.025.

[116] E.Cabrera, A.Schneider, J.Rabanal, P.Ferrada, R.R.Cordero, E.Fuentealba, R.Kopecek, Advancements in the Development of "AtaMo": a Solar Module Adapted for the Climate Conditions of the Atacama Desert in Chile, in: 31st European Photovoltaic Solar Energy Conference and Exhibition, Hamburg, 2015., pp. 1–22.

[117] J. Kapur, A. Bennett, J. Norwood, B. Hamzavytehrany, I. Kueppenbender, Tailoring Ionomer Encapsulants as a low cost solution to potential induced degradation, in: 28th European Photovoltaic Solar Energy Conference and Exhibition, Paris, France, 2013.

[118] A. Pozza, T. Sample, Crystalline silicon PV module degradation after 20 years of field exposure studied by electrical tests, electroluminescence, and LBIC, Progress in Photovoltaics: Research and Application (2016) 368–378. https://doi.org/10.1002/pip.2717.

2 Weathering stability of alternative polyolefin-based backsheets

Parts of this chapter were accepted for publication in the Journal of Applied Polymer Science under the title "Increased reliability of modified polyolefin backsheets over commonly used polyester backsheets for crystalline PV modules" with doi number: 10.1002/app.20183117.

2.1 Motivation

Application of PET-based backsheets

Due to its high strength, temperature resistance and low material price, poly(ethylene-terephthalate) - PET is the most used material in production of PV backsheets. PET is produced via step-growth polycondensation of terephthalic acid (TPA) and ethylene glycol (EG) (see Figure 2.1.) [1,2].
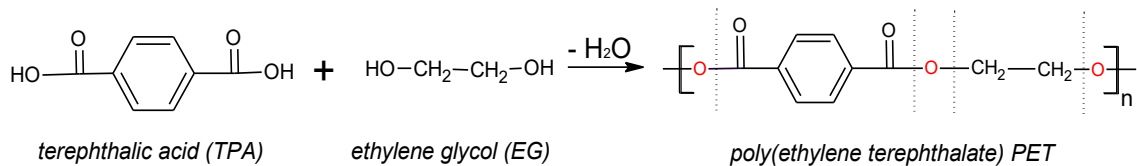
Figure 2.1. Structure of PET

However, mainly due to its structure, reliability of the PET in PV backsheets is a topic of great interest. Being a polyester, PET contains a hydrolysable ester bond in the backbone (see Figure 2.1.) [2,3]. Chain cleavage upon hydrolysis results in molecular weight and initial viscosity reduction, which leads to deterioration of mechanical properties [2–7]. Newly formed shorter polymer chains are then more mobile and able to accumulate on the lamellar surface in a process known as chemo-crystallization [3,5,8]. The deteriorating effect of water is accelerated by other factors such as the presence of effective acids or bases, elevated temperature, cracks and/or high initial content of carboxyl end-groups [3,4,6]. Above the glass transition temperature (T_g, °C), mobility of the shorter polymer chains is even more enhanced, giving rise to higher chemo-crystallization. Therefore, after aging, the initial degree of crystallization is enlarged by the amount of crystals formed by chemo- and/or post-crystallization (physical aging) [3]. An increased degree of crystallinity gives rise to embrittlement, which leads to cracking and/or delamination of the backsheet [6,9–12]. The embrittlement of PET-based

backsheets due to hydrolysis and chemo-crystallization was already reported [4,5,7,10,13].

In order to increase the hydrolysis resistance of the PET films they are usually formulated with anti-hydrolysis additives [3] and are biaxially stretched, which increases the crystalline content and therefore reduces the free fractional volume (FFV) [2,3,6,14,15]. The production of individual biaxial flat PET films and assembling them into a laminate is multiple-step process. This is one of the disadvantages when compared to the one-step co-extrusion process [16,17]. Biaxial PET films need to be bonded with other backsheet layers via an adhesive layer, which increases the costs of the production and eventually could decrease the reliability of the backsheet due to delamination between the backsheet layers [18–20]. A possible solution for overcoming reliability issues related to adhesive layers could be the production of the backsheet via co-extrusion, which could be a limiting factor for polyester-based backsheets.

Due to their high durability and high environmental stability (UV irradiation, water, temperature) fluoropolymers are usually the accompanying material as an outer protective layer in PET-based backsheets [21]. Even though that combination was shown to provide higher reliability in terms of weathering stability compared to other backsheet materials [9,22,23], the utilisation of fluoropolymers has its drawbacks when it comes to costs and sustainable life cycle management. Namely, the recycling of fluoropolymers via conventional methods such as pyrolysis is not possible due to the formation of toxic by-products (e.g. carbonyl fluoride, trifluoroacetic acid, hydrogen fluoride) during the combustion process [24,25].

Therefore, driven with the always-present challenges of cost reduction, reliability of commonly used PET-backsheets and upcoming issues of sustainability and life cycle of PV modules (concerning especially fluoropolymers), the PV industry is seeking new alternatives and polyolefins are increasingly drawing attention of backsheet producers. Polyolefins have been used in backsheets thus far only as individual layers, i.e. an inner layer (e.g. PET/PET/EVA-PPE backsheet) due to their compatibility with the polyolefin encapsulant. In that way, adhesion between encapsulant and backsheet was enhanced. A complete polyolefin backsheet could provide numerous advantages. Namely, aside from low price, one of the perhaps biggest advantages of the fully polyolefin backsheet is the possibility of production via co-extrusion, which is a one-step process and therefore reduces the cost of production. Moreover, co-extrusion requires no adhesive layers, which is another cost-friendly advantage. Furthermore, a polyolefin backsheet is hydrolysis resistant since polyolefins are characterized by very low water uptake, usually less than 0.1% [26]. This eliminates the need for fluoropolymers as protection layers.

Lastly, polyolefins meet the demand for sustainable development since they are compatible with most modern recycling processes [27]. Therefore, a polyolefin-based backsheet could be a promising candidate for the replacement of PET-based backsheets and reduce the reliability issues related to backsheets, while meeting the cost- and sustainability requirements.

Alternative modified polyolefin backsheet

Regarding the production and application relevant requirements for PV applications (melting temperature, coefficient of thermal expansion, thermal conductivity and mechanical properties) polypropylene (PP) stands out among other polyolefin members. Polypropylene is produced via Ziegler-Natta catalysis from propylene (see Figure 2.2.) [27]. Polymerization of the non-symmetrical propylene molecule can result in three sequences depending on the catalyst and polymerization temperature: head-to-tail, head-to-head and tail-to-tail. However, due to steric effects of the -CH$_3$ group, head-to-tail is the favoured sequence and gives rise to high chemical regularity of the PP chain [28,29]. Being a stereoregular polymer, PP exists in three configurational stereoisomeric forms: atactic (aPP), isotactic (iPP) and syndiotactic (sPP) [28,30]. Isotactic PP (iPP) is a product of polymerization of only one isomeric configuration from a propylene monomer and results in head-to-tail sequence (all -CH$_3$ groups are on the same side of the zigzag plane) [28,29,31–33]. Among all three forms, iPP has the highest crystallinity and therefore high strength, stiffness and hardness due to higher packing order [16,27,29,31].

$$H_2C\!=\!CH \underset{CH_3}{|} \quad \xrightarrow{\text{Ziegler-Natta catalysis}} \quad \left[\!-CH_2CH\underset{CH_3}{|}-\!\right]_n$$
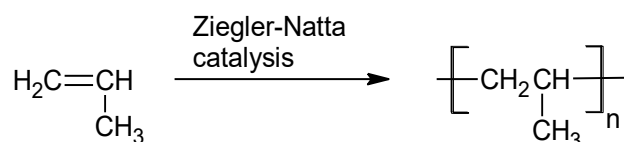
Figure 2.2. Structure of polypropylene

PP crystallizes in four crystalline forms with different chain packing geometries of the helices: monoclinic-α, hexagonal-β, triclinic-γ and the smectic (quenched) form. By far the most common crystalline form of iPP is α-form and it is therefore the most extensively studied crystal structure of iPP [28,34–36]. The β-form is metastable and is usually generated by inclusion of a nucleating agent such as pimelic acid and calcium stearate or calcium dicarboxylates [34,36].

The mechanical properties of the semicrystalline polymers mainly depend on molecular weight, nature of crystal phase, degree of crystallinity and spherulite size [32,34,37]. The α-form is characterized by tangential lamellae connected on radial lamellae, i.e. "cross-hatched" lamellar morphology, which is not observed in the β-form that is made

exclusively of radial lamellae [34]. The morphology of PP has an effect on mechanical properties and degradation [34,36,38]. Tordjeman et al. [34] have shown that the tangential lamellae in the α-phase make the spherulites more rigid and cause an increase in Young's modulus and yield stress. However, the tangential lamellae restrict the elongation at break, which makes PP more brittle.

Polyolefins in general are sensitive to photo-oxidation. Considering sunlight radiation, which is an important factor for polymers which are exposed to outdoors, only carbonyl groups seem to act as UV-light absorbing groups [3]. Therefore, it is to be expected that pure, non-degraded PP should not absorb UV light. However, due to trace amounts of impurities (e.g. hydroperoxides, carbonyl) and contaminations (e.g. catalyst residues and metallic compounds), which are able to absorb UV light, PP is sensitive to photo-oxidation [3,38–42]. Moreover, PP is more sensitive to photo-oxidation than polyethylene (PE) owing to the presence of the tertiary carbon atoms [3,41,43]. Namely, the tertiary carbon atoms at the branch sites are more susceptible to being attacked by free radicals [44]. Due to the helical structure of PP, intramolecular hydrogen abstraction by peroxy radicals dominates intermolecular abstraction [38]. The mechanism of degradation of PP (see Figure 2.3.) is via chain scission according to Norrish type I and ß-scission of alkoxy radicals, which leads to the formation of radicals that further react with molecular oxygen giving rise to further oxidation [3,43].
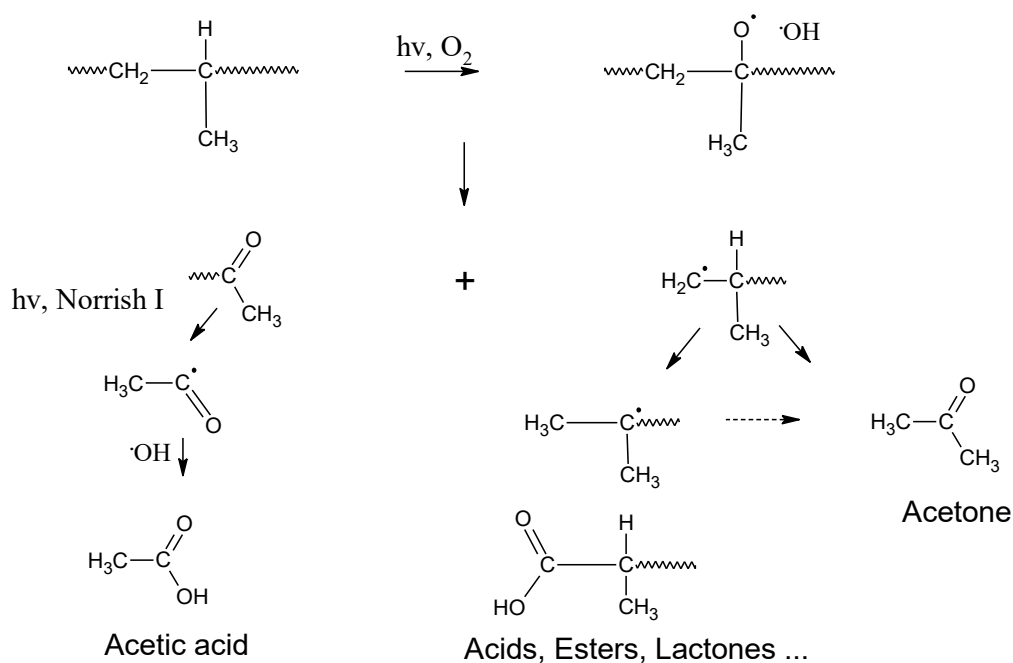

Figure 2.3. Photo-oxidation mechanism of PP (adjusted from [39])

Oxidation affects not only the molecular structure (chemical structure), but also the microstructure (physical structure, morphology) of PP. However, oxidation does not proceed homogenously, but spreads out over the entire material depending on structure and morphology, contaminations, active centres, etc. [3]. Therefore, PP has to be stabilised in order to avoid aging in the environment. One of the most commonly used stabilizers in PP are sterically hindered amine light stabilizers (HALS) and phenolic antioxidants [3,45–47]. HALS were used originally as light stabilizers, but are being increasingly used as well as antioxidants in polyolefins. The degradation mechanism of PP stabilized with sterically hindered amines differs from the PP stabilized with phenolic antioxidants. After an induction period, PP stabilized with phenolic antioxidants exhibits strongly accelerated oxidation at high temperatures, which significantly affects mechanical and physical properties, while those stabilized with HALS immediately exhibit slight loss of physical and mechanical properties at high temperatures with slow propagation over the course of exposure [3].

Being relatively new on the market, the weathering stability of the fully polyolefin backsheets has still not fully investigated. Hence, in this chapter the weathering stability of commonly used PET/fluoropolymer-based (PET-laminate) and newly developed modified polyolefin (MPO) backsheets will be investigated. Their main advantages and disadvantages will be discussed in terms of PV reliability and feasibility of application of MPO as an alternative to PET-based backsheets.

2.2 Experimental part

2.2.1 Preparation and aging of the samples

Two types of PV backsheets were used in this work: PET/PET/fluorocoating laminate (PET-laminate) and co-extruded modified polyolefin composite (MPO). The composition of the backsheets is listed in Table 2.1. The cross-section pictures obtained via light microscopy are shown in Figure 2.4. The layers in the PET-laminate are bonded together via an adhesive layer.

Table 2.1. Composition of the backsheets used in the investigation

Backsheet	Inner layer	Core layer	Outer layer
PET-laminate	Fluorocoating, 5µm	PET, 250 µm	PET, 50 µm
MPO	Modified PP, 25µm	Modified PP, 235µm	Modified PP, 25µm
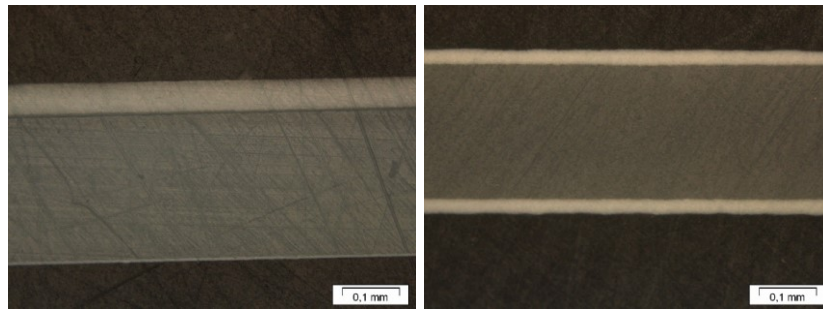
Figure 2.4. Cross-section of PET-laminate (left) and MPO backsheet (right)

Samples were cut before aging according to EN ISO 527-3 [48] and were subjected to a damp heat test (T=85°C; 85% RH) according to IEC 61215 [49] and a sun irradiance test (T=60°C; 40% RH; irradiation in the range λ=300-2500 nm) with a duration of up to 2000h. During the sun irradiance test, samples were irradiated from the inner side, as it would be in real service conditions. Samples were tested prior to aging, after 1000h and 2000h of aging.

The aging behaviour was characterized via UV/Vis/NIR spectroscopy, Fourier transform infrared spectroscopy in attenuated total reflection mode (FTIR-ATR), differential scanning calorimetry (DSC), tensile test and thermo-mechanical analysis (TMA).

2.2.2 UV/Vis/NIR spectroscopy

The optical properties of the backsheets before and after aging were determined via UV/Vis/NIR spectrometer Perkin Elmer Lambda 950 (Waltham, US). The wavelength range was set between 250 and 2500 nm with a measuring interval of 5 nm. Hemispherical reflectance measurements were done with an Ulbricht sphere. The presented spectra had an average of at least 5 measurements per sample and aging

stage. All spectra were used to calculate b* values according to the CIE L a* b* colour space. The yellow-blue opponent colours are represented by the b* axis, with blue at negative values and yellow at positive b* values. Standard light source C was used under a 2° observer angle. The axis maximums for L were 100 and for a* and b* 80, respectively.

2.2.3 FTIR-ATR spectroscopy

The chemical composition of the backsheets before and after the aging was investigated via Fourier transform infrared spectroscopy in attenuated total reflection mode (FTIR-ATR). The measurements were carried out using a Spectrum Two Fourier transform IR spectrometer (Perkin Elmer). The attenuated total reflection unit contained a zinc selenide crystal with a diamond on top (Pike Technologies). The absorption spectra were recorded over the IR range from 4500 to 650 cm^{-1}. The average spectra were taken from 5 measurements from both sides of the backsheets (inner and outer layers).

2.2.4 Differential scanning calorimetry (DSC)

The thermal behaviour of backsheets was characterized via differential scanning calorimetry (DSC) using a Perkin Elmer DSC 4000. Samples of the backsheets with a weight of approximately 10 mg were prepared and put into 50 mL pans with perforated lids. In order to obtain information on reversible and irreversible changes in the material, two heating runs and one cooling run were carried out in the temperature ranges described in the Table 2.2.. For every evaluation, an average of at least two sample runs was taken. Melting points, melting enthalpies and crystallization temperatures were evaluated according to ISO 11357-3 [50]. Since the 1st heating run provided information on the thermal history of material (i.e. processing conditions) the values of melting enthalpies were taken from the 1st heating run.

Table 2.2. Parameters of DSC analysis

Backsheet	Step	Start T [°C]	End T [°C]	Heating rate [°C/min]
PET-laminate	1st heating	25	280	10
	Cooling	280	25	10
	2nd heating	25	280	10
MPO	1st heating	25	200	10
	Cooling	200	25	10
	2nd heating	25	200	10

2.2.5 Tensile test

Tensile tests were performed on the tensile testing machine Zwick Z001 according to EN ISO 527-3 [48]. Rectangular strips were cut prior to aging with a width of 15 mm and length of 150 mm. The test speed applied was 50 mm/min. The average values for yield stress (σ_y, MPa) and strain at break (ε_B, %) were deduced from at least five specimens for each test series.

2.2.6 Thermo-mechanical analysis (TMA)

Thermo-mechanical behaviour was characterized via the thermo-mechanical analyser TMA/SDTA840/841[e]. Measurements were conducted in tensile mode. In order to avoid bending of the sample, a static load of 0.02 N was applied. Measurements were performed under air atmosphere. In order to obtain information on material history, 1st and 2nd heating runs were conducted. Heating of the samples was done from 25°C to 120°C. The heating rate was set to 5°C/min.

2.3 Results and discussion

In the following section, the results of the systematic analysis conducted on PET-laminate and MPO backsheets before and after aging will be presented. For each characterization method applied, the results of PET-laminate before and after aging will be presented and discussed first, followed by the results for MPO backsheet in the same way. At the end of the section, the results of PET-laminate and MPO backsheets will be compared and the possibility of PET-laminate replacement will be discussed.

2.3.1 UV/Vis/NIR spectroscopy

The optical properties of both backsheets before and after aging were investigated via UV/Vis/NIR spectroscopy. In the Figure 2.5. the UV/Vis/NIR spectra of both backsheets before aging are presented. It can be seen that the unaged MPO backsheet has inherently a significantly higher reflectance (due to back scattering) compared to the PET-laminate, which could lead to higher power output of the modules combined with an MPO backsheet.
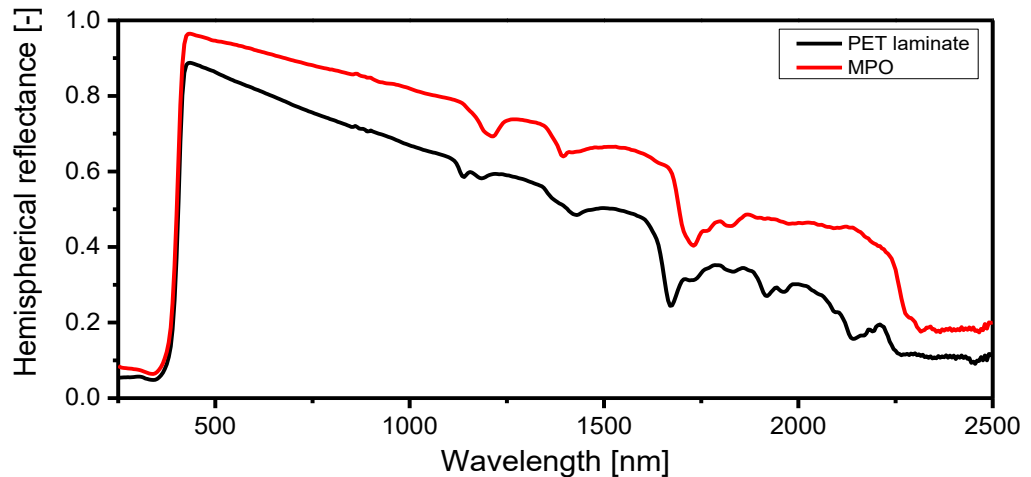
Figure 2.5. UV/Vis/NIR spectra of inner side of PET-laminate and MPO backsheet

PET-laminate

In Figure 2.6. the changes in reflectance spectra on the aging of the inner layer of PET-laminate in the range from 250-800 nm is presented. It can be seen in (Figure 2.6.) that the reflectance in the UV-region did not change after 1000h of aging, but after 2000h of damp heat and sun irradiance testing, it increased slightly, indicating a loss of UV-absorbers. However, no significant shift in the inflection point due to loss of UV absorbers was observed [51–53]. A decrease of the reflectance in the visible region of the spectra was detected. Of special interest is the blue region from 385-485 nm since it is related

to yellowing. Namely, yellowing can represent a serious problem for PV backsheets in the field since it leads to a strong absorption of irradiation and high operating temperatures of the PV module, which in turn can accelerate the degradation processes [3,54,55].

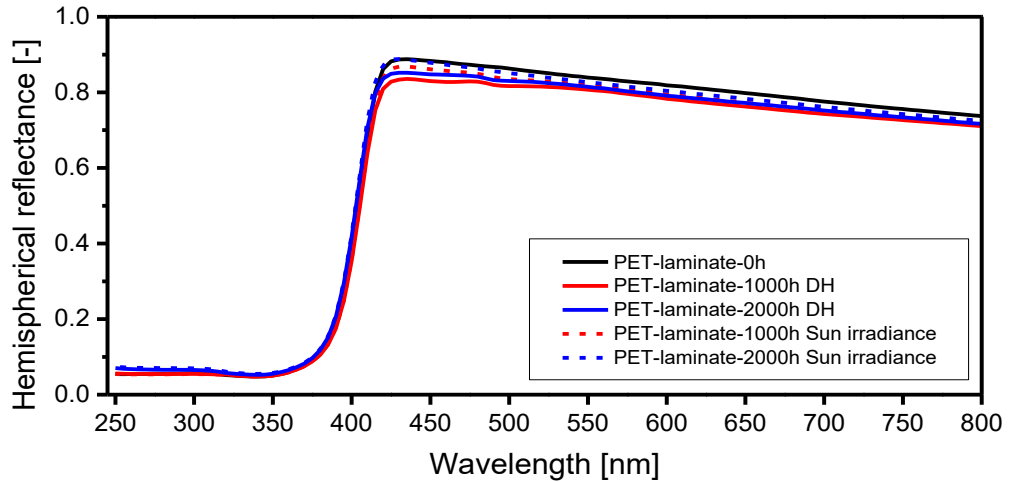**Figure 2.6.** UV/Vis/NIR spectra of inner side of PET-laminate

According the FTIR-ATR and Raman spectroscopy, the inner layer of the PET-laminate is supposed to be a coating based on PVDF mixed with an acrylate resin system as a compatible binder (see Figure 2.7.). The acrylic resin is usually added to fluoropolymer coatings in order to improve pigment wetting and coating adhesion because the PVDF molecule is inert. While the PVDF is highly resistant to outdoor degradation, the acrylic component is expected to be more susceptible to photochemical attack [56]. According to Raman spectra, distinctive peaks of rutile titanium dioxide (TiO_2) pigment are present in the coating as well. TiO_2 is inherently photo-chemically active and could promote the photo-oxidation of the inner layer especially if the pigment is untreated [43,56,57]. The degradation of the PVDF-based inner layer could result in the formation of conjugated groups, which can lead to visible discolouration. It is also possible that the PET-core layer was measured simultaneously since the fluoropolymer layer is very thin (5 µm). Hydrolysis of the PET-core layer can also result in chromophores species, which leads to yellowing [11]. After the sun irradiance test, the decrease of reflectance in the blue region was lower, probably due to a photo-bleaching effect [11]. According to Pern et al. [58], if there is sufficient O_2 and a high enough temperature, no discoloration will occur because the unsaturated bonds (chromophores) are oxidized before colour is produced.
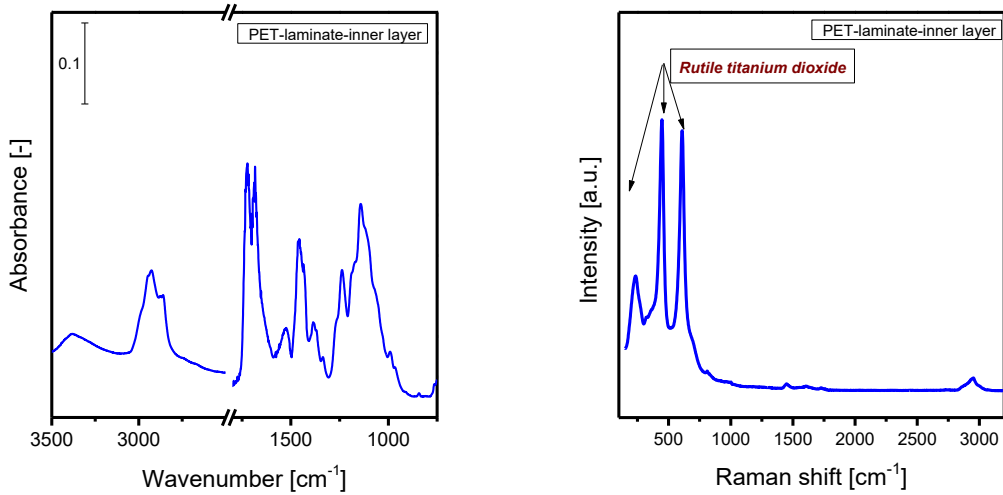
Figure 2.7. FTIR-ATR and Raman spectroscopy spectra of inner layer of PET-laminate

MPO

In Figure 2.8. the UV/Vis/NIR spectra of the inner side of MPO backsheet (based on modified PP) before and after the aging are shown. The decrease of reflectance in the blue region due to yellowing after damp heat aging is clearly observed already after 1000h of aging. The possible reason could be the thermo-oxidation of the inner polypropylene layer during the damp-heat aging. Literature showed that oxidation processes of hindered phenolic oxidants, which are usually added to polyolefins, are associated with an increase in yellowing [45,59]. Sun irradiance did not cause any significant changes in the spectra.

Figure 2.8. UV/Vis/NIR spectra of inner side of MPO backsheet

In order to compare changes in the blue region (385-485 nm) due to yellowing for both backsheets, the spectra were used to calculate b* values. According to the L a* b* colour space, the yellow-blue opponent colours are represented by the b* axis, with blue at negative values and yellow at positive values [11]. In Figure 2.9. it can be seen that damp heat aging caused higher yellowing in the MPO backshe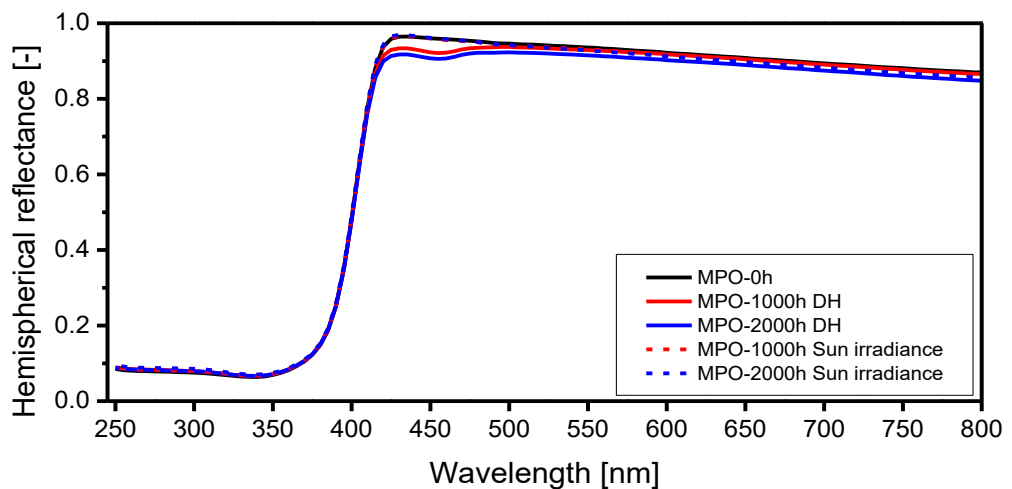et (inner side), compared to the PET-laminate. Sun irradiance resulted in lower yellowing of the MPO backsheet. On the other hand, sun irradiance resulted in shifted b* values towards blue colour in the case of the PET-laminate. The reason for lower yellowing of backsheets after the sun irradiance test could be a photo-bleaching effect, where oxygen and UV irradiation in combination cause the degradation of the chromophore species [11,58].
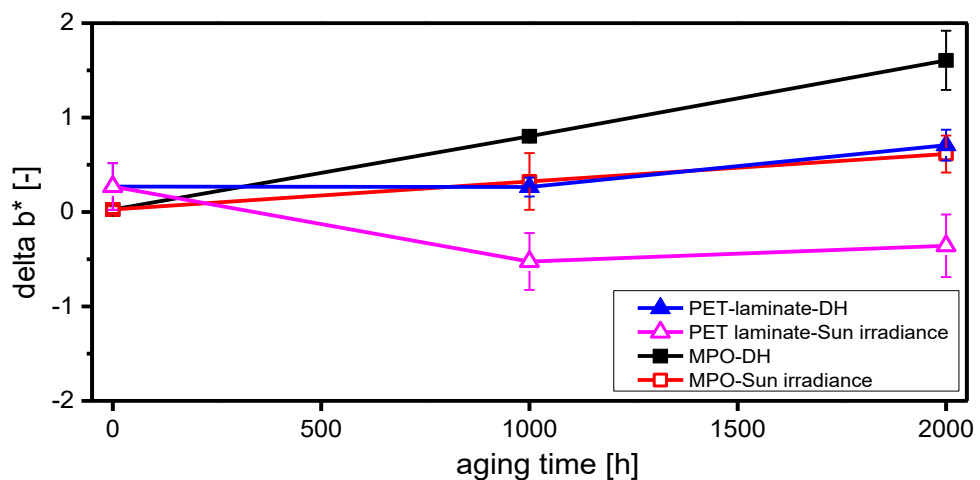
Figure 2.9. UV/Vis/NIR spectra of inner side of MPO backsheet

The change in the optical properties of both backsheets were not significant and it has to be kept in mind that the in real life conditions, the inner side of the backsheet would be protected with the glass and two layers of the encapsulant, while in these tests, films were directly exposed to aging conditions. As the module samples are encapsulated by a glass cover and an encapsulant, atmospheric gases, like oxygen and water vapour are prevented from coming easily into contact with the inner side of the backsheet due to the covering layers. Therefore, such changes in the optical properties are not very likely to happen in the modules.

2.3.2 FTIR-ATR spectroscopy

PET-laminate

The inner layer of the PET-laminate was hard to examine via FTIR-ATR spectroscopy due to the thinness of the coating (5 µm), which caused also peaks of the PET-core layer

to appear in the spectrum. Therefore, the FTIR-ATR data of the inner layer of the PET-laminate were not further evaluated.

The obtained spectra of the outer PET layer of the PET-laminate are presented in Figure 2.10.. The spectra were normalized with respect to the band at 1408 cm^{-1} assigned to the vibrations of phenylene ring, which is insensitive to changes in samples conformation or draw ratio [60]. The assignment of the bands is given in the Table 2.3.

Table 2.3. Band assignments for PET (adjusted from [8,60]

Wavenumber [cm^{-1}]	Feature	Assignment
2962		Asymmetrical -CH$_2$ stretching
2903		Symmetrical -CH$_2$ stretching
1715		C=O stretching
1470	Crystalline	EG *trans* - CH$_2$ bending
1450	Amorphous	EG *gauche* -CH$_2$ bending
1410		In plane C-H bending of the benzene ring
1370	Amorphous	EG *gauche* -CH$_2$ wagging
1340	Crystalline	EG *trans* -CH$_2$ wagging
1255	Amorphous, crystalline	Ester group stretching
1120	Crystalline	EG *trans* Ester group (C-O-C) stretching
1096	Amorphous	EG *gauche* Ester group (C-O-C) stretching
1040	Amorphous	EG *gauche* -CH$_2$ stretching
1020		In plane bending of C-H benzene ring
973	Crystalline	EG *trans* -C-O stretching
898	Amorphous	EG *gauche* -CH$_2$ rocking
874	Crystalline	Out of plane C-H in benzene ring
845	Crystalline	EG *trans* -CH$_2$ rocking
730		Out of plane C-H bending in benzene ring

The region from 3000 to 2800 cm^{-1} is assigned to stretching vibrations of the C-H bond in the ethylene glycol (EG) domains. When di-ethylene glycol (DEG) domains are present in the PET backbone, the bands at 2962 cm^{-1} and shoulder at 2903 cm^{-1} shift to around 2918 cm^{-1} (asymmetrical stretching) and 2854 cm^{-1} (symmetrical stretching) [60]. This shift was observed in the PET investigated in this work.

After aging (see Figure 2.10.), an overall decrease in the bands' intensity could be observed, especially those assigned to -CH$_2$ and -CH$_3$ stretching in the range of 3050-2800 cm^{-1}, carbonyl (C=O) stretching at 1715 cm^{-1}, ester group (C-O-C) stretching at 1255 cm^{-1}, 1120 cm^{-1} and 1094 cm^{-1}, and in plane bending of C-H in the benzene ring at 1020 cm^{-1}.
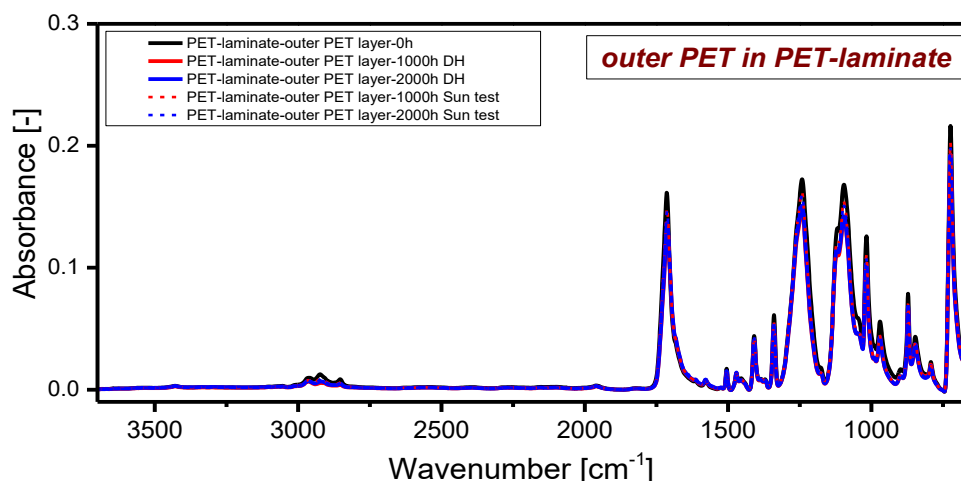
Figure 2.10. FTIR-ATR absorbance spectra of outer PET layer in PET-laminate before and after aging

In order to better depict changes in the outer PET layer upon aging, the part of the spectra that indicates chain scission assigned to $-CH_2$ and $-CH_3$ stretching region is shown in Figure 2.11. The outer layer of the backsheet is a protective layer that is under the direct influence of environmental conditions and needs to be highly stable during its service lifetime. In case of PET-based backsheets, the outer layer needs to be resistant to hydrolysis in order to prevent cracking that could enhance moisture ingress towards the core and inner layer of the backsheet and other PV components. In Figure 2.11. it can be seen that the intensity of the peaks in the wave number region from 3050 to 2800 cm^{-1} significantly decreased with aging time, which is a consequence of chain scission upon hydrolysis. One of the methods to assess the impact of chain scission on the intensity of stretching vibrations is to compare the asymmetrical and symmetrical stretching intensity [60]. Comparing the initial ratio of asymmetrical to symmetrical stretching ($I_{2918}/I_{2854} = 1.3 \pm 0.2$) with the values after aging, it could be seen that the exposure to lower humidity and temperature in sun irradiance tests resulted in a lower decrease of I_{2918}/I_{2854} ratio ($I_{2918}/I_{2854} = 1.1 \pm 0.2$) compared to damp heat tests ($I_{2918}/I_{2854} = 0.9 \pm 0.0$).
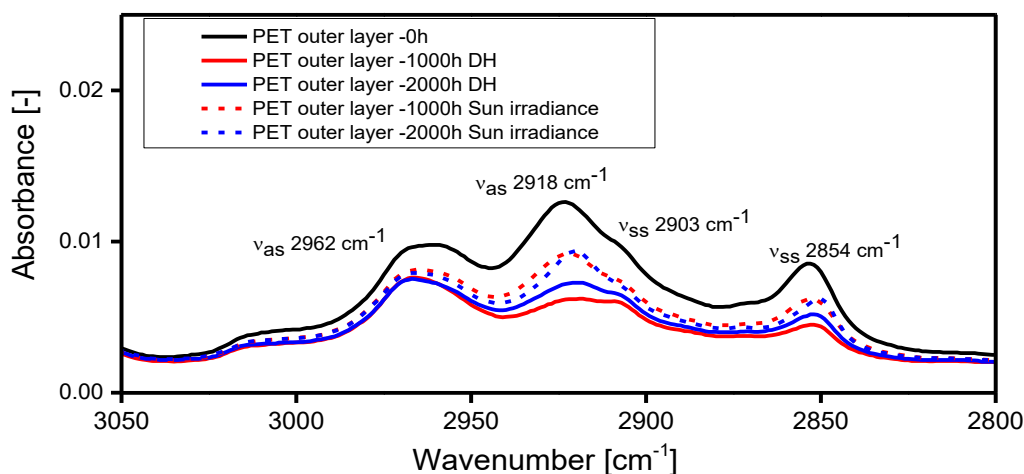
Figure 2.11. FTIR-ATR spectra evolution in the -CH$_2$, -CH$_3$ stretching region of outer PET layer before and after aging

Chain scission is a degradation process that occurs randomly at weak ester bonds. During the accelerated aging tests, temperature, humidity and oxygen were acting simultaneously. Initial cleavage of the bonds occurs due to an increased oscillation of the atoms upon increased temperature, which causes bond overstraining [3,61]. Therefore, at lower temperatures in the sun irradiance test, the bonds' oscillations were presumably lower, which resulted in lower chain scission. The presence of oxygen is a very important factor, since it accelerates the degradation processes significantly [3]. Chain scission results in the radicals that present the starting point for further oxidative reactions, which in turn leads to the formation of various end groups such as hydroxyl, carbonyl and carboxyl [3,8]. Therefore, after the aging of the PET-laminate the increase of the band at 1715 cm^{-1} assigned to carbonyl (C=O) would be expected. However, the investigation of the carbonyl peak did not result in the expected change during aging. Moreover, no changes were observed in the bands assigned to hydroxyl groups. This result indicates that the aging of the PET-laminate did not cause significant changes in the chemical structure of the outer PET layer due to oxidation.

MPO

The FTIR-ATR absorbance spectra of the inner and outer layers of MPO backsheets are shown in Figure 2.12. It can be seen that both layers are PP-based. The spectra were normalized with regards to an internal standard peak at 1168 cm^{-1} assigned to CH$_3$ wagging [62]. The peaks assignments are given in Table 2.4.

Table 2.4. Band assignments for PP (adjusted from [30])

Wavenumber [cm^{-1}]	Assignment
2953	Asymmetrical -CH_3 stretching
2921	Asymmetrical -CH_2 stretching
2869	Symmetrical -CH_2 stretching
2840	Symmetrical -CH_2 stretching
1460	Asymmetrical -CH_3 and -CH_2 bending
1370	Symmetrical -CH_3 bending, -CH_2 wagging, -CH bending, C-C backbone stretching
1305	-CH_2 wagging, -CH_2 twisting
1255	C-H bending, -CH_2 twisting, -CH_3 rocking
1164	C-C backbone stretching, -CH_3 rocking, C-H bending
998	-CH_3 rocking, C-H bending, -CH_2 wagging
973	-CH_3 rocking, C-C backbone stretching
899	-CH_2 and -CH_3 rocking, C-H bending
840	-CH_2 and -CH_3 rocking, C-C and C-CH_3 stretching
809	-CH_2 rocking , C-C and C-CH_3 stretching

The peaks in the wavenumber region from 1800 cm^{-1} to 1500 cm^{-1} probably originate from the processing additives such as erucamid, which is usually added to PP as a slip additive [63], and other processing additives and stabilizers. Analysing the spectrum in the region from 1200-800 cm^{-1} it can be concluded that the PP in MPO is an isotactic PP (iPP) type. Several bands attributed to the 3_1 helix, which is the regular conformation in all iPP polymorphs, could be observed in the absorbance spectrum of MPO: 998, 973 and 841 cm^{-1} (see an insert in Figure 2.12.) [29,30].
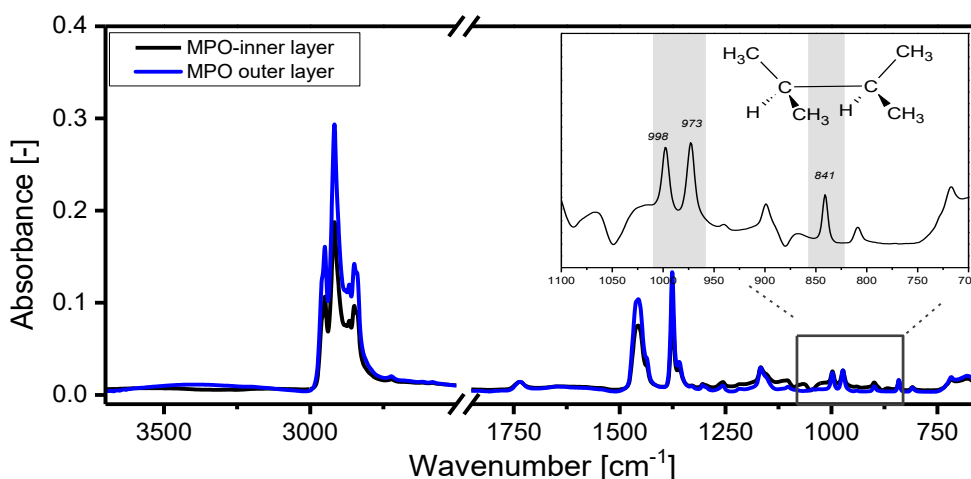

Figure 2.12. FTIR-ATR absorbance spectra of inner and outer layer of MPO backsheet

After the damp heat aging, investigation of the outer layer of MPO revealed certain changes in the region from 1800-1500 cm^{-1}. Other peaks were not affected by aging conditions. In the Figure 2.13. the absorption spectra in the region from 1800-1500 cm^{-1}

after aging is shown. The peak at 1737 cm^{-1} decreased with aging hours and almost disappeared after 2000h of damp heat. Under the sun irradiance conditions, the outer layer was not irradiated and therefore it was exposed only to lower humidity and temperature compared to the damp heat test. Hence, the significant changes of the peak at 1737 cm^{-1} were not observed. The peaks in the region from 1700-1500 cm^{-1} broaden towards the lower wavenumbers during the damp heat test and slightly increase during the sun test. This indicates that there could be a migration or "washing out" of the additives during the aging.
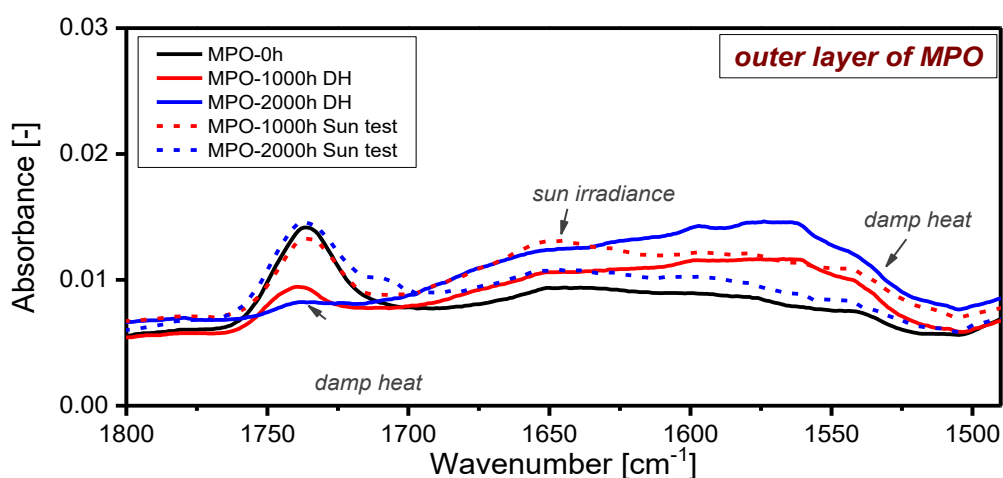
Figure 2.13. FTIR-ATR absorbance spectra of outer layer of MPO in the region from 1800-1500 cm^{-1}

Investigation of the inner layer of the MPO backsheet after the damp heat test revealed the same behaviour as the outer layer. A significant increase in the carbonyl region (C=O) due to photo-oxidation upon irradiance was not observed. No new peaks in the course of aging time indicating a significant change in the chemical structure were observed.

2.3.3 Differential scanning calorimetry (DSC)

During the artificial aging, a change of morphology of the material can occur, which is reflected in the thermal properties as well. Change in the melting enthalpy (ΔH_m, J/g) is a good indicator for the occurrence of aging processes upon physical and chemical aging [64]. Therefore, ΔH_m of both materials was evaluated before and after aging. It is important to note that the data obtained by the DSC measurements are related to the whole backsheet and it is not possible to assign the changes in the values to the individual layers. However, the thicker core layer is expected to dominate the curve.

PET-laminate

The DSC curves of unaged PET-laminate are presented in Figure 2.14. The glass transition temperature (T_g,°C) of unaged PET-laminate was detected at about 78°C and the melting peak (T_m,°C) at about 255°C.
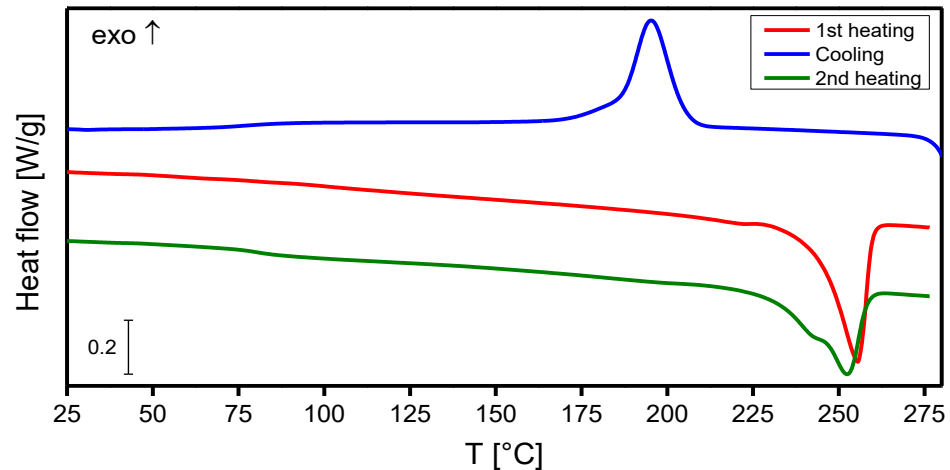
Figure 2.14. DSC curves of the PET-laminate before aging

As the T_g of the PET-laminate is below the exposure temperature in the damp heat test (T=85°C), mobility of the polymer chains was increased during aging, which accelerates the hydrolysis and chain scission. Shorter chains, formed upon hydrolytic chain scission processes, could then rearrange and form newly ordered structures (crystallites) in a process of chemo-crystallization [3]. Chain scission upon hydrolysis was indeed confirmed by the shift of the crystallization temperature (T_c,°C) towards higher values after damp heat aging (see Figure 2.15.) [3,5,64]. This shift in T_c was not that prominent after exposure of the PET laminate in sun irradiance tests due to the lower temperatures applied.
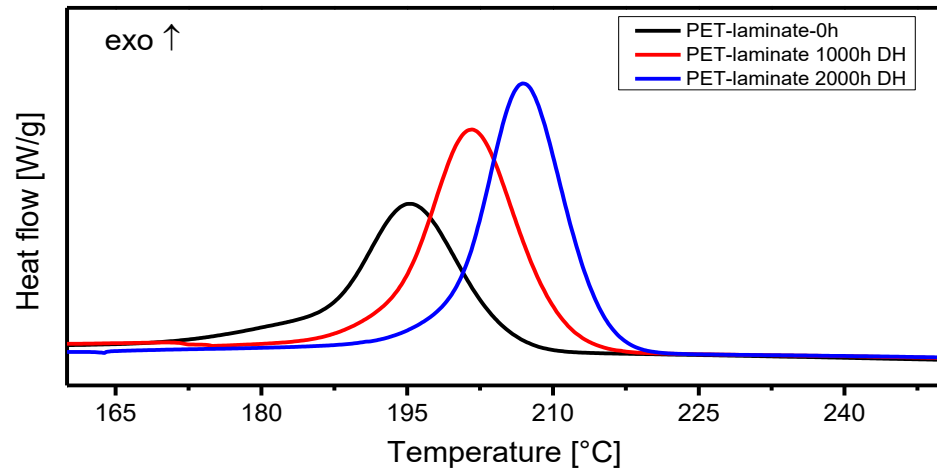
Figure 2.15. Cooling curves of the PET laminate after 0h, 1000h and 2000h of damp heat storage

The ΔH_m of the PET-laminate increased during damp heat aging due to a higher amount of crystalline content formed in chemo-crystallization (see Table 2.5). The sun irradiance test resulted in an increase in the ΔH_m as well, but no significant changes in the T_c were observed, indicating that the chain scission process did not take place. Therefore, an increase in the ΔH_m is probably caused by post-crystallization, which is a sign of physical aging [3,64]. The reversible character was confirmed by the 2nd heating. The formation of any new peaks due to chemical aging was not detected. Exposure to elevated temperature in the damp heat test resulted in a slight increase of T_m as well due to annealing (see Table 2.5.), which led to the unification of the crystallites and/or thickening of the lamellae [64].

Table 2.5. Overview of the melting temperature (T_m,°C) and melting enthalpy (ΔH_m, J/g) values for PET-laminate

	Damp heat		Sun irradiance	
t [h]	*T_m [°C]*	*ΔH_m [J/g]*	*T_m [°C]*	*ΔH_m [J/g]*
0	254.7 ± 0.7	41.7 ± 3.3	254.7 ± 0.7	41.7 ± 3.3
1000	256.1 ± 0.2	46.6 ± 8.9	255.0 ± 0.2	47.1 ± 4
2000	256.1 ± 0.2	54.1 ± 5.3	255.5 ± 0.3	53.3 ± 3.1

MPO

The DSC curves of unaged MPO are presented in Figure 2.16. The T_m of MPO was detected at about 166°C indicating an α-crystalline structure which is distinguished from the β-crystalline structure by a higher melting temperature [34]. Another melting peak at about 38°C was detected, which could be assigned to the melting of the crystallites

formed by secondary crystallization, which was confirmed by the disappearance of the peak in the 2nd heating run [3,32].
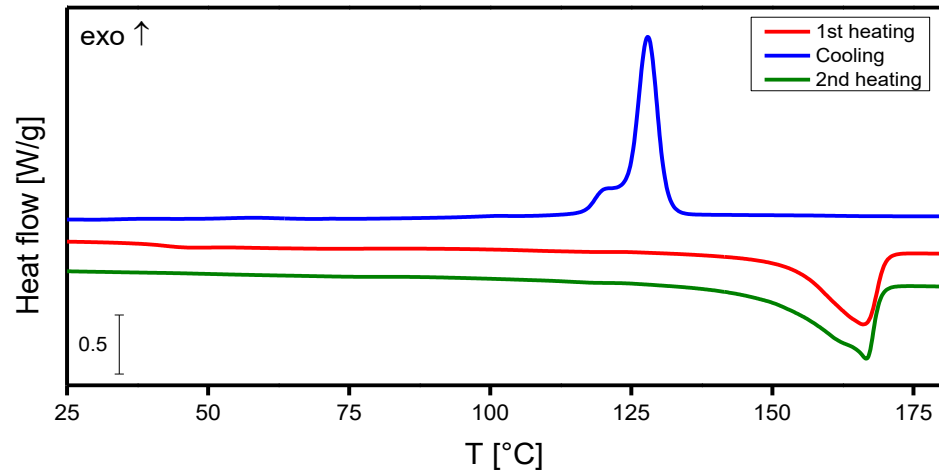
Figure 2.16. DSC curves of MPO before aging

After aging, the MPO backsheet showed a slight increase in ΔH_m upon damp heat exposure due to post-crystallization (see Table 2.6.). Furthermore, after aging a slight annealing shoulder at around 95°C (damp heat) and 60°C (sun irradiance) occurred in the 1st heating curves of MPO, as indicated by the black line in Figure 2.17. If the temperature of the accelerated aging test is between the T_g and T_m for a certain time, re-ordering of the molecular chains by releasing and rearranging physical bonds and relaxing entangled molecular chains may occur [3,36]. It can result in the formation of very small crystallites, which melt around 10-15°C above the annealing temperature [64].
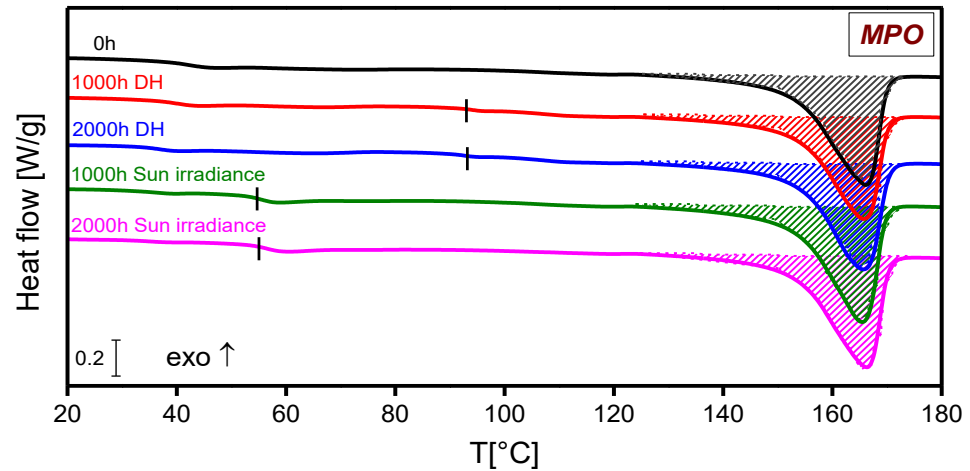
Figure 2.17. DSC curves of the 1st heating of MPO after aging

From the values in Table 2.6. it can be seen that the T_m shifted towards lower values with aging time for both tests. These results could indicate the deterioration of the crystalline structure or thinner crystalline lamellae [3,64].

Table 2.6. Overview of the melting temperature (T_m,°C) and melting enthalpy (ΔH_m, J/g) values for MPO backsheet

|	Damp heat		Sun irradiance	
t [h]	T_m [°C]	ΔH_m [J/g]	T_m [°C]	ΔH_m [J/g]
0	169.9 ± 0.4	49.6 ± 2.6	169.9 ± 0.4	49.6 ± 2.6
1000	165.8 ± 0.1	53.2 ± 3.6	165.9 ± 0.8	52.5 ± 2.4
2000	165.5 ± 0.2	54.4 ± 4.1	166.1 ± 0.1	58.3 ± 2.8

The cooling curves of the MPO backsheet did not show any significant changes upon accelerated aging under damp heat or irradiance tests indicating that no stress-induced chain scission took place. Furthermore, no new peaks, which would indicate chemical aging, were detected. Hence, it can be concluded that artificial aging under the chosen stress conditions did not cause significant changes in the thermal properties of the MPO backsheet.

2.3.4 Tensile test

Upon exposure at elevated temperatures, the crystallite thickness can increase or certain crystallites can rearrange in processes of post- and/or re-crystallisation. An increased degree of crystallinity leads to embrittlement of the material which is indicated by an increase in the yield stress [3–5,10,12,64–66]. Due to chain cleavage processes (chemical aging), the polymer chains become shorter, which affects the load transfer

along the chain, i.e. ability of the material to elongate with increasing load. This is reflected in a decrease in the strain-at-break, ε_B (%) values. Hence, the yield stress, σ_y (MPa) and ε_B (%) are two good indicators of the mechanical properties and their changes can be closely correlated to physical and/or chemical aging processes [3,10,65,67].

PET-laminate

The stress-strain curves of the PET-laminate in machine direction are shown in Figure 2.18. The Young's modulus, *E* (MPa) is measured at about 2800 MPa.
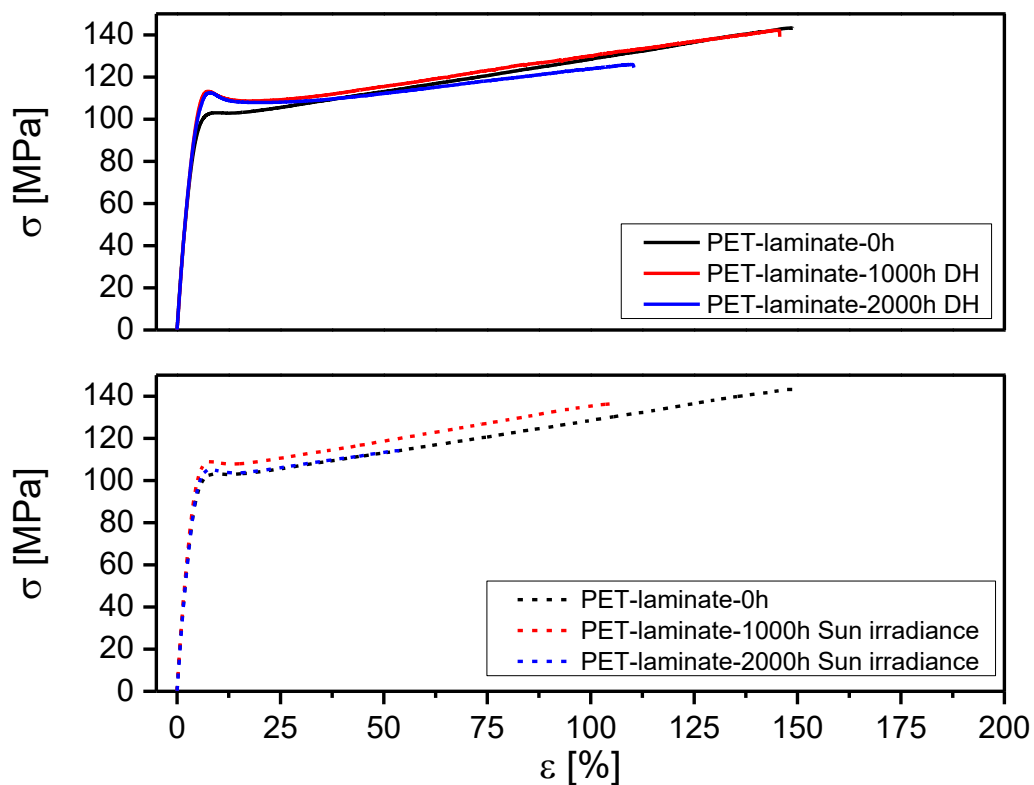
Figure 2.18. Stress-strain curves of the PET-laminate before and after aging

After aging, the PET-laminate showed a reduction in ε_B (%), which can be explained by the on-going chain scission (see Figure 2.19.) starting at 1000h. The relative decrease of the ε_B (%) values was higher after the sun irradiance test (70% decrease of ε_B after 2000h) than after the damp heat test due to the presence of certain amounts of UV light. Because of annealing, i.e. physical aging, the values of σ_y increased with the exposure time, as shown in Figure 2.19. [10,68]. The relative increase in σ_y was slightly more prominent after damp heat aging than upon accelerated aging with irradiance due to the higher increase in crystallinity.
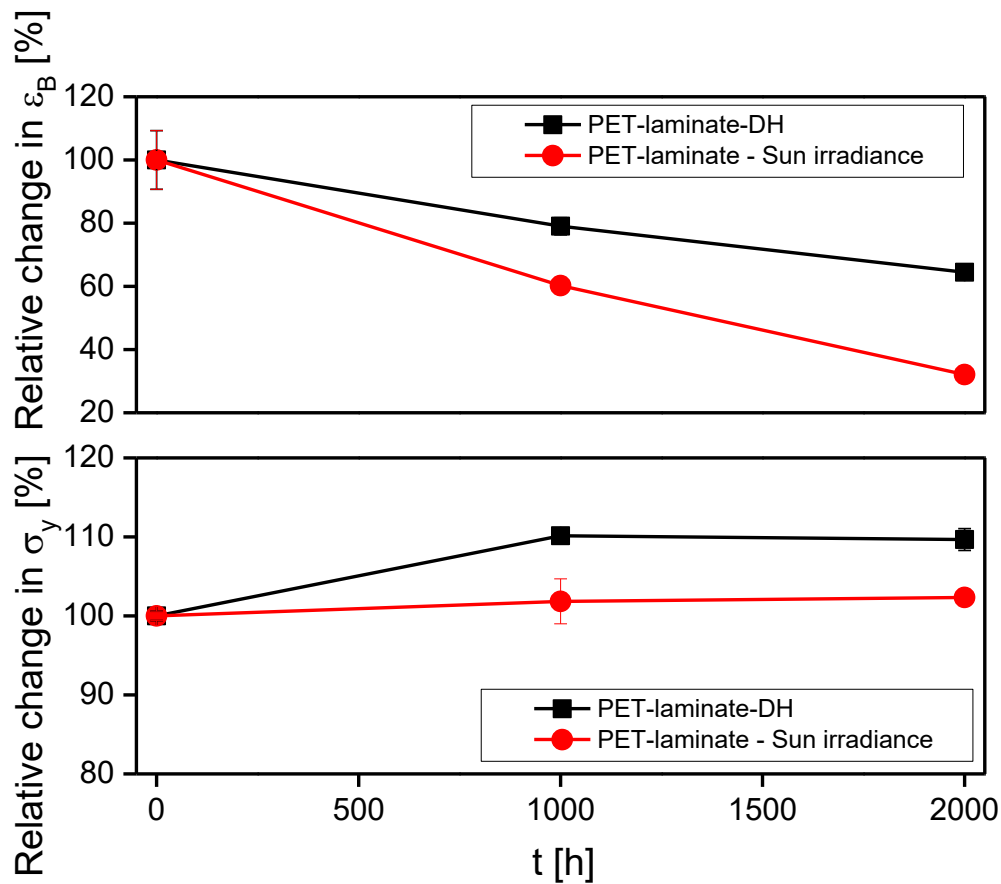
Figure 2.19. Relative change of strain-at-break, ε_B and yield stress, σ_y for PET-laminate before and after aging

Visual observation during the tensile testing revealed a more homogenous failure, i.e. simultaneous break of all layers for samples with increasing aging hours compared to the unaged samples where the failure of each layer was obtained at mostly different stress levels. In some unaged PET-laminate samples even delamination occurred. The observed changes in mechanical properties are in good correlation with the results of DSC analysis since an increased degree of crystallinity and chain scission directly influence the mechanical properties [12,32,64].

MPO

The stress-strain curves of unaged MPO are shown in Figure 2.20. The shape of the curves is typical for ductile polymers with strain hardening. At very low strain rates, a total orientation in the plane parallel region of the specimen is achieved. Here the load is no longer absorbed by intermolecular forces but primarily by valence bonds which increases an effect within the material known as work hardening [69]. A value of about

1130 MPa is obtained for the Young's modulus with elongation of up to almost 1100 % (almost 10 times higher than the PET-laminate). In Figure 2.20. it is also visible that MPO exhibits a yield point at which local necking followed by a constant stress plateau occurs (also known as cold yielding) [32,69]. According to Grellmann et al. [69] such a stress plateau is the result of a stretching of the material accompanied by a pulling out of the un-stretched part of the specimen. This leads to an orientation by aligning the molecules in the direction of the loading [69]. According to Albertsson et al. [41] the initial stage of deformation is a result of a simple rigid displacement of crystalline lamellas when the service temperature of semi-crystalline polyolefins is above their T_g, (which usually is the case). The tie-chains that are present in the amorphous inter-lamellar zones seem to play a key role in the plastic deformation since they allow load transfer between crystallites and ensuing destruction of the lamellar structure by chain-slip and lamellar break-up [37,67].
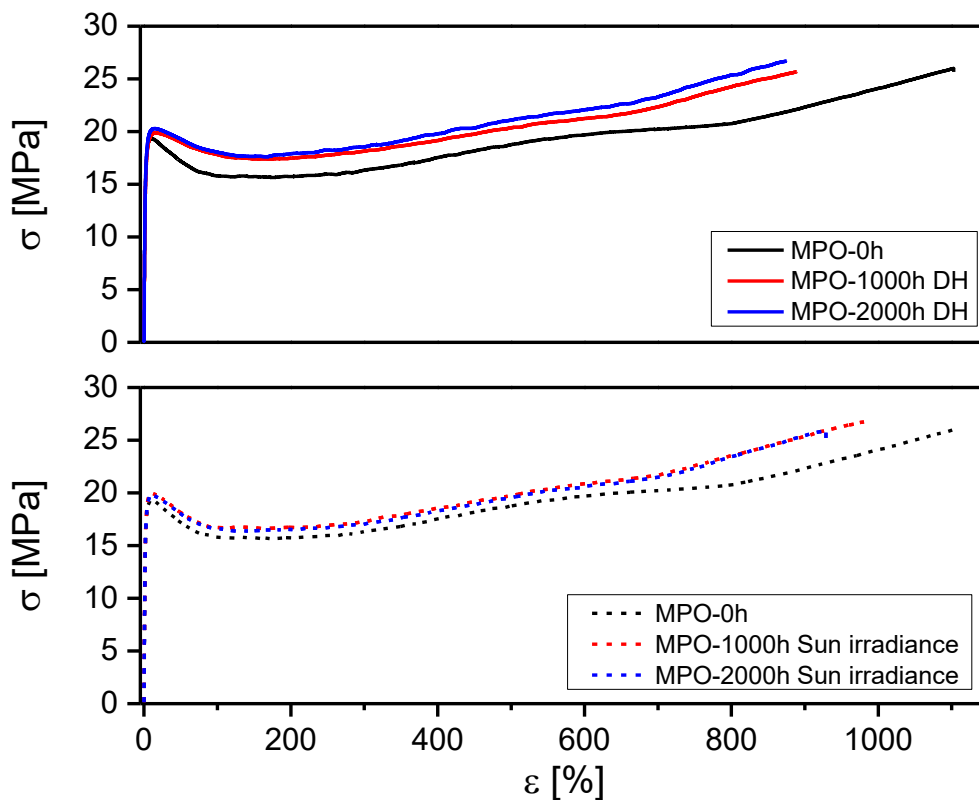

Figure 2.20. Stress-strain curves of MPO backsheet before and after aging

After the accelerated aging, the MPO backsheet showed a reduction of ε_B of up to 20% (see Figure 2.21.). The decrease of ε_B was slightly more pronounced after the damp heat test. According to Fayolle et al. [67] material fracture occurs when a hyper oriented

domain (which transmits load to less oriented domains through a decrease of the cross sectional area) contains a critical size defect. This defect creates a stress concentration which leads to rupture. Of course, the rupture point depends then on the homogeneity of the sample. However, the thicker crystallites that are formed during post-crystallization could present such defects [67]. An increase in σ_y (see Figure 2.21.) occurred due to an increased crystallinity upon annealing (physical aging). Yield stress depends essentially on the crystallinity ratio (especially through the crystallite thickness) which increases through annealing [3,32,64,67]. If oxidation takes place in the amorphous phase only, then it is not expected to have much influence on the yield properties except when extensive chain scission results in chemo-crystallisation [37,38,67,70]. Essentially all polyolefins, especially PE and PP oxidise exclusively in the amorphous phase because the crystalline phase is impermeable to oxygen [70]. The observed increase in σ_y of the MPO backsheet is not as significant as was observed for the PET-laminate, which can be easily explained by the missing chain scission upon oxidation and a lower increase in crystallinity in MPO.
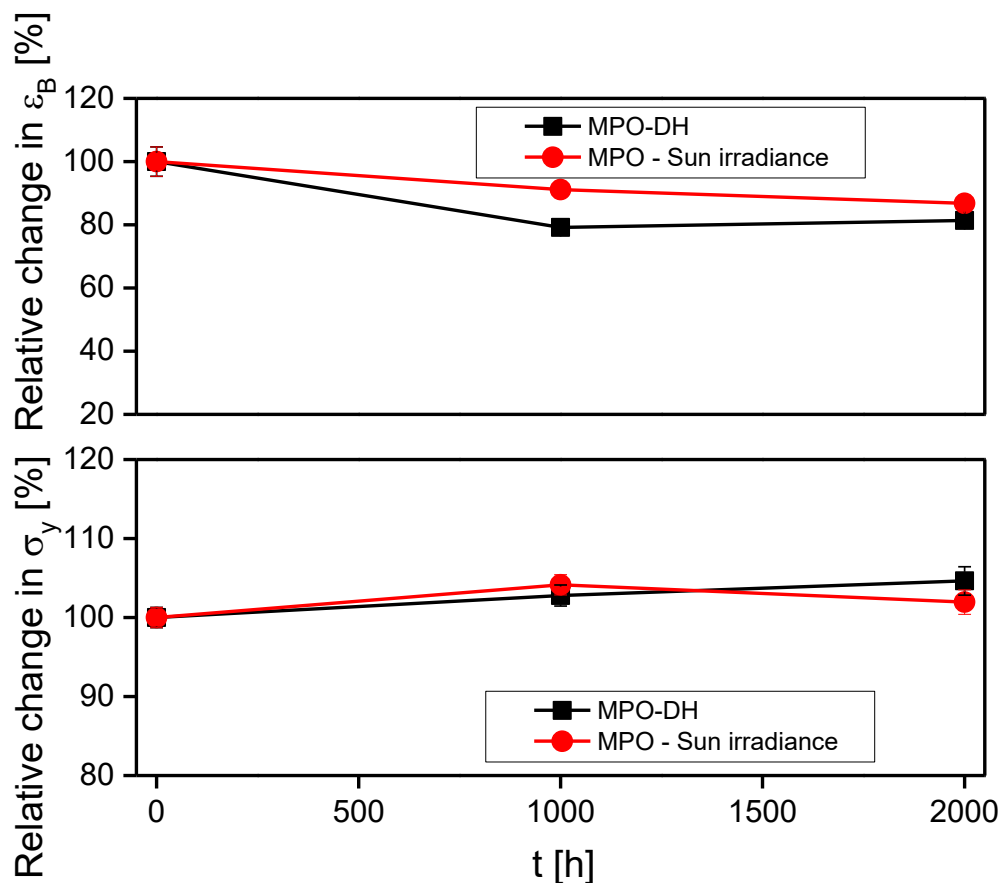

Figure 2.21. Relative change of strain-at-break, ε_B and yield stress, σ_y for MPO backsheets before and after aging

2.3.5 Thermo-mechanical analysis (TMA)

Thermo-mechanical properties of the PV backsheets are of great importance during lamination and outdoor operation of the modules. The high temperature of lamination can induce certain changes in material behaviour such as a relaxation from orientations and stresses, which can lead to dimensional instability of the backsheet (shrinkage, appearance of waves) [71]. Moreover, mismatches in the coefficient of thermal expansion (CTE) of different PV components can introduce internal stresses, which can, immediately or during service, lead to different failure modes (e.g. delamination of the backsheet, delamination from the encapsulant, cracking of the cell) [32,71].

Exposure of polymers to elevated temperatures, humidity and UV irradiation causes certain changes in the physical and/or chemical structure of the material which can be reflected in their thermo-mechanical properties as well [3,32,64]. When thermoplastics are exposed to temperatures above the T_g, orientations and stresses may relax, resulting in post-crystallization and re-crystallization processes [64]. Therefore, the thermo-mechanical curves could be a good indicator of the aging processes, in particular physical aging processes. The thermo-mechanical behaviour of the backsheets during lamination could be determined from the first heating curve. On the other hand, application-relevant thermo-mechanical behaviour could be determined from the second heating curve, where the thermal history of the material is removed via lamination. Since the operating temperature for most of the PV modules is in the range of 25°C to 85°C, this range will be considered when discussing the thermomechanical behaviour of the investigated backsheets before and after aging.

PET-laminate

The thermal expansion curves of unaged PET-laminates in machine direction (MD) and counter direction (CD) are shown in the Figure 2.22. Unaged PET-laminates showed anisotropic behaviour with shrinkage in MD and expansion in CD, which is a consequence of the drawing off of the film during production and is a well known behaviour of extruded polymers [64,71–74]. From the morphology point of view, anisotropic behaviour is a consequence of the alignment of crystals along the chain axis and the formation of inter-crystalline bridges, which are correlated with the negative CTE, as observed for MD [74–76]. The reason for shrinkage in MD could be a higher degree of orientation in MD during production, which means that polymer chains in CD have higher mobility, leading to expansion under applied conditions [64,77]. Anisotropic behaviour could exclude biaxial orientation. It has to be kept in mind that the investigated PET-laminate backsheet is a laminate of three different layers (see Table 2.1.). It is

possible that only the outer PET-layer is biaxial in order to prevent moisture ingress towards core layer and it is usually not a requirement that the core layer is biaxially stretched as well. Anisotropic behaviour could lead to dimensional instability and therefore induce certain stresses in the PET-laminate during the lamination of PV modules [3]. In the 2nd heating run anisotropy disappears, since another heating provides higher mobility of the frozen chains and allows oriented molecules to move into their thermo-dynamically preferred position [3,78,79]. Since the processing history is removed with the 1st heating run, the 2nd heating run provides information on material constants. The difference in CTE between the 1st and 2nd heating runs in both direction indicates a relaxation from orientations and/or stresses [64,71,80]. In the 1st heating run the slope starting at about 70°C in MD and 90°C in CD was observed. This corresponds to the higher mobility of the polymer chains as the T_g range (T_g of PET-laminate is about 78°C) was crossed [32,64]. Since the 1st heating run of the backsheet could be related to the lamination of the PV module, it can be said that the 2nd heating run is relevant for application. Therefore, from the different CTE obtained in the 2nd heating curves in MD and CD it can be seen that the lamination could import certain stresses, which could be relevant for the application.
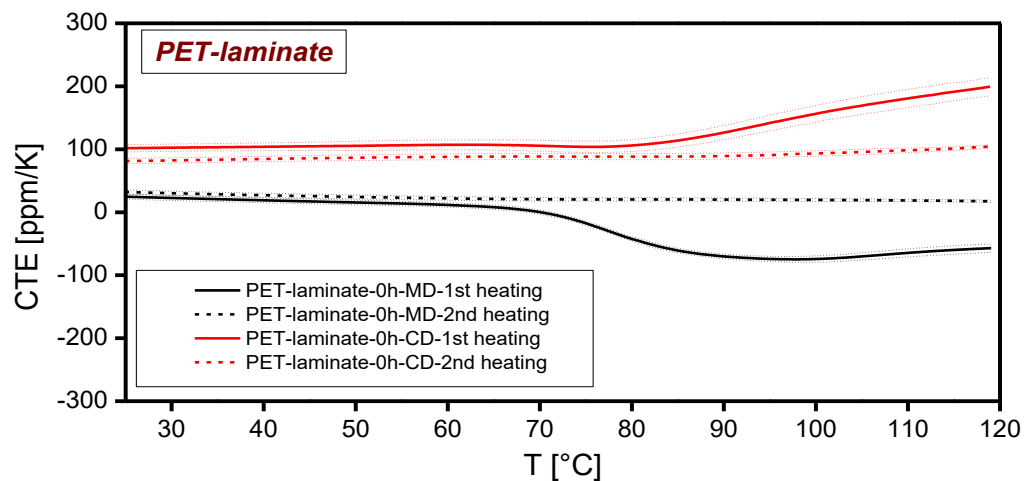
Figure 2.22. TMA curves of PET-laminate before aging in MD and CD with standard deviation as an envelope

Exposure of the PET-laminate at elevated temperatures during aging in damp heat conditions led to an increased degree of crystallinity upon chain scission and chemo-crystallization processes, as revealed by DSC analysis. Chain scission resulted in the shorter polymer chains and maybe disturbed the existing degree of orientation of the polymer chains. Due to the shortening of the polymer chains, their mobility increased,

which could explain an increased expansion in MD after aging. This effect was more pronounced in CD, again, probably due to the initially higher degree of mobility of the polymer chains. Due to the higher temperature in the damp heat test and shorter polymer chains (as indicated by cooling curves), this effect was more pronounced for the damp heat aged samples (see Figure 2.23a.) than for those aged under sun irradiance conditions (see Figure 2.23b.). The 2nd heating run showed differences in CTE values compared to unaged samples. For comparison, the CTE values in the range from 25°C to 85°C before and after aging are summarized in the Table 2.7.. The values of CTE in the 2nd heating run after aging indicated changes in the thermo-mechanical behaviour upon aging and the effect was stronger after damp heat aging.

Figure 2.23. TMA curves of PET-laminate before and after a) damp heat aging and b) Sun irradiance test in MD and CD with standard deviation as an envelope
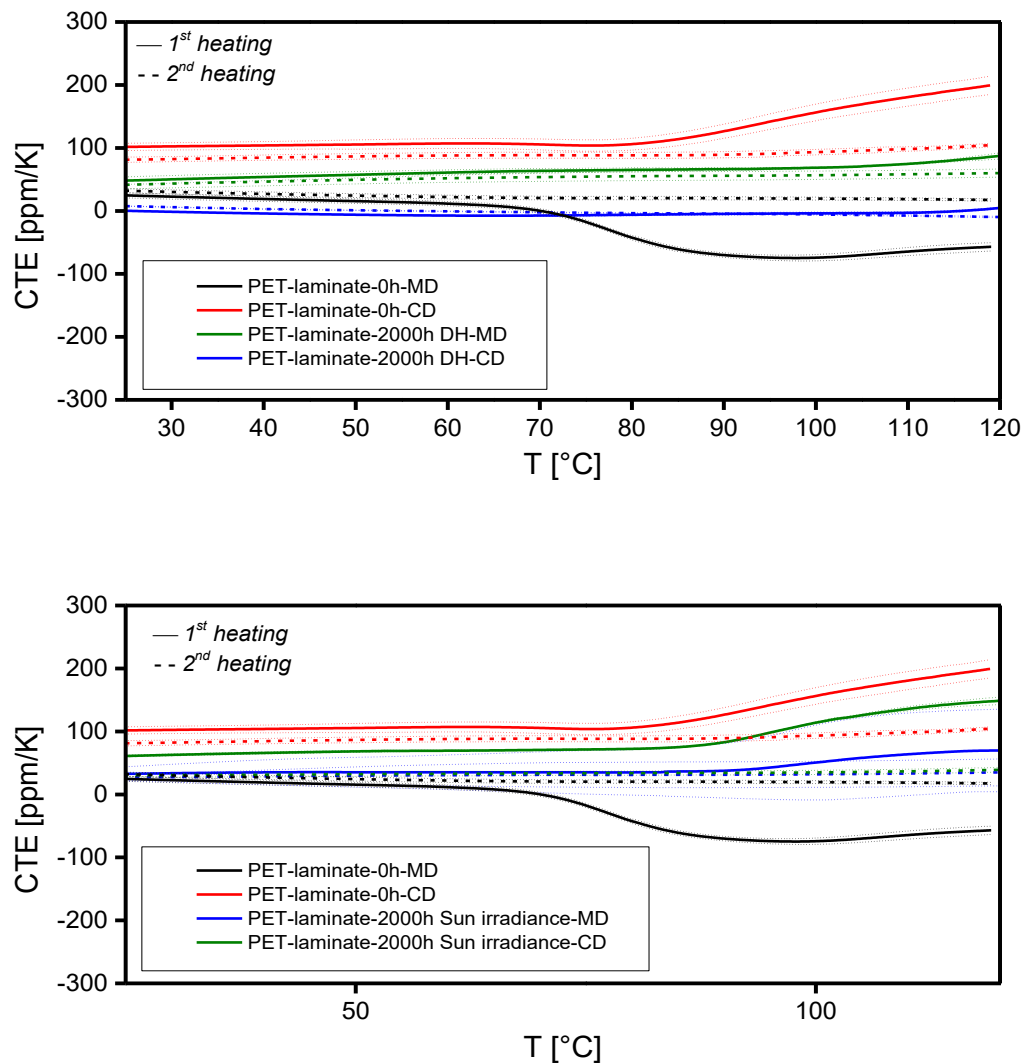
Table 2.7. CTE values of the 1st and 2nd TMA heating run for PET-laminate backsheet in the range from 25°C to 85°C

PET-laminate	1st MD	2nd MD	1st CD	2nd CD
Unaged	-61 ± 3.6	20.3 ± 2.6	114.2 ± 10.4	88.5 ± 4.8
Damp heat	65.7 ± 2.7	55.5 ± 7	-5.4 ± 1.7	-3.4 ± 0.6
Sun irradiance	36.5 ± 40	31.2 ± 20.4	75.1 ± 0.7	34 ± 3.2

MPO

In Figure 2.24. TMA curves of MPO in the MD and CD directions before aging are presented. It can be seen that the 1st heating resulted in expansion in both directions indicating biaxial orientation. Biaxial stretching improves mechanical, optical and barrier properties of the polymeric films [81,82]. The CTE is higher in the CD compared to MD direction. This observation could indicate a lower degree of crystallite orientation in CD, which enabled higher mobility of the polymer chains in the applied temperature range. Such a difference in the expansion between CD and MD could introduce certain stresses during lamination. The difference in the CTE between the 1st and 2nd heating runs in both directions indicates relaxation from orientations and stresses upon applied heating [64,71,80]. The 2nd TMA heating run curves are almost overlapped in both directions, which indicates that lamination would not induce stresses caused by a difference in CD and MD. The slope of about 45°C in MD and 55°C in CD occurs in the 1st heating run curve. This slope could be assigned to the melting of the crystals from secondary crystallization and is in good correlation with the thermal behaviour of MPO (see section 2.3.3.) For semi-crystalline polymers, secondary crystallization can significantly contribute to thermo-mechanical behaviour [3,80]. Secondary crystallization is influenced by the molecular structure and thermal history (during processing and storage time) [3,83].
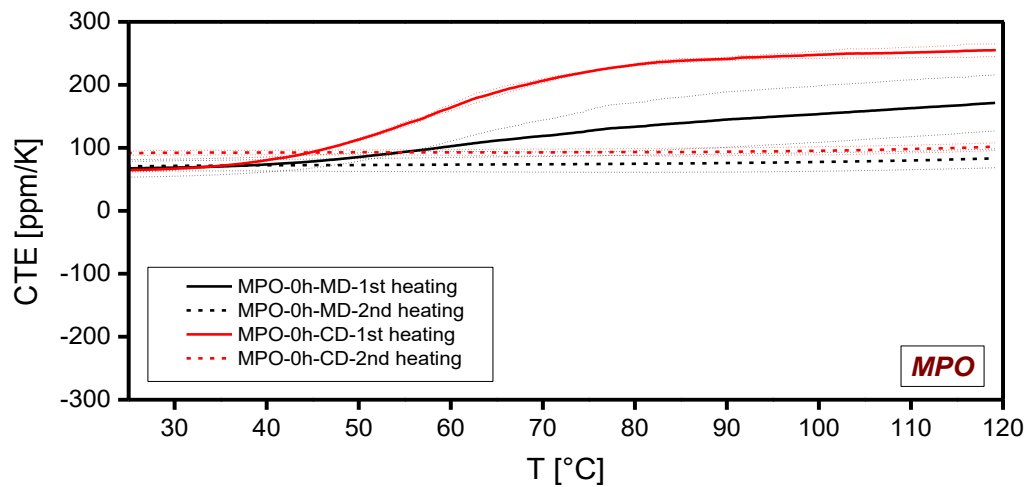
Figure 2.24. TMA curves of MPO backsheet before aging in MD and CD with standard deviation as an envelope

After the damp aging (see Figure 2.25a.), the 1st heating in MD resulted in high deviation and it is hard to evaluate whether the CTE indeed increased or decreased. The expansion in CD decreased due to an increased degree of crystallinity, as revealed by DSC analysis. After sun irradiance, the 1st heating in both directions resulted in a decreased expansion. Since DSC results revealed an increased degree of crystallinity due to post-crystallization of MPO, this could be the reason for decreased expansion upon aging. With increased crystallinity, the amount of free volume available for polymer chain motions is reduced, which affects the thermo-mechanical behaviour [14]. The 2nd heating run resulted in isotropic expansion after damp heat aging. This observation indicates that lamination and aging of the MPO would not affect its CTE behaviour during service. The sun irradiance test resulted in the shift of the slope in MD to higher values of about 60°C, which can be correlated with the melting of crystallites formed by annealing as revealed by DSC analysis (see section 2.3.3.). The CTE values of the 2nd heating run after sun irradiance changed, compared to unaged MPO (see Table 2.8.), which could indicate irreversible changes in the material [64] However, the observed changes in CTE after aging are lower compared to PET-laminate indicating higher thermo-mechanical stability.
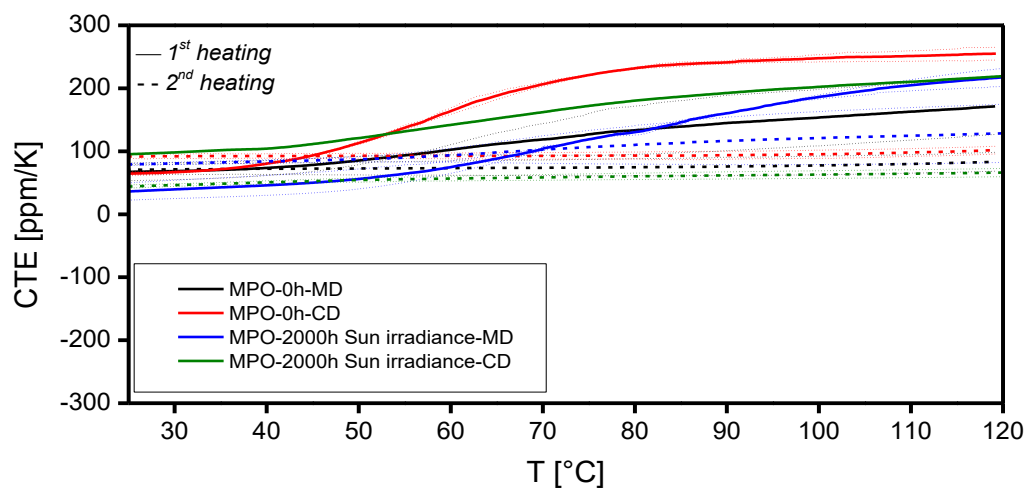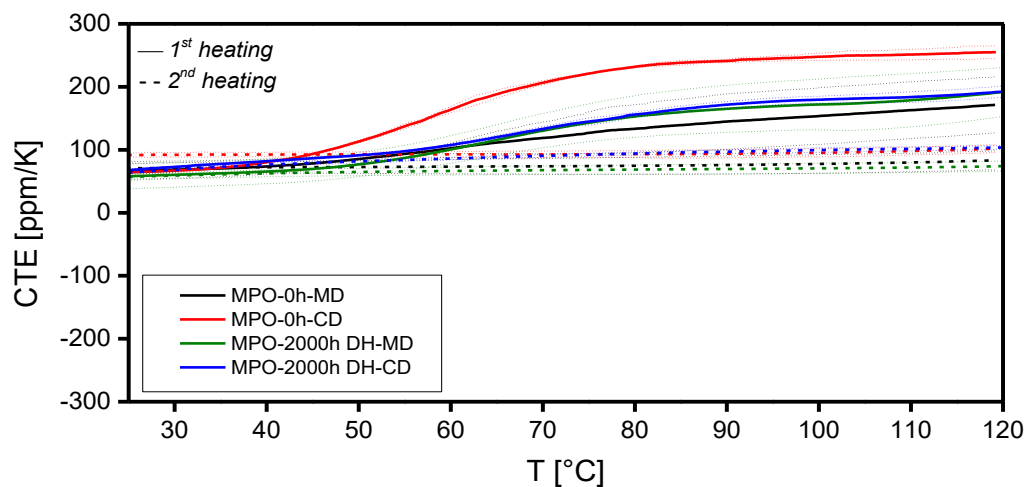
Figure 2.25. TMA curves of MPO before and after a) damp heat aging and b) Sun irradiance test in MD and CD with standard deviation as an envelope

Table 2.8. CTE values of the 1st and 2nd TMA heating run for MPO backsheet in the range from 25°C to 85°C

MPO	1st MD	2nd MD	1st CD	2nd CD
Unaged	139.1 ± 41.3	75.1 ± 13.9	236.2 ± 3.6	93.2 ± 6.4
Damp heat	160 ± 35.3	69.1 ± 7.6	164.9 ± 4.7	95.8 ± 2.5
Sun irradiance	146.6 ± 3	61 ± 5.4	113.2 ± 34	85.3 ± 0.7

2.3.6 Feasibility of PET replacement via MPO backsheets

The systematic investigation of a PET-laminate as a state-of-the-art backsheet and of an MPO backsheet as an alternative was done in order to determine their weathering stability under applied accelerated aging tests. As revealed by FTIR-ATR spectroscopy, the outer PET layer in the PET-laminate showed a decrease of the peaks assigned to the stretching vibration of the backbone, indicating chain scission upon hydrolysis. However, no oxidation products were detected, which indicated that the chemical structure of the outer PET layer was not affected significantly. Chain scission led to chemo-crystallization that was confirmed by DSC analysis via a gradual shift in the crystallization temperature and an increase of crystallinity. Changes in the morphology, in turn, affected the mechanical properties and resulted in embrittlement and reduced elongation-at-break, which was additionally accelerated under sun irradiance tests due to the portion of UV irradiation. These results highlighted typical drawbacks of PET-based backsheets (embrittlement and cracking). Such behaviour in the field was reported to give rise to many other failure modes, due to an increased moisture ingress, such as delamination of the backsheet, corrosion of the interconnections and cell, delamination of the front encapsulant, etc. [84]. On the other hand, due to an inherent hydrolysis resistance of polyolefins, the MPO did not show any significant change in the morphology that could affect its thermal and mechanical properties after accelerated aging. In fact, MPO retained its flexibility even after 2000h of aging. TMA analysis showed the thermal expansion of MPO in both directions in the applied temperature range (25°C-120°C) which could lead to fewer internal stresses after lamination compared to the PET-laminate that showed anisotropic behaviour. Moreover, CTE values of MPO backsheets are closer to the CTE values of encapsulants (see Chapter 4), which could also contribute to lower stresses in the PV module upon lamination. However, in order to assess the actual build-up of internal stresses in the PV module after lamination, more in-depth measurements are necessary, which have not been the scope of this work.

Based on the presented results, it can be concluded that the MPO backsheet could provide excellent weathering stability in the field. Moreover, due to an inherent resistance to hydrolysis and great stability against UV irradiation, it could be an excellent backsheet for harsh climatic conditions such as high humidity and/or irradiation. From the reliability and sustainability point of view, MPO could be a great alternative to standard PET-based backsheets.

2.4   Summary and conclusions

To overcome the always-rising challenges of reliability of the PV modules, cost reduction and sustainability, one of the solutions is the application of new materials for PV components. For this, the co-extruded polyolefin backsheets are drawing attention over commonly used PET/fluoropolymer backsheets as they exhibit many favourable characteristics. However, being new on the market, their weathering stability has not been fully investigated yet. Hence, in this work, the weathering stability of a newly developed modified polyolefin (MPO) backsheet as an alternative to currently used PET/fluoropolymer (PET-laminate) backsheets was systematically investigated. For this purpose, UV/Vis/NIR and FTIR-ATR spectroscopy, differential scanning calorimetry (DSC), tensile tests and thermo-mechanical analysis (TMA) were chosen as characterization methods.

Artificial aging of the PET-laminate under damp heat conditions resulted in chain scission and chemo-crystallization, which led to the deterioration of mechanical properties in terms of embrittlement and decreased elongation-at-break. Deterioration of the mechanical properties was even more pronounced in the presence of irradiance as an accelerating factor (70% decrease in elongation). The results of TMA showed that the lamination of the PET-laminate could induce certain stresses in the PV module due to an anisotropic expansion. Thermomechanical properties were affected by aging due to an increased degree of crystallinity, which reduced the free fractional volume available for mobility of polymer chains. Such deterioration of the thermal and mechanical properties could result in cracking in the field, which can give rise to many failure modes of PV modules.

A slight post-crystallization of the MPO did not affect the mechanical properties significantly. A slight reduction in the elongation-at-break (20% decrease) and a slight increase of the yield stress due to annealing was detected after damp heat testing and is acceptable for PV applications. TMA analysis revealed thermal expansion in both directions, which could induce fewer internal stresses upon lamination compared to a PET-laminate. Aging did not result in significant changes in thermomechanical properties.

In order to increase the reliability of PV modules in the field, it is important to make sure that materials for PV components provide sufficient weathering stability during service time. The characterization methods applied in this work were shown to be convenient and reliable in determining the weathering stability of both types of backsheets.

Based on the results presented in this work, it can be concluded that the weathering stability of the MPO laminate is higher than of the PET-laminate under the conditions of the applied accelerated aging tests. Due to an inherent resistance to hydrolysis and great stability against UV irradiation, it could be a good backsheet for harsh climatic conditions such as high humidity and/or irradiation. The MPO backsheet could be a good candidate as a replacement for the PET-based backsheet concerning the reduction of cracking and embrittlement in the field without compromising the reliability of PV modules.

2.5 References

[1] S. Koltzenburg, M. Maskos, O. Nuyken, Polymer Chemistry, 1st ed., Springer Berlin Heidelberg, 2017.

[2] J. Scheirs, T.E. Long, Modern polyesters: Chemistry and technology of polyesters and copolyesters, John Wiley & Sons, Hoboken, N.J., 2003.

[3] G.W. Ehrenstein, S. Pongratz, Resistance and stability of polymers, Hanser Publishers, Munich, 2013.

[4] B. Ottersböck, G. Oreski, G. Pinter, Correlation study of damp heat and pressure cooker testing on backsheets, J. Appl. Polym. Sci. (2016). https://doi.org/10.1002/APP.44230.

[5] M. Knausz, G. Oreski, G.C. Eder, Y. Voronko, B. Duscher, T. Koch, G. Pinter, K.A. Berger, Degradation of photovoltaic backsheets: Comparison of the aging induced changes on module and component level, J. Appl. Polym. Sci. 132 (42093) (2015) 1–8. https://doi.org/10.1002/app.42093.

[6] N.S. Allen, M. Edge, M. Mohammadian, K. Jones, Physicochemical aspects of the environmental degradation of poly(ethylene terephthalate), Polymer Degradation and Stability 43 (2) (1994) 229–237. https://doi.org/10.1016/0141-3910(94)90074-4.

[7] K. Kanuga, Degradation of Polyester Film Exposed to Accelerated Indoor Damp Heat Aging, in: 37th IEEE Photovoltaic Specialists Conference, Seattle, Washington, 19-24 June, 2011.

[8] F. Dubelley, E. Planes, C. Bas, E. Pons, B. Yrieix, L. Flandin, The hygrothermal degradation of PET in laminated multilayer, European Polymer Journal 87 (2017) 1–13. https://doi.org/10.1016/j.eurpolymj.2016.12.004.

[9] G. Griffini, S. Turri, Polymeric materials for long-term durability of photovoltaic systems, Journal of Applied Polymer Science 133 (11) (2016). https://doi.org/10.1002/app.43080.

[10] G. Oreski, G.M. Wallner, Aging mechanisms of polymeric films for PV encapsulation, Solar Energy 79 (6) (2005) 612–617. https://doi.org/10.1016/j.solener.2005.02.008.

[11] B. Ottersböck, Natural and artificial weathering tests of polymer films used in solar applications. Doctoral Thesis, Leoben, AUT, April/2017.

[12] K.P. Menard, Dynamic Mechanical Analysis: A practical introduction, 1st ed., CRC Press, USA, 1999.

[13] Z. Xia, J.H. Wohlgemuth and D.W. Cunningham, A Lifetime Prediction of PV Encapsulant and Backsheet via Time Temperature Superposition Principle, in: 34th IEEE Photovoltaic Specialists Conference (PVSC), Philadelphia, Pennsylvania, USA, 7-12 June, 2009.

[14] John Wiley and Sons, Encyclopedia of Polymer Science and Technology - Barrier polymers, 1999-2012.

[15] Z. Shi, A. Fujita, Extremely enhanced hydrolytic stability of poly(ethylene terephthalate) films, Polym Eng Sci 58 (3) (2018) 261–271. https://doi.org/10.1002/pen.24562.

[16] I.M. Ward, Structure and Properties of Oriented Polymers, Applied Science Publishers LTD, London, 1997.

[17] J.-F. Tassin, M. Vigny, D. Veyrat, Biaxial stretching of pet films: A molecular description, Macromol. Symp. 147 (1) (1999) 209–220. https://doi.org/10.1002/masy.19991470121.

[18] P. Sánchez-Friera, M. Piliougine, J. Peláez, J. Carretero, M. Sidrach de Cardona, Analysis of degradation mechanisms of crystalline silicon PV modules after 12 years of operation in Southern Europe, Prog. Photovolt: Res. Appl. 19 (6) (2011) 658–666. https://doi.org/10.1002/pip.1083.

[19] Chiao-Chi Lin, Peter J. Krommenhoek, Stephanie S. Watson, Xiaohong Gu, Depth profiling of degradation of multilayer photovoltaic backsheets after accelerated laboratory weathering: Cross-sectional Raman imaging, Solar Energy Materials and Solar Cells 144 (2016) 289–299. https://doi.org/10.1016/j.solmat.2015.09.021.

[20] Fernando D. Novoa, David C. Miller, Reinhold H. Dauskardt, Environmental mechanisms of debonding in photovoltaic backsheets, Solar Energy Materials and Solar Cells 120, Part A (0) (2014) 87–93. https://doi.org/10.1016/j.solmat.2013.08.020.

[21] M. DeBergalis, Fluoropolymer films in the photovoltaic industry, Journal of Fluorine Chemistry 125 (8) (2004) 1255–1257. https://doi.org/10.1016/j.jfluchem.2004.05.013.

[22] H. Hu, W.M. Wang, O. Fu, A. Bradley, T. Felder, W. Gambogi and T.J. Trout, Typical Photovoltaic Backsheet Failure Mode Analysis Under Different Climates in China, in: SNEC 2016, Shanghai.

[23] A. Lefebvre, G. O'Brien, D. Althouse, B. Douglas, G. Moeller, D. Garcia, T. Fine, A. Bonnet, Weathering Performance of PV Backsheets, in: 2013 PV Module Reliability Workshop.

[24] S.Huber, M.K. Moe, N. Schmidbauer, G. Hansen and D. Herzke, Emissions from incineration of fluoropolymer materials: A literature survey, 2009.

[25] L. Maras, Environmental challenges disposing of backsheets at PV module EOL, in: EU PVSEC, Munich, Germany 2016.

[26] K. Oberbach (Ed.), Kunststoff Taschenbuch, 27th ed., Carl Hanser Verlag München Wien, 1998.

[27] R. Mülhaupt, Ziegler-Natta catalysis and propylene polymerization: In: Karger-Kocsis J. (eds) Polypropylene, Springer, Dordrecht, 1999.

[28] J. Karger-Kocsis, Polypropylene Structure, blends and composites: Volume 1 Structure and Morphology, Springer Science & Business Media, 1995.

[29] F.A. Miller, D.W. Mayo, R.W. Hannah, Course notes on the interpretation of infrared and Raman spectra, Wiley-Interscience, Hoboken N.J., 2004.

[30] E. Andreassen, Infrared and Raman spectroscopy of polypropylene: In: Karger-Kocsis J. (eds) Polypropylene, Springer, Dordrecht, 1999.

[31] M.T. DeMseuse, Biaxial Stretching of Film: Polyolefins used in biaxial stretched films, 1st ed., Woodhead Publishing Limited, Daryaganj, New Delhi, India, 2011.

[32] G.W. Ehrenstein, Polymeric Materials: Structure, Properties, Application, Carl Hanser Verlag GmbH & Co. KG, 2001.

[33] B. Wunderlich, Thermal Analysis of Polymeric Materials, Springer-Verlag Berlin Heidelberg, Berlin, Heidelberg, 2005.

[34] P. Tordjeman, C. Robert, G. Marin, P. Gerard, The effect of α, β crystalline structure on the mechanical properties of polypropylene, The European Physical Journal E 4 (4) (2001) 459–465. https://doi.org/10.1007/s101890170101.

[35] S.C. Tjong, J.S. Shen, R. Li, Morphological behaviour and instrumented dart impact properties of β-crystalline-phase polypropylene, Polymer 37 (12) (1996) 2309–2316. https://doi.org/10.1016/0032-3861(96)85340-7.

[36] H.B. I. Karacan, The Influence of Annealing Treatment on the Molecular Structure and the Mechanical Properties of Isotactic Polypropylene Fibers, Journal of Applied Polymer Science 122 (2011.).

[37] J.M.Schultz, Microstructural aspects of failure in semicrystalline polymers, Polymer Engineering and Science 24 (10) (1984) 770–785.

[38] G.M. A.B. Mathur, Thermo-oxidative degradation of isotactic polypropylene film: Structural changes and its correlation with properties, Polymer 23 (1982) 54–56.

[39] C. Rouillon, P.-O. Bussiere, E. Desnoux, S. Collin, C. Vial, S. Therias, J.-L. Gardette, Is carbonyl index a quantitative probe to monitor polypropylene photodegradation? Polymer Degradation and Stability 128 (2016) 200–208. https://doi.org/10.1016/j.polymdegradstab.2015.12.011.

[40] W.S. Subowo, M. Barmawi, O.B. Liang, Growth of carbonyl index in the degradation of polypropylene by UV irradiation, J. Polym. Sci. A Polym. Chem. 24 (6) (1986) 1351–1362. https://doi.org/10.1002/pola.1986.080240618.

[41] A.-C. Albertsson (Ed.), Long-Term Properties of Polyolefines, Springer, Berlin Heidelberg, 2004.

[42] C. Vasile (Ed.), Handbook of polyolefins, 2nd ed., Marcel Dekker, New York, 2000.

[43] H. Zweifel, Macromolecular Systems - Materials Approach: Stabilization of Polymeric Materials, Springer, 1998.

[44] T. Ojeda, A. Freitas, K. Birck, E. Dalmolin, R. Jacques, F. Bento, F. Camargo, Degradability of linear polyolefins under natural weathering, Polymer Degradation and Stability 96 (4) (2011) 703–707. https://doi.org/10.1016/j.polymdegradstab.2010.12.004.

[45] S. Beißmann, M. Stiftinger, K. Grabmayer, G. Wallner, D. Nitsche, W. BUCHBERGER, Monitoring the degradation of stabilization systems in polypropylene during accelerated aging tests by liquid chromatography combined with atmospheric pressure chemical ionization mass spectrometry, Polymer Degradation and Stability 98 (9) (2013) 1655–1661. https://doi.org/10.1016/j.polymdegradstab.2013.06.015.

[46] F. Gugumus, The performance of light stabilizers in accelerated and natural weathering, Polymer Degradation and Stability (58) (1995).

[47] C. Kósa, Š. Chmela, G. Theumer, W. Habicher, New combined phenol-hindered amine stabilizers for polymers based on diphenylmethane-4,4'-diisocyanate and dicyclohexylmethane-4,4'-diisocyanate, Polymer Degradation and Stability 86 (3) (2004) 391–400. https://doi.org/10.1016/j.polymdegradstab.2004.04.018.

[48] International Organisation for Standardisation, ISO 527-3, Plastics - Determination of tensile properties: Part 3: Test conditions for films and sheets, 1995.

[49] International Organisation of Standardisation, IEC 61215, Crystalline silicon terrestrial photovoltaic (PV) modules - Design Qualification and Type Approval, International Electrotechnical Commission, Geneva, CH, 2005.

[50] International Organisation for Standardisation, ISO 11357-3, Plastics - Differential scanning calorimetry (DSC) Part 3: Determination of temperature and enthalpy of melting and crystallization, 1999.

[51] B. Ottersböck, G. Oreski, G. Pinter, Comparison of different microclimate effects on the aging behavior of encapsulation materials used in photovoltaic modules, Polymer Degradation and Stability (2017) 182–191. https://doi.org/10.1016/j.polymdegradstab.2017.03.010.

[52] A. Beinert, C. Peike, I. Dürr, M. Kempe, K.-A. Weiß, The Influence of the Additive Composition on the Photochemical Degradation of EVA, in: 29th European Photovoltaic Solar Energy Conference and Exhibition, Amsterdam, Netherlands, 2014.

[53] G. Oreski, G.M. WALLNER, R.W. Lang, Ageing characterization of commercial ethylene copolymer greenhouse films by analytical and mechanical methods, Biosystems Engineering 103 (4) (2009) 489–496. https://doi.org/10.1016/j.biosystemseng.2009.05.003.

[54] O. Fu, H. Hu, W.J. Gambogi, J.G. Kopchick, T. Felder, H. Babak, B. Alex, H. Yushi, T. John, Understanding backsheet durability through field studies and accelerated stress testing, in: SNEC 2014.

[55] F. Liu, L. Jiang, S. Yang, Ultra-violet degradation behavior of polymeric backsheets for photovoltaic modules, Solar Energy 108 (0) (2014) 88–100. https://doi.org/10.1016/j.solener.2014.06.027.

[56] K. Wood, The Effect of Fluoropolymer Architecture on the Exterior Weathering of Coatings, Macromol. Symp. 187 (2002.) 469–479.

[57] V. Wachtendorf, A. Geburtig, P. Trubiroha, The Influence of Humidity and Wetness on Weathering Results, Christ Church College Oxford, England, 15., 2008.

[58] A.W. Czanderna, F. J. Pern, Encapsulation of PV modules using ethylene vinyl acetate copolymer as a pottant: A critical review, Solar Energy Materials and Solar Cells (43) (1996) 101–181.

[59] Klaus J. Geretschläger, Gernot M. Wallner, Jörg Fischer, Structure and basic properties of photovoltaic module backsheet films, Solar Energy Materials and Solar Cells 144 (2016) 451–456. https://doi.org/10.1016/j.solmat.2015.09.060.

[60] J. Badia, E. Strömberg, S. Karlsson, A. Ribes-Greus, The role of crystalline, mobile amorphous and rigid amorphous fractions in the performance of recycled poly (ethylene terephthalate) (PET), Polymer Degradation and Stability 97 (1) (2012) 98–107. https://doi.org/10.1016/j.polymdegradstab.2011.10.008.

[61] H. W. Siesler, K. Holland-Moritz, IR and Raman Spectroscopy Of Polymers, Marcel Dekker, Inc., New York, 1980.

[62] M. Sclavons, M. Laurent, J. Devaux, V. Carlier, Maleic anhydride-grafted polypropylene: FTIR study of a model polymer grafted by ene-reaction, Polymer 46 (19) (2005) 8062–8067. https://doi.org/10.1016/j.polymer.2005.06.115.

[63] P. Eyerer, Thomas Hirth, P. Elsner, Polymer Engineering: Kapitel 3: Eigenschaften von Kunststoffen in Bauteilen, Springer, Berlin Heidelberg, 2008.

[64] G.W. Ehrenstein, G. Riedel, P. Trawiel, Thermal analysis of plastics: Theory and practice, Carl Hanser Verlag, Munich, 2004.

[65] G. Oreski, G. Pinter, Aging Characterization of Multi-Layer Films Used As Photovoltaic Module Backsheets: 4AV.4.13, in: 28th European Photovoltaic Solar Energy Conference and Exhibition, Paris, France, 2013, pp. 3050–3054.

[66] H. Lee, F.J.M. Garry, Changes in free volume and mechanical properties of PVC films incurred by quenching and aging, J. of Macromolecular Sc., Part B 29 (1) (1990) 11–29. https://doi.org/10.1080/00222349008212333.

[67] B. Fayolle, L. Audouin, J. Verdu, Oxidation induced embrittlement in polypropylene - a tensile testing study, Polymer Degradation and Stability (70) (2000) 333–340.

[68] L. G. E. Struik, Physical Aging in Amorphous Polymers and Other Materials, Elsevier Sci. Publ. Comp., Amsterdam-Oxford-New York, 1978.

[69] W. Grellmann, S. Seidler, V. Alstädt, Polymer testing, 2nd ed., Carl Hanser Verlag, Munich, 2011.

[70] J. Pospíšil, Z. Horák, J. Pilař, N. Billingham, H. Zweifel, S. Nešpůrek, Influence of testing conditions on the performance and durability of polymer stabilisers in thermal oxidation, Polymer Degradation and Stability 82 (2) (2003) 145–162. https://doi.org/10.1016/S0141-3910(03)00210-6.

[71] M. Knausz, G. Oreski, M. Schmidt, P. Guttmann, K. Berger, Y. Voronko, G. Eder, T. Koch, G. Pinter, Thermal expansion behavior of solar cell encapsulation materials, Polymer Testing 44 (2015) 160–167. https://doi.org/10.1016/j.polymertesting.2015.04.009.

[72] H. Domininghaus, P. Elsner, P. Eyerer, T. Hirth, Kunststoffe: Eigenschaften und Anwendungen, Springer Berlin Heidelberg New York, 2004.

[73] E. Baur, J.G. Brinkman, T.A. Osswald, E. Schmachtenberg, Saechtling Kunststoff Taschenbuch, 30th ed., Carl Hanser, Munich, 2007.

[74] C. Choy, F. Chen, E. Ong, Anisotropic thermal expansion of oriented crystalline polymers, Polymer 20 (10) (1979) 1191–1198. https://doi.org/10.1016/0032-3861(79)90142-3.

[75] A.G. Gibson, I.M. Ward, Thermal expansion behaviour of hydrostatically extruded linear polyethylene, Journal of Material Science 14 (8) (1979) 1838–1842. https://doi.org/10.1007/BF00551022.

[76] C. L. CHOY, F. C. CHEN, and K. YOUNG, Negative thermal expansion in oriented crystalline polymers.

[77] Cantor Kirk, Blown Film Extrusion, 2nd ed., Hanser Verlag, München, 2011.

[78] A. Genovese, R.A. Shanks, Time-Temperature Creep Behaviour of Poly(propylene) and Polar Ethylene Copolymer Blends, Macromol. Mater. Eng. 292 (2) (2007) 184–196. https://doi.org/10.1002/mame.200600346.

[79] I.M. Ward, J. Sweeney, An Introduction to the Mechanical Properties of Solid Polymers, 2nd ed., Wiley, 2004.

[80] M. Omazic, The influence of polymer carrier films on semiconductor processing. Doctoral thesis, Leoben, 2018.

[81] S.H. Tabatabaei, P.J. Carreau, A. Ajji, Structure and properties of MDO stretched polypropylene, Polymer 50 (16) (2009) 3981–3989. https://doi.org/10.1016/j.polymer.2009.06.059.

[82] T. Lüpke, S. Dunger, J. Sänze, H.-J. Radusch, Sequential biaxial drawing of polypropylene films, Polymer 45 (20) (2004) 6861–6872. https://doi.org/10.1016/j.polymer.2004.07.075.

[83] A.J. Peacock, Handbook of Polyethylene: Morphology and Crystallization of Polyethylene, Marcel Dekker, Inc., New York, N.Y., 2000.

[84] A. Omazic, G. Oreski, M. Halwachs, G.C. Eder, C. Hirschl, L. Neumaier, G. Pinter, M. Erceg, Relation between degradation of polymeric components in crystalline silicon PV module and climatic conditions: A literature review, Solar Energy Materials and Solar Cells 192 (2019) 123–133. https://doi.org/10.1016/j.solmat.2018.12.027.

3 Weathering stability of polyolefin encapsulants in standard and double-glass modules

3.1 Motivation

In order to protect brittle and always thinner c-Si cells in photovoltaic (PV) modules from environmental stress factors, c-Si cells are encapsulated with polymeric materials. The encapsulant which is most often used in PV modules is by far ethylene vinyl-acetate (EVA) mainly due to its satisfying properties at a low price. EVA is a co-polymer of ethylene and randomly dispersed polar vinyl-acetate (VAc) segments in the ethylene backbone [1]. Since the acetate groups are bulky and prevent the packing of PE chains into crystal lattices, their content greatly influences the crystallinity and therefore the final properties of the material [1]. During lamination of the PV module, EVA is cross-linked via a peroxide radical reaction, which transforms it from the original thermoplastic, opaque and easily deformable material into an elastomeric, highly transparent material via the formation of a loose 3-D polymer network (see Figure 3.1.) [2]. In this way, the thermal and mechanical stability of EVA film is acquired, which makes the crosslinking degree of EVA a very important parameter for reliability of PV modules [2–4]. However, there is always a certain amount of residual peroxides left in the EVA after lamination that can keep reacting with additives giving rise to failure modes such as discoloration, corrosion and delamination [2,5,6]. Therefore, the crosslinking mechanism of EVA, i.e. peroxides can represent a weak point for reliability of EVA, i.e. PV modules.
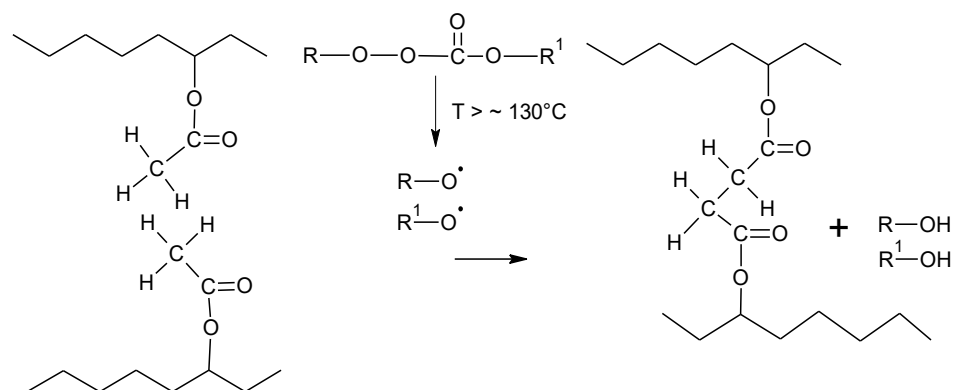

Figure 3.1. Crosslinking of EVA during lamination [7]

When exposed to different environmental stresses (temperature, oxygen, humidity, irradiation, etc.) EVA undergoes thermo- and photo-oxidation, which leads to the deterioration of its mechanical, optical and thermal properties and finally loss of the PV

modules' efficiency [2,8–10]. The main degradation mechanism of EVA was reported to be via Norrish I and II reactions, which results in the formation of different degradation products including lactones, ketones, acetaldehyde and most important - acetic acid [1,3,8,11]. Acetic acid promotes many failure modes such as corrosion of metallization [12–14], delamination of the front encapsulant [15,16], potential induced degradation (PID) [17] and autocatalytic degradation of EVA [8,18].

The main drawbacks of EVA as an encapsulant and failure modes of PV modules related to degradation of EVA have already been discussed in details in Chapter 1. Moreover, it was shown that the occurrence of certain failure modes linked with EVA degradation is closely related to the operating conditions (climate) [19]. Discoloration, accompanied by delamination of EVA above the cell and a certain degree of corrosion are the most often observed failure modes in arid climates [8,19–27]. PV modules installed in tropical climates show a higher degree of delamination compared to other climate types due to a combination of high temperature and humidity, which leads to the decomposition of adhesive Si-O-Si bonds at the glass/encapsulant interface and finally corrosion [19,28–30] [30–32]. Modules in polar climate mostly suffer from failure modes related to mechanical loads (e.g. cell cracks), which could be promoted by an increased stiffness of EVA at lower temperatures [19]. Despite being linked to many failure modes, EVA is still the most widely used encapsulant in PV modules installed worldwide.

Alternatives to EVA

In order to overcome the reliability issues related to EVA, alternative materials are starting to get more attention. Thermoplastic polyolefin (TPO) and polyolefin elastomer (POE) seem to be the best alternatives since they would not require change in the production line and are economically better options compared to, for example, reliable but expensive silicones [33].

TPO does not crosslink, which diminishes failure modes related to residual peroxides and reduces lamination time for up to 10 min, which could reduce production costs. Moreover, TPO does not contain VAc segments (no acetic acid formation), which would potentially minimize the occurrence of failure modes such as corrosion, discoloration and delamination. Those features combined with hydrolysis resistance could be of special interest for application in climates with higher humidity levels.

On the other hand, POE crosslinks via peroxides but is free of VAc segments. As in the case of TPO, there is no production of acetic acid and therefore there is no occurrence of related failure modes in the field. Due to the higher volume resistivity, TPO and POE are assumed to be PID resistant compared to EVA, which is PID sensitive [34]. However,

both materials are also sensitive to thermo- and photo-oxidation, mainly due to remaining catalysts residues and contaminations from the production process [35–39]. Degradation results in chain scission and crosslinking, which can lead to changes in molecular weight and formation of different oxygen containing groups [9,40,41].

Being relatively new in solar applications, the reliability of PV modules with TPO and POE has still not been fully investigated. As shown by Ottersböck et al. [9], TPO undergoes less degradation under Xenon aging conditions compared to EVA. Cabrera et al. [42] have shown that TPO results in higher resistance to long-term humidity exposure compared to EVA. Govaerts et al. [43] reported that cell corrosion could be reduced by the application of a polyolefin encapsulant. Oreski et al. [44] have shown that ethylene copolymers based on acrylates and acrylic acid (such as POE) provide similar or better mechanical and optical properties compared to EVA without the formation of acetic acid.

Influence of backsheet type on degradation of front encapsulant

The role of the backsheet material in degradation behaviour of encapsulants within PV modules has already been recognized as an important factor for reliability of PV modules [9,18,45,46]. Moisture (water vapour) and oxygen, that can enter through the polymeric backsheet and penetrate towards the front encapsulant and cell, can lead to many failure modes such as delamination, corrosion and degradation of EVA resulting in corrosive acetic acid formation. While the water vapour transmission rate (WVTR) and oxygen transmission rate (OTR) should be minimized, the permeation of the degradation product acetic acid (AATR) is beneficial to be high in order to provide a fast diffusion of corrosive acetic acid out of the PV module laminate [46]. Therefore, selective permeation properties (low WVTR, high AATR) of backsheets are receiving more attention as a reliability factor for PV modules.

Double glass (or glass-glass) modules are one of the approaches in design of PV modules. In these modules, glass is not only used for the front cover (as in standard modules) but also for back cover instead of standard polymeric backsheets. Such assembly is claimed to provide higher robustness towards mechanical and thermal loads, which guarantees longer life [47]. Another advantage of glass as a backsheet compared to polymeric is its chemical resistance and impermeability, which could be beneficial in climates with, for example, high concentrations of salt in the air such as in coastal areas or high humidity levels. However, the impermeability of the glass could represent problem for acetic acid if EVA is used as an encapsulant and lead to an accumulation of acetic acid at interfaces of the PV components. If EVA were replaced

with other encapsulation materials such as TPO or POE, then acetic acid would not represent problem. Suleske [26] investigated degradation of double glass modules installed in hot and dry climates and showed that the occurrence of hot-spots and delamination is a major failure mode of double glass modules compared to modules with a polymeric backsheet. According to [26,48], the reason for such behaviour is actually excessive heating of double glass modules. Therefore, high temperatures (such as in the desert) could represent problems for the installation of the double glass modules. Due to obviously different microclimatic conditions in double glass modules, different degradation mechanisms of encapsulants compared to standard modules are expected. However, the findings on the degradation behaviour of front encapsulants in double glass modules are, in general, very poor.

Although the use of alternative encapsulants and/or changes in PV module design could represent possible solutions to increase reliability and/or reduce costs of PV modules, the actual impact of such steps on the reliability of PV modules has still not been fully investigated. Hence, the focus of this work is to (i) investigate the degradation of the standard (EVA) and alternative (TPO and POE) front encapsulants on the PV module level and (ii) to understand the influence of PV design, i.e. backsheet type on degradation of front encapsulants in PV modules.

3.2   Experimental part

3.2.1   Preparation and aging of the samples

In order to investigate the influence of PV design on the weathering stability of standard (EVA) and alternative (TPO and POE) front encapsulants in the PV module, the single-cell test modules with different compositions (see Table 3.1.) were laminated according to standard lamination procedures [9]. Butyl rubber was applied as the sealant in double-glass modules.

Table 3.1. Composition of the single-cell test modules

Test module	Glass	Encapsulant	Backsheet	
Standard module	2 mm	EVA	PET-laminate	
		TPO		
		POE		
Double-glass module	2 mm	EVA	Glass (2mm)	
		TPO		
		POE		

Modules were artificially aged at OFI up to 1000h according to parameters listed in the Table 3.2.. In order to extract encapsulants from the single-cell test modules for the destructive measurements, modules were manually destroyed via mechanical cutting. The encapsulants were delaminated from the area (i) in contact with the c-Si cell and (ii) in contact with the backsheet (PET-laminate in standard modules and glass in double-glass modules).

Table 3.2. Artificial aging parameters

Aging test	Parameters	Duration
Damp heat	85°C, 85% RH	1000h
Sun irradiation	60°C, 40% RH; 1000 W/m^2 $_{\lambda=300-2500\ nm}$	

3.2.2   UV/Vis/NIR spectroscopy

The degradation of front encapsulants on PV module level was investigated non-destructively via Lambda 950 spectrometer from Perkin Elmer. Measurements were carried out on single-cell modules in reflectance mode above the cell and PET-laminate

i.e. transmittance mode above the glass backsheet. Spectra were recorded in the range from 250 to 2500 nm with a resolution of 5 nm. Since the measurements were done on the modules, the spectra of encapsulants also include reflectance of the glass and inner side of the backsheet. The presented spectrum is an average of at least three measurements at each position.

3.2.3 FTIR-ATR spectroscopy

In order to identify changes in the chemical structure of the encapsulants, Fourier Transform Infrared spectroscopy in attenuated total reflectance mode (FTIR-ATR) was conducted on Spectrum GX FTIR spectrometer (Perkin Elmer, Waltham, USA) with ATR unit Pike VeeMax II (Pike Technologies, Madison, USA) using a ZnSe crystal with a diamond on top. The spectra were recorded over the range of 4000 to 650 cm^{-1} for all samples. The measurements were obtained from an average of 16 scans and at a resolution of 4 cm^{-1}. The presented spectrum is an average of at least three measurements at each position. The spectra of encapsulants were normalized with respect to the peak at 2850 cm^{-1} assigned to methylene C-H stretching of ethylene segments [5].

3.2.4 Differential scanning calorimetry (DSC)

Thermal properties of the encapsulants before and after the aging were investigated via DSC 4000 from Perkin Elmer. In order to obtain information on reversible and irreversible properties of the material, two heating runs were applied. The measurement parameters are listed in Table 3.3. Melting enthalpy was evaluated from the 1st heating curve according to [49]. The mass of the samples ranged from 9 to 11 mg. In order to avoid oxidation of the samples, a nitrogen atmosphere with a flow of 50 mL/min was kept during the measurements.

Table 3.3. Parameters of DSC analysis

Step	Start T [°C]	End T [°C]	Heating rate [°C/min]
1st heating	-70	150	10
Cooling	150	-70	10
2nd heating	-70	300	10

3.3 Results and discussion

In the following section, the results of the UV/Vis/NIR spectroscopy, FTIR-ATR spectroscopy and DSC analysis will be presented. Before presenting the results of each characterization method after aging, the properties of all three encapsulants will be compared before aging in order to point out their differences due to composition. At the end of the section, the weathering stability of all three types of the encapsulants will be compared and discussed in terms of PV application. Finally, the feasibility of the EVA replacement in PV modules operating under harsh climatic conditions and the influence of the backsheet type on their degradation will be discussed.

3.3.1 UV/Vis/NIR spectroscopy

In Figure 3.2. UV/Vis/NIR spectra of unaged and laminated single films of EVA, TPO and POE are presented. It can be seen that TPO and crosslinked POE have higher hemispherical transmittance in the UV region than crosslinked EVA. This implies that more light from the UV part of the spectra could be transmitted onto the cell with TPO and POE as encapsulants, which could lead to higher power output of the PV module.
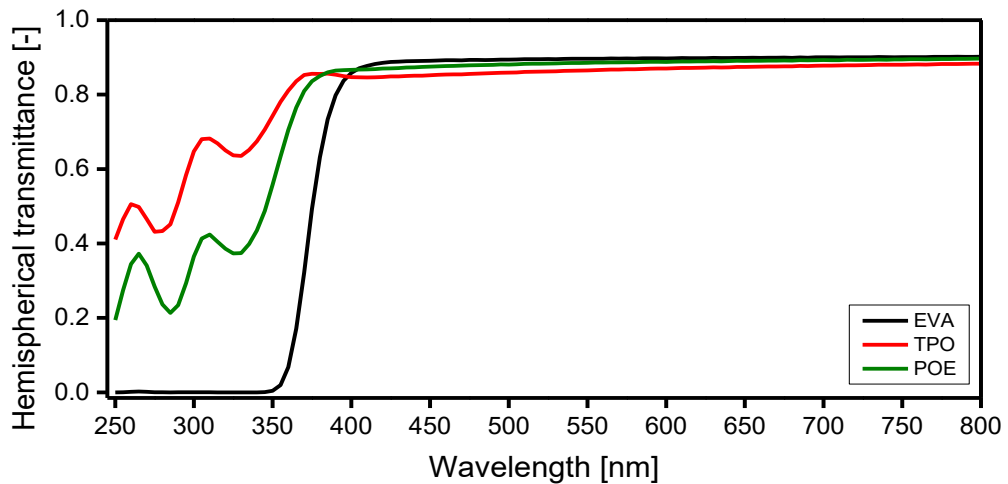
Figure 3.2. Comparison of optical properties of unaged and laminated films of EVA, TPO and POE encapsulants

The UV/Vis/NIR measurements were carried out on single cell modules above the cell and above the back-cover. However, the area above the back-cover was not always sufficient to conduct accurate measurements. Therefore, the part of either cell or modules' edge was measured as well, which could affect the results. Moreover, since the modules were frameless, higher moisture ingress was expected at the edges and

this could also be a potential cause for deviation between results of the modules of the same composition.

EVA

In Figure 3.3a-3.3b. the UV/Vis/NIR spectra of EVA above the cell and backsheet are shown. The reflectance intensity above the cell (Figure 3.3a.) is very low due to the absorption of c-Si cell. Damp heat aging of standard modules resulted in slight increase of reflectance in the UV-region probably due to a loss of an UV-absorber and consequently slight decrease of the reflectance in the blue region indicating yellowing of the EVA encapsulant. Discoloration of the encapsulant could directly influence the power output of PV module [19]. A slight increase of reflectance in the UV-region was also observed in double glass modules, but no significant yellowing could be detected. The sun irradiance test did not result in significant changes in either of the PV module types. A reason could be the photo-bleaching effect, where oxygen and UV irradiation in combination cause the degradation of the chromophore bonds [9].

Above the backsheet (see Figure 3.3b), no significant changes were observed after both aging types due to yellowing or loss of UV-absorbers. Slight increase of the reflectance, i.e. transmittance after aging could be assigned to thickness changes.
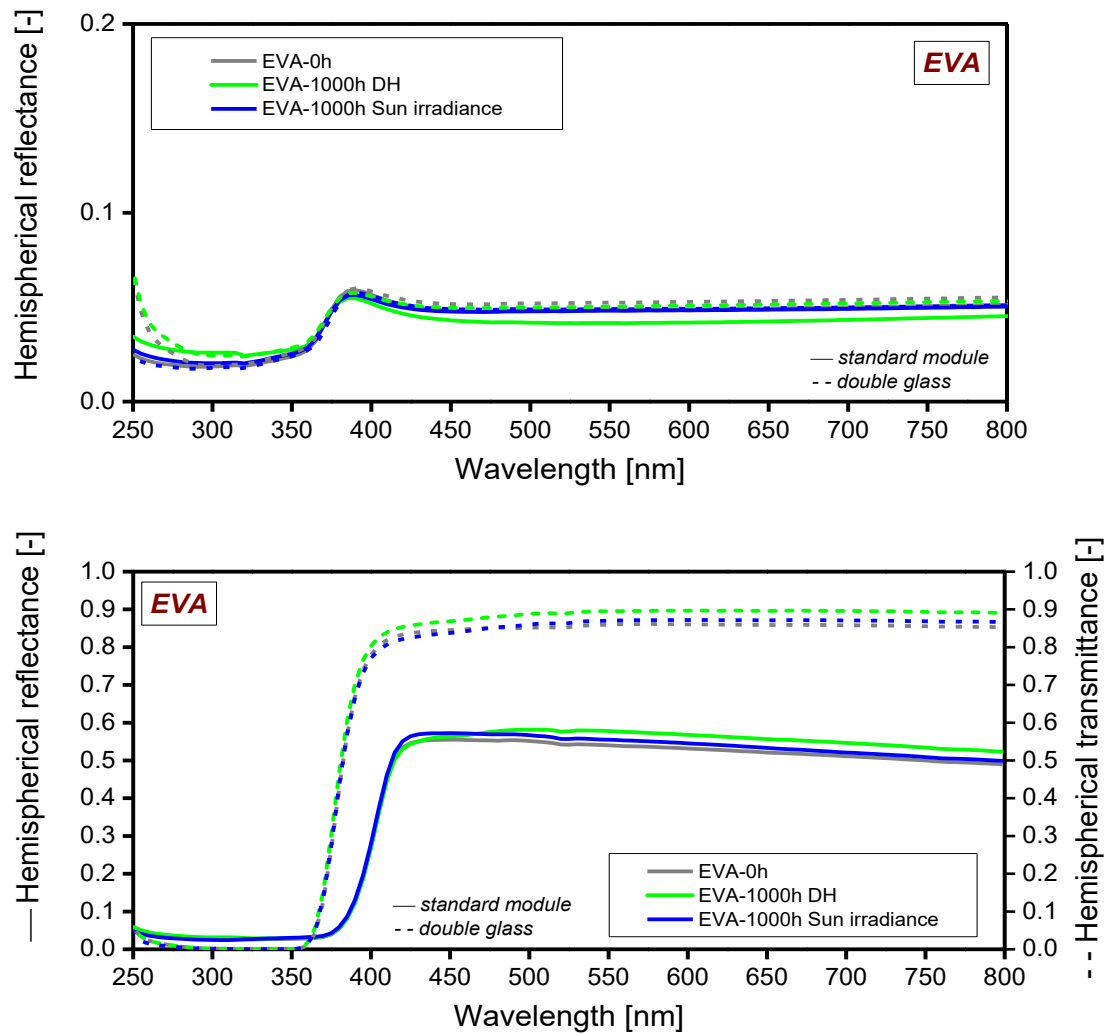
Figure 3.3. UV/Vis/NIR spectra of EVA: a) above the cell; b) above the backsheet before and after aging

TPO

In Figure 3.4a-3.4b. the UV/Vis/NIR spectra of TPO above the cell and above the backsheet before and after aging are shown. Damp heat aging of the standard modules and double glass modules did not result in significant changes except a slight increase of reflectance in the UV region indicating a loss of UV-absorbers. Sun irradiance resulted in an increase of reflectance in UV region due to loss of UV absorbers.

Above the PET-laminate a strong decrease of reflectance was observed in the blue region due to yellowing after damp heat aging (see Figure 3.4b.). Since such yellowing was not observed above the cell, it indicated the influence of PET-laminate on yellowing of TPO. According to Drobny et al. [50] the TPO should not discolour since it does not contain any unsaturation in its backbone, but aging of compounding ingredients or the presence of impurities (e.g. residual catalysts) may cause discoloration. Sun irradiance

resulted in an increase of reflectance in the UV region indicating a loss of UV-absorbers. The TPO in double-glass modules showed no yellowing after damp heat aging. The differences in the spectra are due to the changes in the thickness.
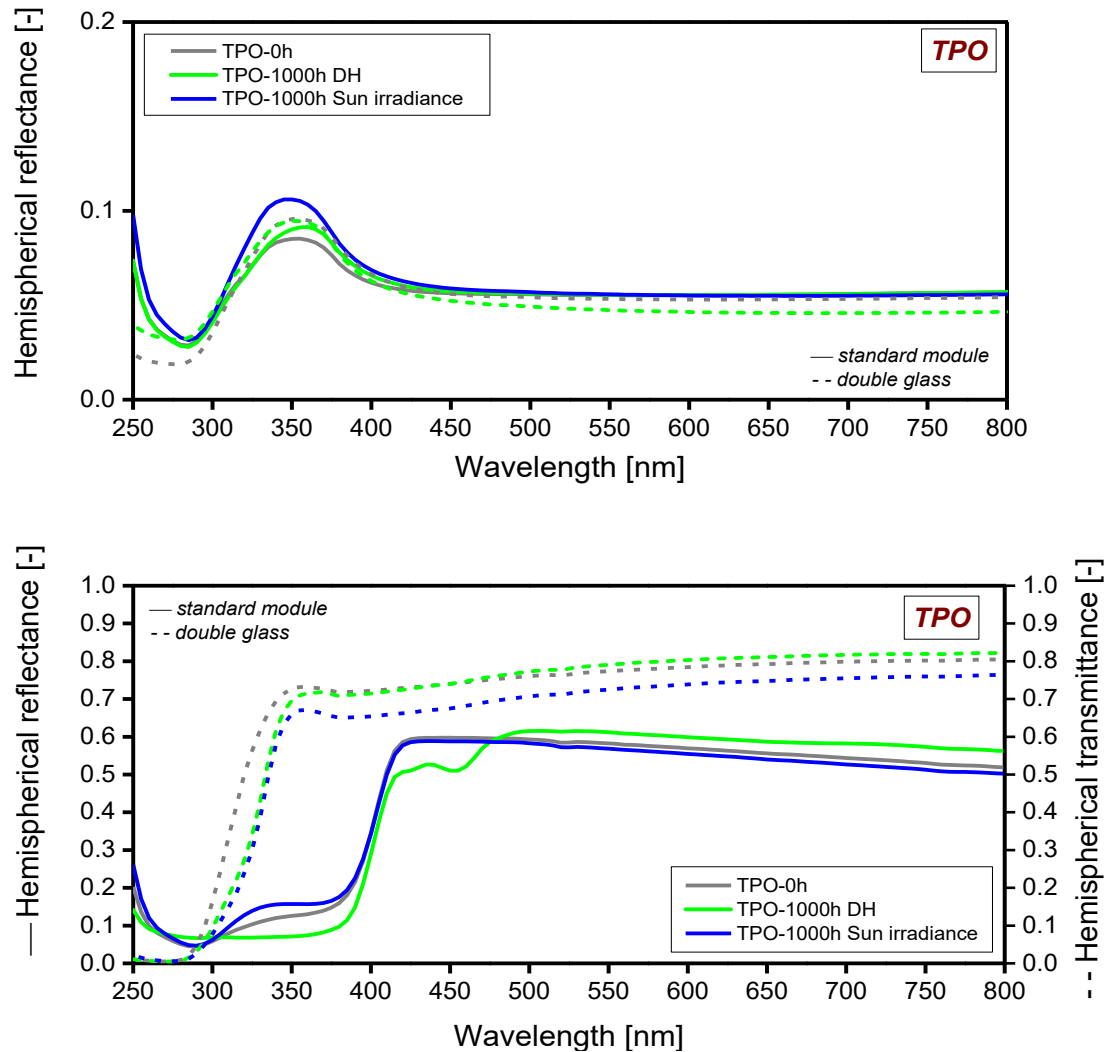
Figure 3.4. UV/Vis/NIR spectra of TPO: a) above the cell; b) above the back-cover before and after aging

POE

The UV/Vis/NIR spectra of the POE after the aging is presented in Figure 3.5a-3.5b. A slight increase of reflectance in the UV region and a decrease of reflectance in the blue region indicated yellowing due to loss of UV-absorbers. The same was observed for double glass modules as well. The trend after sun irradiance was the same but the effect was lower.

Damp heat aging resulted in a decrease of reflectance in the blue region due to yellowing of POE above the PET-laminate, while in the double glass modules no significant yellowing could be detected. No changes in the UV-region were observed. Sun irradiance tests resulted in a slight increase of reflectance in both modules compared to unaged POE, which could be a consequence of the photo-bleaching effect [8,9].
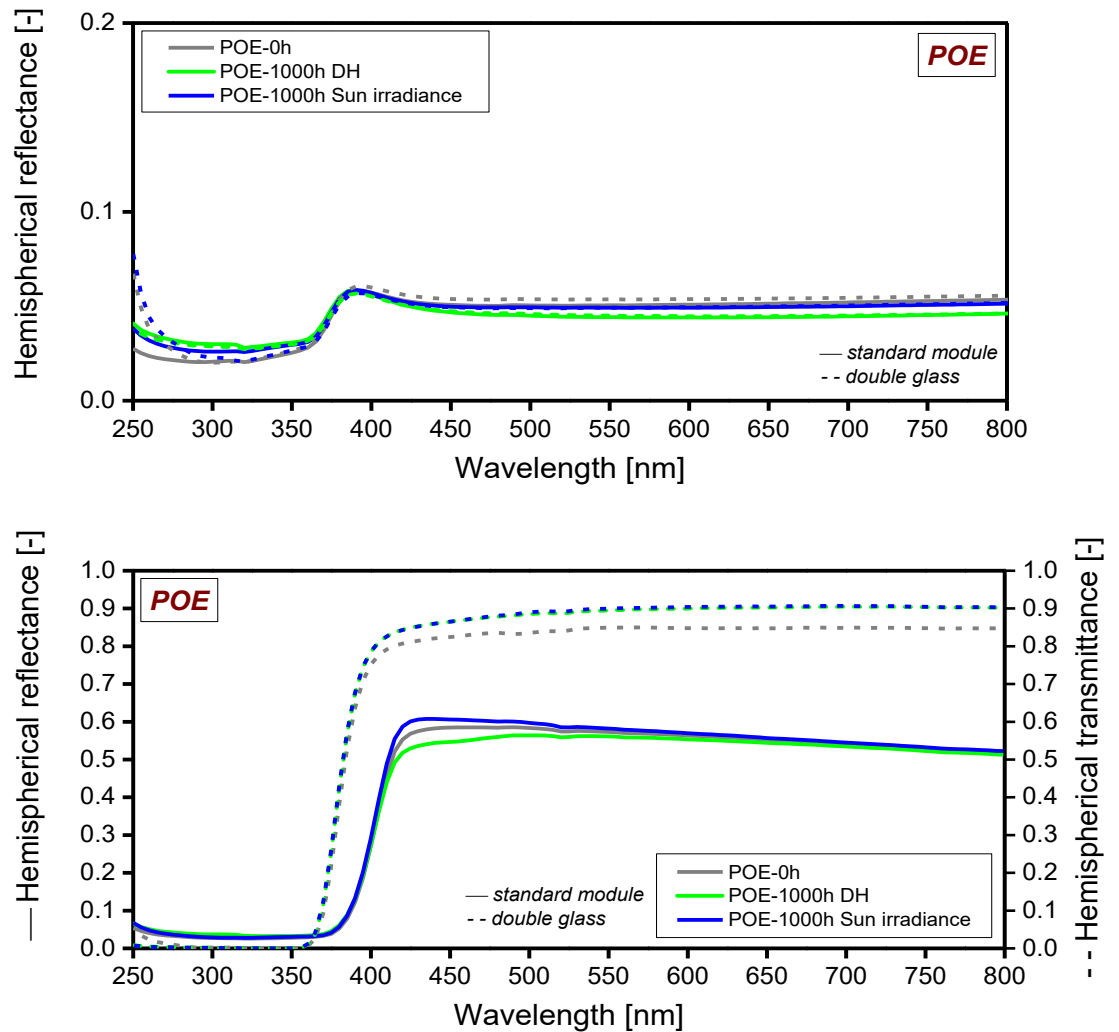
Figure 3.5. UV/Vis/NIR spectra of POE: a) above the cell; b) above the backsheet before and after aging

The optical properties of all three encapsulants laminated in standard and double glass modules above the cell and backsheet were investigated. Damp heat aging showed higher impact on yellowing compared to the sun irradiance test, probably due to the photo-bleaching effect. Encapsulants showed a slight loss of UV absorbers that was usually followed by a slight yellowing above the cell, mostly in both types of modules. Nevertheless, the highest impact of aging was observed in combination of TPO and PET-laminate after damp heat aging. Strong yellowing was even visually observable. Damp

heat aging of standard modules with POE resulted in significant yellowing above the PET-laminate as well. Modules with EVA, on the other hand, did not result in such yellowing above the PET-laminate. These observations indicated an incompatibility between materials but should not, however, affect the power output of the module. In fact, the power output of the 6-cell modules with EVA and TPO aged up to 3000h showed a comparable behaviour without any decrease of power output (see Figure 3.6.).
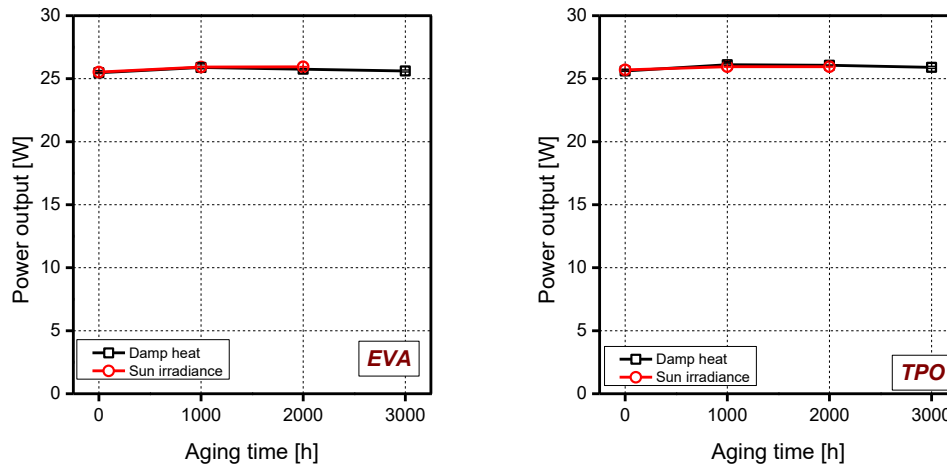

Figure 3.6. Power output of modules using the EVA and TPO encapsulant

UV/Vis/NIR spectroscopy was applied in this work since it is a non-destructive method that provides information on optical properties of encapsulants. Moreover, it is possible to follow the degradation of optical properties at module level, which is of special importance since in that way microclimate effects are included. It was shown that aging of single encapsulant films does not result in the same data as the encapsulants aged within modules [9]. The obtained data above the cell resulted in higher repeatability compared to data above the backsheet. The results obtained above the backsheet showed very high deviation between the samples of the same composition. The reason is most probably the design of the test-modules that were frameless, which could promote moisture ingress. Furthermore, it was often hard to obtain proper spectra due to lack of space between the edge of the module and cell. This finding pointed out the importance of test-module design, the applied characterization method and the interpretation of the data when assessing the weathering stability of materials on the PV module level.

3.3.2 FTIR-ATR spectroscopy

In order to show the differences in the chemical structure of laminated and unaged crosslinked EVA, TPO and crosslinked POE encapsulants, their FTIR-ATR absorbance spectra are shown in the Figure 3.7. All three encapsulants are polyethylene-based, which is evident by characteristic peaks about 2916, 2848, 1463 and 730 cm^{-1} that originated from symmetric, asymmetric and deformation vibrations of the CH_2 and CH_3 groups of ethylene segments [51]. EVA shows additional peaks at 1740, 1238 and 1020 cm^{-1} related to carbonyl (C=O) and ether groups (C-O-C) originating from ester groups of the vinyl acetate (VAc) segments [9,11]. Aside from PE peaks, TPO showed an additional peak around 1080 cm^{-1}, which most probably stems from the sterically hindered phenols that are usually used as stabilizers [51]. As a copolymer of PE and an acrylate-based co-monomer, POE does not have vinyl acetate groups. The peaks around 1160 and 1266 cm^{-1} originate from C=O and C-O groups of acrylate that is added to POE as an elastomeric compound [44,51,52].
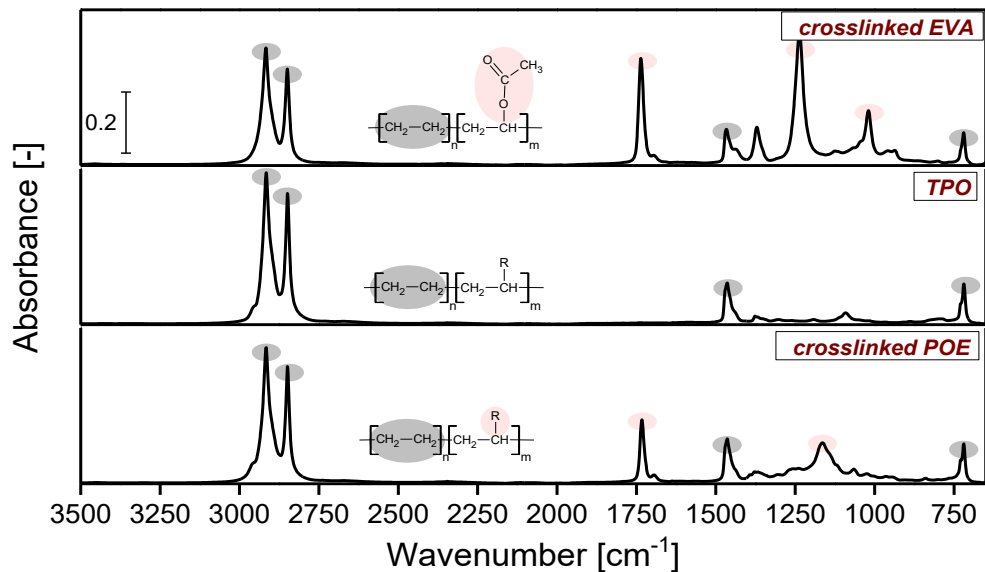
Figure 3.7. Exemplary graph of FTIR-ATR absorbance spectra of unaged and laminated encapsulants

EVA

In Figure 3.8.-3.9. the FTIR-ATR spectra of EVA above the cell before and after DH and sun irradiance test in the standard and double-glass modules are shown. After damp heat aging, the EVA extracted from the standard module above the cell (Figure 3.8.) showed a very small increase of the broad peak in the range from 3500-3000 cm^{-1}, which

is assigned to the OH group of alcohols, peroxides and hydro-peroxides. An increase in this area is an indication of hydrolysis [1,9,53–59]. Furthermore, an increase of the carbonyl (C=O) peak around 1735 cm^{-1} was observed after both aging tests, which is due to the formation of ester and aldehyde groups formed via back-biting of VAc moieties upon oxidation [1,9,57,60]. As support, an increase of the peak at 1120 cm^{-1} was observed, which is assigned to the C-O-C stretch vibration. This indicates either (i) evolution of the acetaldehyde or (ii) hydro-peroxides that broke down to ketones and water [1,9,56,57,60]. Since a slight increase in the region 3500-3000 cm^{-1} was observed, most probably the latter is the reason. No broadening of the carbonyl peak due to the formation of lactones, ketones, anhydride and acid groups was observed [1,60]. Furthermore, the slight formation of the peak at around 1600 cm^{-1}, which is assigned to conjugated double bonds, i.e. unsaturated ketones and/or vinylidene esters, was observed above the cell [1,44,56,57,59]. The peak at 995 cm^{-1}, which is assigned to terminal =CH double bond groups showed a slight increase as well [44,57,59]. This fact combined with the emergence of the peak at 1600 cm^{-1} could indicate chemical degradation, i.e. chain cleavage of the EVA in the modules under damp heat conditions [1,9,11,56]. However, the observed changes in EVA spectra from standard modules were minimal after both aging tests indicating overall stability of EVA.

Figure 3.8. FTIR-ATR absorbance spectra of EVA above the cell before and after DH and sun irradiance test within standard module (PET-laminate backsheet)

In the double glass modules (Figure 3.9.), no matter what type of aging and position in the module, no formation of the broad band at 3700-3000 cm^{-1} was observed, indicating that the EVA did not undergo hydrolysis. Since the glass is impermeable, it could prevent penetration of moisture and oxygen to the cell and encapsulant. A slight increase in the

carbonyl region due to an increase in the ester and aldehyde groups formed via backbiting of VAc moieties was observed and further supported by an increase of the band at 1120 cm^{-1} [1,9]. It can be clearly seen that the increase of the peaks 1120 cm^{-1}, 1020 cm^{-1} and 995 cm^{-1} is more pronounced compared to the standard modules indicating stronger oxidation (thermo- and photo-oxidation) of the EVA encapsulant in double-glass modules above the cell. The formation of double bonds was confirmed by an increase in the peaks at 995 and 909 cm^{-1}[11,44]. The oxidation of EVA in double-glass modules could be triggered by the decomposition of the oxygen containing compounds in the material or residual oxygen from the production. Moreover, slightly higher temperature of double-glass modules upon irradiation in the sun irradiance test could accelerate photo-oxidation.
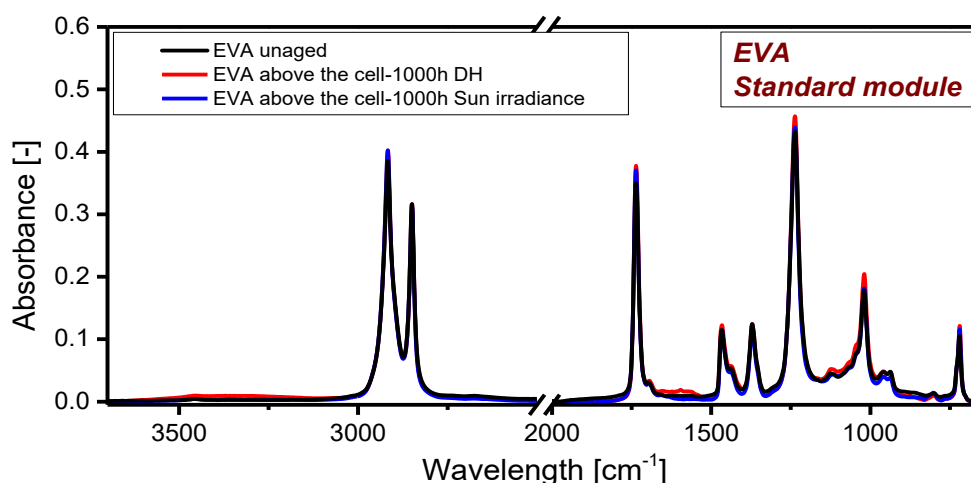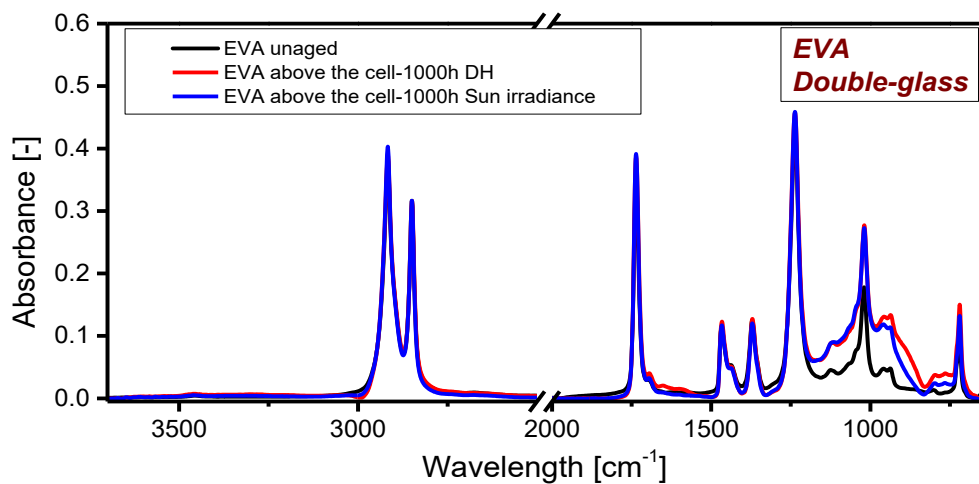

Figure 3.9. FTIR-ATR absorbance spectra of EVA above the cell before and after DH and sun irradiance test within double-glass module (glass backsheet)

In general, EVA showed high stability in terms of thermo- and photo-oxidative degradation in both types of modules. The photo-oxidation of EVA above the cell was more pronounced in the double-glass modules probably due to higher temperatures upon irradiation in the sun irradiance test. The EVA above the PET-laminate (standard modules) and glass (double-glass modules) backside was examined as well in order to investigate the degradation of EVA in "extreme conditions". Namely, standard modules were frameless, which can promote higher moisture ingress from the edges. Therefore, higher degradation of EVA in contact with PET-laminate at the edges of the standard modules is expected. On the other hand, the edges of double-glass modules were sealed with butyl rubber sealant, which was supposed to reduce the moisture ingress. Therefore, above the PET-laminate (see Figure 3.10.) a strong increase in the region from 3500-3000 cm^{-1} after sun irradiance test could be observed. An additional increase

of the peak around 1560 cm^{-1} was detected, which could originate from the degradation of the additives or from carboxylic acids that are built up at high degrees of oxidative degradation [61]. The photo-oxidation of EVA above the PET-laminate was further supported by an increase of the carbonyl (C=O) peak around 1735 cm^{-1} and peaks at 1120 cm^{-1} (C-O-C), 1600 cm^{-1} (C=C) and 995 cm^{-1} (=CH) [1,9,57,60]. The possible chain scission was more emphasized compared to damp heat aging as indicated by stronger increase of the peak at 995 cm^{-1} [1,9,11,44,56]. Above the glass backside in double-glass modules only the changes in the region from 1200-950 cm^{-1} due to the oxidation were observed, while no hydrolysis could be observed. It has to be noted that, in standard PV modules exposed outdoors, such degradation is not expected due to the frame and bigger distance between the edge of the modules and cell, which supresses the moisture ingress. However, those results showed the clear impact of moisture ingress on degradation of EVA encapsulant.

Figure 3.10. FTIR-ATR absorbance spectra of EVA above the back cover before and after DH and sun irradiance testing within standard and double-glass module

TPO

The FTIR-ATR spectra of the TPO front encapsulant before and after aging in the standard and double-glass modules are shown in the Figure 3.11. and Figure 3.14. After damp heat aging, almost no difference in the TPO spectra could be observed above the cell. Only a slight increase of the carbonyl peak at 1735 cm^{-1} could be observed indicating oxidation of the TPO and a slight increase of the peaks in the range from 1160-990cm^{-1} indicating changes in the additives. After the sun irradiance test, only the change in the area assigned to additives was detected.

Figure 3.11. FTIR-ATR absorbance spectra of TPO above the cell before and after DH and sun irradiance test within standard module (PET-laminate backsheet)

After damp heat aging of the standard modules with TPO, the broad band assigned to OH groups could be found only above the PET-laminate (see Figure 3.12.). TPO above the PET-laminate showed strong changes upon damp heat aging in the region from 1800 cm^{-1} to 1450 cm^{-1}, which is assigned to C=O, and indicated oxidation processes [9,61]. The peak at 1736 cm^{-1} is probably due to the formation of aliphatic esters. The broad peak around 1130 cm^{-1} corresponds to the carbonyl stretch vibration of ketone and C-O-C stretch vibration of aliphatic ester. An increase of these bands indicates oxidation during aging [1,9,62]. The formation of the double bonds upon degradation was confirmed by the peak at 1640 cm^{-1} (C=C) and 995 cm^{-1} (trans vinylidene). The strong peak at around 1550 cm^{-1} could originate from carboxylic acids that are built up at high degrees of oxidative degradation [61].
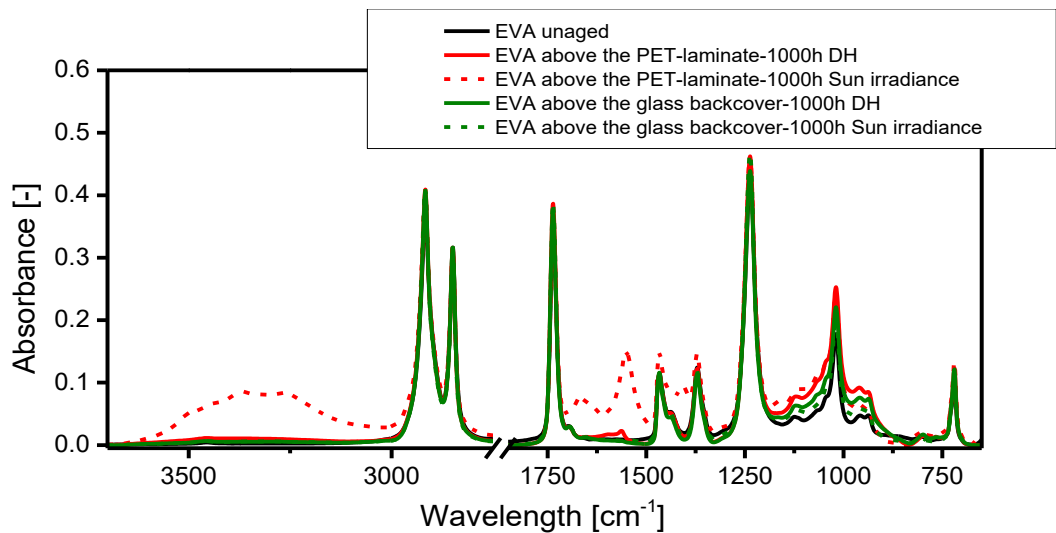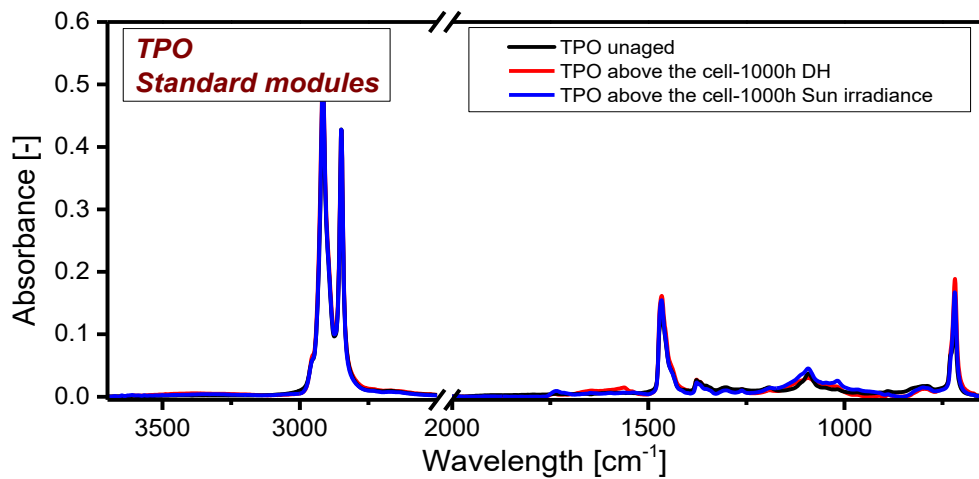
Figure 3.12. FTIR-ATR absorbance spectra of TPO above the back cover before and after DH and sun irradiance testing within the standard modules (PET-laminate)

The strong changes in the absorbance spectra of TPO are in good correlation with the observed yellowing via UV/Vis/NIR spectroscopy. In fact, the strong incompatibility between the TPO and PET-laminate (i.e. the innerside of the PET-laminate) was even visually observable as strong yellowing (see Figure 3.13.). The manual delamination of the modules revealed that the yellowing was indeed in the encapsulant and not on the inner side of the PET-laminate. As suggested by Edge et al. [63] the possible reason for such yellowing could be an interaction of phenolic-antioxidants in TPO with the rutile TiO_2 in the PET-laminate, which is used as pigment and stabilizer. The disappearance of the antioxidant butylhydroxytoluol after damp heat aging was confirmed via TD-GC-MS.
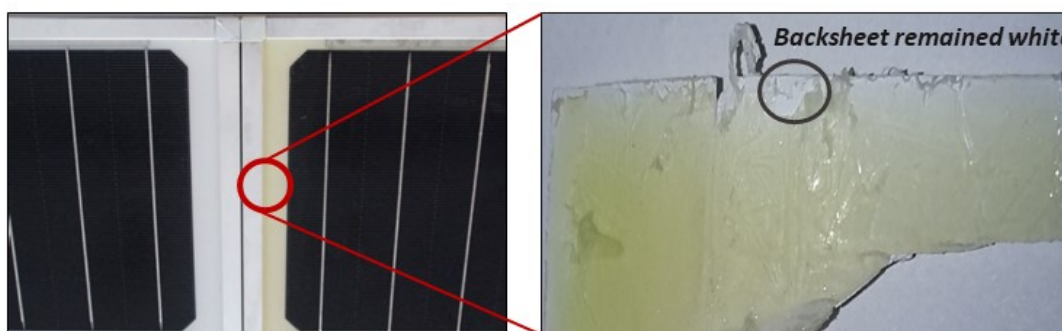
Figure 3.13. Yellowing of TPO encapsulant after damp heat aging in contact with PET-laminate

After the sun irradiance test, the observed changes in the TPO spectra above the PET-laminate were not so significant compared to damp heat aging either due to photo-

bleaching effect, i.e. photo-oxidation of the conjugated double bond groups formed [3,8,9] or the conditions of the test were not sufficient to initiate an interaction between TPO and the inner side of the PET-laminate. A slight increase of the peak at 1550 cm^{-1} and broadening of the peak around 1120 cm^{-1} could be observed due to additives and the carbonyl stretch vibration of ketone and C-O-C stretch vibration of aliphatic ester respectively. The peak at 1080 cm^{-1} related to antioxidants resulted in broadening and increase regardless of position or aging test. This indicates migration or degradation of the antioxidant.

In the double glass modules, a slight increase of the OH band was observed and this could be due to an ingress of moisture from the edges where a butyl rubber-based sealant was applied. However, as in the case of the EVA encapsulant, aside from a slight increase around 1640 and 1080 cm^{-1} due to the migration of the additives, no significant changes were found.

Figure 3.14. FTIR-ATR absorbance spectra of TPO above the cell before and after DH and sun irradiance test within double-glass module (glass backsheet)

POE

In Figure 3.15.-3.16. the FTIR-ATR spectra of POE in standard and double-glass modules before and after aging are shown. After damp heat aging of the standard module, the FTIR-ATR spectra of POE revealed certain changes. Due to oxidation, peaks at 3500-3000, 1670, 1550, 1120, 995 cm^{-1} increased after damp heat and sun irradiance tests, no matter what the position within the module. According to Glikman et al. [64], the presence of ester groups contributes to higher sensitivity towards photo-oxidation of copolymers of PE and acrylic monomers compared to PE. Dole et al. [59] showed that oxidation of co-polymers of PE and acrylate monomers lead to the formation

of C-O groups (evident by an increase between 1300 and 1000 cm^{-1}), while carbonyl groups remain mainly constant.

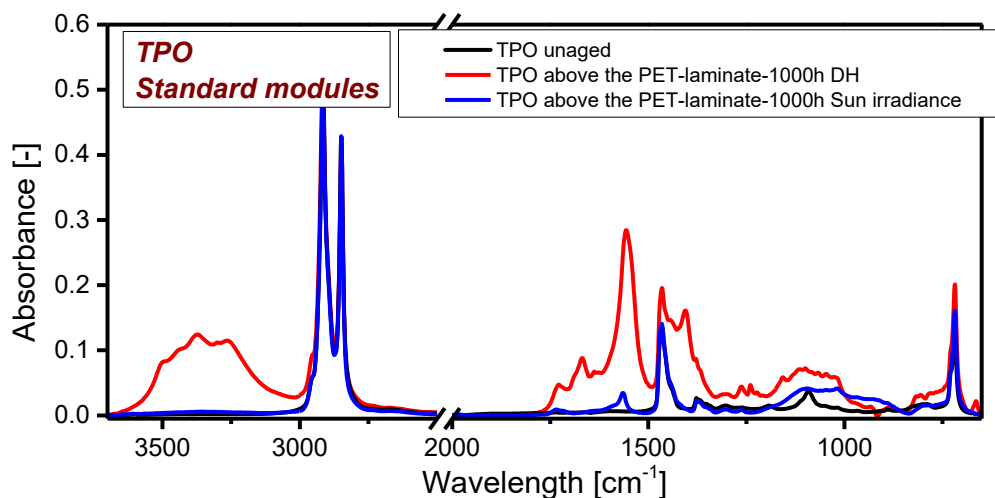**Figure 3.15.** FTIR-ATR absorbance spectra of POE above the cell before and after DH and sun irradiance test within standard module (PET-laminate backsheet)

In the double-glass module, as was case with the EVA and TPO, no significant changes were observed except an increase of the peak around 1100-800 cm^{-1}, which could be due to the changes in the additives or in the stretching and wagging vibrations of double C=C bonds [44].
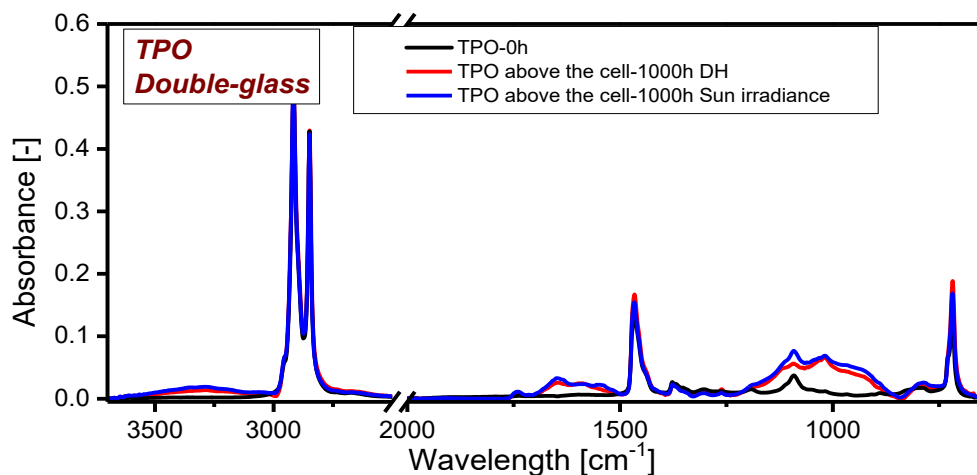

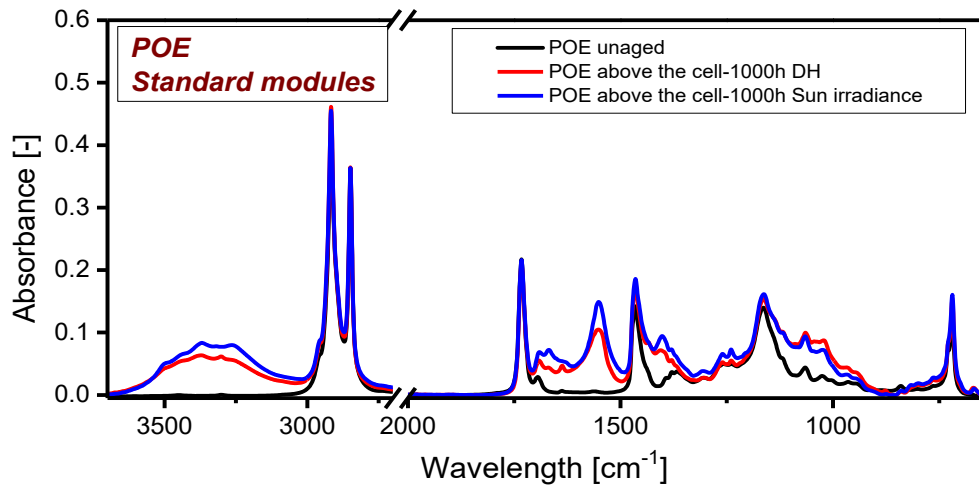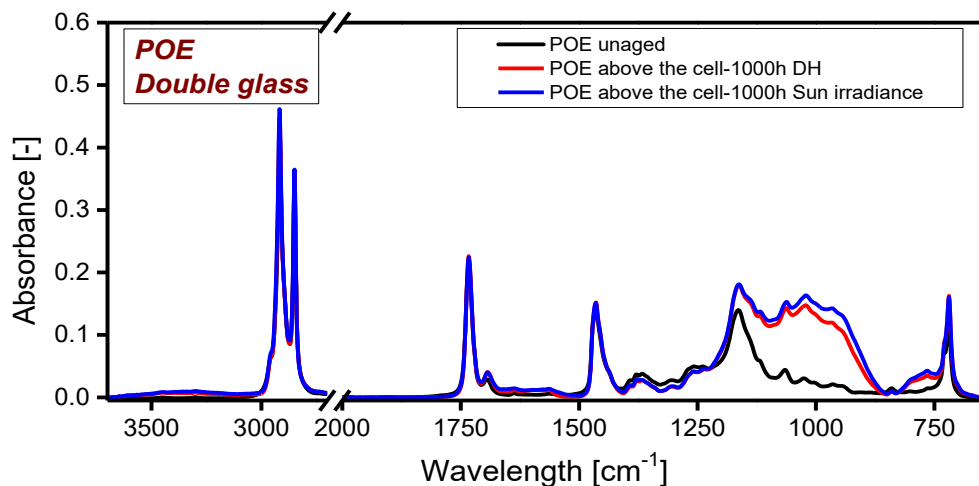**Figure 3.16.** FTIR-ATR absorbance spectra of POE above the cell before and after DH and sun irradiance test within double-glass module (glass backsheet)

The results of the FTIR-ATR analysis revealed a significant difference in absorption spectra between encapsulants in standard and double-glass modules, indicating different aging processes. Since glass backside is impermeable it could prevent the

ingress of moisture towards the encapsulants above the cell. Therefore, encapsulants extracted from double-glass modules did not suffer from hydrolysis compared to encapsulants from the standard modules. However, photo-oxidation of encapsulants was more pronounced in double-glass modules, probably due to higher temperature (caused by irradiation) in the centre of the modules that could accelerate degradation processes. Oxidation of polyolefins was shown to lead to loss of mechanical properties. This observation proves that permeation properties of the backsheet material influence the degradation of the encapsulants above the cell. The degradation of the encapsulants above the PET-laminate was higher compared to position above the cell, but as already stated, this can be regarded as "extreme conditions" since the modules were frameless and moisture ingress was highly enhanced.

3.3.3 Differential scanning calorimetry (DSC)

The DSC curves of unaged and laminated EVA, TPO and POE are shown in Figure 3.17. In the DSC curve of crosslinked EVA a very broad melting range with the melting peaks at 40°C and 65°C is observed. Those peaks are related to the existence of two predominant crystals sizes, one less perfect at 45°C and highly organized crystals of PE chains at 65°C [65–67]. The crystallization of the PE sequences is hindered by the vinyl-acetate groups since they can affect the length of PE sequences [65,66,68]. The DSC curve of TPO shows two melting peaks around 45°C and 109°C, which is higher than the melting temperatures of EVA and POE since it does not contain any groups that could hinder crystallization of the PE sequences. The first peak most probably originates from the melting of the crystals formed in the secondary crystallization and its reversible character is confirmed by its absence in the 2nd heating curve [69,70]. According to Jäger at al. [52], POE should provide better thermal stability than EVA, but otherwise the properties are similar to EVA. Therefore, a crosslinked POE shows the similar melting behaviour as EVA but with a second melting peak at higher temperatures, around 85°C. Since the damp heat aging is expected to have more impact on thermal properties due to the physical aging, only the modules after damp heat aging were used for the DSC measurements. Furthermore, only the thermal properties of the encapsulants above the cell are investigated due to the fact that above the backsheet there are two layer of the encapsulants (front and back encapsulant), which usually have slightly different composition. This could cause misleading interpretation of the data. Moreover, the properties of the encapsulants in contact with cell are of higher importance since change in those can significantly contribute to the reduction of power output.
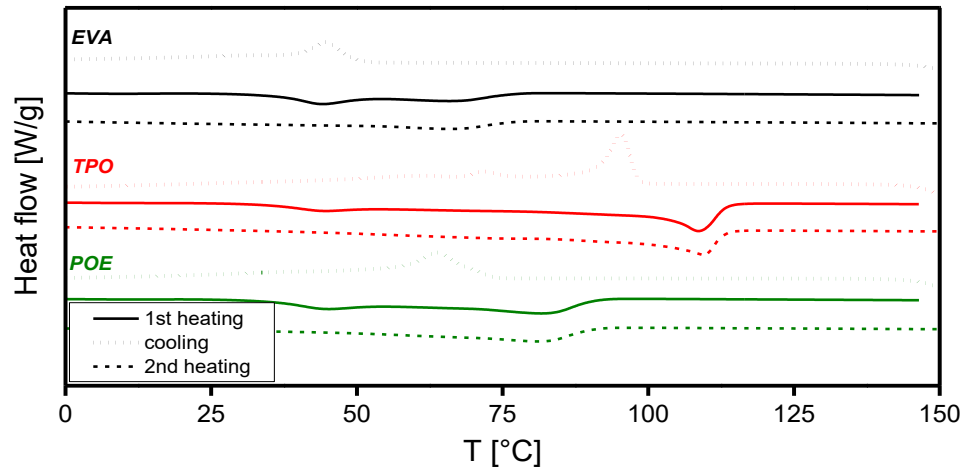
Figure 3.17. DSC thermogram of unaged and laminated EVA, TPO and POE encapsulant

The thermogram of EVA from the standard and double-glass modules before and after aging is shown in Figure 3.18. The melting temperature, melting enthalpy from the 1st heating run and the crystallization temperature from the cooling run before and after aging are summarized in Table 3.4. It can be seen that 1000h of damp heat test resulted in a shifting of the peak at 40°C assigned to less organized crystal segments towards slightly higher values of ~45°C (see Table 3.4.). This result indicates that exposure to higher temperatures resulted in a physical aging process, i.e. formation of more organized crystals and/or recrystallization [10,60,70]. On the other hand, the main melting peak shifted to the slightly lower values. Physical aging processes are related to changes in the physical structure of the polymer, while the molecular chains remain intact compared to chemical aging. They are the result of the thermodynamically unstable states caused by process-dependent cooling conditions during manufacturing [35,70]. Although the primary crystalline region (PE) is stable during aging, chain segments containing VAc units in the amorphous and ethylene chain segments in the secondary crystallization are able to re-arrange [60,69]. Considering the high standard deviation, it is hard to determine whether the overall melting enthalpy increased with aging time. In the 1st heating run no exothermic crosslinking peak could be observed, confirming that EVA was fully crosslinked in the test modules, which provides sufficient thermal and thermo-oxidative stability [2,6,71] and could be linked to overall good stability of EVA as confirmed by spectroscopy measurements. The cooling curves and 2nd heating run did not show any changes that could indicate chain scission or other processes of chemical aging. From the presented data, it could be concluded that EVA in contact with cell did

not undergo chemical aging processes since all observed changes were shown to be reversible [35,70]. The 1st heating curves of EVA from double-glass modules revealed the same thermal behaviour indicating that double-glass setup did not cause higher degradation of thermal properties compared to standard modules.

Figure 3.18. DSC thermogram of unaged and aged EVA encapsulant above the cell

In Figure 3.19. the thermogram of TPO above the cell before and after aging is shown. It can be seen that annealing at 85°C in a damp heat test allowed the formation of less organized crystallites that melt at ~ 95°C, which is slightly higher than exposure temperature, indicating physical aging [35,70]. This reversible-character was further confirmed by the disappearance of the same peak after the 2nd heating run. Furthermore, the two peaks at around 45°C and 65°C became more pronounced with aging probably due to re-crystallization. Due to the formation of the additional peak at 95°C, melting enthalpy (ΔH_m, J/g) increased from 89.7 J/g ± 2.2 to 99.7 J/g ± 3.9 (see Table 3.4.). No significant changes were observed in the main melting peak or cooling curves indicating that TPO did not undergo chemical aging processes. The same physical aging effects were observed in the TPO from double-glass modules as well.
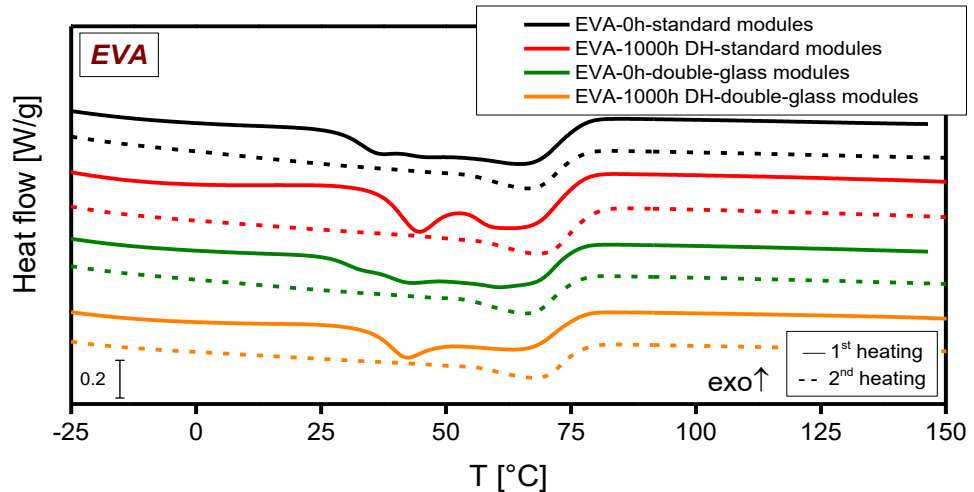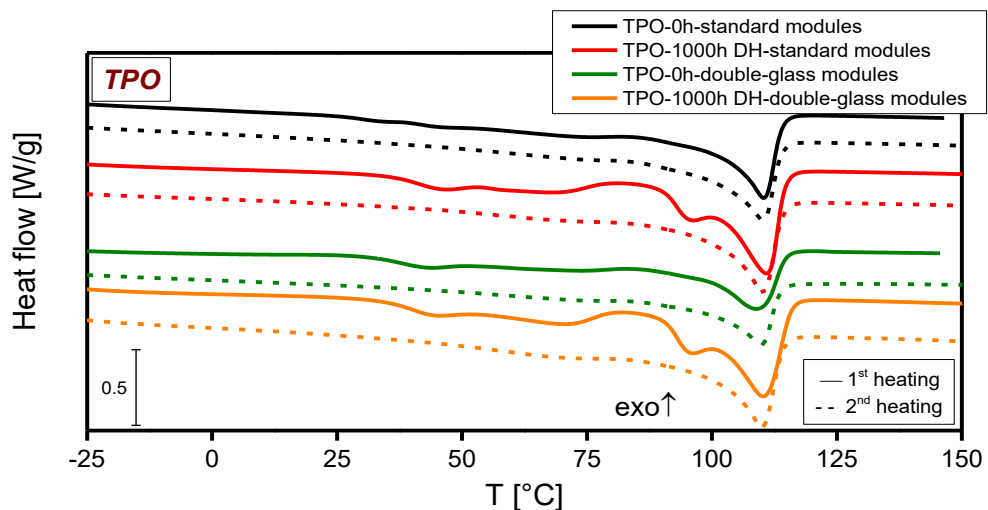
Figure 3.19. DSC thermogram of unaged and aged TPO encapsulant above the cell

In Figure 3.20. the thermogram of POE before and after aging is shown. It can be seen that the main melting peak shifted from 80.3°C to 73.5°C and a new melting peak emerged at 93°C after aging. Although the new melting peak is quite sharp, it could be assigned to annealing since its temperature is around 10°C higher than the exposure temperature and its reversible character is confirmed by its disappearance in the 2nd heating run [70]. According to Ojeda et al. [72], a shift of melting temperature towards lower values could result from an increase in crystal defects as a consequence of oxidative degradation, which results in smaller crystallites with more imperfections. During oxidative degradation, the chain rupture can occur in crystalline and non-crystalline phases. Since the crystalline phase is impermeable to oxygen, the most likely oxidation sites could be fold surfaces, loose chain ends and inter-lamellar tie molecules [35,72,73]. In fact, analysing the cooling curves and 2nd heating curves it could be seen that the T_c shifted to slightly lower values (see Table 3.4.) indicating the possible chain scission [35]. Chain scission leads to the formation of shorter and more mobile chains that are able to crystallize faster [35,70,74]. Accordingly, T_m in the 2nd heating run shifted to slightly lower values as well [35,70]. Less organized crystallites, indicated by T_m around 39°C, could rearrange upon aging or their crystallites thickness could increase, which is indicated by a slight shift towards higher temperature [70]. Analysis of POE from double-glass modules revealed the same behaviour.
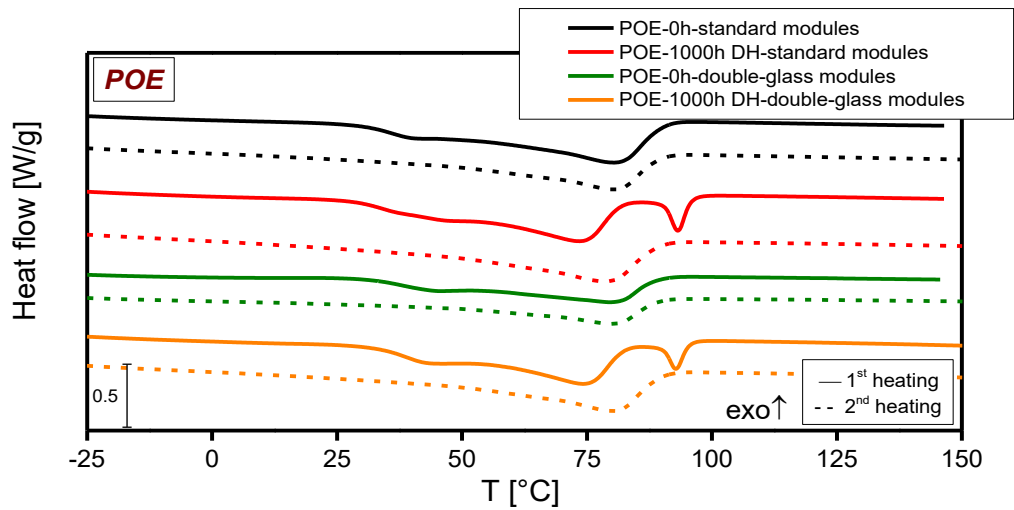
Figure 3.20. DSC thermogram of unaged and aged POE encapsulant above the cell

Table 3.4. Melting enthalpy (ΔH_m) and melting temperature (T_m) of main melting peak of encapsulant before and after aging (1st heating run)

		0h			1000h DH		
		T_m [°C]	ΔH_m [J/g]	T_c [°C]	T_m [°C]	ΔH_m [J/g]	T_c [°C]
Standard modules	EVA	65.1 ± 0.1	49.1 ± 3.1	44.9 ± 0.2	62.5 ± 0.3	50.6 ± 4.4	44.6 ± 0.2
	TPO	110.4 ± 0.1	89.7 ± 2.2	95.5 ± 0.1	111.3 ± 0.7	99.7 ± 3.9	94.3 ± 1.1
	POE	80.3 ± 0.1	68.1 ± 1.8	61.8 ± 0.1	73.5 ± 0.1	74.4 ± 4.4	59.7 ± 0.0
Double-glass modules	EVA	62.7 ± 2.2	47.2 ± 1.1	44.5 ± 0.2	64.3 ± 0.6	37.8 ± 3.5	44.2 ± 0
	TPO	109.5 ± 1.1	70.5 ± 1.9	94.9 ± 0.4	110.7 ± 0.2	104.7 ± 0.4	95.1 ± 0
	POE	79.3 ± 0.2	43.8 ± 0.1	60.8 ± 0.2	74.3 ± 0.6	67.2 ± 4.0	61.9 ± 0.0

Except for slight shifts in T_m and changes in ΔH_m due to physical aging processes, thermal properties of EVA and TPO encapsulants in the modules did not change significantly upon aging. However, POE showed the emergence of a sharp annealing peak upon exposure to elevated temperature and possible chemical aging as indicated by a shift of T_c towards lower values. Double-glass composition did not influence significantly degradation of thermal properties of encapsulants.

3.3.4 Feasibility of EVA replacement

In order to investigate the weathering stability of alternative encapsulants (TPO and POE) systematic analysis was done on the test modules. Furthermore, modules were

prepared in two different designs: with polymeric PET-laminate (standard modules) and glass backsheet (double-glass), which gave insights into the influence of PV design, i.e. permeation properties of backsheet on the degradation of front encapsulants.

The results of UV/Vis/NIR spectroscopy revealed similar degradation of optical properties above the cell in terms of yellowing in both module types. Based on the results of FTIR-ATR spectroscopy, TPO showed excellent stability above the cell, regardless of aging test or module design. The reason for good stability of TPO could be its hydrolysis resistance and absence of oxygen- and double-bonds containing groups (e.g. VAc segments). On the other hand, EVA and POE resulted in hydrolysis and photo-oxidation. Oxidation of the PE-based encapsulants can lead to loss of mechanical [57,75,76] and optical properties [9], which can lead to failure modes such as discoloration, delamination, cracking of the cells. The FTIR-ATR data showed the clear influence of backsheet type and microclimate on the degradation of front encapsulants. The permeation properties of the PET-laminate allowed ingress of moisture and oxygen, which resulted in hydrolysis and stronger oxidation of EVA and POE in standard modules compared to impermeable double-glass modules. The degradation of the all three types of encapsulants was usually more pronounced above the backsheet than above the cell due to permeation of moisture and oxygen from the edges that were not protected with the frame (usually should not happen outdoors). The results for TPO showed the highest degradation above the PET-laminate, which is most probably the consequence of interactions between the TiO_2 in the inner side of the backsheet and additives in TPO (photo-yellowing). The observed yellowing indicated an incompatibility of those two materials, but should not affect the power output. Thermal analysis (DSC) revealed physical aging of EVA and TPO encapsulants above the cell in terms of re- and post-crystallization. An increased degree of crystallinity could lead to a loss of mechanical and optical properties (reduced transmittance), which could affect power output of the modules. DSC analysis of the POE indicated possible chemical aging.

Based on the results presented in this work, it can be concluded that alternative encapsulants showed similar (POE) or better (TPO) weathering stability compared to the state-of-the-art encapsulant (EVA). The type of backsheet plays an important role in the degradation of front encapsulant due to the permeation properties. TPO encapsulant showed the highest weathering stability above the cell no matter what aging conditions or type of the backsheet used, which indicates its good performance in the modules operating under harsh climatic conditions.

3.4   Summary and conclusions

Although the most widely used encapsulant in PV modules, EVA comes with its drawbacks such as peroxide-induced crosslinking and production of corrosive acetic acid, which are linked to reduced reliability of the PV modules. Therefore, alternative thermoplastic polyolefin (TPO) and polyolefin elastomer (POE) are drawing more attention as encapsulating materials. In order to replace EVA, alternative materials need to provide comparable or even better properties. Hence, the main aim of Chapter 3 was to investigate weathering stability of alternative encapsulants at PV module level and to understand the role of permeation properties of backsheet in their degradation.

Systematic analysis in terms of UV/Vis/NIR spectroscopy, FTIR-ATR spectroscopy and differential scanning calorimetry (DSC) was conducted on front encapsulants at PV module level. UV/Vis/NIR spectroscopy conducted above the cell revealed a slight loss of UV-absorbers that led to slight yellowing in both types of modules regardless of the type of encapsulant.

FTIR-ATR spectroscopy showed the clear influence of backsheet type and microclimate on the degradation of front encapsulants. The degradation of encapsulants above the PET-laminate was stronger due to the permeation of the moisture and oxygen through the polymeric backsheet that could lead to hydrolysis and oxidation of the encapsulants. The strongest effect of degradation was observed for TPO above the PET-laminate after damp heat aging due to the interaction between TiO_2 from the inner side of the backsheet and additives in TPO. In the presence of sun irradiation, the effect was minimized due to photo-bleaching effect. Hydrolysis and photo-oxidation of encapsulants in double glass modules was minimized, compared to standard modules with polymeric backsheet. This confirmed the assumption that the permeability of the polymeric backsheet could drive the degradation of the encapsulant faster compared to impermeable glass. However, observed changes in the area assigned to C-O-C and terminal =CH (in case of EVA and POE) and additives (TPO) seemed to be higher, which is probably due to higher temperature in the centre of the double glass modules compared to standard modules.

Results of DSC analysis showed that EVA and TPO encapsulants underwent similar physical degradation processes (re- and post-crystallization), which did not affect their chemical structure, while POE showed chemical aging.

In order to increase the reliability of PV modules, weathering stability of encapsulants is of great importance. The characterization methods applied in this chapter were shown to be effective and reliable in the investigation of weathering stability of polymeric encapsulants. Based on the data obtained in this work, it can be concluded that TPO

showed the highest weathering stability in contact with solar cell. Combined with a good chemical composition (no peroxides, no acetic acid production) it is a promising encapsulant that could provide increased reliability of PV modules, especially those operating under harsh climatic conditions.

3.5   References

[1] M. Rodríguez-Vázquez, C.M. Liauw, N.S. Allen, M. Edge, E. Fontan, Degradation and stabilisation of poly(ethylene-stat-vinyl acetate): 1 – Spectroscopic and rheological examination of thermal and thermo-oxidative degradation mechanisms, Polymer Degradation and Stability 91 (2006) 154–164. https://doi.org/10.1016/j.polymdegradstab.2005.04.034.

[2] C. Hirschl, M. Biebl–Rydlo, M. DeBiasio, W. Mühleisen, L. Neumaier, W. Scherf, G. Oreski, G. Eder, B. Chernev, W. Schwab, M. Kraft, Determining the degree of crosslinking of ethylene vinyl acetate photovoltaic module encapsulants—A comparative study, Solar Energy Materials and Solar Cells 116 (2013) 203–218. https://doi.org/10.1016/j.solmat.2013.04.022.

[3] F.J. Pern, A.W. Czanderna, Characterization of ethylene vinyl acetate (EVA) encapsulant: Effects of thermal processing and weathering degradation on its discoloration, Solar Energy Materials and Solar Cells (1992) 3–23.

[4] C. Peike, T. Kaltenbach, K.-A. Weiß, M. Koehl, Non-destructive degradation analysis of encapsulants in PV modules by Raman Spectroscopy, Solar Energy Materials and Solar Cells 95 (2011) 1686–1693. https://doi.org/10.1016/j.solmat.2011.01.030.

[5] P. Klemchuk, E. Ezrin, G. Lavigne, W. Holley, J. Galica, S. Agro, Investigation of the degradation and stabilization of EVA-based encapsulant in field-aged solar energy modules, Polymer Degradation and Stability (1997) 347–365.

[6] G. Oreski, A. Rauschenbach, C. Hirschl, M. Kraft, G.C. Eder, G. Pinter, Crosslinking and post-crosslinking of ethylene vinyl acetate in photovoltaic modules, J. Appl. Polym. Sci. 134 (2017) 101. https://doi.org/10.1002/app.44912.

[7] C. Hirschl, M. Biebl-Rydlo, M. Kraft, W. Mühleisen, L. Neumaier, G.C. Eder, B.S. Chernev, Raman Spectroscopic Determination of the Degree of Encapsulant Crosslinking in PV Modules, in: 28th European Photovoltaic Solar Energy Conference and Exhibitiom, pp. 3020–3025.

[8] A.W. Czanderna, F. J. Pern, Encapsulation of PV modules using ethylene vinyl acetate copolymer as a pottant: A critical review, Solar Energy Materials and Solar Cells (1996) 101–181.

[9] B. Ottersböck, G. Oreski, G. Pinter, Comparison of different microclimate effects on the aging behavior of encapsulation materials used in photovoltaic modules, Polymer Degradation and Stability (2017) 182–191. https://doi.org/10.1016/j.polymdegradstab.2017.03.010.

[10] K. Agroui, G. Collins, Determination of thermal properties of crosslinked EVA encapsulant material in outdoor exposure by TSC and DSC methods, Renewable Energy 63 (2014) 741–746. https://doi.org/10.1016/j.renene.2013.10.013.

[11] S.-S. Choi, C.E. Son, Novel analytical method for determination of contents of backbone and terminal/branch vinyl acetate groups of poly(ethylene-co-vinyl acetate) using deacetylation reaction, Polymer Testing 56 (2016) 214–219. https://doi.org/10.1016/j.polymertesting.2016.10.012.

[12] U. Weber, R. Eiden, C. Strubel, T. Soegding, M. Heiss, P. Zachmann, K. Nattermann, H. Engelmann, A. Dethlefsen, N. Lenck, Acetic Acid Production, Migration and Corrosion Effects in Ethylene-Vinyl-Acetate- (EVA-) Based PV Modules, in: 27th European Photovoltaic Solar Energy Conference and Exhibition, Frankfurt, 2012.

[13] T. Geipel, M. Moeller, A. Kraft, U. Eitner, A Comprehensive Study of Intermetallic Compounds in Solar Cell Interconnections and their Growth Kinetics, Energy Procedia 98 (2016) 86–97. https://doi.org/10.1016/j.egypro.2016.10.084.

[14] C. Peike, S. Hoffmann, P. Hülsmann, B. Thaidigsmann, K.-A. Weiß, M. Koehl, P. Bentz, Origin of damp-heat induced cell degradation, Solar Energy Materials and Solar Cells 116 (2013) 49–54. https://doi.org/10.1016/j.solmat.2013.03.022.

[15] D. Wu, J. Zhu, T.R. Betts, R. Gottschalg, Degradation of interfacial adhesion strength within photovoltaic mini-modules during damp-heat exposure, Prog. Photovolt: Res. Appl. 22 (2014) 796–809. https://doi.org/10.1002/pip.2460.

[16] D. Wu, J. Zhu, D. Montiel-Chicharro, T.R. Betts, R. Gottschalg, Influence of different lamination conditions on the reliability of encapsulation of PV modules, in: 29th European Photovoltaic Solar Energy Conference and Exhibition, Amsterdam, Netherlands, 2014.

[17] Sachiko Jonai, Kohjiro Hara, Yuji Tsutsui, Hidenari Nakahama, Atsushi Masuda, Relationship between cross-linking conditions of ethylene vinyl acetate and potential induced degradation for crystalline silicon photovoltaic modules, Japanese Journal of Applied Physics 54 (2015) 08KG01.

[18] A.Mihaljevic, G.Oreski, G.Pinter, Influence of Backsheet Type on Formation of Acetic Acid in PV Modules, in: 32nd European Photovoltaic Specialists Conference and Exhibition, Munich, 2016.

[19] A. Omazic, G. Oreski, M. Halwachs, G.C. Eder, C. Hirschl, L. Neumaier, G. Pinter, M. Erceg, Relation between degradation of polymeric components in crystalline silicon PV module and climatic conditions: A literature review, Solar Energy Materials and Solar Cells 192 (2019) 123–133. https://doi.org/10.1016/j.solmat.2018.12.027.

[20] E. Kaplani, Detection of Degradation Effects in Field-Aged c-Si Solar Cells through IR Thermography and Digital Image Processing, International Journal of Photoenergy 2012 (2012) 1–11. https://doi.org/10.1155/2012/396792.

[21] S. Chattopadhyay, R. Dubey, V. Kuthanazhi, J.J. John, C.S. Solanki, A. Kottantharayil, B.M. Arora, K.L. Narasimhan, V. Kuber, J. Vasi, A. Kumar, O.S. Sastry, Visual Degradation in Field-Aged Crystalline Silicon PV Modules in India and Correlation With Electrical Degradation, IEEE J. Photovoltaics 4 (2014) 1470–1476. https://doi.org/10.1109/JPHOTOV.2014.2356717.

[22] F. Bandou, A. Hadj Arab, M.S. Belkaid, P.-O. Logerais, O. Riou, A. Charki, Evaluation performance of photovoltaic modules after a long time operation in Saharan environment, International Journal of Hydrogen Energy 40 (2015) 13839–13848. https://doi.org/10.1016/j.ijhydene.2015.04.091.

[23] Y.Tang, B.Raghuraman, J.Kuitche, G.TamizhMani, C.E.Backus, C.Osterwald, An evaluation of 27+ years old photovoltaic modules operated in a hot-dessert climatic conditions, in: 2006 IEEE 4th World Conference on Photovoltaic Energy Conversion, Waikoloa, Hawai, 2006.

[24] M. Chicca, G. TamizhMani, Nondestructive techniques to determine degradation modes: Experimentation with 18 years old photovoltaic modules, in: IEEE 42nd Photovoltaic Specialists Conference (PVSC), New Orleans, 2015., pp. 1–5.

[25] A. Bouraiou, M. Hamouda, A. Chaker, M. Mostefaoui, S. Lachtar, M. Sadok, N. Boutasseta, M. Othmani, A. Issam, Analysis and evaluation of the impact of climatic conditions on the photovoltaic modules performance in the desert environment, Energy Conversion and Management 106 (2015) 1345–1355. https://doi.org/10.1016/j.enconman.2015.10.073.

[26] A.A.Suleske, Performance Degradation of Grid-Tied Photovoltaic Modules in a Desert Climatic Condition. Master Thesis, 2010.

[27] K.Yedidi, S.Tatapudi, J.Mallineni, B.Knisely, K.Kutiche, G.TamizhMani, Failure and Degradation Modes and Rates of PV Modules in a Hot-Dry Climate: Results after 16 years of field exposure, in: Photovoltaic Specialist Conference (PVSC), 2014 IEEE 40th, pp. 3245–3247.

[28] D. C. Jordan, J. H. Wohlgemuth, and S. R. Kurtz, Technology and Climate Trends in PV Module Degradation, in: 27th European Photovoltaic Solar Energy Conference and Exhibition, Frankfurt, 2012.

[29] A. Limmanee, S. Songtrai, N. Udomdachanut, S. Kaewniyompanit, Y. Sato, M. Nakaishi, S. Kittisontirak, K. Sriprapha, Y. Sakamoto, Degradation analysis of photovoltaic modules under tropical climatic conditions and its impacts on LCOE, Renewable Energy 102 (2017) 199–204. https://doi.org/10.1016/j.renene.2016.10.052.

[30] M.Makenzi, N.Timonah, M.Benedict, I.Abisai, Degradation Prevalence Study of Field-Aged Photovoltaic Modules Operating Under Kenyan Climatic Conditions, SJEE 3 (2015) 1. https://doi.org/10.11648/j.sjee.20150301.11.

[31] P. Sánchez-Friera, M. Piliougine, J. Peláez, J. Carretero, M. Sidrach de Cardona, Analysis of degradation mechanisms of crystalline silicon PV modules after 12 years of operation in Southern Europe, Prog. Photovolt: Res. Appl. 19 (2011) 658–666. https://doi.org/10.1002/pip.1083.

[32] Neelkanth G. Dhere, Reliability of PV Modules and Balance-of-System Components, in: Proceedings of the 31st IEEE Photovoltaic Specialist Conference, 2005., pp. 1570–1576.

[33] M.D. Kempe, Overview of Scientific Issues Involved in Selection of Polymers for PV Applications: Preprint, in: 37th IEEE Photovoltaic Specialists Conference, Seattle, USA, 2011.

[34] M.C. López-Escalante, L.J. Caballero, F. Martín, M. Gabás, A. Cuevas, J.R. Ramos-Barrado, Polyolefin as PID-resistant encapsulant material in 5PV6 modules, Solar Energy Materials and Solar Cells 144 (2016) 691–699. https://doi.org/10.1016/j.solmat.2015.10.009.

[35] G.W. Ehrenstein, S. Pongratz, Resistance and stability of polymers, Hanser Publishers, Munich, 2013.

[36] G.M. A.B. Mathur, Thermo-oxidative degradation of isotactic polypropylene film: Structural changes and its correlation with properties, Polymer 23 (1982) 54–56.

[37] C. Rouillon, P.-O. Bussiere, E. Desnoux, S. Collin, C. Vial, S. Therias, J.-L. Gardette, Is carbonyl index a quantitative probe to monitor polypropylene photodegradation?, Polymer Degradation and Stability 128 (2016) 200–208. https://doi.org/10.1016/j.polymdegradstab.2015.12.011.

[38] A.-C. Albertsson (Ed.), Long-Term Properties of Polyolefines, Springer, Berlin Heidelberg, 2004.

[39] C. Vasile (Ed.), Handbook of polyolefins, 2nd ed., Marcel Dekker, New York, 2000.

[40] A. Valadez-Gonzalez, J.M. Cervantes-U, L. Veleva, Mineral fller influence on the photo-oxidation of high density polyethylene: I. Accelerated UV chamber exposure test, Polymer Degradation and Stability (1999) 253–260.

[41] G. Oreski, G.M. WALLNER, R.W. Lang, Ageing characterization of commercial ethylene copolymer greenhouse films by analytical and mechanical methods, Biosystems Engineering 103 (2009) 489–496. https://doi.org/10.1016/j.biosystemseng.2009.05.003.

[42] E.Cabrera, A.Schneider, J.Rabanal, P.Ferrada, R.R.Cordero, E.Fuentealba, R.Kopecek, Advancements in the Development of "AtaMo": a Solar Module Adapted for the Climate Conditions of the Atacama Desert in Chile, in: 31st European Photovoltaic Solar Energy Conference and Exhibition, Hamburg, 2015., pp. 1–22.

[43] J. Govaerts, B.Geyer, A.van der Heide, T.Borgers, S.Hellstrom, B.Broeders, E.Voroshazi, J.Szlufcik and J.Poortmans, Extended Qualification Testing of 1-cell Crystalline Si PV Laminates: Impacts of Advanced Cell Metallization and Encapsulation Schemes, in: 33rd European Photovoltaic Solar Energy Conference and Exhibition, Amsterdam, 2017.

[44] G. Oreski, G.M. WALLNER, Evaluation of the aging behavior of ethylene copolymer films for solar applications under accelerated weathering conditions, Solar Energy 83 (2009) 1040–1047. https://doi.org/10.1016/j.solener.2009.01.009.

[45] C. Peike, P. Hülsmann, M. Blüml, P. Schmid, K.-A. Weiß, M. Köhl, Impact of Permeation Properties and Backsheet-Encapsulant Interactions on the Reliability of PV Modules, ISRN Renewable Energy 2012 (2012) 1–5. https://doi.org/10.5402/2012/459731.

[46] G. Oreski, A. Mihaljevic, Y. Voronko, G.C. Eder, Acetic acid permeation through photovoltaic backsheets: Influence of the composition on the permeation rate, Polymer Testing 60 (2017) 374–380. https://doi.org/10.1016/j.polymertesting.2017.04.025.

[47] J. Tang, C. Ju, R. Lv, X. Zeng, J. Chen, D. Fu, J.-N. Jaubert, T. Xu, The Performance of Double Glass Photovoltaic Modules under Composite Test Conditions, Energy Procedia 130 (2017) 87–93. https://doi.org/10.1016/j.egypro.2017.09.400.

[48] A. Skoczek, T. Sample, E.D. Dunlop, The results of performance measurements of field-aged crystalline silicon photovoltaic modules, Progress in Photovoltaics: Research and Application (2009) 227–240. https://doi.org/10.1002/pip.874.

[49] International Organisation for Standardisation, ISO 11357-3, Plastics - Differential scanning calorimetry (DSC) Part 3: Determination of temperature and enthalpy of melting and crystallization, 1999.

[50] J.G. Drobny, Handbook of Thermoplastic Elastomers: Polyolefin-Based Thermplastic Elastomers.

[51] H.I. Mattausch, Infrarot-spektroskopische Charakterisierung von Polymeren und Additiven. Bachelorarbeit, Leoben, 2008.

[52] K. M. Jäger, R. C. Dammert, B. A. Sultan, Thermal degradation studies of different polar polyethylene copolymers, J. Appl. Polym. Sci. 84 (2002) 1465–1473. https://doi.org/10.1002/app.10510.

[53] H. W. Siesler, K. Holland-Moritz, IR and Raman Spectroscopy Of Polymers, Marcel Dekker, Inc., New York, 1980.

[54] H. Lobo, J.V. Bonilla (Eds.), Handbook of plastics analysis, Marcel Dekker, New York, 2003.

[55] Arijit Ghosh, Degradation of polymer/substrate interfaces – an attenuated total reflection Fourier transform infrared spectroscopy approach. Masterthesis, Ohio, 2010.

[56] N.S. Allen, M. Edge, M. Rodriguez, C.M. Liauw, E. Fontan, Aspects of the thermal oxidation, yellowing and stabilisation of ethylene vinyl acetate copolymer, Polymer Degradation and Stability (2001) 1–14.

[57] Adams Tidjani, Comparison of formation of oxidation products during photo-oxidation of linear low density polyethylene under different natural and accelerated weathering conditions, Polymer Degradation and Stability (2000) 465–469.

[58] F.P. La Mantia, V. Malatesta, M. Ceraulo, M.C. Mistretta, P. Koci, Photooxidation and photostabilization of EVA and cross-linked EVA, Polymer Testing 51 (2016) 6–12. https://doi.org/10.1016/j.polymertesting.2016.01.018.

[59] P. Dole, J. Chauchard, Thermooxidation of poly(ethylene-co-methyl acrylate) and poly(methy1 acrylate) compared to oxidative thermal aging of polyethylene, Polymer Degradation and Stability (1996) 63–72.

[60] J. Jin, S. Chen, J. Zhang, UV aging behaviour of ethylene-vinyl acetate copolymers (EVA) with different vinyl acetate contents, Polymer Degradation and Stability 95 (2010) 725–732. https://doi.org/10.1016/j.polymdegradstab.2010.02.020.

[61] K. Grabmayer, G.M. WALLNER, S. Beißmann, U. Braun, R. Steffen, D. Nitsche, B. Röder, W. Buchberger, R.W. Lang, Accelerated aging of polyethylene materials at high oxygen pressure characterized by photoluminescence spectroscopy and established aging characterization methods, Polymer Degradation and Stability 109 (2014) 40–49. https://doi.org/10.1016/j.polymdegradstab.2014.06.021.

[62] B. Ottersböck, Natural and artificial weathering tests of polymer films used in solar applications. Doctoral Thesis, Leoben, AUT, April/2017.

[63] N.S. Allen, D.J. Bullen, J.F. McKellar, Photo-yellowing of a phenolic anti-oxidant in the presence of various stabilizer/titanium dioxide pigment combinations in polyethylene, Journal of Material Science 13 (1978) 2692–2696.

[64] J.-F. Glikman, R. Arnaud, J. Lemaire, H. Seinera, Photolysis and photo-oxidation of ethylene-ethyl acrylate copolymers, Polymer Degradation and Stability 16 (1986) 325–335. https://doi.org/10.1016/0141-3910(86)90089-3.

[65] S. Bistac, P. Kunemann, J. Schultz, Crystalline modifications of ethylene-vinyl acetate copolymers induced by a tensile drawing: effect of the molecular weight, Polymer 39 (1998) 4875–4881.

[66] M. Brogly, M. Nardin, J. Schultz, Effect of Vinylacetate Content on Crystallinity and Second-Order Transitions in Ethylene–Vinylacetate Copolymers, J. Appl. Polym. Sci. 64 (1997) 1903–1912. https://doi.org/10.1002/(SICI)1097-4628(19970606)64:10<1903:AID-APP4>3.0.CO;2-M.

[67] A. Badiee, I.A. Ashcroft, R.D. Wildman, The thermo-mechanical degradation of ethylene vinyl acetate used as a solar panel adhesive and encapsulant, International Journal of Adhesion and Adhesives 68 (2016) 212–218. https://doi.org/10.1016/j.ijadhadh.2016.03.008.

[68] Rufina Alamo, Roman Domszy, Leo Mandelkern, Thermodynamic and structural properties of copolymers of ethylene, Journal of Physical Chemistry (1984) 6587–6595.

[69] A.J. Peacock, Handbook of Polyethylene: Morphology and Crystallization of Polyethylene, Marcel Dekker, Inc., New York, N.Y., 2000.

[70] G.W. Ehrenstein, G. Riedel, P. Trawiel, Thermal analysis of plastics: Theory and practice, Carl Hanser Verlag, Munich, 2004.

[71] K. Agroui, A. Belghachi, G. Collins, J. Farenc, Quality control of EVA encapsulant in photovoltaic module process and outdoor exposure, Desalination 209 (2007) 1–9. https://doi.org/10.1016/j.desal.2007.04.001.

[72] T. Ojeda, A. Freitas, K. Birck, E. Dalmolin, R. Jacques, F. Bento, F. Camargo, Degradability of linear polyolefins under natural weathering, Polymer Degradation and Stability 96 (2011) 703–707. https://doi.org/10.1016/j.polymdegradstab.2010.12.004.

[73] John Wiley and Sons, Encyclopedia of Polymer Science and Technology - Barrier polymers, 1999-2012.

[74] M. Knausz, G. Oreski, G.C. Eder, Y. Voronko, B. Duscher, T. Koch, G. Pinter, K.A. Berger, Degradation of photovoltaic backsheets: Comparison of the aging induced changes on module and component level, J. Appl. Polym. Sci. 132 (2015) 1–8. https://doi.org/10.1002/app.42093.

[75] Eiichi Miyagawa, Koh-hei Nitta, Akira Tanaka, Effects of photo-oxidation on tensile deformation behaviour in low-density polyethylene, e-Polymers (2005).

[76] J. Pospíšil, Z. Horák, J. Pilař, N.C. Billingham, H. Zweifel, S. Nešpůrek, Influence of testing conditions on the performance and durability of polymer stabilisers in thermal oxidation, Polymer Degradation and Stability 82 (2003) 145–162. https://doi.org/10.1016/S0141-3910(03)00210-6.

4 Influence of damp heat aging on thermo-mechanical stability of polyolefin encapsulants at single film level

4.1 Motivation

One of the main purposes of encapsulating materials is the protection of brittle c-Si solar cells and soldered interconnections from breakage during the production and service of PV modules. Already during the production of PV modules, all of the PV components expand at different rates in the applied temperature range. Thermal expansion or shrinkage of the encapsulation material during the lamination of PV modules can lead to the sliding of the c-Si cells or other components [1,2]. According to Ehrenstein [3], joining materials that have different expansion properties can lead to thermal stresses. Mismatches in the coefficient of thermal expansion (CTE) between PV components can lead to breakage of the Si-cell and interconnectors, delamination on the interfaces with the encapsulation, warpage of the backsheet, etc. PV encapsulants have the highest CTE among PV components [1,4–6]. Therefore, it is evident that thermal expansion behaviour of the encapsulant is a key parameter for a stable PV module lamination process and high product quality [1].

During operation in the field, PV modules additionally experience different daily and seasonal thermal cycles, depending on the operation conditions, which adds additional internal stresses within the PV module [1,4,7]. The variations in the CTE must be considered during the design of PV modules. CTE is a material characteristic value and remains constant as long as the temperature changes occur within the same state, e.g. below as well as above the T_g temperature. However, if a transition is crossed, significant changes in the material properties can occur. If a certain component cannot be deformed within given conditions (such as PV components in a PV module), it can result in internal stresses [3,8]. When polymers reach temperatures above the softening temperature, depending on the pre-existing degree of molecular orientation, shrinkage (negative expansion) can occur because the increased temperature allows molecular movement. Since the molecules tend to return to the natural coiled state, the final result is shrinkage of the material [3].

Some attempts have been made to understand the thermal expansion behaviour of solar cell encapsulants, but the data are very poor. Knausz et al. [1] investigated thermal expansion of different un-crosslinked encapsulants during lamination of the PV modules

in order to identify possible deficiencies in production process and allow for the optimization of the process parameters. The authors [1] found that there is a strong anisotropic expansion of encapsulants and that there are significant differences between different types of encapsulants as well. This indicates that the choice of material is important not only for the reliability of the PV modules but also should be considered prior to lamination of the PV modules since it can lead to serious damage of the PV components and/or introduce internal stresses that can lead to failure modes during operation in the field.

Exposure of polymers to elevated temperatures, humidity and irradiation causes certain changes in their physical and/or chemical structure, which can be reflected in their optical, thermal, mechanical and thermo-mechanical properties [8]. When polymers are exposed to temperatures above the glass transition temperature (T_g), internal aging can occur, i.e. orientations and stresses may relax, post-crystallization and/or re-crystallization processes may take place [3,8,9]. Such conditions have impact on the properties of the material. Relaxation from orientations and stresses can result in a change in the initial dimensions of the material [1,3]. Since PV modules operate outdoors, the polymeric PV components are exposed to harsh environmental conditions (elevated temperatures, humidity, UV irradiation, mechanical loads, etc.) during their whole service time, which can affect their properties during service and give rise to different failure modes. For example, changes in thermal and thermo-mechanical properties of EVA upon field exposure were found to be triggers for delamination of the front encapsulant [10–12]. Wang et al. [11] assume that UV exposure leads to an increased crystallinity and therefore increased stiffness of the EVA encapsulant. Damp heat aging was found to influence the polymer morphology of the EVA due to an increased crystallinity, which has an effect on the stiffness of material as well [12–15].

Thermo-mechanical analysis (TMA) has already been proven as a good method for investigation of thermo-mechanical properties of thin polymeric films [1,16–20]. Used in combination with differential scanning calorimetry (DSC), the information on the influence of polymer morphology and thermal properties on thermo-mechanical behaviour can be obtained. DSC is a very good tool for detecting changes in the polymer morphology caused by physical and chemical aging processes. The effects of the changed morphology on aging should be manifested in thermo-mechanical behaviour as well. However, according to the author's knowledge, so far there are no published studies on the influence of aging on the thermo-mechanical behaviour of polyolefin solar encapsulants.

Hence the main idea behind this chapter was to investigate how the changes in the materials' morphology upon aging under damp heat conditions affect the thermo-mechanical behaviour of laminated EVA, TPO and POE encapsulants at the single film level. Of special interest was to investigate changes of thermal and thermo-mechanical properties in the application relevant range for PV encapsulants from 25°C to 80°C. These findings could help evaluate the applicability of each encapsulant under specific operating conditions.

4.2 Experimental part

4.2.1 Preparation and aging of the samples

The encapsulants investigated in this work are ethylene vinyl-acetate (EVA), thermoplastic polyolefin (TPO) and polyolefin elastomer (POE). Their detailed structure can be found in Chapter 3. As the main objective of this work was to investigate the influence of damp heat aging on the thermo-mechanical stability of the encapsulants in the PV module during service time, thermal and thermo-mechanical properties of the encapsulants were investigated prior to and after 1000h of damp heat aging. For that purpose, the encapsulant single films were cut into A4 sheets and laminated in the same way as PV modules according to the parameters listed in Table 4.1. After lamination, the samples were subjected to damp heat tests (T=85°C, RH=85%) in the climate chamber for 1000h. The reason why single films were used in this work is because the encapsulants could not be manually delaminated from the modules in the proper dimensions needed for the TMA measurements.

Table 4.1. Lamination parameters [15]

Step	Time [min]	Temperature [°C]	Pressure [mbar]
Closing laminator	0.5	144	atmospheric
Evacuation	6.0	144	atmospheric to 850
Pressure	1.0	144	850
Curing	9.3	144	850
Ventilation	0.3	144	850 to atmospheric
Opening laminator	0.5	144	atmospheric

4.2.2 Thermo-mechanical analysis (TMA)

The thermal expansion behaviour was characterized using a Mettler Toledo TMA/SDTA 840 (Schwerzenbach, CH). Due to the influence of drawing off during film extrusion, thermal expansion of the films was measured in machine (MD) and counter (CD) direction in tensile mode before and after aging. The measurements were performed under air atmosphere. In order to obtain information on reversible and irreversible changes in the materials, two heating runs were carried out. The end temperature of the first heating run for TMA was set below the melting region, while for the second heating

run it was set in the region of melting to detect all transitions influencing thermo-mechanical expansion.

In order to avoid bending of the films and to ensure maximum accuracy when determining CTE, samples need to be in tension during measurements. Therefore, a static load of 0.02 N was applied. The applied load exerts hardly any influence in the temperature range where melting still has not started [16]. However, with the start of the melting range, due to the enhanced mobility of molecular chains and the introduction of relaxation (internal stresses and orientations), the influence of the static load increases rapidly. For thin films, static loads of F = 0.01 N to F = 1 N are recommended [9]. Therefore, the static load of F = 0.02 N was used in this study. Each sample was measured at least two times per direction according to the parameters listed in Table 4.2..

Table 4.2. Parameters of TMA analysis

Step	Start temperature [°C]	End temperature [°C]	Heating rate [°C/min]
1st heating	25	80	5
Cooling	80	25	5
2nd heating	25	100	5

The coefficient of thermal expansion (CTE) was evaluated from the first and second heating curves. The evaluation of the data was done according to ISO 11359-2 [21] or DIN 53 752 [22] standards. The CTE was calculated according to Equation 4.1.

$$CTE(T_1, T_2) = \frac{1}{l_0} * \frac{l_2 - l_1}{T_2 - T_1} \ [10^{-6} K^{-1}]$$

where l_0 is the initial length of the sample at room temperature, l_1 is the length of the sample at 25°C and l_2 is the length at the end temperature [9]. The initial length of the sample was 10 mm and width 6 mm. CTE was calculated for both heating runs.

In the first heating run, reversible and irreversible effects overlap. Therefore, the first heating run yielded information about the actual state of the specimen, including the thermal and mechanical history, processing influences and service conditions. During the first heating run, all reversible effects (internal stresses, post-crystallization, post-polymerization etc.) are eliminated. The second heating run provides the coefficient of thermal expansion as a material characteristic and, in order to determine it, the material must not undergo irreversible changes (post-polymerization, post-crystallization).

Therefore, the end temperature of the first heating was set at lower values compared to the second heating run.

4.2.3 Differential scanning calorimetry (DSC)

Thermal properties of the encapsulants before and after aging were investigated via DSC 4000 from Perkin Elmer. In order to obtain information on reversible and irreversible properties of the material, two heating runs were applied. The measurement parameters are listed in Table 4.3. Melting enthalpy was evaluated from the 1st heating run according to [23]. The mass of the samples ranged from 9 to 11 mg. In order to avoid oxidation of the samples, nitrogen atmosphere with flow of 50 mL/min was maintained during the measurements. Each sample was measured at least twice.

Table 4.3. Parameters of DSC analysis

Step	Start temperature [°C]	End temperature [°C]	Heating rate [°C/min]
1st heating	-70	150	10
Cooling	150	-70	10
2nd heating	-70	300	10

The degree of crystallinity (w_c, %) of each sample was calculated according to Equation 4.2.:

$$w_c = \frac{\Delta Hm}{\Delta Hm^0} * 100 \ [\%]$$

Where ΔH_m is the experimental melting enthalpy (heat of fusion) and ΔH_m^0 is the literature value for 100% crystalline material [9]. In the case of EVA, TPO and POE, a component that is able to crystallize is PE and its ΔH_m^0 value of 293 J/g was considered in the calculations [9].

4.3   Results and discussion

In the following part, each material will be discussed separately starting with EVA. Their thermo-mechanical properties will be correlated with their thermal properties before and after aging. At the end of the section, three types of encapsulants will be compared and a critical overview of their thermal and thermo-mechanical stability will be given.

4.3.1   Ethylene vinyl-acetate (EVA)

In Figure 4.1. TMA curves of crosslinked EVA before aging in MD and CD direction are shown. The measurements were starting at room temperature, which means that the T_g range could not influence the shape of the curves presented in this work. As can be seen, the 1st heating of the EVA film resulted in expansion in both directions, which could indicate biaxial stretching of the film during production [1]. Otherwise, the material would result in expansion in one and shrinkage in other direction (anisotropic expansion), which indicates drawing off of the film during production and is a well known behaviour of extruded polymers [1,9,24–26]. Biaxial extrusion improves mechanical, optical and barrier properties of the polymeric films [27,28]. The expansion in CD is lower compared to MD throughout whole temperature range (see Figure 4.13.). During heating, the material can pass through certain transition temperatures such as secondary transition (ß-transitions), glass transition (T_g) and melting, which gives polymer chains mobility and allows relaxation of orientations introduced during the extrusion process [9,29]. Another heating of the EVA (2nd TMA heating) provided frozen chains mobility and allowed the oriented chain molecules to move into their thermodynamically preferred position [1,9], which resulted in the difference in expansion between the 1st and 2nd TMA heating run. Since the expansion of the EVA film in both directions indicated biaxial extrusion, it can be assumed that the chains are oriented in both directions and therefore the same effect of relaxation from orientations or stresses was observed in the 2nd TMA heating in both directions. Furthermore, the 1st TMA heating run resulted in a slope that begins at about 55°C in both directions. In the 2nd TMA heating run the slope shifted to about 60°C and correlates well with the main melting endotherm of EVA as discussed later (see Figure 4.2.). However, the slope starts at a slightly higher temperature in CD compared to MD, which could indicate slightly more organized crystals and/or thicker lamellae in the CD direction.
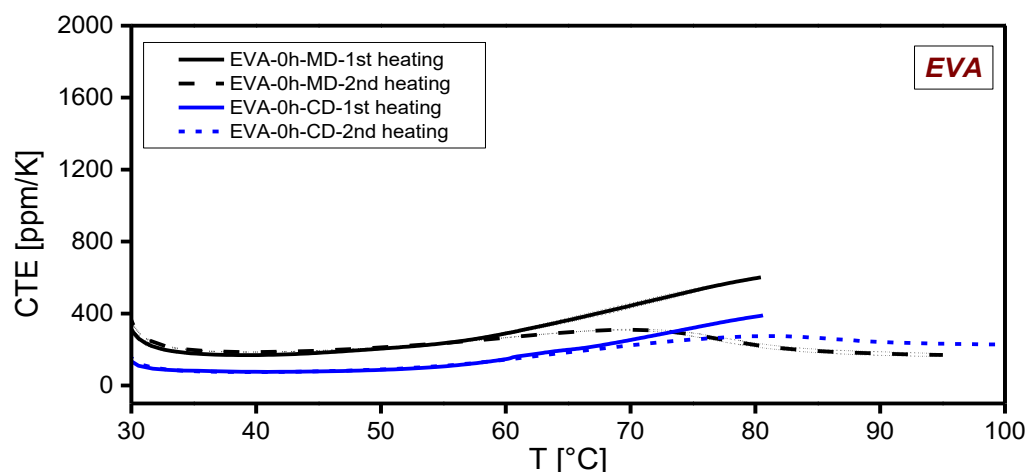
Figure 4.1. TMA curves of crosslinked and unaged EVA in MD and CD direction with standard deviation as an envelope

As can be seen in Figure 4.2., the 1st DSC heating run of EVA revealed a broad melting area that starts already at about 40°C and continues to about 80°C [1,15,30], with a melting temperature detected about 45°C and 67°C. The broad melting range is a result of a series of overlapping melting points corresponding to the melting of the lamellae of various thicknesses [3,9,29]. Therefore, the first melting peak of about 45°C can be attributed to the less organized crystals, which are formed in the area among the primary crystals during slow cooling or storage at ambient temperatures [1,15,31,32]. High branch content of bulky acetate side groups results in lower crystallization and low lamellar thickness, which translates into low melting and processing temperatures [29]. The 2nd DSC heating run shows material-specific behaviour and revealed a melting peak of about 67°C, which corresponds to the thermodynamic melting point of the EVA [1,15,29]. Observed melting endotherms are in good correlation with the slopes that occurred in the 1st and 2nd TMA heating runs.
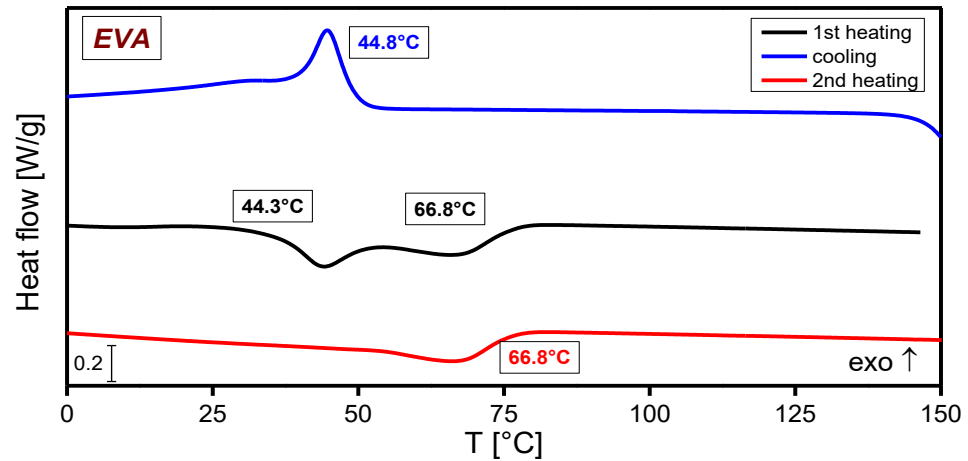
Figure 4.2. DSC curves of crosslinked and unaged EVA

After the damp heat aging, higher expansion in both directions in the 1st TMA heating run (see Figure 4.3.) compared to the 1st TMA heating of unaged EVA could be observed. However, there was rather high deviation, which could be related to inhomogeneity of the sample caused by aging and/or uneven distribution of the cross-linker. In fact, due to uneven distribution of peroxide cross-linkers in EVA, the properties of EVA can vary significantly across the entire material even before aging. Comparing the 1st TMA heating curves of EVA before and after aging, it can be seen that the curves in MD and CD are overlapped after aging. The reason could be a reorganization or even melting of the crystals formed via secondary crystallization before aging. For semi-crystalline polymers, secondary crystallization can significantly contribute to thermo-mechanical behaviour as well [8,16]. Secondary crystallization is influenced by the molecular structure and thermal history (during processing and storage time) [8,29]. According to Peacock [29], secondary crystallization is unlikely to increase the degree of crystallinity more than 2-3%. However, it does affect the amount of crystalline fraction and/or leads to improved packing within the non-crystalline regions. There are several modes of secondary crystallization, any or all of which can take place to some extent such as thickening of pre-existing crystallites, lamellae may anneal to relieve crystal defects or thin, poorly ordered crystallites may form in inter-lamellar zones [29]. The reason why this effect was not observed before aging but after exposure to elevated temperatures is probably due to the thermal load that the material experienced. Namely, during applied heating in TMA measurements, the material receives a certain thermal load for a short time, depending on the heating rate. However, the aged material was additionally exposed to elevated temperatures for 1000h and afterwards again during the measurements. Probably this

fact could lead to either a reorganization of the less organized crystals formed by secondary crystallization or their melting after aging.
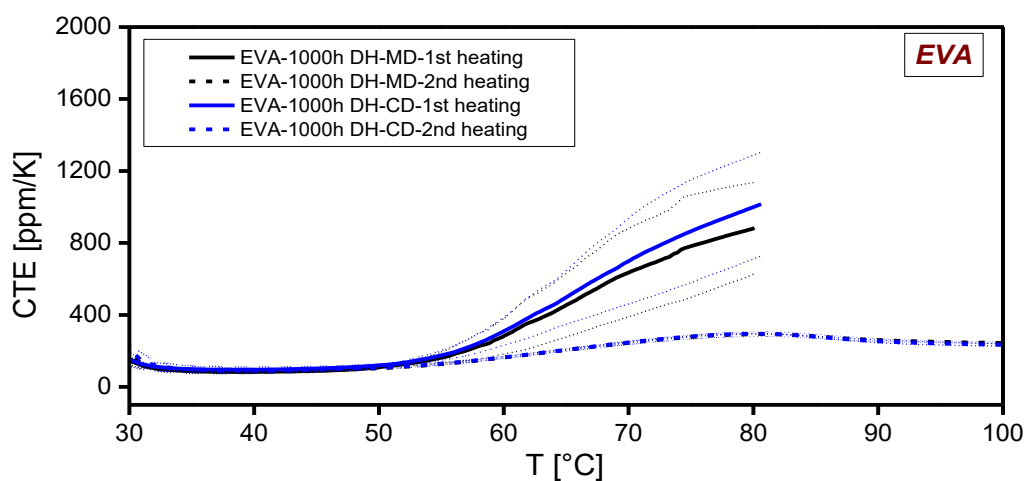

Figure 4.3. TMA curves of crosslinked EVA in MD and CD direction after damp heat aging with standard deviation as an envelope

The 1st DSC heating run revealed a shift of the first melting endotherm to lower temperatures (see Figure 4.4.), i.e. from 44.1°C ± 0.4 to 41.6°C ± 0.2 after aging, which could indicate either the deterioration of the crystalline structure, thinner lamellae or the formation of the less organized crystals [8,9]. The melting enthalpy (ΔH_m, J/g) increased after aging from 41.2 ± 6 J/g to 44.4 ± 0 J/g, which could indicate that more crystals were formed in the process of post-crystallization upon storage at elevated temperatures. However, the standard deviation of the ΔH_m before aging was quite high and therefore the eventual increase after aging needs to be considered with the following precaution. If one assumes that crystallinity indeed increased after aging, then it is to keep in mind that a higher crystalline content should decrease mobility of the polymer chains due to a reduction of the free fractional volume (FFV) [9,33]. Then the higher expansion observed in TMA curves after aging would seem contradictory. According to Ehrenstein et al. [3,9], there are few possible explanations: the changes in the material can occur in the crystalline region or in amorphous region. (By the means of the crystalline region, the changes could be either lower or higher crystallinity, i.e. formation of less organized crystals or post-crystallization, which can induce the relaxation of residual stresses. Since the 1st DSC heating run revealed a shift of the melting endotherm to lower temperatures, which could indicate deterioration of the crystalline structure, it is possible that the crystalline region was affected by aging and resulted in a decrease of its volume content. The main crystalline region of the PE segment could split into smaller fragments

(without a decrease of the overall degree of crystallinity), which would provide more space for mobile polymer chains. It is known that the morphology of semicrystalline PE cannot be strictly considered as having pure crystalline (ordered) and pure amorphous (disordered) regions [29]. It is rather considered as three-phase morphology where at the boundary between disordered regions and crystallite surfaces there exists a third phase made up of chain segments that exhibit varying degrees of order. This boundary layer is usually called the interfacial region, interface or partially ordered region [29]. Eventually the crystals formed by post-crystallization could attach on to those smaller deteriorated parts that act as nucleation points. Formation of the crystals in post-crystallization also induces certain stresses as well [3,29]. It is therefore possible that the melting of those crystals leads to the release of the residual stresses that is stronger compared to the original material that did not contain those crystals and related stresses. In the amorphous region, the changes could include breakage of intra- or intermolecular bonds, which increases free fractional volume (FFV) and therefore provides more space for chain mobility [3,9]. After the 2nd TMA heating run, the expansion curves in MD and CD are overlapped. This observation could be a result of annealing at elevated temperature that led to a uniform reorganization of the crystal in both directions. As expected, the 2nd DSC run did not show any changes after aging, which confirmed that no chemical aging took place and that the observed changes are assigned to physical aging and have a reversible character [8,9].
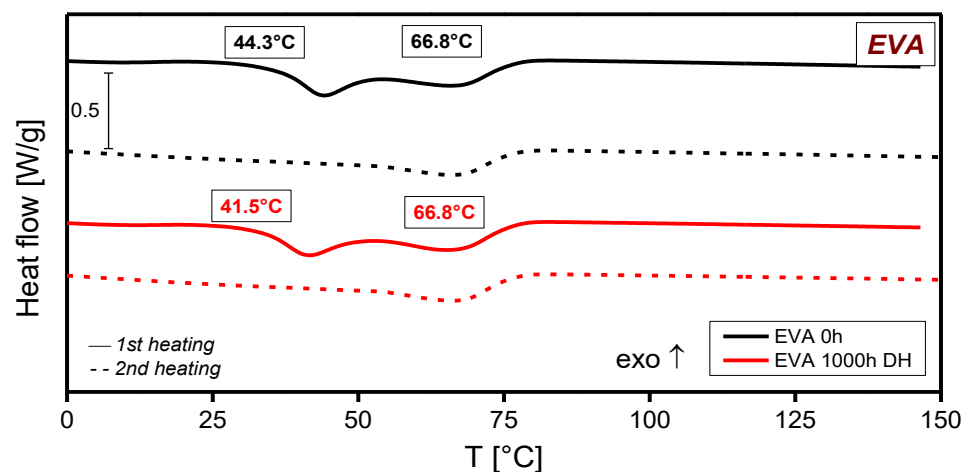

Figure 4.4. DSC curves of crosslinked EVA before and after damp heat aging

4.3.2 Thermoplastic polyolefin (TPO)

The TMA curves of laminated TPO before aging in MD and CD are shown in Figure 4.5. The slight difference in expansion between MD and CD can be observed, which could indicate slightly higher degree of orientation in MD compared to CD direction. It can be also seen that TPO showed significantly lower expansion in both directions compared to crosslinked and unaged EVA (see Table 4.4.). The reason for higher thermo-mechanical stability of TPO in the investigated temperature region is its higher melting temperature, as indicated by the DSC results [3,8,9,29], which will be discussed later. The 1st TMA heating curve resulted in a slope of about 50°C, which can be correlated with the onset of the melting of less organized crystals formed via secondary crystallization (as seen on DSC). The thermal expansion of PE in this case depends on two factors: the relative proportions of the ordered and disordered regions and the orientation of crystallite axes with respect to the direction in which the expansion is being measured. Furthermore, disordered regions exhibit substantially greater expansion than crystalline regions since they inherently possess greater degrees of freedom of movement [29]. The DSC analysis showed that the degree of crystallinity (w_c, %) of TPO is ~32.8 %, which is higher compared to EVA (~14%). Therefore, it can be concluded that there is a lower number of disordered regions that could contribute to the expansion of TPO, which resulted in lower CTE compared to crosslinked EVA. In other words, the crystalline structure, i.e. morphology has a dominant effect on thermo-mechanical behaviour of TPO.
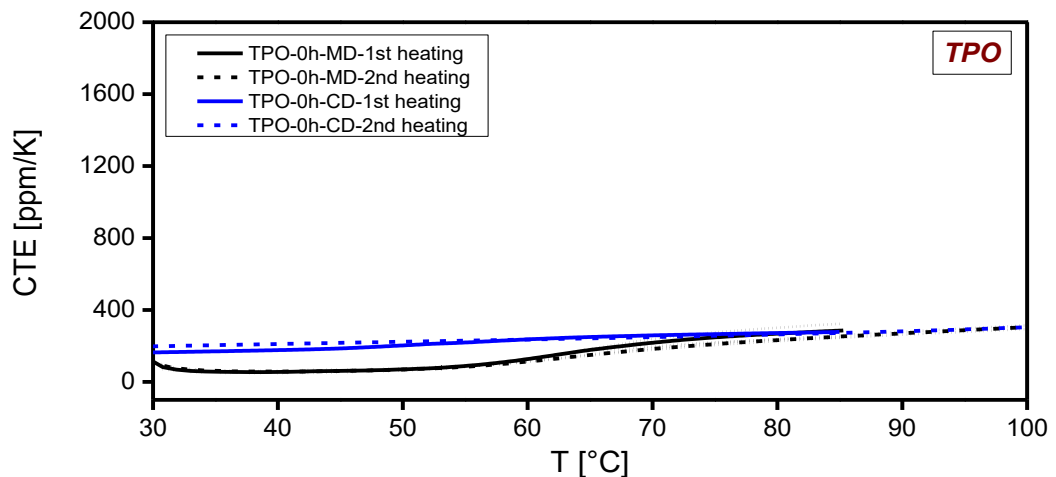

Figure 4.5. TMA curves of laminated and unaged TPO in MD and CD direction with standard deviation as an envelope

TPO is a copolymer of low density polyethylene (LDPE) and α-olefins. The 1st DSC heating of TPO (see Figure 4.6.) resulted in two melting peaks at about 44°C and 108°C.

The first melting peak is most probably the result of secondary crystallization that occurred during the storage time at usually ambient temperatures [29]. The absence of the same peak in the 2nd heating run confirms that it is not coming from the added elastomeric component. The second melting peak is assigned to melting of the LDPE crystals and is in accordance with the reported literature values of about 105-118°C [25,34].
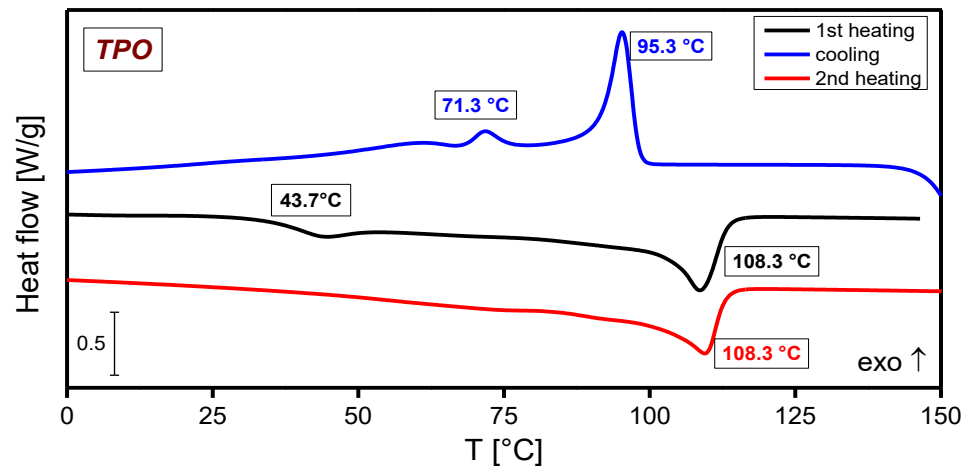

Figure 4.6. DSC curves of laminated and unaged TPO

The thermal expansion curves of TPO after damp heat aging are shown in Figure 4.7. The 2nd heating curve of TPO in MD is missing due to slipping of the sample from the clamps upon reaching a certain temperature even after multiple repetitions and therefore no results could be extracted. The aging of TPO resulted in isotropic expansion behaviour. The 1st TMA heating after aging showed slightly higher expansion in MD direction compared to unaged TPO. In CD direction, a decrease of expansion in the range from 25-50°C compared to unaged TPO could be observed and was most probably caused by relaxation from orientations or residual stresses in that temperature range. The slope at about 55°C was observed in the 1st TMA heating run in both directions and could be correlated with the first melting endotherm.
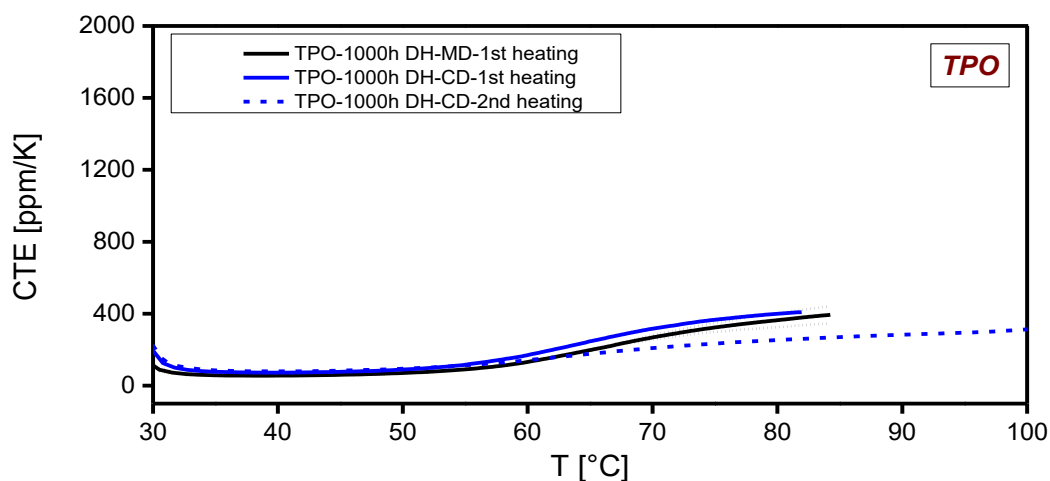
Figure 4.7. TMA curves of laminated TPO in MD and CD direction after damp heat aging with standard deviation as an envelope

DSC analysis (see Figure 4.8.) showed physical aging of the TPO after damp heat exposure; new melting peaks at about 65°C and 96°C due to post-crystallization and possibly re-crystallization were observed. Their reversible-character was confirmed by the disappearing of the same peaks after the 2nd DSC heating run [8,9]. Because of physical aging, ΔH_m increased from 96.3 J/g ± 6.3 to 100.6 J/g ± 1.8. Again, as in the case of EVA, increased crystallinity should lead to lower mobility of the polymer chains due to reduction of the FFV [3,8,33] and therefore lower thermal expansion. However, the explanation for increased expansion could apply as in the case of EVA (see above). It is possible that the crystalline regions were split into smaller portions, which enabled more space for mobility of the polymer chains or the changes occurred in the amorphous regions, which could increase FFV as well. Moreover, it is possible that the melting of the crystals formed in post-crystallization process led to the release of the residual stresses that is stronger compared to the original material that did not contain those crystals and related stresses [3,9].
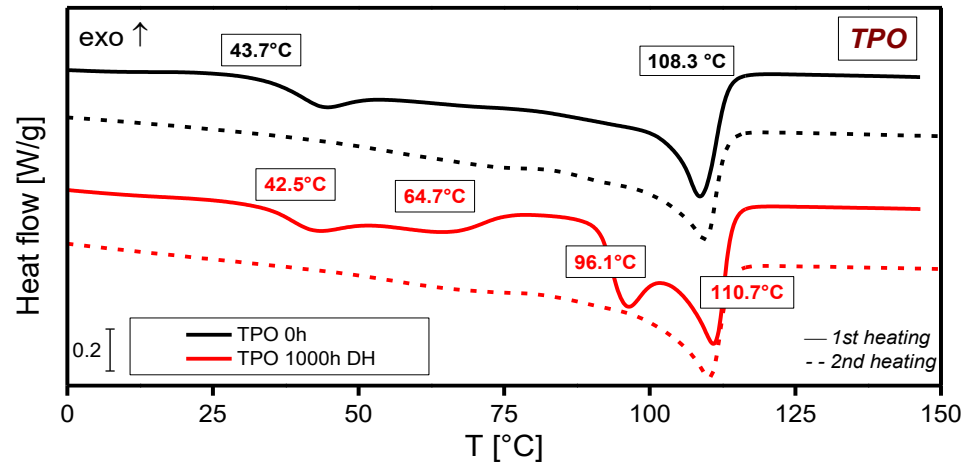
Figure 4.8. DSC curves of laminated TPO before and after damp heat aging

4.3.3 Polyolefin elastomer (POE)

The TMA curves of crosslinked and unaged POE before aging are shown in Figure 4.9. It can be seen that the POE is showing isotropic expansion behaviour, indicating biaxial orientation. Measurements in MD resulted in very high deviation, probably due to the inhomogeneity of the sample. The CTE in MD is lower compared to EVA (see Figure 4.13.). The curves of the 1st and the 2nd TMA run are quite overlapped, indicating that the effect of relaxation from orientations is lower in unaged POE compared to unaged EVA and TPO. It indicates that the degree of orientation of polymer chains in the POE is lower compared to EVA and TPO. In the 1st TMA heating curve slope about 55°C is observed in both directions and could be related to the thermal behaviour of POE as will be discussed later.
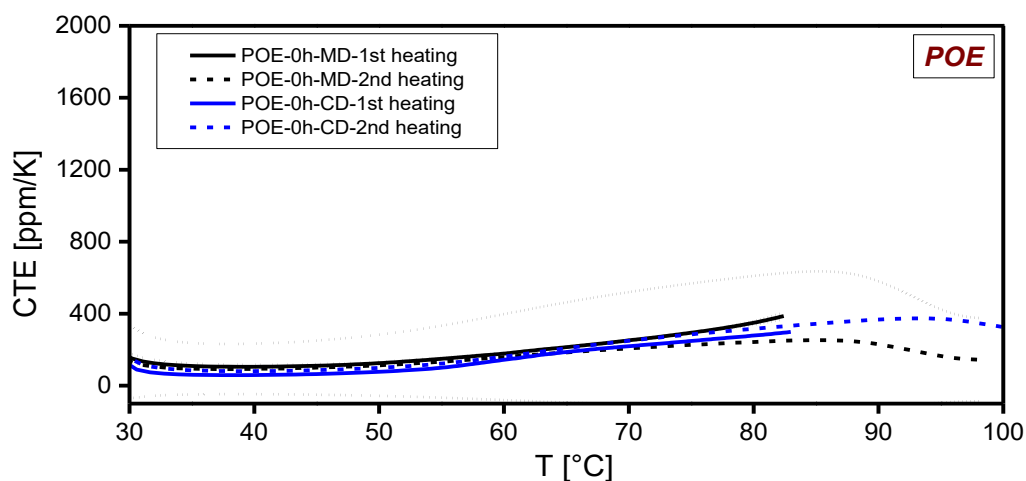
Figure 4.9. TMA curves of crosslinked and unaged POE in MD and CD direction with standard deviation as an envelope

The DSC results of POE are presented in Figure 4.10. POE is a co-polymer of LDPE and acrylate monomer. The broad melting range has two distinctive melting peaks of about 45°C and 82°C. The first peak can be assigned to the melting of the less organized crystals with probably thinner lamellae, while the latter is assigned to melting of the PE crystals. The 2nd DSC run reveals one melting peak at about 82°C, which corresponds to the thermodynamic melting point of the POE. Based on the higher melting point, POE should provide higher thermal stability compared to EVA [35]. The degree of crystallinity of crosslinked and unaged POE is ~24%, which is higher compared to EVA and therefore it can be assumed that there are fewer disordered regions that could contribute to the expansion of POE by providing free volume for mobility of the polymer chains. Hence, the POE showed lower thermal expansion than EVA before aging.
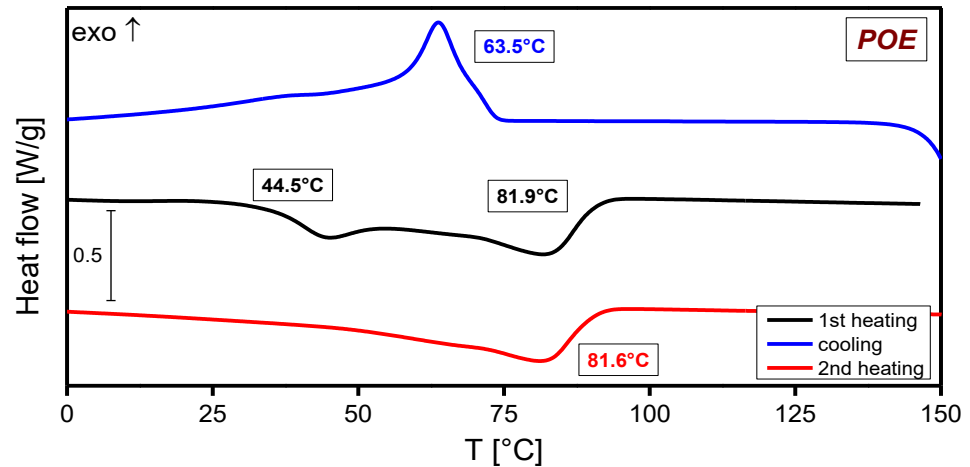
Figure 4.10. DSC curves of crosslinked and unaged POE

After the aging of POE (see Figure 4.11.), significantly higher thermal expansion in both directions could be observed in the 1st TMA heating in the temperature range from 55-80°C. The 2nd TMA heating run after aging did not show any significant changes compared to unaged POE. This leads to the conclusion that the observed difference between the 1st and the 2nd TMA run is either a relaxation of residual stresses and orientations or a change in the thermal behaviour of POE, i.e. changes in the morphology caused by aging.
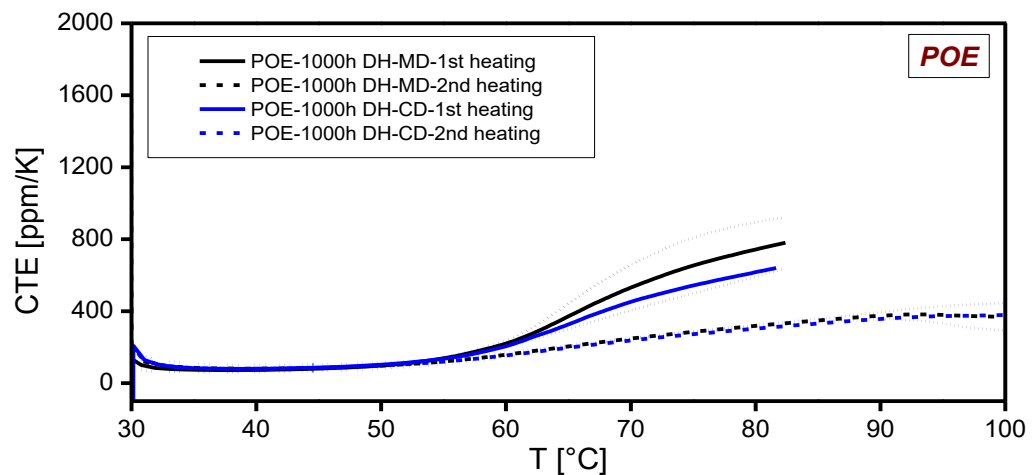

Figure 4.11. TMA curves of crosslinked POE in MD and CD direction after damp heat aging with standard deviation as an envelope

As results of DSC analysis has shown, damp heat aging resulted in the formation of a very sharp melting peak with T_m about 92°C, which caused shifting of the main melting

endotherm from about 82°C to 75°C (see Figure 4.12.). Since the exposure in the damp heat test was at 85°C, the sharp peak at 92°C could be assigned to a post-crystallization peak due to annealing and its aging-induced character is confirmed by its disappearance in the 2nd heating run [8,9]. Another possible reason is that the exposure to 85°C caused a unification of the crystal lamellae thickness, as observed by Oreski et al. [14] in the case of ionomers. One assumption was that maybe certain crystals are agglomerating upon aging, as can be case with ionomers. Therefore, one of the samples was taken for further DSC analysis, where two heating runs were applied and afterwards the material rested for 24h and then measured again. In case of agglomeration, the peak would be observable again after 24 h upon applied heating. However, the peak was absent and it confirmed that agglomeration is not the cause of the peak at 92°C. Despite the formation of the new peak, the overall melting enthalpy of POE decreased after aging from 71.5 J/g ± 2.8 to 62.5 J/g ± 1.8, which, together with the shift of the melting temperature to lower values, could indicate chemical aging [8]. In chemical aging changes take place in the chemical composition, molecular structure and/or molecular weight of the material and are usually manifested as chain scission, crosslinking and cyclization [8]. Analysis of cooling curves of POE did not reveal a significant shift in the crystallization temperature that could confirm chain scission. Therefore, the deterioration of crystalline structure upon aging is most probably the reason for the observed changes. The FTIR-ATR analysis of the POE did not show the formation of any bonds (hydroxyl or carbonyl) that would indicate oxidation of the sample.
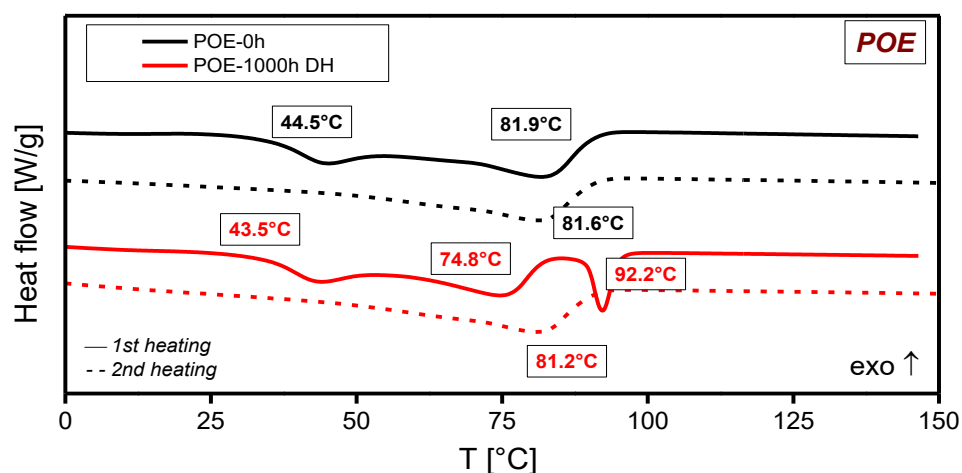

Figure 4.12. DSC curves of crosslinked POE before and after damp heat aging

4.3.4 An overview of thermo-mechanical stability of polyolefin encapsulants

In order to determine the influence of aging on the morphology and thermo-mechanical properties of polyolefin encapsulants, TMA and DSC analysis were conducted on EVA, TPO and POE encapsulants. All three types of encapsulants showed thermal expansion in the applied temperature range in both directions, indicating biaxial orientation. The 1st heating of EVA showed the highest deviation between MD and CD of $\Delta CTE= 211.3 \pm 1.2 \cdot 10^{-6} K^{-1}$ (see Figure 4.13.), which could lead to higher stress in the module during production. Accordingly, TPO showed the smallest difference between the two directions in the 1st heating run ($\Delta CTE= 0.5 \pm 18.2 \cdot 10^{-6} K^{-1}$), which could indicate lower internal stresses within PV module after production. The thermal analysis of all three types of encapsulants revealed physical aging in terms of post- and re-crystallization after exposure to damp heat conditions. POE additionally showed a decrease of T_m and ΔH_m after aging, indicating chemical aging. Such changes in the material morphology affected the thermo-mechanical properties of the encapsulants as well. TPO in general showed the highest thermal and thermo-mechanical stability before and after aging, which was expected since it has the highest melting temperature among the investigated materials. The reason for high thermal stability is the absence of the side groups that could limit the crystallization of the PE such as vinyl acetate side groups or acrylate-based side groups as in case of EVA and POE. In order to compare the thermal expansion of the materials in the relevant temperature range, CTE values of all three encapsulants before and after aging at 80°C (~ max temperature of the module) are summarized and presented in Figure 4.13.. It can be seen that EVA resulted in the highest CTE values before and after aging (1st heating run), followed by POE and finally by TPO. The obtained trend in CTE values is in good correlation with the calculated degree of crystallinity, which indicates that crystallinity has a dominating effect on thermo-mechanical behaviour of the investigated encapsulants.

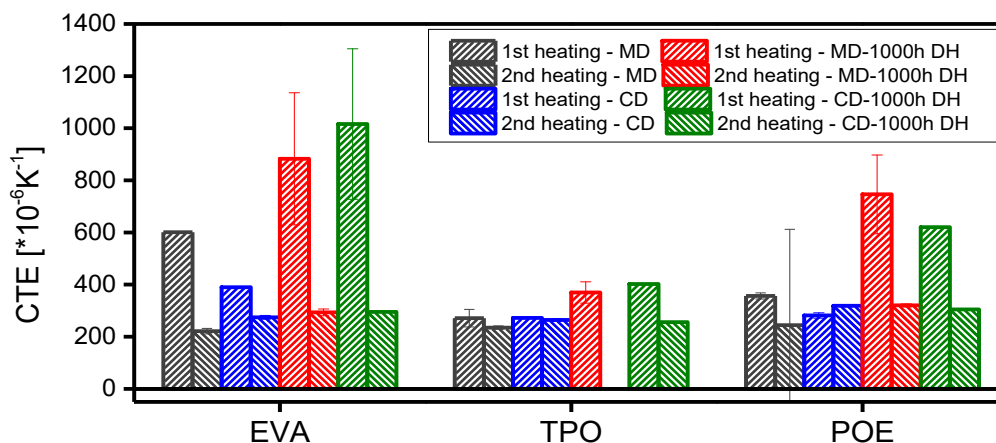**Figure 4.13.** CTE values of the 1st and 2nd TMA heating run for all tested encapsulants at 80°C

However, in order to better understand the influence of thermal expansion of the encapsulants on other PV components and to assess the amount of eventual internal stress that could occur within the PV module during outdoor service, more investigations are needed not only on single materials but also at module level.

4.4   Summary and conclusions

The thermo-mechanical stability of polymeric PV components is of great importance for the reliability of PV modules during production and operation in the field. Changes in the thermo-mechanical properties can result in internal stresses that are linked to different failure modes such as cracking of the thin c-Si cells and soldering and/or delamination. Hence, in Chapter 4 an overview on the thermo-mechanical and thermal behaviour of three types of polyolefin encapsulants has been given. The main aim was to understand the influence of damp heat aging on morphology and thermo-mechanical stability of the polyolefin encapsulants.

Thermo-mechanical analysis (TMA) was conducted on three types of encapsulants: state-of-the-art EVA and alternative TPO and POE encapsulants. In order to correlate findings of TMA with the morphology of each material, additional differential scanning calorimetry (DSC) measurements were conducted. In the first TMA heating run, all three types of encapsulants showed thermal expansion in both directions indicating biaxial orientation, which is common in solar applications since it leads to better mechanical, optical and barrier properties. Unaged EVA, showed the highest difference in CTE between the MD and CD directions, which could indicate the incorporation of internal stresses within the PV module during production. Another heating provided polymer chains enough mobility and allowed the oriented chain molecules to move into their thermo-dynamically preferred isotropic position. Therefore, the 2nd TMA curves revealed lower expansion due to the relaxation from orientations and/or stresses. From the thermo-mechanical stability point of view, TPO showed the most stable behaviour, i.e. the lowest thermal expansion, which is a consequence of the highest melting temperature of all three types of encapsulants, as revealed by DSC analysis.

After damp heat aging, all three encapsulants showed an increase in expansion. In the case of EVA and TPO, DSC analysis confirmed physical aging in terms of an increased degree of crystallinity due to post-crystallization. Since an increased degree of crystallinity leads to reduced free fractional volume (FFV) available for polymer chain mobility, an increased thermal expansion could indicate a deterioration of the crystalline structure and/or changes in the amorphous regions of the EVA and TPO. On the other hand, POE resulted in an increased thermal expansion, which was well supported with decreased crystallinity indicating chemical aging.

The results presented in this work have shown that morphology, i.e. the crystalline content, has a dominating effect on thermo-mechanical behaviour of polyolefin encapsulants. Due to the highest crystalline content, TPO showed the most stable

thermo-mechanical behaviour among the investigated encapsulants before and after aging. On the other hand, EVA with the lowest crystalline content showed the highest thermal expansion, which could lead to the formation of stresses within PV modules during production and service time and give rise to different failure modes.

Thermo-mechanical analysis combined with differential scanning calorimetry proved to be suitable for the systematic investigation of the thermo-mechanical stability of polyolefin encapsulants. Moreover, the methods used proved to be convenient, effective and reliable techniques for the characterization of the various physical aging mechanisms in the encapsulants. In order to increase the reliability of PV modules from a thermo-mechanical point of view, it is necessary to reduce internal stresses that could be caused by encapsulant expansion during production and service of PV modules. In those terms, TPO would seem to be a good solution, not only during production, but also during operation in the harsh climatic conditions.

4.5   References

[1] M. Knausz, G. Oreski, M. Schmidt, P. Guttmann, K. Berger, Y. Voronko, G. Eder, T. Koch, G. Pinter, Thermal expansion behavior of solar cell encapsulation materials, Polymer Testing 44 (2015) 160–167. https://doi.org/10.1016/j.polymertesting.2015.04.009.

[2] G. Oreski, M. Knausz, G. Pinter, C. Hirschl, G.C. Eder, Advanced methods for discovering PV module process optimization potentials and quality control of encapsulation materials, in: 28th European Photovoltaic Solar Energy Conference and Exhibition, Paris, France, 2013.

[3] G.W. Ehrenstein, Polymeric Materials: Structure, Properties, Application, Carl Hanser Verlag GmbH & Co. KG, 2001.

[4] U. Eitner, M. Pander, S. Kajari-Schröder, M. Köntges, H. Altenbach, Thermomechanics of PV Modules Including the Viscoelasticity of EVA, in: 26th European Photovoltaic Solar Energy.

[5] U. Eitner, Thermomechanics of photovoltaic modules. Doctor thesis, Martin-Luther-Universitaet Halle-Wittenberg, 2011.

[6] S. Kalpakjian, S.R. Schmid, E. Werner, Werkstofftechnik: Herstellung, Verarbeitung, Fertigung, 5th ed., Pearson Studium, Munich, 2011.

[7] A.W. Czanderna, F. J. Pern, Encapsulation of PV modules using ethylene vinyl acetate copolymer as a pottant: A critical review, Solar Energy Materials and Solar Cells (43) (1996) 101–181.

[8]   G.W. Ehrenstein, S. Pongratz, Resistance and stability of polymers, Hanser Publishers, Munich, 2013.

[9] G.W. Ehrenstein, G. Riedel, P. Trawiel, Thermal analysis of plastics: Theory and practice, Carl Hanser Verlag, Munich, 2004.

[10] Neelkanth G. Dhere, Reliability of PV Modules and Balance-of-System Components, in: Proceedings of the 31st IEEE Photovoltaic Specialist Conference, 2005., pp. 1570–1576.

[11] E. Wang, H.E. Yang, J. Yen, S. Chi, C. Wang, Failure Modes Evaluation of PV Module via Materials Degradation Approach, Energy Procedia 33 (2013) 256–264. https://doi.org/10.1016/j.egypro.2013.05.066.

[12] G. Oreski, G.M. WALLNER, Evaluation of the aging behavior of ethylene copolymer films for solar applications under accelerated weathering conditions, Solar Energy 83 (7) (2009) 1040–1047. https://doi.org/10.1016/j.solener.2009.01.009.

[13] S. Chen, J. Zhang, J. Su, Effect of damp-heat aging on the properties of ethylene-vinyl acetate copolymer and ethylene- acrylic acid copolymer blends, J. Appl. Polym. Sci. 114 (5) (2009) 3110–3117. https://doi.org/10.1002/app.30859.

[14] G. Oreski, G.M. WALLNER, Damp Heat induced physical ageing of PV encapsulation materials, in: 12th Intersociety Conference on Thermal and Thermomechanical Phenomena in Electronic Systems, Las Vegas, USA, 2010.

[15] B. Ottersböck, G. Oreski, G. Pinter, Comparison of different microclimate effects on the aging behavior of encapsulation materials used in photovoltaic modules, Polymer Degradation and Stability (2017) 182–191. https://doi.org/10.1016/j.polymdegradstab.2017.03.010.

[16] M. Omazic, The influence of polymer carrier films on semiconductor processing. Doctoral thesis, Leoben, 2018.

[17] C. L. CHOY, F. C. CHEN, and K. YOUNG, Negative thermal expansion in oriented crystalline polymers.

[18] A.G. Gibson, I.M. Ward, Thermal expansion behaviour of hydrostatically extruded linear polyethylene, Journal of Material Science 14 (8) (1979) 1838–1842. https://doi.org/10.1007/BF00551022.

[19] M. Knausz, G. Oreski, P. Guttmann, Investigation in the thermal expansion behavior of PV module encapsulation materials, in: Centre of Excellence PoliMaT (Ed.), The proceedings of the Austrian--Slovenian Polymer Meeting 2013, Narodna in univerzitetna knjižnica, Ljubljana, 2013, pp. 44–46.

[20] G. Orchard, G. Davies, I. Ward, The thermal expansion behaviour of highly oriented polyethylene, Polymer 25 (8) (1984) 1203–1210. https://doi.org/10.1016/0032-3861(84)90364-1.

[21] International Organisation for Standardisation, ISO 11359-2, Plastics- Thermomechnical Analysis (TMA). Determination of CTE and Tg, 1999.

[22] DIN 53 752, Prüfung von Kunststoffen Bestimmung des thermischen Längenausdehnungskoeffizienten, 1980.

[23] International Organisation for Standardisation, ISO 11357-3, Plastics - Differential scanning calorimetry (DSC) Part 3: Determination of temperature and enthalpy of melting and crystallization, 1999.

[24] H. Domininghaus, P. Elsner, P. Eyerer, T. Hirth, Kunststoffe: Eigenschaften und Anwendungen, Springer Berlin Heidelberg New York, 2004.

[25] E. Baur, J.G. Brinkman, T.A. Osswald, E. Schmachtenberg, Saechtling Kunststoff Taschenbuch, 30th ed., Carl Hanser, Munich, 2007.

[26] C. Choy, F. Chen, E. Ong, Anisotropic thermal expansion of oriented crystalline polymers, Polymer 20 (10) (1979) 1191–1198. https://doi.org/10.1016/0032-3861(79)90142-3.

[27] S.H. Tabatabaei, P.J. Carreau, A. Ajji, Structure and properties of MDO stretched polypropylene, Polymer 50 (16) (2009) 3981–3989. https://doi.org/10.1016/j.polymer.2009.06.059.

[28] T. Lüpke, S. Dunger, J. Sänze, H.-J. Radusch, Sequential biaxial drawing of polypropylene films, Polymer 45 (20) (2004) 6861–6872. https://doi.org/10.1016/j.polymer.2004.07.075.

[29] A.J. Peacock, Handbook of Polyethylene: Morphology and Crystallization of Polyethylene, Marcel Dekker, Inc., New York, N.Y., 2000.

[30] K. Agroui, G. Collins, Determination of thermal properties of crosslinked EVA encapsulant material in outdoor exposure by TSC and DSC methods, Renewable Energy 63 (2014) 741–746. https://doi.org/10.1016/j.renene.2013.10.013.

[31] M. Brogly, M. Nardin, J. Schultz, Effect of Vinylacetate Content on Crystallinity and Second-Order Transitions in Ethylene–Vinylacetate Copolymers, J. Appl. Polym. Sci. 64 (10) (1997) 1903–1912. https://doi.org/10.1002/(SICI)1097-4628(19970606)64:10<1903:AID-APP4>3.0.CO;2-M.

[32] Y.-L. Loo, K. Wakabayashi, Y.E. Huang, R.A. Register, B.S. Hsiao, Thin crystal melting produces the low-temperature endotherm in ethylene/methacrylic acid ionomers, Polymer 46 (14) (2005) 5118–5124. https://doi.org/10.1016/j.polymer.2005.04.043.

[33] John Wiley and Sons, Encyclopedia of Polymer Science and Technology - Barrier polymers, 1999-2012.

[34] H. Domininghaus, P. Eyerer, P. Elsner, T. Hirth, Kunststoffe: Eigenschaften und Anwendungen, Springer, Berlin Heidelberg, 2007.

[35] K. M. Jäger, R. C. Dammert, B. A. Sultan, Thermal degradation studies of different polar polyethylene copolymers, J. Appl. Polym. Sci. 84 (7) (2002) 1465–1473. https://doi.org/10.1002/app.10510

5 Non-destructive investigation of influence of climate-specific accelerated tests on degradation of EVA at module level

5.1 Motivation

One obstacle to the development of PV modules with long-term reliability is the fact that current qualification standards are only useful for detecting premature failures and do not include long-term reliability or service life considerations [1]. The common qualification test for PV modules prior to installation is IEC 61215 [2], which indicates early product life (infant) failures due to choice of design, process and materials [2–6]. It is based on a set of defined experiments which, among many others, includes visual inspection, thermal cycling test, humidity-freeze test, damp heat test, mechanical load test and hail test [2]. The test is based on strict pass/fail criteria for infant failures and is recognized as not predictive of long term performance [4,6–10]. It defines power loss of more than 5% as a fail, while values below 5% are considered as pass [2,8,10,11]. According the IEC 61215, damp heat testing of modules performed at 85°C and 85% RH for a duration of 1000h provides the most information for aging and degradation of encapsulation materials (encapsulant and backsheet) [2,10,12]. These test results are expected to represent a real life time behaviour after 20-25 years [12]. However, the conditions in IEC 61215 in general are not climate specific, i.e. this test does not provide adequate UV exposure or combined multiple factors and therefore it cannot accurately predict long-term performance of PV modules [1].

According to Wohlgemuth et al. [9], it is necessary to use reliability tests that go beyond the qualification test. Reliability tests are designed to evaluate failures, to quantify them and to help understand the failure mechanisms in order to improve the reliability of the PV module. These tests can be done by applying lower or higher stresses depending on exposure times, i.e. long- or short-term (accelerated) testing [7,10]. But, some processes are not easy to accelerate and therefore sometimes the defects that appear or do not appear in qualification or reliability tests are different from those reported from the field [1,7,8,10,13]. A few authors [1,4,6,8,12,14–17] have emphasized the necessity of considering aging conditions when predicting the outdoor lifetime of PV materials, in order not to over or under accelerate degradation mechanisms that are observed in the field. As discussed already in Chapter 1, different operating conditions (climate) drive

different degradation processes. Therefore, it is necessary to assess the reliability of the PV modules for those specific climatic conditions. In order to do so, it is important to develop climate-specific accelerated aging tests. However, thorough research is needed to understand the impact of aging parameters on over-/under-acceleration of failure modes on the PV module level. For example, increasing the temperature and humidity (above the conditions in the damp heat test) in order to simulate harsher climatic conditions or to shorten the test times could be a problem for the polymeric components that have a glass transition (T_g, °C) in that range, since the mobility of the polymer chains increases in the T_g range. Parameters like this could drastically accelerate degradation processes [12,17–19]. Furthermore, the addition of irradiation, which is necessary for simulating outdoor conditions, often over-accelerates degradation processes [1,3,3,16] and it is very hard to replicate outdoor irradiation conditions in the accelerated tests. Moreover, irradiation also contributes to additional heating of the sample, which accelerates degradation as well.

The design of accelerated aging tests is not the only challenge that researchers are faced with. Another obstacle with testing PV modules is their design; it is hard to address the degradation of the laminated PV components without destroying the PV modules. On the other hand, by aging and testing single PV components, the influence of the microclimate within the PV module is completely excluded and could result in misleading results as well. Ottersböck et al. [20] have shown that the microclimate has a strong influence on the aging behaviour of the polymeric encapsulants. On the other hand, Knausz et al. [21] have shown that the backsheets are not influenced by the microclimate in the PV modules and that the results obtained by testing of the single films can be correlated with the behaviour of the backsheets laminated within a module.

There are various non-destructive methods which are used to assess the degradation of the PV modules such as UV/Vis/NIR spectroscopy, fluorescence spectroscopy, UV-fluorescence, electroluminescence, thermographic cameras, etc.. However, most of these methods do not provide a clear picture of the degradation mechanism behind the failure and usually just confirm that a failure mode occurred without a clear picture about chemical nature of the degradation.

Raman spectroscopy was already shown to be a good tool for non-destructive investigation of the degradation of an encapsulant within the PV module [22–30]. The confocal setup allows the measurement of individual layers within a multilayer system, which provides information on each component level and makes it possible to follow the actual origin of degradation. According to Peike et al. [24] an increase in the baseline of

the EVA spectrum, which occurs due to the formation of a fluorescence background, is an indication of degradation of EVA. Namely, during the degradation of EVA, it is assumed that different compounds such as lactones, ketones and/or acetaldehyde are formed and act as chromophores, giving rise to the formation of fluorescence background [24,28,31]. It is assumed that the formation of the chromophores is responsible for the yellowing of EVA, which is the most frequently reported failure mode of EVA in field aged PV modules [10]. Therefore, an increase in the baseline could be used as an indicator of EVA degradation [23,24,28,29,32,33]. Beinert et al. [28] followed an increase in the fluorescence background as a function of EVA degradation due to the decomposition of additives. Mihaljevic et al. [29] used an increase in the fluorescence background as an indication of EVA degradation caused by the permeation properties of backsheets in PV module. Lee at el. [32] investigated yellowing of EVA by following an increase in the fluorescence background.

An exemplary EVA spectrum is shown in Figure 5.1. The highest intensity is obtained from the peaks in the region from 2800-3000 cm^{-1}, which are assigned to CH_2 and CH_3 stretching of ethylene and acetate units [24]. Deconvoluted Raman spectra of EVA in the C-H stretching region based on the Lorentzian fit is shown as an insert in Figure 5.1. It can be seen that this region is very complex. However, due to rather high intensity compared to, for example C=O stretching at 1735 cm^{-1}, the changes in this region can be easily followed after degradation. Nevertheless, this region has not been studied extensively so far. Peike et al. [24] studied the change in the ratio of symmetric to asymmetric stretching before and after aging and found that the ratio decreases with aging time due to degradation of EVA. However, the authors [24] did not discuss in detail the reason for the decrease of stretching intensity. Hirschl et al. [34] investigated this area in order to determine the degree of crosslinking in finished PV modules and showed that the Raman would be a good tool for in-line checking of EVA crosslinking.
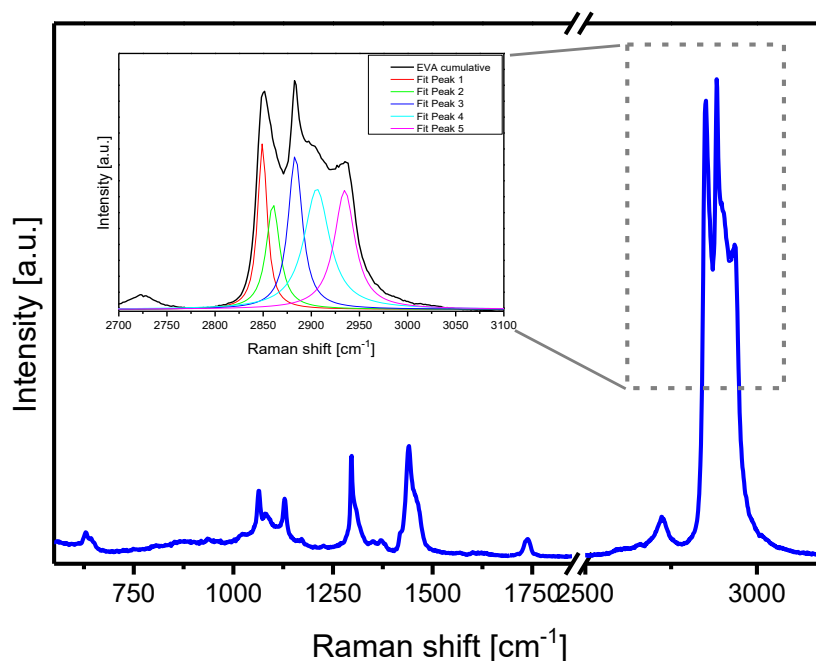
Figure 5.1. Exemplary EVA spectrum with the insert of the deconvoluted peaks

The formation of acetic acid upon degradation of EVA should affect the stretching intensity of the C-H groups in the backbone due to a depletion of the VAc segments. According to Czanderna et al. [35] the depletion of the VAc segments during deacetylation leaves behind the C=C in the backbone (see Figure 5.2.).
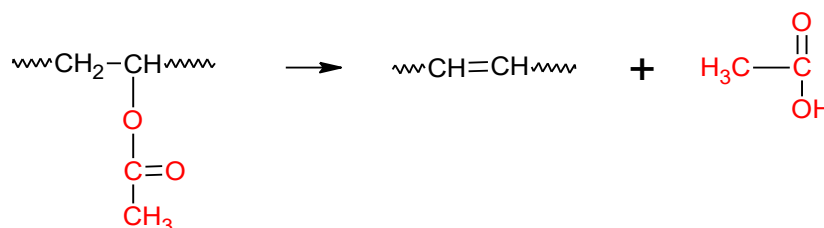

Figure 5.2. Deacetylation of EVA via Norrish I and II reactions

The peak normally assigned to C=C bonds is around 1635 cm^{-1}, but its intensity is too low compared to the intensity of the peaks caused by stretching and cannot be used to follow deacetylation with high accuracy. However, the degradation of EVA upon deacetylation can be followed as a change in the intensity ratio of CH_2 and CH_3 stretching in the range from 2800-3000 cm^{-1}. According to the authors' knowledge, unfortunately there are no published studies so far that deal with the effect of deacetylation on the CH stretching region upon degradation of EVA.

Hence, the main objective of this chapter is to investigate the degradation of EVA at PV module level non-destructively via the application of Raman confocal spectroscopy and to understand the influence of the different aging parameters on degradation of EVA. Those insights could help in optimizing the climate-specific tests, which is mandatory for the increased reliability of the PV modules operating outdoors.

5.2 Experimental part

5.2.1 Preparation and aging of the samples

The composition of the modules for all accelerated aging tests was the same: glass/EVA/c-Si cell/EVA/PET-laminate. The modules were prepared in the laminator according to the standard lamination procedure as described in [20]. All of the samples were aged at OFI. The parameters of the aging tests are summarized in Table 5.1. The wavelength range of the irradiance was 300-2500 nm (metal halide lamps). The arid climate tests were conducted only until 500h of aging. Due to an extensive testing plan, the machine availability did not allow each test to be conducted until the same time.

Table 5.1. Parameters of accelerated aging tests

Climate	Duration [h]	T [°C]	RH [%]	Irradiance [W/m^2]	Intervals
Tropical 1	3000	85	85	-	Constant
Tropical 2	3000	90	90	-	Constant
Moderate	1000	85	85	1000	Constant
Alpine	2000h=4 cycles	85	85	-	250h
		85	85	1200	250h
Arid	1000h	95	50	1200	Constant

5.2.2 Raman confocal spectroscopy

The degradation of the EVA front encapsulant was followed non-destructively via Raman confocal spectrometer LabRAM HR (HoribaJobin Yvon) with the external Ar+ laser (λ=514 nm). The confocal hole and slit were adjusted to 200µm. The objective used was an Olympus x10 and grating was set to 600 grooves/mm. The irradiation time was 5 seconds with 5 scans within one acquisition time. At least 5 measuring points above the cell were taken. The focus was mainly on the middle of the module since the temperature is expected to be the highest in the centre of the module during exposure and therefore the degradation effects should be higher. Moreover, the reliability of EVA above the cell is of the highest importance for the reliability of the PV modules and the power output. Processing of the data was done in the LabSpec 5 and Origin 9.0 software. The spectra were normalized according to the peak at 1295 cm^{-1} assigned to C-C stretching of ethylene unit [24].

5.2.3 UV-fluorescence measurements

Non-destructive UV-fluorescence (UV-f) measurements were performed in OFI. Measurements were conducted in a dark environment by illuminating the PV modules with UV light and detecting the fluorescing light in the visible region by a photographic camera system (Olympus OM-D, equipped with high pass filter to cut off the UV irradiation). Excitation with UV light was performed with a self-made UV lamp consisting of 3 power-tuneable light emitting diode (LED) arrays with an emission maximum at 365 nm and a low pass filter to cut off all visible light. The power supply was a modified DC/DC converter with controllable and piecewise constant voltage/constant current characteristics, sourced by a 12-cell, lithium-polymer accumulator with a capacity of 5000 mAh. An exposure time of 30 s was sufficient to achieve a well contrasted UV fluorescence image of a module.

5.3　Results and discussion

In the following section, the results of Raman confocal spectroscopy and UV-f measurements will be presented and discussed. Raman confocal spectroscopy was used as a tool for qualitative and quantitative assessment of EVA degradation in the modules aged under climate-specific accelerated tests. First, the results of the qualitative analysis (following an increase in fluorescence background) will be discussed. Afterwards, the results of the quantitative analysis will be presented where the relative change in the stretching area as a function of degradation of EVA for each climate test was followed. The findings of the Raman confocal spectroscopy will be compared with the results of UV-f measurements as another non-destructive method. Finally, the outcomes of each method will be compared and discussed in terms of their applicability, relevance and complexity.

5.3.1　Raman confocal spectroscopy

Qualitative analysis of EVA degradation

In Figure 5.3. the Raman spectra of EVA aged according to tropical 1 conditions are shown. The aging parameters applied in tropical 1 test are equal to those applied in a standard damp heat aging test (T=85°C, RH=85%) and therefore this test can be used as a reference for other tests. In Figure 5.3. it can be seen that EVA spectra did not show any increase in the baseline that could indicate formation of a fluorescence background, i.e. degradation of EVA. As can be seen in Table 5.1., in this test no irradiation was applied. Therefore, the temperature in the centre of the module did not deviate from the one set by the test and was measured to be 85°C (see Table 5.3.). The temperature of the modules during aging was monitored with PT1000- temperature sensor adhered to the backsheet in the middle of test-module (behind the cell). This temperature was found to be nearly identical to the black panel temperature in the climate chamber. The overall decrease of the peaks intensity with aging time is due to focusing on the interface of EVA and c-Si cell and not due to degradation.
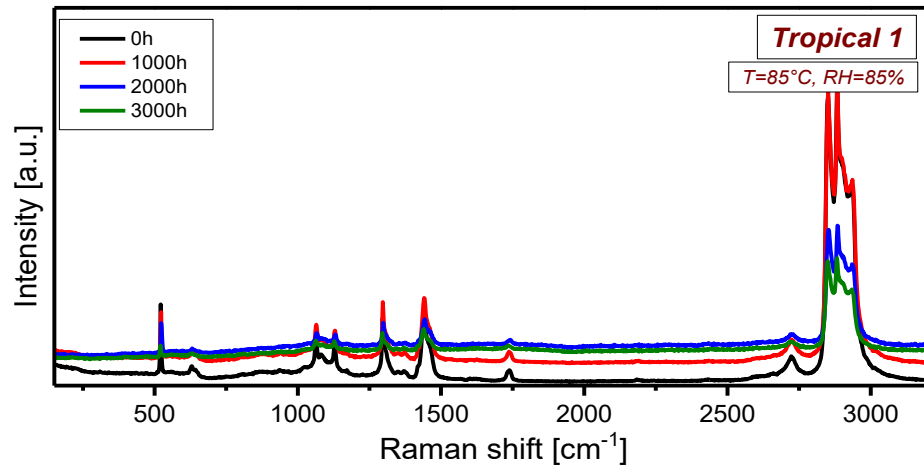
Figure 5.3. EVA spectrum after the tropical 1 climate-specific accelerated aging test

In this test, the degradation of EVA was influenced by temperature, humidity and oxygen that could penetrate through the backside of the polymeric backsheet. The backsheet used in the investigated modules was a PET-laminate. The permeation properties of the PET-laminate in terms of water vapour transmission rate (WVTR), oxygen transmission rate (OTR) and acetic acid transmission rate (AATR) were measured and are shown in Table 5.2.

Table 5.2. Permeation properties of PET-laminate at 25°C

Material	WVTR [g/m$^2\cdot$d]	AATR [g/m$^2\cdot$d]	OTR [cm^3/m$^2\cdot$d$\cdot$bar]
PET-laminate	0.6 ± 0	< 0.1	4.5 ± 0.1

As can be seen from the data in Table 5.2., the permeation properties of the PET-laminate at room temperature are very low. However, with increased temperature the permeation properties increase as well due to the higher mobility of the polymer chains especially if the temperature is above the T_g [19,36–38], which was the case for all conducted tests. Since PET is a polycondensate, it is very sensitive to increased temperature and humidity, which can lead to an increased rate of hydrolysis (see Chapter 2). Nevertheless, the conditions set by tropical 1 climate test did not cause degradation of EVA that could be qualitatively assessed.

In Figure 5.4. Raman spectra of EVA after the tropical 2 test are shown. As in the case of tropical 1, irradiation was not applied here either. Instead, the temperature and relative humidity level were increased to 90°C and 90% RH. The measured temperature in the centre of the module was 90°C. As can be seen on the Figure 5.4., these conditions were

not sufficient to induce higher degradation of EVA compared to tropical 1 conditions. Therefore, no increase in the baseline was observed.
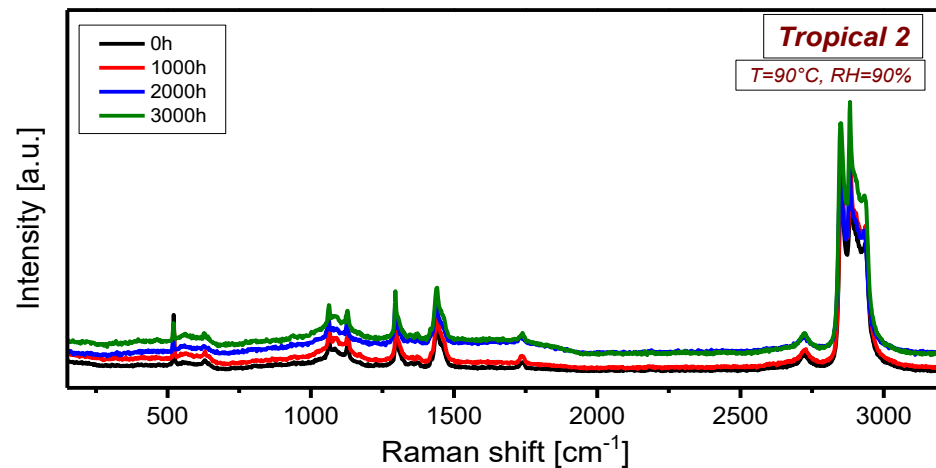

Figure 5.4. EVA spectrum after the tropical 2 climate-specific accelerated aging test

However, the temperature applied in this test was already so high above the T_g of the PET-laminate backsheet, that even visual degradation of the backsheet was caused. Figure 5.5. shows the backside of the backsheet with increasing aging hours. Increased temperature and relative humidity led to an extreme degradation (yellowing and cracking) of the PET-laminate backsheet compared to other climate-specific tests. The reason for such behaviour is an increased mobility of the polymer chains in PET upon exposure to the exposure temperature higher than the glass transition temperature ($T_g \sim 78°C$), which has an accelerated influence on hydrolysis. The beginning of the cracking was observed visually for the first time after 2000h of aging (crack indicated by red arrow). Such degradation of the backsheet was not observed in other climate tests since the conditions and/or exposure time were not as harsh as in tropical 2 test. This observation confirms that more attention needs to be paid to the types of materials used when setting the parameters of the accelerated test since certain degradation mechanisms could be over-accelerated. Since the backsheet was so degraded, it would be expected that the more moisture and oxygen would penetrate into the PV module and lead to higher degradation of EVA. Surprisingly, no such effect was observed (at least from qualitative point of view) and this could indicate that the core layer of the backsheet remained intact and prevented further degradation of the EVA.

0h	1000h	1500h	2000h	2500h	3000h

Figure 5.5. Cracking of the PET-laminate backsheet after tropical 2 test

In Figure 5.6.-5.8. Raman EVA spectra in climates with applied irradiation (moderate, alpine and arid) are shown. Raman spectra of EVA aged under a moderate climate are shown in Figure 5.6. The exposure of modules resulted in gradual increase in the baseline above the c-Si cell. According to the literature [24,28,29,31], an increase in the baseline is due to an increased fluorescence background, which could be caused by the formation of chromophore species upon degradation of EVA. The reason for higher degradation of EVA in a moderate climate compared to tropical climate tests is an addition of irradiation as an accelerating factor. In this study, applied irradiation was in the range of 300 nm to 2500 nm, which means that the EVA received a certain amount of the UV irradiation as well. Moreover, since the applied irradiation range was up to 2500 nm it also contributed to the additional warming up of the EVA, especially in the centre of the modules. Therefore, the temperature at the centre of the modules was about 113°C. This increase in temperature accelerated degradation reactions [19].
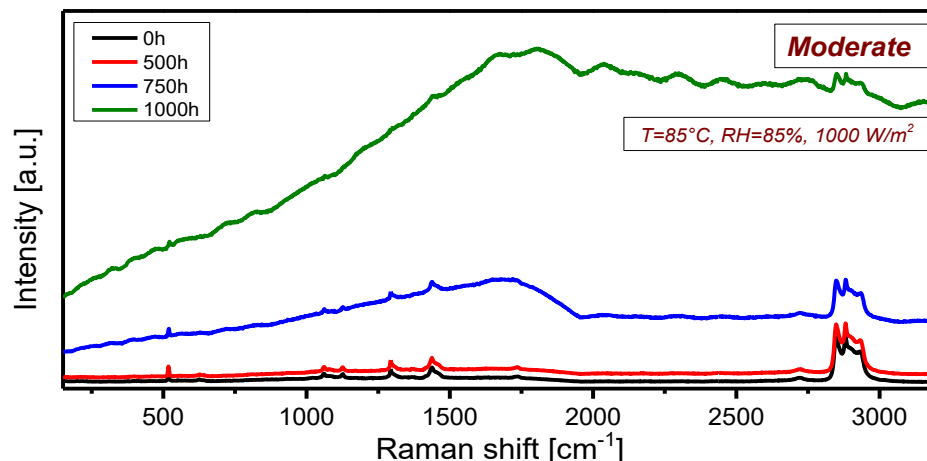
Figure 5.6. EVA spectrum after the moderate climate-specific accelerated aging test

It was already observed that the combination of UV and humidity drives the degradation of EVA stronger than damp heat conditions alone [20,24,25,32]. The radiation of sunlight that is the main cause of degradation in plastics is in the range of 300-400 nm. The energy of light radiation at 350 nm (343 kJ/mol) is sufficient to split many bonds and lead to chain cleavage, crosslinking, alteration of existing or formation of new functional groups etc. [19]. The effective wavelength of light that causes maximum degradation (initiates photochemical reactions) for PE is 300 nm. Further effective wavelengths of interest for EVA (as a PE copolymer) are at ~ 270 nm (C-H in ethylene), ~ 357 nm (aliphatic C-C) and ~ 362 nm (C-O ether) [19] which correspond to the wavelengths applied in the accelerated aging tests in this study. Concerning EVA, the C-O group has the bond energy of 331 kJ/mol, which is lower than C-H or C-C bond energy and therefore the chain splitting is expected to be at C-O-C bridges connecting ethylene and VAc segments (see Figure 5.2.). In order to increase its reliability while operating outdoors, EVA is stabilized with different light stabilizers. However, the stabilizing additives are consumed over time or even can interact with residual peroxides giving rise to the additional formation of chromophores and degradation of EVA [28,39–41]. The quantum yield, i.e. the amount of the absorbed radiation in the wavelength range that is sufficient to initiate a photochemical reaction that leads to a reaction such as chain cleavages, ranges between 10^{-2} and 10^{-5} for plastics. This means that only one of 100 to 100,000 polymer molecules that have absorbed radiation reacts under cleavage. This quantum yield is raised almost to 1 in the presence of chromophores, such as hydrogen peroxides or carbonyl groups present in the polymer, which explains their influence on weathering processes [19]. Therefore, the combination of an increased temperature,

humidity, irradiation and possibly residual peroxides resulted in the formation of a fluorescence background due to the formation of chromophores.

Raman spectra of EVA aged under an alpine climate are shown in Figure 5.7. As was observed for a moderate climate, the modules aged under alpine climate conditions showed an increase in the baseline as well. This climate test consisted of two parts applied at intervals (see Table 5.1.). UV irradiation was not applied constantly as it was in the moderate climate test, but sequentially. However, since the dose of irradiation was higher, the measured temperature in the centre of the modules was higher as well and was measured to be 118°C during the irradiation cycles. During cycles without irradiation, it was 85°C.
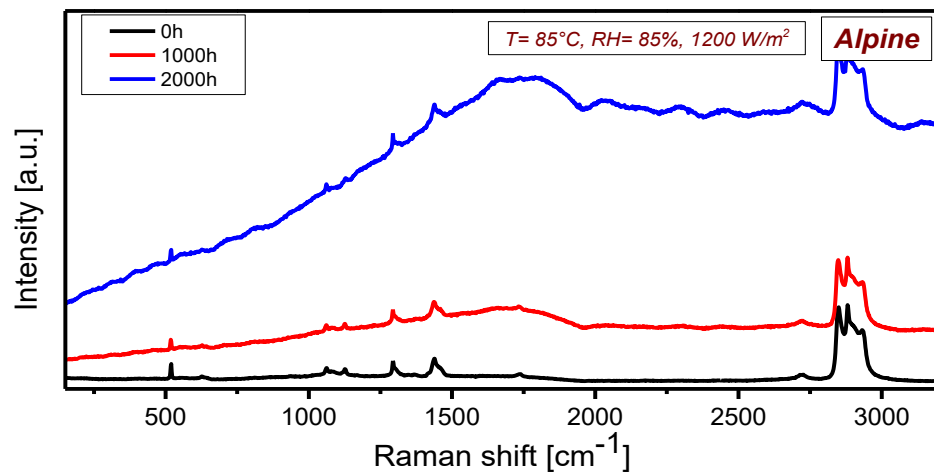

Figure 5.7. EVA spectrum after the alpine climate-specific accelerated aging test

Raman spectra of EVA aged under an arid climate are shown in Figure 5.8. This test was conducted only until 500h. However, a strong increase in the baseline was already observed after 500h of exposure. The high test temperature of 90°C combined with a high radiation of 1200 W/m^2 resulted in a temperature in the centre of the module of 129°C, which was the highest measured temperature among all climate tests (see Table 5.3.). Moreover, compared to the alpine climate where high UV dosage was applied at intervals, in the arid tests UV irradiation was applied constantly. That means that such a high temperature of the module was constant as well, which resulted in a strong increase in baseline already after 500h (compared to other climates) due to stronger degradation of EVA. The degradation reactions were therefore accelerated not only by irradiation, but also by the high temperature in the centre of the module [19].
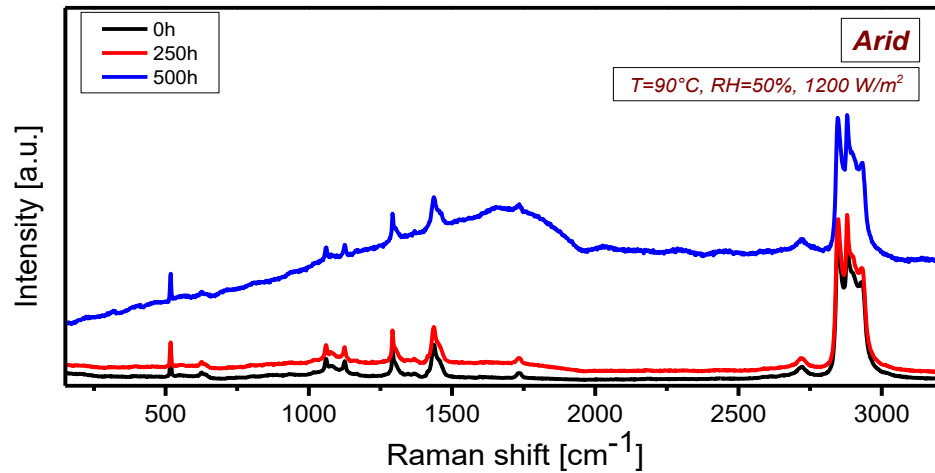
Figure 5.8. EVA spectrum after the arid climate-specific accelerated aging test

Table 5.3. Chamber temperature vs. measured module temperature

Climate test	Chamber T [°C]	Irradiation [W/m²]	Module T [°C]
Tropical 1	85°C	-	85°C
Tropical 2	90°C	-	90°C
Moderate	85°C	1000	113°C
Alpine	85°C	-	85°C
	85°C	1200	118°C
Arid	90°C	1200	129°C

Quantitative analysis of EVA degradation

In order to quantitatively assess the degradation of EVA in the modules aged under climate-specific accelerated tests, the stretching region of EVA assigned to ethylene and acetates stretching vibrations was analysed after each climate-specific test and aging step. The peaks assigned to CH_3 symmetric stretching of acetates (2882 cm^{-1}) and CH_3 asymmetric stretching of acetates and ethylene segments (2936 cm^{-1}) were analysed. Both peaks showed gradual decreases with aging time in each test, which could indicate changes in the EVA backbone i.e. reduced chain length (probably caused by deacetylation) [31,42].

Figure 5.9. depicts the relative change in the ratio of 2882 cm^{-1}/2936 cm^{-1} as a function of EVA degradation under different climate tests. In order to highlight the difference in EVA degradation between the climate tests with and without irradiation, tropical 1 was chosen as a reference since the aging conditions were set according to the standard damp heat test. The tests under moderate climate conditions were conducted only until 1000h, while the tests under an arid climate were conducted only until 500h.

Nevertheless, it can be clearly seen that the investigated peaks showed the most prominent decrease in the climate tests where the UV irradiation was added as an accelerating factor (moderate, alpine and arid climate). The combination of high temperature, humidity and irradiance accelerates the degradation of EVA. As shown in Table 5.3., the addition of irradiation significantly increased the temperature in the centre of the module, which additionally accelerated degradation of EVA. The reason why the moderate climate showed a stronger decrease in the peaks compared to the alpine climate (which had a higher dosage of irradiation) is because in the moderate climate UV irradiation was applied constantly, while in the alpine climate UV irradiation was applied at intervals (see Table 5.1.). The relative change in the peaks in the arid climate was relatively strong considering that it was aged for only 500h. The reason could be the highest temperature among all climate tests followed by a high dosage of irradiation, which also led to a very high temperature in the centre of the module. With increasing temperature, the bonds are loaded by oscillating atoms until bond cleavage occurs, which results in the formation of radicals that represent the starting point for further oxidative degradation reactions [19]. In the case of EVA, the small amounts of residual peroxides can initiate the formation of radicals as well, which also accelerates degradation.
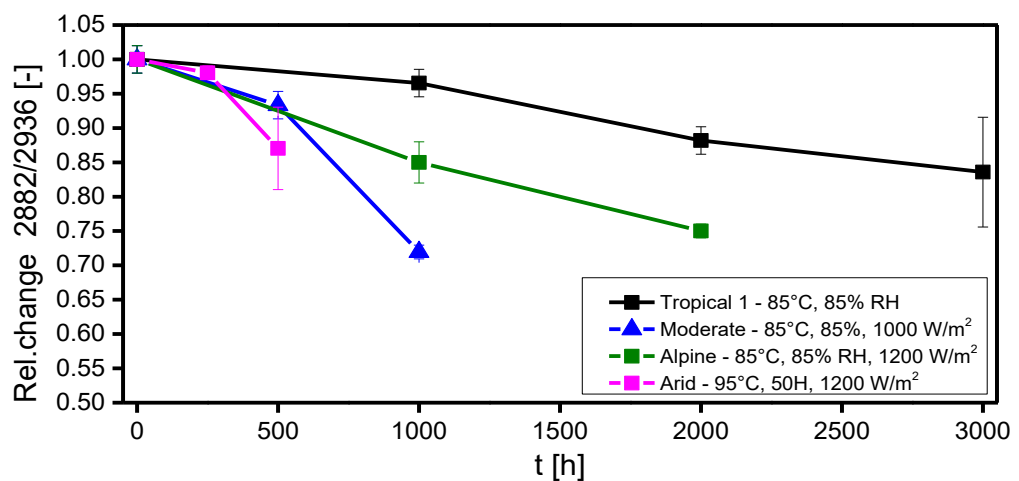

Figure 5.9. Decrease of the peaks in the stretching region upon degradation of EVA

Qualitative and quantitative analysis of EVA degradation in PV modules under climate-specific accelerated aging tests showed that different aging conditions lead to different extents of EVA degradation. Higher degradation was observed when irradiation was added as an accelerating factor compared to the reference test (damp heat=tropical 1). Furthermore, it was observed that different dosages of irradiation, as well as duration of

the applied irradiation, have a great impact on the degradation rate of EVA. These observations clearly indicated that there is an important difference in EVA degradation between the climate-specific tests compared to standard damp heat test. In other words, if the PV modules are tested under damp heat conditions and have passed the test, it does not necessarily mean that they will be reliable under all operating (climatic) conditions. Namely, the most often reported failure modes of EVA in field aged PV modules is discoloration followed by delamination of the front encapsulant and corrosion of metallization due to moisture ingress and evolution of acetic acid [10]. Discoloration is caused by the degradation of EVA whereas chromophores are formed and result in an increase in fluorescence background. Discoloration is a failure mode that is observed in every climate, but to different extents [10]. However, the results of this work confirmed that if only the damp heat test is applied it will not predict the reliability of the EVA correctly even after extensive aging. On the other hand, a variation of aging parameters (T, RH, and UV) could give more insights into reliability of the EVA outdoor. The observed changes in ratios of stretching vibrations with aging time indicated changes along the EVA backbone that could be caused by processes such as chain scission (deacetylation) or aging induced crosslinking. However, the change in the ratios upon aging cannot be directly correlated with the amount of acetic acid formed or even confirm that the degradation of EVA was necessarily followed by deacetylation.

5.3.2 UV-fluorescence measurements (UV-f)

The results of UV-f imaging for tropical 1 as a reference, moderate and alpine climate test are presented in Figure 5.10. Original modules, as expected, did not show any fluorescence after manufacturing. Fluorescence is a form of luminescence and is the physical effect of emission of light by a material that has absorbed light or other electromagnetic radiation [19,43–45]. The emitted light in the visible region has a longer wavelength than the absorbed radiation from UV light. If the fluorophore, i.e. a fluorescent chemical compound is formed, then the light can be re-emitted upon light excitation [43]. In order to re-emit light, the fluorophore needs to contain several π bonds such as those in combined aromatic groups or cyclic molecules [43,45]. Typical fluorophores are degradation products of polymers and/or additives with chromophoric/fluorophoric groups [43,44].

After damp heat exposure, i.e. the tropical 1 climate test, EVA showed fluorescing effects, especially between the cells (interface between encapsulant and backsheet). An increased fluorescence after aging is related to an increased water vapour ingress through the backsheet and it increases with aging time [43,44]. It can be seen that the

fluorescence is not homogeneously distributed due to limited permeation through the backsheet only. However, with the addition of the irradiance in moderate and alpine climate, it can be seen that the fluorescing effect is more evenly distributed (between the cells and along the ribbons), which indicates an additional formation of the fluorophores upon degradation of EVA [44]. The formation of fluorescence indicates degradation of EVA or additives in EVA.

From visual comparison between individual figures in Figure 5.10. until 1000h, it can be seen that the module aged under moderate climate test exhibited the strongest fluorescence effect. The effect was observed between the cells and along the ribbons above the cells. However, from the UV-f imaging it is not possible to quantify the extent of EVA degradation. This method did not provide insight into the real origin or the extent of the degradation, i.e. the chemical nature of the degradation. It rather provided information that fluorophores groups were formed upon degradation of EVA in the area between the cells or around ribbons. Therefore, it could not be completely correlated with the degree of degradation of EVA as revealed by Raman spectroscopy (quantitative analysis). However, the observed increase in the baseline due to the formation of fluorescence background as revealed by Raman can be correlated with the observed fluorescence via UV-f measurements.
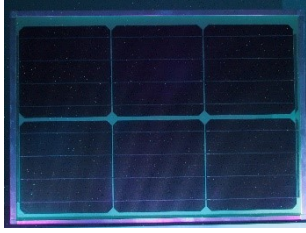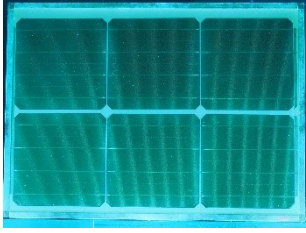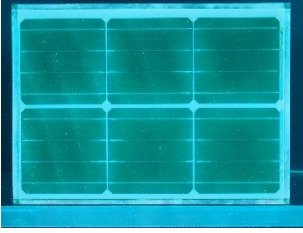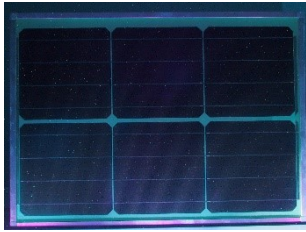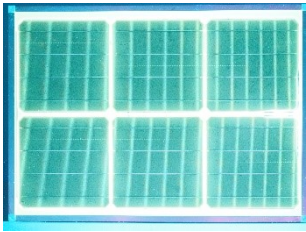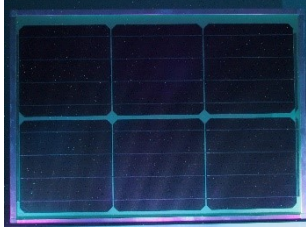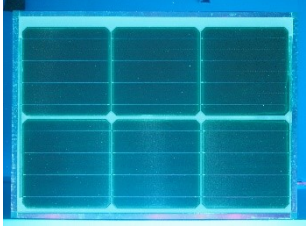
	0h	1000h	2000h
Tropical 1 (T=85°C, RH=85%)			

	0h	1000h	
Moderate (T=85°C, RH=85%, 1000 W/m²)			

	0h	1000 h	2000h
Alpine (T=85°C, RH=85%, 1200 W/m²)			

Figure 5.10. UV-fluorescence images of modules before and after aging under tropical 1, moderate and alpine climate tests

5.3.3 Comparison of applied non-destructive methods

In this work, two non-destructive methods were applied in order to investigate the degradation of EVA under different climate-specific tests: Raman confocal spectroscopy and UV-fluorescence measurements. Both methods revealed degradation of EVA with increasing aging time. However, Raman spectroscopy allowed for qualitative and quantitative assessment of EVA degradation and clearly showed a correlation between the aging parameters and the extent of EVA degradation. The highest degradation of EVA was observed under climate tests with included irradiation as an accelerating factor.

Furthermore, it was shown that the duration of the applied irradiation has a great impact on degradation behaviour as well. On the other hand, UV-f measurements indicated degradation of EVA via formation of fluorescence signal. The difference in the formation of fluorescence signal in climate tests with and without applied irradiation could be seen. The irradiation caused more uniform distribution of the fluorescence, since the formation of fluorophores was not limited by permeation properties only (as in case of tropical 1 test). However, no clear, i.e. quantitative assessment of EVA degradation could be made based on the results obtained via the UV-f method.

From the applicability point of view, both methods are applicable for non-destructive investigation of degradation of polymeric encapsulants in PV modules. However, Raman confocal spectroscopy gives information on the chemical nature of degradation of the encapsulant at a defined measuring point, while UV-f imaging measurements give the spatial distribution of UV-fluorescence in the whole sample without revealing information on the chemical nature of EVA degradation

5.4   Summary and conclusion

A service life prediction of PV modules is a complex task since it requires extensive experiments to generate reliable results, demands a considerable amount of time and it is very hard to obtain an accurate correlation between experimental results and field data. According to the IEC 61215 qualification test, a damp heat test performed at 85°C and 85% RH in duration of 1000h is assumed to provide the most information for aging and degradation of encapsulation materials (encapsulant and backsheet). However, the conditions in this test are not climate-specific and do not predict reliability of PV modules accurately since the irradiation is not included as an aging factor. Therefore, climate-specific accelerated tests need to be developed. In order to assess the impact of accelerated tests, non-destructive methods are of great importance. In this Chapter, the main aim was to non-destructively investigate the influence of climate-specific tests on the reliability of the EVA encapsulant in the PV module.

Non-destructive Raman confocal spectroscopy was conducted on PV modules aged under different sets of climate-specific accelerated tests to assess the EVA degradation. In order to qualitatively assess the degradation, an increase in the baseline due to the formation of fluorescence background was taken as an indicator for EVA degradation. It was shown that higher fluorescence background formed in the modules that were aged under climate-specific tests with included irradiation (moderate, alpine and arid) as an accelerating factor. For quantitative analysis, the relative change in C-H stretching area assigned to ethylene and acetate segments, as a measure of EVA degradation, was evaluated over aging time. It was observed that the relative change was the highest in the arid and moderate climate tests due constant irradiation and high temperature in the centre of the module. The results of Raman confocal spectroscopy showed that the degradation of EVA depends strongly on the aging parameters. A combination of aging factors (elevated T, RH and UV) as in moderate, alpine and arid climates caused stronger and faster degradation of EVA within the standardized aging time of 1000h. On the other hand, increased T and RH alone (T=85°C, RH=85%) as recommended by IEC 61215 standard (as in tropical 1) or slightly increased (as in tropical 2) did not cause such strong degradation of EVA (in terms of increased fluorescence background and changes along the EVA backbone) even after 3000h of aging. However, increased temperature and relative humidity in the tropical 2 led to an extreme degradation of the PET-laminate backsheet after 2000h of aging due to higher mobility of the polymer chains, which accelerated hydrolysis of PET. Those results have highlighted the importance of the type

of materials and operating conditions of the module when conducting the accelerated aging tests.

UV-fluorescence measurements revealed an increased fluorescence upon aging due to the formation of fluorophores, which indicated degradation of the EVA polymer and/or additives. Irradiation of the samples in the accelerated ageing tests induced the formation of UV-fluorescence, with the intensity of the fluorescence signal being dependent on the storage time and sample temperature. The irradiation caused a more uniform distribution of the fluorescence, since the formation of fluorophores was not limited to the permeation properties of the backsheet (as in the case of tropical 1 test).

Raman confocal spectroscopy proved to be suitable, convenient and reliable method for the non-destructive investigation of EVA degradation at the PV module level. Compared to UV-f imaging method, it gave insights into chemical nature of degradation and provided qualitative and quantitative assessments of EVA degradation. In order to increase the reliability of PV modules, it is necessary to conduct proper accelerated tests and to understand the degradation mechanisms behind PV failure modes.

5.5 References

[1] Y. Lyu, J. Hyun Kim, X. Gu, Developing methodology for service life prediction of PV materials: Quantitative effects of light intensity and wavelength on discoloration of a glass/EVA/PPE laminate, Solar Energy 174 (2018) 515–526. https://doi.org/10.1016/j.solener.2018.08.067.

[2] International Organisation of Standardisation, IEC 61215, Crystalline silicon terrestrial photovoltaic (PV) modules - Design Qualification and Type Approval, International Electrotechnical Commission, Geneva, CH, 2005.

[3] E.Parnham, A.Whitehead, S.Pain, W.Brennan, Comparison of Accelerated UV Test Methods With Florida Exposure for Photovoltaic Backsheet Materials EU PVSEC 2017, in: 33rd European Photovoltaic Solar Energy Conference and Exhibition, Amsterdam, 2017.

[4] W. Gambogi, O. Fu, A. Bradley, K.M. Stika, B. Hamzavy, R. Smith, T. Sample, The Impact of Materials Properties on PV Module Performance and Durability, 2012.

[5] Neelkanth G. Dhere, Reliability of PV Modules and Balance-of-System Components, in: Proceedings of the 31st IEEE Photovoltaic Specialist Conference, 2005., pp. 1570–1576.

[6] C.R. Osterwald, T.J. McMahon, History of accelerated and qualification testing of terrestrial photovoltaic modules: A literature review, Prog. Photovolt: Res. Appl. 17 (2009) 11–33. https://doi.org/10.1002/pip.861.

[7] M. Vázquez, I. Rey-Stolle, Photovoltaic module reliability model based on field degradation studies, Prog. Photovolt: Res. Appl. 16 (2008) 419–433. https://doi.org/10.1002/pip.825.

[8] J.H. Wohlgemuth, D.W. Cunningham, P. Monus, J. Miller and A. Nguyen, Long Term Reliability of Photovoltaic Modules, in: 2006 IEEE 4th World Conference on Photovoltaic Energy Conversion, Waikoloa, Hawaii, May 7-12, 2006.

[9] J. Wohlgemuth and S. Kurtz, Reliability testing beyond qualification as a key component in photovoltaic's progress toward grid parity, in: IEEE Internationl Reliability Physics Symposium, Monterey, CA, USA, 2011.

[10] A. Omazic, G. Oreski, M. Halwachs, G.C. Eder, C. Hirschl, L. Neumaier, G. Pinter, M. Erceg, Relation between degradation of polymeric components in crystalline silicon PV module and climatic conditions: A literature review, Solar Energy Materials and Solar Cells 192 (2019) 123–133. https://doi.org/10.1016/j.solmat.2018.12.027.

[11] A. Skoczek, T. Sample, E.D. Dunlop, The results of performance measurements of field-aged crystalline silicon photovoltaic modules, Progress in Photovoltaics: Research and Application (2009) 227–240. https://doi.org/10.1002/pip.874.

[12] Z. Xia, J.H. Wohlgemuth and D.W. Cunningham, A Lifetime Prediction of PV Encapsulant and Backsheet via Time Temperature Superposition Principle, in: 34th IEEE Photovoltaic Specialists Conference (PVSC), Philadelphia, Pennsylvania, USA, 7-12 June, 2009.

[13] X.Dong, H.Wang, Y.Jin, J.Huang and H.Shen (Ed.), Degradation and Reliability of Fielded c-Si PV Modules Over 28 Years in China, 2015.

[14] E.R. Parnham, K. Forsyth, W.A. MacDonald, W.J. Brennan, PET Backsheets: The robust balance between performance and cost, in: Polymers in Photovoltaics, Cologne, Germany, 2014.

[15] W.J. Gambogi, Comparative Performance of Backsheets for Photovoltaic Modules, in: 25th European Photovoltaic Solar Energy Conference and Exhibition, Valencia, Spain, 2010, pp. 4079–4083.

[16] E. Parnham, A. Seaman, A. Whitehead, W. Brennan, E. Ashford, Yellowing of PV backsheets in accelerated tests can be used as a realistic indication of possible field failures-fact or fiction?, in: 32nd European Photovoltaic Solar Energy Conference and Exhibition.

[17] K. Kanuga, Degradation of Polyester Film Exposed to Accelerated Indoor Damp Heat Aging, in: 37th IEEE Photovoltaic Specialists Conference, Seattle, Washington, 19-24 June, 2011.

[18] B. Ottersböck, G. Oreski, G. Pinter, Correlation study of damp heat and pressure cooker testing on backsheets, J. Appl. Polym. Sci. (2016). https://doi.org/10.1002/APP.44230.

[19] G.W. Ehrenstein, S. Pongratz, Resistance and stability of polymers, Hanser Publishers, Munich, 2013.

[20] B. Ottersböck, G. Oreski, G. Pinter, Comparison of different microclimate effects on the aging behavior of encapsulation materials used in photovoltaic modules, Polymer Degradation and Stability (2017) 182–191. https://doi.org/10.1016/j.polymdegradstab.2017.03.010.

[21] M. Knausz, G. Oreski, G.C. Eder, Y. Voronko, B. Duscher, T. Koch, G. Pinter, K.A. Berger, Degradation of photovoltaic backsheets: Comparison of the aging induced changes on module and component level, J. Appl. Polym. Sci. 132 (2015) 1–8. https://doi.org/10.1002/app.42093.

[22] C. Peike, S. Hoffmann, P. Hülsmann, B. Thaidigsmann, K.-A. Weiß, M. Koehl, P. Bentz, Origin of damp-heat induced cell degradation, Solar Energy Materials and Solar Cells 116 (2013) 49–54. https://doi.org/10.1016/j.solmat.2013.03.022.

[23] C. Peike, T. Kaltenbach, M. Köhl, K.-A. Weiß, N.G. Dhere, J.H. Wohlgemuth, K. Lynn, Lateral distribution of the degradation of encapsulants after different dampheat exposure times investigated by Raman spectroscopy, in: SPIE Solar Energy + Technology, San Diego, California, SPIE, 2010, p. 77730.

[24] C. Peike, T. Kaltenbach, K.-A. Weiß, M. Koehl, Non-destructive degradation analysis of encapsulants in PV modules by Raman Spectroscopy, Solar Energy Materials and Solar Cells 95 (2011) 1686–1693. https://doi.org/10.1016/j.solmat.2011.01.030.

[25] C. Peike, S. Hoffmann, I. Dürr, K.-A. Weiß, N. Bogdanski, M. Köhl, PV module degradation in the field and in the lab - how does it fit together?, in: 29th European Photovoltaic Solar Energy Conference and Exhibition, Amsterdam, Netherlands, 2014.

[26] C. Peike, S. Hoffmann, I. Dürr, K.-A. Weiß, M. Koehl, The Influence of Laminate Design on Cell Degradation, Energy Procedia 38 (2013) 516–522. https://doi.org/10.1016/j.egypro.2013.07.311.

[27] C. Peike, L. Purschke, K.-A. Weiß, M. Köhl, M.D. Kempe, Towards the origin of photochemical EVA discoloration, in: 39th Photovoltaic Specialists Conference IEEE, Tampa Bay, USA, 2013.

[28] A. Beinert, C. Peike, I. Dürr, M. Kempe, K.-A. Weiß, The Influence of the Additive Composition on the Photochemical Degradation of EVA, in: 29th European Photovoltaic Solar Energy Conference and Exhibition, Amsterdam, Netherlands, 2014.

[29] A.Mihaljevic, G.Oreski, G.Pinter, Influence of Backsheet Type on Formation of Acetic Acid in PV Modules, in: 32nd European Photovoltaic Specialists Conference and Exhibition, Munich, 2016.

[30] E. Planes, B. Yrieix, C. Bas, L. Flandin, Chemical degradation of the encapsulation system in flexible PV panel as revealed by infrared and Raman microscopies, Solar Energy Materials and Solar Cells 122 (2014) 15–23. https://doi.org/10.1016/j.solmat.2013.10.033.

[31] Ian.R.Lewis, Howell G.M. Edwards, Handbook of Raman Spectroscopy: From the Research Laboratory to the Process Line, Taylor & Francis Group, LLC, New York, 2011.

[32] Y.-H. Lee, Y.-T. Li, B.-F. Wang, Y.-W. Lin, H.-S. Wu, D.-R. Huang, A novel approach to yellowing process and formation of chromophores in EVA Sheets by two UV-aging methods, in: 29th European Photovoltaic Solar Energy Conference and Exhibition, Amsterdam, Netherlands, 2014.

[33] C. Peike, P. Hülsmann, M. Blüml, P. Schmid, K.-A. Weiß, M. Köhl, Impact of Permeation Properties and Backsheet-Encapsulant Interactions on the Reliability of PV Modules, ISRN Renewable Energy 2012 (2012) 1–5. https://doi.org/10.5402/2012/459731.

[34] C. Hirschl, M. Biebl–Rydlo, M. DeBiasio, W. Mühleisen, L. Neumaier, W. Scherf, G. Oreski, G. Eder, B. Chernev, W. Schwab, M. Kraft, Determining the degree of crosslinking of ethylene vinyl acetate photovoltaic module encapsulants—A comparative study, Solar Energy Materials and Solar Cells 116 (2013) 203–218. https://doi.org/10.1016/j.solmat.2013.04.022.

[35] A.W. Czanderna, F. J. Pern, Encapsulation of PV modules using ethylene vinyl acetate copolymer as a pottant: A critical review, Solar Energy Materials and Solar Cells (1996) 101–181.

[36] John Wiley and Sons, Encyclopedia of Polymer Science and Technology - Barrier polymers, 1999-2012.

[37] G.W. Ehrenstein, Polymeric Materials: Structure, Properties, Application, Carl Hanser Verlag GmbH & Co. KG, 2001.

[38] J. Scheirs, T.E. Long, Modern polyesters: Chemistry and technology of polyesters and copolyesters, John Wiley & Sons, Hoboken, N.J., 2003.

[39] A. Jentsch, K.-J. Eichhorn, B. Voit, Influence of typical stabilizers on the aging behavior of EVA foils for photovoltaic applications during artificial UV-weathering, Polymer Testing 44 (2015) 242–247. https://doi.org/10.1016/j.polymertesting.2015.03.022.

[40] P. Klemchuk, E. Ezrin, G. Lavigne, W. Holley, J. Galica, S. Agro, Investigation of the degradation and stabilization of EVA-based encapsulant in field-aged solar energy modules, Polymer Degradation and Stability (1997) 347–365.

[41] I. HINTERSTEINER, L. Sternbauer, S. Beissmann, W.W. Buchberger, G.M. WALLNER, Determination of stabilisers in polymeric materials used as encapsulants in photovoltaic modules, Polymer Testing 33 (2014) 172–178. https://doi.org/10.1016/j.polymertesting.2013.12.004.

[42] J.L. Koenig, Spectroscopy of Polymers, 1992.

[43] G. Eder, Y. Voronko, C. Hirschl, R. Ebner, G. Újvári, W. Mühleisen, Non-Destructive Failure Detection and Visualization of Artificially and Naturally Aged PV Modules, Energies 11 (2018) 1053. https://doi.org/10.3390/en11051053.

[44] Jan Schlothauer, Sebastian Jungwirth, Beate Röder, Michael Köhl, Flourescence as powerful tool for the inspection of polymer degradation in photovoltaic modules, in: PV Module Reliability Workshop 2011, Berlin.

[45] J. R. Lakowicz, Principles of fluorescence spectroscopy, 3rd ed., Springer, New York, 2006.

6 Summary

Harsh environmental conditions and different internal stresses were shown to be responsible for the degradation of PV modules before meeting the manufacturers' warranty of 25 years lifetime. Higher reliability could be achieved by (i) changes of materials for PV components, (ii) changes in PV design and/or production processes and (iii) development of new, or adjusting the current qualification and reliability tests. Hence, this thesis deals with the influence of each of these steps on reliability of PV modules.

The first part of this thesis dealt with the possibility of PET replacement with alternative materials. PET/fluoropolymer laminates are state-of-the-art in PV backsheets. Due to the susceptibility to hydrolysis, application of adhesive layers and the unsustainability of fluoropolymers, PET/fluoropolymer compositions need to be replaced with alternative materials. Therefore, the weathering stability of alternative co-extruded polyolefin backsheet (MPO) was systematically investigated in terms of optical, chemical, thermal, mechanical and thermo-mechanical properties before and after accelerated aging. Exposure at elevated temperature and humidity in damp heat tests resulted in chain scissions at hydrolysable ester bonds in PET-laminate, which led to the formation of shorter and more mobile chains that can crystallize faster. As a result, the overall degree of crystallinity increased (chemo-crystallization), as detected by DSC analysis. An increased degree of crystallinity affected the mechanical properties in terms of decreased elongation-at-break and increased embrittlement. The presence of irradiance accelerated the loss of mechanical properties significantly (70% loss of initial elongation-at-break). An increased crystallinity affected the thermo-mechanical properties in terms of reduced thermal expansion due to the reduction of available free fractional volume (FFV). On the other hand, a slight increase of crystallinity due to post-crystallization did not affect the mechanical and thermomechanical properties of MPO significantly. High weathering stability, combined with high flexibility, selective permeation properties and the absence of adhesive and fluoropolymer layers are great features that could make co-extruded polyolefin backsheets the candidate of choice in future PV modules.

Even though it is the most widely used PV encapsulant, ethylene vinyl-acetate (EVA) has major drawbacks such as peroxide-induced crosslinking and formation of corrosive acetic acid upon degradation, which are linked with several common failure modes of PV modules (discoloration, delamination, corrosion, etc.). Therefore, the second and third parts of this thesis dealt with the possibility of EVA replacement with alternative materials. Since the microclimate within the PV module and permeation properties of the

backsheet play important roles in the degradation of front encapsulants, the weathering stability of state-of-the-art EVA and the alternative thermoplastic polyolefin (TPO) and polyolefin elastomer (POE) encapsulants was investigated at PV module level (microclimate effect). Results of UV/Vis/NIR spectroscopy revealed a slight yellowing of encapsulants above the cell due to loss of UV-absorbers regardless of the type of backsheet used. FTIR-ATR spectroscopy revealed a strong influence of the type of the backsheet and microclimate within test module on the degradation of the front encapsulants. Due to the permeation of moisture and oxygen through the polymeric backsheet, aging of EVA and POE resulted in hydrolysis and photo-oxidation. On the other hand, the impermeability of the glass backsheet did not allow ingress of moisture and oxygen. TPO showed the highest stability above the cell, regardless of backsheet type. The results of these investigations have confirmed that PV design, i.e. type of backsheet can indeed influence degradation of front encapsulants in PV modules.

Another part of the feasibility study of EVA replacement dealt with the thermo-mechanical properties of state-of-the-art and alternative encapsulants. Mismatches in coefficient of thermal expansion (CTE) of different PV components can add additional stresses in PV modules during production and service, which can lead to cracking of the cells and interconnection and/or delamination. In order to assess the thermo-mechanical stability of polyolefin encapsulants (EVA, TPO and POE) during service time, thermo-mechanical analysis (TMA) was conducted on laminated and aged (1000h damp heat) single films. Differential scanning calorimetry (DSC) provided insights into the relation between morphology and thermo-mechanical behaviour. All three types of encapsulants showed expansion in both directions upon heating. Due to its highest crystalline content, TPO showed the most stable thermo-mechanical behaviour among the investigated encapsulants before and after aging. On the other hand, EVA, with the lowest crystalline content, showed the highest thermal expansion, which could lead to the formation of stresses within the PV module during production and service time and give rise to different failure modes. An increased thermal expansion of EVA and TPO after aging could be correlated with deteriorated crystalline structures. POE showed an increased thermal expansion after aging, which is in good correlation with the observed decrease in crystallinity, which provided enough space for mobile polymer chains. The results presented in this work have shown that morphology, i.e. the crystalline content has a dominating effect on the thermo-mechanical behaviour of polyolefin encapsulants. Thermo-mechanical behaviour of solar encapsulants has not been extensively studied so far. The findings from this work indicated differences in thermo-mechanical behaviour of different polyolefin encapsulants and proved that thermo-mechanical analysis

combined with differential scanning calorimetry is a suitable method for the systematic investigation of the thermo-mechanical stability of polyolefin encapsulants.

In the last part of the thesis, the focus was on the influence of adjusted accelerated tests on the degradation of EVA, and special emphasis was on the application of non-destructive methods. According to the state-of-the-art IEC 61215 qualification test, damp heat testing of modules performed at 85°C and 85% RH for a duration of 1000h provides the most information for aging and degradation of encapsulation materials. However this test is recognized as not predictive of long term performance. In order to predict long term performance under different operating conditions as accurately as possible, the development of climate-specific tests is necessary. The impact of these conditions on the degradation of polymeric components needs to be well understood to avoid under-/over-acceleration of degradation mechanisms. Besides demanding service life prediction, another challenge is the testing of PV modules which usually requires the use of destructive methods in order to assess the origin of the degradation of PV modules. Raman confocal spectroscopy and UV-fluorescence measurements were applied as non-destructive methods to assess the degradation of EVA in the PV modules aged under climate-specific accelerated tests. To qualitatively assess the degradation of EVA, an increase in the baseline due to the formation of the fluorescent background, which indicates the formation of chromophores upon degradation, was followed with aging time. For a quantitative determination of EVA degradation, the relative change in C-H stretching vibrations assigned to ethylene and acetate segments as a function of degradation of EVA was evaluated for each climate-specific test. It was observed that there was a clear difference in degradation of EVA between climate tests where high temperature, humidity and irradiance were involved as opposed to the standard test (damp heat test). The addition of irradiance as an accelerating factor increased the degradation rate of EVA significantly. The fastest degradation was observed for the arid climate where the set temperature and irradiance were the highest. Raman confocal spectroscopy was shown to be a good tool for the non-destructive analysis of PV modules. Compared to UV-f measurements, it allowed qualitative and quantitative assessment of EVA degradation. The results of this work point out the importance of aging conditions and could be valuable for the development of accelerated tests and an overall understanding of EVA degradation in PV modules.

The results presented in this work could contribute to the overall knowledge on polymer degradation and give valuable inputs necessary for PV module reliability. The proposed characterization methods and evaluation procedures have been shown as efficient and reliable in understanding polymer degradation mechanisms.

In order to increase reliability of PV modules, reduce costs and follow sustainability trends, it is necessary to continuously gain knowledge on polymer degradation and to develop beyond state-of-the-art new characterization techniques and accelerated tests. Further investigation on the role of the thermo-mechanical behaviour of polymeric components in the formation of internal stresses in PV modules would be beneficial to prevent related failure modes. Moreover, further development and application of non-destructive methods would provide great opportunities for further understanding of different degradation mechanisms at PV module level.